(2)

DOE/ET/25202-1(Vol.2)

DATA BASE ON BATTERIES, POWER CONDITIONING EQUIPMENT, AND PHOTOVOLTAIC ARRAYS

Volume 2. Final Report

By
Amitava Podder
Mark Kapner
Terence Morse

February 1981

Work Performed Under Contract No. AC01-79ET25202

Hittman Associates, Inc.
Columbia, Maryland

U.S. Department of Energy

Solar Energy

DISCLAIMER

DISCLAIMER

DOE/ET/25202-1(Vol.2)
Distribution Category UC-63a

DATA BASE ON BATTERIES, POWER CONDITIONING EQUIPMENT, AND PHOTOVOLTAIC ARRAYS VOLUME 2

H-C3002-80-973

Contract No. DE-AC01-79ET25202
Final Report

Prepared by:

Amitava Podder
Mark Kapner
Terence Morse

Submitted to:

U.S. Department of Energy
Division of Energy Storage Systems
Washington, DC

Submitted by:

Hittman Associates, Inc.
9190 Red Branch Road
Columbia, Maryland 21045

February 1981

THIS PAGE

WAS INTENTIONALLY

LEFT BLANK

ACKNOWLEDGEMENTS

The authors would like to express their appreciation to all those who provided guidance and assistance in the preparation of this report. In particular, we would like to thank Dr. Albert Landgrebe of the Department of Energy, and Dr. David Caskey of Sandia Laboratories, who supervised the preparation of the report; Larry Carter of Hittman Associates, who acted as the Program Manager for this project; and Dr. Henry Curran of Hittman Associates, who acted as the in-house consultant. We would also like to thank the industry representatives who provided us with valuable information on batteries, power conditioning equipment, and photovoltaic arrays.

TABLE OF CONTENTS

TABLE OF CONTENTS (CONTINUED)

LIST OF FIGURES

LIST OF FIGURES (CONTINUED)

LIST OF FIGURES (CONTINUED)

LIST OF FIGURES (CONTINUED)

LIST OF FIGURES (CONTINUED)

LIST OF FIGURES (CONTINUED)

LIST OF FIGURES (CONTINUED)

LIST OF TABLES

EXECUTIVE SUMMARY

This volume contains the data used to develop end-use scenarios and identify R&D needs for batteries to be used in photovoltaic power systems. In addition to its specific application to the present study, this data base is intended to provide state-of-the-art information to manufacturers of the various components of photovoltaic power systems, system designers, and researchers in this field.

An extensive literature search was conducted to obtain technical data on batteries, power conditioners, and photovoltaic arrays. Manufacturers and developers of each of the three technologies were contacted to obtain published brochures as well as other technical data not yet published. The data obtained from published technical literature and from direct communication with manufacturers and developers are compiled in this volume.

Table 1 contains data on various battery parameters. Many of these values are projections. Percentage uncertainties are shown for the estimated selling prices. Ultimate cycle life projections were obtained from the battery developers. The degree of uncertainty with regard to the ultimate characteristics of batteries depends on the present development status of that system. All costs in Table 1 are in 1980 dollars.

There are a number of power conditioner manufacturers, but most of them do not have experience with photovoltaic systems. An extensive search was made for the manufacturers of power conditioners. Ten manufacturers of power conditioners for solar photovoltaic applications were identified. It is expected that as the market develops, more manufacturers will be attracted to the production of these systems. Table 2 presents a summary of power conditioning equipment by manufacturers. All costs in Table 2 are in 1980 dollars.

Manufacturing photovoltaic arrays is a high-risk business. There are three basic product areas:

- Photovoltaic cell production
- Flat-plate array assembly
- Concentrating collector manufacture.

Photovoltaic cell manufacture technology is well known by all semiconductor manufacturers; but since the market is not large, few firms are serving it. Market entry in the future would only require capital for gearing up for production and minor technology perfections, neither of which would

involve large periods of time. Most semiconductor manufacturers are content with manufacturing only the cells and have no current interest in selling arrays or photovoltaic systems.

Most photovoltaic arrays are manufactured by companies that are either independent or backed by parent corporations in the energy field. Many of these firms manufacture their own solar cells, but several buy cells from semiconductor manufacturers. The sale of flat-plate collectors to the public is the only area being actively pursued within the terrestrial marketplace.

Concentrating photovoltaic collectors are in the early stages of development and are not actively marketed to the public. Firms involved in concentrator research will custom-design a system, but only one firm has a standard developed concentrating (hybrid) system for which it has published literature. Concentrators require more development before they can achieve commercialization. Several manufacturers carrying on R&D on collectors feel that the only viable market for concentrators is for very large systems.

Table 3 shows the characteristics of arrays of different manufacturers. All costs in Table 3 are in 1980 dollars.

TABLE 1. SUMMARY OF BATTERY PARAMETERS

BATTERY	PROJECTED SELLING PRICE (1980$)	ENERGY EFFICIENCY (%) AT C/5 RATE	SELF-DISCHARGE RATE	LONGEST CYCLE LIFE ACHIEVED (CYCLES)	ULTIMATE CYCLE LIFE PROJECTED BY BATTERY DEVELOPER (CYCLES)
Lead-Acid	$72/kWh (±20%)* (current deep discharge Pb-Acid Batteries $125 to $189/kWh)	75	1 - 15%/mo	1,800	4,000
Nickel-Iron	$82/kWh (±40%)	65	80%/mo	1,600	2,000
Nickel-Zinc	$55/kWh (±30%)	65 ± 5	No data	300	1,000
Redox Cr/Fe	$450/kW + 27/kWh (±35%)*	65	Nil	5,000 cycles for electrodes alone	10,000
Zinc-Chlorine	$128/kW + $14/kWh (±15%)	60	80%/mo	1,050	5,000
Zinc-Bromine	$50/kWh (±40%)*	70	25%/mo	600	5,000
Nickel-Hydrogen	$215/kWh (±20%)*	65	20%/day	10,000	30,000
Zinc-Ferricyanide	$230/kW + $32/kWh (±30%)	70	No data	650	50,000
Lithium-Metal Sulfide	$57/kWh (±25%)*	LiAl/FeS - 80 (±5) LiSi/FeS - 73 (±4)	25%/mo	LiAl/FeS 1,000 LiSi/FeS 300	LiAl/FeS - 2,000 LiSi/FeS - 3,000
Sodium-Sulfur (Glass Fiber)	$40/kWh (±15%)	84	Nil	250	2,500

TABLE 1. (CONTINUED)

BATTERY	PROJECTED SELLING PRICE (1980$)	ENERGY EFFICIENCY (%) AT C/5 RATE	SELF-DISCHARGE RATE	LONGEST CYCLE-LIFE ACHIEVED (CYCLES)	ULTIMATE CYCLE LIFE PROJECTED BY BATTERY DEVELOPER (CYCLES)
Sodium-Sulfur (β Alumina)	$48/kWh (±10%)	75	Nil	1,500	2,500
Calcium-Metal Sulfide	$36/kWh (±11%)*	70	No data	120	2,500

*Indicates selling price projection by Hittman Associates, Inc. Other selling price estimates were supplied by battery developers.

TABLE 2. SUMMARY OF THE CHARACTERISTICS OF POWER CONDITIONING EQUIPMENT BY MANUFACTURER

MANUFACTURER	CHARACTERISTICS						
	Efficiency	Cost	Max Input Voltage	Minimum Input Voltage	Normal Input Operating Voltage Range	Output Frequency	Output Voltage
Windworks	96% max -1Ø 98% max -3Ø	$350-$800 per kW	213.6V DC for 240V AC systems	No Minimum	0-500V	60 cycles	120V AC 240V AC 480V AC
Abacus	90% max	$1,200-$1,525 per kW	310V DC	190V DC	200-300V DC	50, 60 cycles	240/120V AC 208V AC 480V AC
AiResearch	93% max	ND	600V DC	ND	200-300V DC	60 cycles	480/277V
Westinghouse	92% max	$600 per kW	350V DC	200V DC	200-300V DC	60 cycles	208/120V AC 480/277V AC
Soleq	93% max	$750-$2,440	ND	ND	10.5-140V DC	60 cycles	240V AC 120V AC
Delta	95% max	$150-$1,000 per kW	650V DC	ND	200-500V DC	60 cycles	480/277V AC 75-500V DC
United Technologies	89.5% max	ND	ND	ND	130-240V DC	60 cycles	208V DC
Elgar	89% max	$2,600 per kW	ND	ND	21-60V	60, 50 cycles	115V AC 230V AC

ND = No data available

TABLE 2. (CONTINUED)

MANUFACTURER	CHARACTERISTICS						
	Output Power	Total Harmonic Distortion	Power Factor	Reliability (MTBF)	Life	Lead Time on Orders	Operation Mode
Windworks	2 kW-100 kW	ND	ND	ND	ND	8-20 weeks	Utility
Abacus	4 kW-60 kW	4%	0° lead to 0° lag	30,000 hrs	Indefinite	13-18 weeks	Utility & Stand Alone
AiResearch	20-250 kW	<5%	>.90	20,000 hrs	10-20 years	12-18 months	Utility
Westinghouse	62.5 kW	<5%	0.9 lead -0.7 lag	--	20 years	10 months	Utility & Stand Alone
Soleq	2 kW - 60 kW	5%	ND	10,000 hours	30 years	8-12 weeks	Stand Alone
Delta	60-400 kW	<3%	ND	20,000 hrs	20 years	6-9 months	Stand Alone & Utility
United Technologies	48.8 kVA	<15%	.85	ND	ND	29 weeks	Stand Alone & Utility
Elgar	.6 kW-1 kW	5-10%	ND	15,000-30,000 hrs	ND	2-8 weeks	Stand Alone

ND = No data available

TABLE 3. PHOTOVOLTAIC MODULE DATA

	MANUFACTURER										
	Amperex				Applied Solar Energy Corp.			Arco Solar			Mobil Tyco
Model	BPX-47A	BPX-47B-15	BPX-47B-20	BPX-47C	CPS-14	609-3039	60-3040	16-500	16-1000	16-2000	M28
Electrical Performance[2]:											
V_{oc} (V)	-	-	-	-	-	-	-	20.3	20.3	20.3	-
I_{sc} (A)	-	-	-	-	-	-	-	0.6	1.2	2.3	-
Pmax (W)	11	16.5	18.3	33.0	1.4	23.4 23.4 23.4	84 84	8.2	16.6	33	41.3
V_{Pmax} (V)	15.5	8.2	9.1	16.4	14.0	18 9 6	30 15	16.1	16.1	16.1	8.6
I_{Pmax} (A)	0.7	2.01	2.01	2.01	0.1	1.3 2.6 3.9	2.8 5.6	0.51	1.03	2.05	4.8
η (%)	5.4	6.1	6.8	7.3	6.4	10.1	12.4	6.8	8.5	8.9	8.5
Dimensions[3]:											
(in)	18.4 x 16.9	23 x 18.4	23 x 18.4	41.5 x 16.9	7.3 x 6.75	30 x 12	47.75 x 22	35.9 x 11.9	25.9 x 11.9	47.9 x 11.9	-
(cm)	47 x 43	58 x 47	58 x 47	105 x 43	19 x 17	76 x 30	121 x 56	40 x 30	66 x 30	122 x 30	-
Surface Area[3]:											
(sq ft)	2.2	2.9	2.9	4.9	0.34	2.5	7.3	3.3	2.1	4.0	-
(m^2)	0.2	0.27	0.27	0.46	0.03	0.23	0.68	0.12	0.20	0.37	-
Weight: (lb)	5.29	8.8	8.8	24.3	2	9	-	3.3	5.4	10	20
(kg)	2.40	3.99	3.99	11.0	0.91	4.08	-	1.50	2.45	4.54	9.07

Notes: 1. *All modules are monocrystalline silicon except for SES which is cadmium sulfide.*

2. a. *Tolerance on data is ± 10%.*

b. *All data was measured at 100 mw/cm of light intensity.*

c. *All data was measured with a cell temperature of 25-28°C. Information is not available from manufacturers to calculate compensating differences for this 3°C temperature differential. However, the error due to this temperature difference is negligible (1%).*

3. *All dimensions are approximate.*

XX

TABLE 3. (CONTINUED)

	MANUFACTURER										
	Motorola						Sensor Technology				
Model	MSP01E	MSP10D	MSP01B	MSP01A	MSF02A	MSP26A	2018 BXX17	2018 JXX19	2036 EXX19	2036 FXX11	3035 JXX18
Electric Performance[2]:											
V_{oc} (V)	4.1-4.5	6.25-6.75	12.5-13.5	25-27	18.75-20	18.75-20	-	-	-	-	-
I_{sc} (A)	6.6-7.8	4.4-5.2	2.2-2.6	1.1-1.3	1.1-1.3	0.5-0.6	-	-	-	-	-
P_{max} (W)	21.7-26.5	21.7-26.5	21.7-26.5	21.7-26.5	16.3-20	7.3-9.1	3.6	4.32	4.32	2.16	8.4
$V/_{Pmax}$ (V)	3.52	5.28	10.55	21.1	15.84	15.84	7.2	7.2	14.4	14.4	14.0
$I/_{Pmax}$ (A)	5.88-7.19	3.92-4.8	1.96-2.4	.98-1.2	.98-1.2	.44-.55	0.5	0.6	0.3	0.15	0.6
η(%)	7.0	7.0	7.0	7.0	6.3	2.8	4.8	5.2	5.2	4.7	6.5
Dimensions[3]:											
(in)	23 x 23	23 x 23	23 x 23	23 x 23	22.8 x 19.3	22.8 x 19.3	6.5 x 17	6.5 x 19	6.5 x 19	6.5 x 11	11.28 x 18.5
(cm)	58 x 58	58 x 58	58 x 58	58 x 58	58 x 49	58 x 49	17 x 43	17 x 48	17 x 48	17 x 28	29 x 47
Surface Area[3]:											
(sq ft)	3.7	3.7	3.7	3.7	3.1	3.1	0.8	0.9	0.9	0.5	1.4
(m^2)	0.34	0.34	0.34	0.34	0.29	0.29	0.07	0.08	0.08	0.05	0.13
Weight: (lb)	12	12	12	12	9.2	9.2	-	-	-	-	-
(kg)	5.44	5.44	5.44	5.44	4.17	4.17	-	-	-	-	-

Notes: 1. All modules are monocrystalline silicon except for SES which is cadmium sulfide.

2. a. Tolerance on data is ± 10%.

b. All data was measured at 100 mw/cm of light intensity.

c. All data was measured with a cell temperature of 25-26°C. Information is not available from manufacturers to calculate compensating differences for this 3°C temperature differential. However, the error due to this temperature difference is negligible (1%).

3. All dimensions are approximate.

TABLE 3. (CONTINUED)

	MANUFACTURER									
	Solar Power Corp.				Spectrolab					Tideland Signal
Model	G-12-361	M12-401	M12-369	M12-361						MG-600
Electrical Performance[2]:										
V_{oc} (V)	-	-	21	21	-	-	-	-	-	9.35
I_{sc} (A)	-	-	1.63	2.05	-	-	-	-	-	0.62
P_{max} (W)	27.6	28.7	25	31	5.4	8.1	4.05	8.1	9.45	3.5
$V/_{Pmax}$ (V)	14.7	16.6	16.5	16.5	5.4	8.1	8.1	16.2	18.9	7
$I/_{Pmax}$ (A)	1.88	1.73	1.52	1.9	1	1	0.5	0.5	0.5	-
(%)	5.7	-	5.5	6.8	5.8	6.2	5.4	6.2	6.0	5.4
Dimensions[3]:										
(in)	44 x 17	-	46 x 15.3	46 x 15.3	4.88 x 28.9	4.88 x 42.1	4.88 x 22.4	4.88 x 42.1	4.88 x 48.7	10 x 10
(cm)	112 x 43	-	117-39	117-39	12 x 73	12 x 107	12 x 57	12 x 107	12 x 124	25 x 25
Surface Area[3]:										
(sq ft)	5.13	-	4.9	4.9	1.0	1.4	0.8	1.4	1.7	0.7
(m^2)	0.48	-	0.46	0.46	0.09	0.13	0.07	0.13	0.16	0.07
Weight: (lb)	20	-	18	18	3.6	5.2	2.8	5.2	6	20 lb
(kg)	9.07	-	8.16	8.16	1.63	2.36	1.27	2.36	2.72	9.07

Notes: 1. All modules are monocrystalline silicon except for SES which is cadmium sulfide.

2. a. Tolerance on data is ± 10%.

b. All data was measured at 100 mw/cm of light intensity.

c. All data was measured with a cell temperature of 25-28°C. Information is not available from manufacturers to calculate compensating differences for this 3°C temperature differential. However, the error due to this temperature difference is negligible (1%).

3. All dimensions are approximate.

TABLE 3. (CONTINUED)

	MANUFACTURER																	
	SES				Solarex													
Model	Basic	12-2	12-6	12-12	435	1480	480	4200	4200J	4300	220	230	1270	280	785	615	460	9200J
Electrical Performance[2]:																		
V_{oc} (v)	-	-	-	-	20	20	20	20	20	20	18	18	18	18	10	9	6.6	23
I_{sc} (A)	-	-	-	-	-	-	-		-	-	-	-	-	-	-	-	-	-
P_{max} (W)	1.52	3	6	12	6	10	12	20	22	36	2.5	5	9	11	10	2.5	6.5	25
V_{Pmax} (V)	8	16	16	16	14	14	14	14	14	14	12	12	12	12	7	6	4	16
I_{Pmax} (A)	0.19	0.19	0.38	0.76	0.4	0.65	0.8	1.3	1.5	2.1	0.18	0.4	0.65	0.8	1.3	0.4	1.3	1.5
(%)	3.68	3.68	3.68	3.68	8.1	7.7	8.1	7.7	7.0	8.1	6.7	6.7	7.5	7.9	7.2	6.7	7.0	7.5
Dimensions[3]:																		
(in)	8 x 8 Module	-	-	-	10 x 12	12.9 x 15.8	14.9 x 15.5	20 x 20	23 x 21	26 x 26.5	7 x 8.5	10 x 11	12.9 x 14	10.5 x 20	10.5 x 20	5.5 x 11	7.5 x 20	22.9 x 22.9
(cm)	20 x 20	-	-	-	25 x 31	33 x 40	38 x 39	51 x 51	58 x 53	66 x 67	18 x 22	25 x 28	33 x 36	27 x 51	27 x 51	14 x 28	19 x 51	58 x 58
Surface Area[3]:																		
(sq ft)	0.4	-	-	-	0.8	1.4	1.6	2.8	3.4	4.8	0.4	0.8	1.3	1.5	1.5	0.4	1.0	3.6
(m^2)	0.04	-	-	-	0.07	0.13	0.15	0.26	0.32	0.45	0.04	0.07	0.12	0.14	0.14	0.04	0.09	0.06
Weight: (lb)	-	6	12	24	-	-	-	-	-	-	-	-	-	-	-	-	-	-
(kg)	-	2.72	5.44	10.9	-	-	-	-	-	-	-	-	-	-	-	-	-	-

Notes: 1. *All modules are monocrystalline silicon except for SES which is cadmium sulfide.*

2. a. *Tolerance on data is ± 10%.*

b. *All data was measured at 100 mw/cm of light intensity.*

c. *All data was measured with a cell temperature of 25-28°C. Information is not available from manufacturers to calculate compensating differences for this 3°C temperature differential. However, the error due to this temperature difference is negligible (1%).*

3. *All dimensions are approximate.*

I. INTRODUCTION

Hittman Associates performed an assessment of batteries suitable for use in various photovoltaic applications. The objective of this study was to compile an up-to-date comprehensive data base for research, design, and development of photovoltaic systems, primarily in the areas of applications and battery technology, and secondarily in the area of power conditioning and photovoltaic array technology.

The study involved the compilation and systematic organization of the available data on existing and potential terrestrial photovoltaic applications, with particular emphasis on six specific applications.

For each end-use area, a scenario was developed in which the most promising storage battery systems have been identified. The R&D needed for the most promising battery systems have also been determined.

The six applications studied were:

- Remote - A remote village
- Residential - A single-family house
- Commercial/Institutional - A commercial office building
- Industrial/Utility - A small utility
- Agricultural - A dairy farm
- Military - A field telephone office.

The documentation of this study consists of two volumes. This volume contains the data base used to develop the end-use scenarios and identify the R&D needed for batteries to be used in photovoltaic power systems. In addition to its specific application to the present study, this data base is intended to provide state-of-the-art information to manufacturers of the various components of photovoltaic power systems, system designers, and researchers in this field.

An extensive literature search was conducted to obtain technical data on batteries, power conditioners, and photovoltaic arrays. Manufacturers and developers of each of the three technologies were contacted to obtain published brochures as well as other technical data not yet published. The data obtained from published technical literature and direct communication with manufacturers and developers are compiled in this volume.

Sections II, III, and IV contain the data on batteries, power conditioning equipment, and photovoltaic arrays, respectively. Data obtained from literature and personal communication with manufacturers and developers are included in these sections. Principles of operation, types of systems, performance characteristics, test data, and cost data are included for each of the components.

Section V contains the Bibliography, and Section VI contains a list of abbreviations used in this volume.

II. DATA BASE ON BATTERIES

A. Definition of Batteries

The battery component of a photovoltaic electric system (see Figure II-1) serves two functions: (1) storing energy from the array when this energy is being supplied at a faster rate than required by the load, and (2) supplying energy to the load when the power required exceeds that being supplied by the array.

Energy is stored in a secondary battery by using direct current electricity to separate reactive materials in a reversible electrochemical reaction. Charging is accomplished by placing the proper potential difference (voltage) across the battery terminals.

Energy is recovered from the battery (e.g., discharged) by allowing the reactive materials to recombine via the reverse of the charging electrochemical reaction. Direct current flows between the battery terminals when a load is connected across them, until the battery is discharged.

Table II-1 presents data on the most important battery parameters described in this section. Many of these values (especially the production costs) are projections. The assumptions on which these projections are based are discussed in the following pages.

B. Definition and General Discussion of Battery Parameters

1. Production Cost and Selling Price

The production cost for batteries is the factory cost. It consists of the cost of materials, labor, overhead, taxes, and depreciation on plant and equipment. Selling price is the production cost plus the return on investment. Batteries with fixed electrolytes are rated in terms of kWh capacity. For such batteries (which include all conventional storage batteries) cost is expressed in dollars per kWh of battery capacity ($/kWh). For flowing electrolyte batteries, the power-related and energy-related components can be independently sized. Flow batteries are generally rated in kW and kWh. The cost for flow batteries is therefore expressed as two components:

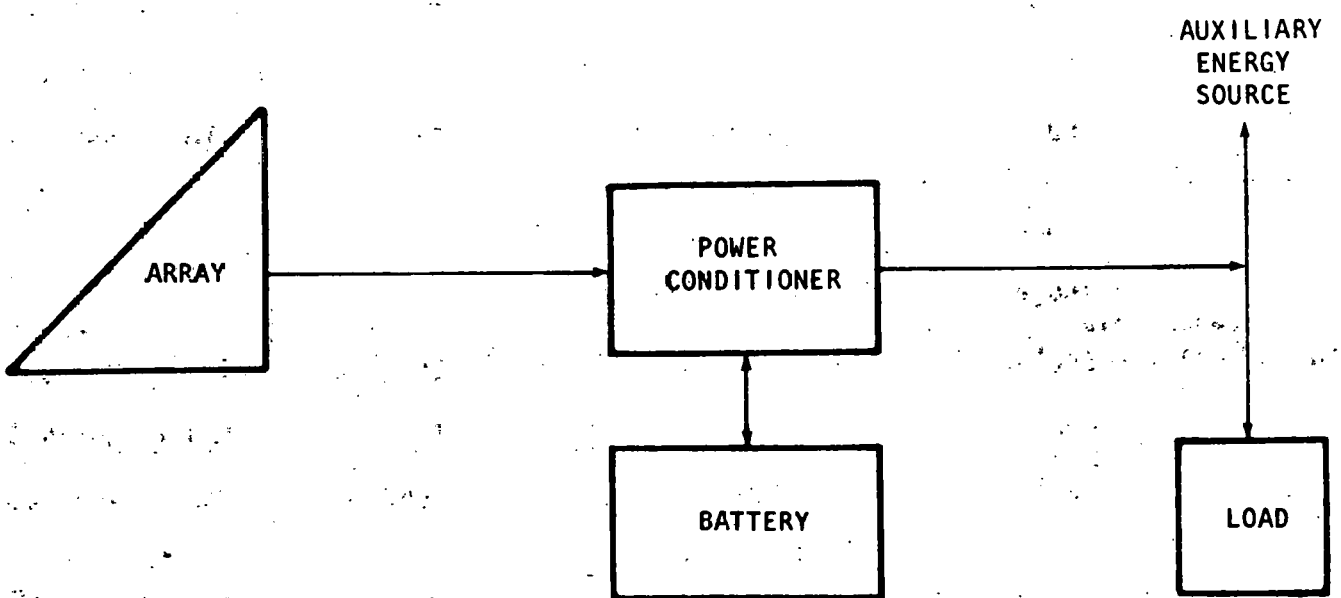

Figure II-1. Simplified Block Diagram of a Photovoltaic System

TABLE II-1. SUMMARY OF BATTERY PERFORMANCE PARAMETERS

BATTERY	PROJECTED SELLING PRICE (1980$)	ENERGY EFFICIENCY (%) AT C/5 RATE	SELF-DISCHARGE RATE	LONGEST CYCLE LIFE ACHIEVED (CYCLES)	ULTIMATE CYCLE LIFE PROJECTED BY BATTERY DEVELOPER (CYCLES)
Lead-Acid	$72/kWh (±20%)* (current deep discharge Pb-Acid Batteries $125 to $189/kWh)	75	1 - 15%/mo	1,800	4,000
Nickel-Iron	$82/kWh (±40%)	65	80%/mo	1,600	2,000
Nickel-Zinc	$55/kWh (±30%)	65 ± 5	No data	300	1,000
Redox Cr/Fe	$450/kW + 27/kWh (±35%)*	65	Nil	5,000 cycles for electrodes alone	10,000
Zinc-Chlorine	$128/kW + $14/kWh (±15%)	60	80%/mo	1,050	5,000
Zinc-Bromine	$50/kWh (±40%)*	70	25%/mo	600	5,000
Nickel-Hydrogen	$215/kWh (±20%)*	65	20%/day	10,000	30,000
Zinc-Ferricyanide	$230/kW + $32/kWh (±30%)	70	No data	650	50,000
Lithium-Metal Sulfide	$57/kWh (±25%)*	LiAl/FeS - 80 (±5) LiSi/FeS - 73 (±4)	25%/mo	LiAl/FeS 1,000 LiSi/FeS 300	LiAl/FeS - 2,000 LiSi/FeS - 3,000
Sodium-Sulfur (Glass Fiber)	$40/kWh (±15%)	84	Nil	250	2,500

TABLE II-1. (CONTINUED)

BATTERY	PROJECTED SELLING PRICE (1980$)	ENERGY EFFICIENCY (%) AT C/5 RATE	SELF-DISCHARGE RATE	LONGEST CYCLE-LIFE ACHIEVED (CYCLES)	ULTIMATE CYCLE LIFE PROJECTED BY BATTERY DEVELOPER (CYCLES)
Sodium-Sulfur (b Alumina)	$48/kWh (±10%)	75	Nil	1,500	2,500
Calcium-Metal Sulfide	$36/kWh (±11%)*	70	No data	120	2,500

*Indicates selling price projection by Hittman Associates, Inc. Other selling price estimates were supplied by battery developers.

(a) Energy-dependent cost ($/kWh of storage capacity)

(b) Power-dependent cost ($/kW).

Power- and energy-dependent costs can be combined into a single total cost parameter for a specific discharge time, T, by the equation:

$$C = C_E + \frac{C_p}{T}$$

Where:

C = total cost in $/kWh

C_E = energy-dependent cost in $/kWh

C_p = power-dependent cost in $/kW

T = discharge time in hours.

Energy-related components are the reactants and reactant containment vessels. Power-related components are the cell stacks, pumps, and control apparatus.

Production cost estimates for near-term batteries can be made with a high degree of confidence, since the manufacturing processes are similar to conventional batteries (e.g. lead-acid). For those batteries which will require unusual materials processing and handling techniques, a complete production engineering study must be performed before accurate cost projections can be made.

Whenever possible, cost estimates in this report are based on the Standard Costing Methodology developed for potential electric utility load-leveling batteries and described in EPRI 1198-2, "Revised Guidelines for Estimating the Capital Costs of Advanced Battery Systems" (September 1979). The methodology can be applied to batteries for which all materials requirements are known, and a conceptualized manufacturing process has been developed. It is based on an annual production of 25 load-leveling 100-MWh battery plants. Other assumptions in the Standard Costing Methodology are:

(a) Materials and purchased component costs are based on quotes from creditable suppliers for quantities appropriate for the scale of production.

(b) Scarce materials will be available at current costs.

(c) Labor rate is $10/hr.

(d) Overhead is 150 percent on direct labor and 10 percent on materials and purchased components.

(e) Factory space for manufacturing is leased at $50/$m^2$.

(f) Investment consists of 1.25 x equipment cost (to account for installation) plus 30 percent of the value of annual production at factory cost.

(g) Depreciation on manufacturing equipment is 10 percent annually.

(h) Taxes and after-tax return on investment are each 15 percent of investment.

For the zinc-chlorine, sodium-sulfur, and lithium-metal sulfide batteries, labor, overhead, and materials account for more than 85 percent of the selling price. The production cost projections in this report reflect first costs; they do not assume a credit for recycled materials from used batteries. All costs are expressed in 1980 dollars.

2. Battery System Life

Two measures of battery system life are: (1) calendar life and (2) cycle life. Calendar life is important for batteries which degrade over time regardless of how much they are cycled, and for battery systems which are expected to spend a great deal of time in standby mode.

Cycle life is generally defined as the number of times the battery can be charged and discharged at specified charge and discharge rates and depth of discharge before its capacity degrades to 80 percent of original capacity. Most cycle testing has been done using a uniform charge rate, discharge rate, and depth of discharge for each cycle. Photovoltaic applications, however, will involve a somewhat random cycling process with significant seasonal fluctuation in depth of discharge, and potentially rapid switching between charging and discharging mode. The effect of such random cycling on storage battery cycle life has not yet been determined.

Cycle life can also be shortened by extremes of temperature and humidity, and improper maintenance.

3. Failure Mechanisms

A failure mechanism is the process or occurrence by which battery capacity decreases below 80 percent of original capacity. Some mechanisms cause sudden failure (e.g. internal shorting between electrodes; others are gradual (e.g. corrosion of the positive grid causing increase in internal resistance). In developmental-stage batteries, there are often several possible failure mechanisms.

4. Reliability

Reliability of a device or system is defined as the probability that it will satisfactorily perform its specified function for a specified period of time under a given set of operating conditions.

Reliability functions have not yet been developed for advanced batteries. Qualitative estimates for reliability are given where available. When data on mean life of cells become available for a battery, the following reliability functions can be derived:

Assuming that an electrochemical cell displays exponential time-to-failure characteristic, the reliability R(t) of a cell with mean life (based on sample test data) of ML is given by: $R(t) = \exp(-t/ML)$.

Considering only cell failures which result in open circuit, it is possible to estimate the reliability of a battery system composed of such cells. For n equal cells connected in series to form a module, the module reliability is given by the formula:

$$R_m(t) = R_c(t)^n$$

where $R_m(t)$ = module reliability

$R_c(t)$ = cell reliability (probability that an open cell failure will not occur in time t)

The reliability of a battery consisting of a set of modules in parallel where the failure of N of the modules constitutes battery failure (i.e., if fewer than N modules fail, the battery is still operable) is given by:

$$R_B(t) = 1 - \left[1 - R_m(t)\right]^N$$

where $R_m(t)$ = module reliability

$R_B(t)$ = battery reliability.

5. Efficiency

The energy efficiency of a battery is defined as the ratio of energy discharged to charging energy for a specified charge and discharge rate. Energy efficiency is defined for the full range of battery capacity (i.e., fully charged to fully discharged to fully charged). Important efficiency relationships are defined below:

$$\text{Energy efficiency} = (\text{electrochemical efficiency}) \times \left(1 - \frac{\text{parasitic energy loss per cycle}}{\text{discharge energy per cycle}}\right)$$

$$\text{Electrochemical efficiency} = \text{Coulombic efficiency} \times \text{voltaic efficiency}$$

$$\text{Coulombic efficiency} = \frac{\text{time-averaged current during discharge}}{\text{time-averaged charging current}}$$

$$\text{Voltaic efficiency} = \frac{\text{time-averaged discharge voltage}}{\text{time-averaged charging voltage}}$$

6. Maintenance Requirements

Maintenance requirements have not yet been fully determined for batteries still in the developmental stage.

Some of the maintenance operations in advanced batteries such as redox flow batteries will be automated. These operations include venting or recombining hydrogen gas produced during charging, rebalancing cells in series so that all are at the same state of charge, and maintaining proper operating temperatures. Other maintenance procedures are manual, e.g. servicing pumps and filters, replacing chemicals, and replacing defective cells. Maintenance cost estimates are included where available.

7. Voltage/Current Characteristics

The electrical characteristics of primary concern in photovoltaic applications are:

(a) Open circuit voltage

(b) Charge cut-off voltage

(c) Discharge cut-off voltage

(d) The voltage vs. state of charge curve at constant current density. This is often shown as a voltage-time profile or voltage amp-hour profile

(e) The voltage vs. current density curve (fixed state of charge).

8. Charging Characteristics

Important charging characteristics are:

(a) Minimum charging time

(b) Voltage or current regulation required to assure proper charging without damage.

9. Self-Discharge Rate

Self-discharge of a battery is defined as loss of capacity on storage when battery is on open-circuit. This is due to spontaneous decomposition of battery materials from the charged to the discharged state. Self-discharge rate is measured in percent of rated capacity lost per unit time (usually month or day).

10. Operating Temperatures

Most batteries operate best in a particular temperature range. Where data are available, the relationship between temperature and battery performance is shown.

11. Energy and Power Densities

Energy and power densities of batteries may be important in those photovoltaic system applications where there are critical weight and space limitations. The four parameters which define these characteristics are:

(a) Specific energy (Wh/kg)

(b) Volumetric energy density (Wh/liter)

(c) Specific power (W/kg)

(d) Volumetric power density (W/liter).

For flow batteries (Redox, $Zn\text{-}Cl_2$, $Zn\text{-}Br_2$, and $H_2\text{-}Cl_2$), a more appropriate measure of power density is W/A, where the cell stack area is represented by A.

For nonflow batteries, in which energy capacity and power (e.g., discharging rate) are interdependent, the energy density is given at defined discharge rates. Discharge rates are expressed in terms of nominal capacity C (amp-hours) divided by a number of hours, e.g., C/5 means 200 amps if nominal capacity, C, were 1,000 amp-hours.

A battery has a peak power capability which is limited by the maximum current density and physical size of current-carrying components of the battery. Since peak power capability generally diminishes as the battery is discharged, specific and volumetric power densities are specified at full charge and at 80 percent depth of discharge.

12. Scarce Materials and Potential for Recycling

The use of scarce materials in a battery introduces uncertainty in the future price of the battery because the future price of such materials is inherently unstable.

This report identifies the scarce materials required for each advanced battery, the quantity of material per unit of battery capacity, and the possibility of recycling materials which could be recovered from used batteries. The production cost of a battery is particularly difficult to predict if the quantity of any material required for large-scale production of that battery would be a significant portion of existing production capacity for that material. The feasibility of producing such a battery depends on the potential for expanding production capacity of the scarce material, which, in turn, depends on proven reserves and the cost of extraction and refining. The problem is further complicated if a large percentage of the scarce material now consumed in the United States is imported.

13. Environmental, Health, and Safety Concerns

Toxic substances which will be used in the manufacture of some storage batteries pose a potential occupational safety or health hazard and are a public safety concern in the event that the battery is damaged or disposed of improperly. Other health and safety concerns are potentially toxic or explosive substances formed during battery operation, such as hydrogen (formed during overcharge of most batteries), chlorine in $ZnCl_2$ batteries, or stibine in lead-acid systems. Proper controls and containment are required to minimize the risks of human exposure to leakage from storage batteries.

14. Development Cost

The development cost is the estimated expenditure which will be required to advance the battery technology to the point where it either meets the performance and cost objectives established by DOE, or it can be successfully introduced on the market.

C. Battery Manufacturers and Developers

The following is a partial list of organizations that are actively involved in battery development:

1. Lead-Acid Battery

C&D Batteries Division of Eltra Corp.
3043 Walton Road
Plymouth Meeting, PA 19462
(215) 828-9000

Exide
Exide Engineering and Development Center
19 W. College
Yardley, PA 19067
(215) 493-7000

El Power Corp.
2117 S. Anne Street
Santa Ana, CA 92704
(714) 540-6155

Gates Rubber Co.
Electrochemistry R&D Division
P.O. Box 5887
999 S. Broadway
Denver, CO 80217
(303) 744-4806

Globe-Union, Inc.
5757 N. Green Bay Avenue
Milwaukee, WI 53201
(414) 228-2437

Gould, Inc.
40 Gould Center
Rolling Meadows, IL 60008
(312) 640-4400

Matsushita Electric Corp. of America
Panasonic - ECD Division
One Panasonic Way
Secaucus, NJ 07094
(201) 348-7000

Prestolite Battery Co.
511 Hamilton Street
Toledo, OH 43694
(419) 244-2811

2. Nickel-Iron Battery

Nife, Inc.
P.O. Box 100
George Washington Highway
Lincoln, RI 02865
(401) 333-1170

International Nickel Corp.
R&D Center
Sterling Forrest
Suffern, NY 10901
(914) 753-2707

Eagle-Picher Industries, Inc.
P.O. Box 47
Joplin, MI 64801
(417) 623-8000

Westinghouse Electric Corp.
Research & Development Center
1310 Beulah Road
Pittsburgh, PA 15235
(412) 256-7000

3. Nickel-Zinc Battery

McGraw-Edison Co.
333 W. River Road
Elgin, IL 60120
(312) 741-8900

Yardney Electric Corp.
82 Mechanic Street
Pawcatuck, CT 02891
(203) 599-1100

Gould, Inc.
40 Gould Center
Rolling Meadows, IL 60008
(312) 640-4400

G.M. Research Laboratories
Warren, MI 48090
(313) 556-5000

Gates Rubber Co.
Electrochemistry R&D Division
P.O. Box 5887
999 S. Broadway
Denver, CO 80217
(303) 744-4806

Exide
Exide Engineering and Development Center
19 W. College Avenue
Yardley, PA 19067
(215) 493-7000

Energy Research Corporation
3 Great Pasture Road
Danbury, CT 06810
(203) 792-1460

Eagle-Picher Industries, Inc.
P.O. Box 47
Joplin, MO 64801
(417) 623-8000

4. Redox Flow Battery

NASA-Lewis Research Center
Mail Stop 302-1
21000 Brook Park Road
Cleveland, OH 44135
(216) 433-4000

Battelle, Geneva Research Center
Electrochemistry Department
1227 Carouge - Geneva
SWITZERLAND CH-12

5. Zinc-Chlorine Battery

Energy Development Associates
1100 Whitcomb Avenue
Madison Heights, MI 48171
(713) 583-9434

6. Zinc-Bromine Battery

PPG Industries, Inc.
Chemical Division
One Gateway Center
Pittsburgh, PA 15222
(412) 434-3133

Gould, Inc.
40 Gould Center
Rolling Meadows, IL 60008
(312) 640-4400

General Electric Co.
G.E. Corporate R&D Center
P.O. Box 8
Schenectedy, NY 12301
(518) 385-2011

Exxon Research & Engineering Company
Exxon Research
Box 45
Linden, NJ 07036
(201) 474-2270

Eco-Control, Inc.
56 Rogers Street
Cambridge, MA 02142
(617) 661-8080

7. Hydrogen-Chlorine Battery

Brookhaven National Laboratory
Upton, NY 11973
(516) 345-2123

8. Nickel-Hydrogen Battery

Eagle-Picher Industries, Inc.
Electronics Division
P.O. Box 47
Joplin, MO 64801
(417) 623-8000

Energy Research Corporation
3 Great Pasture Road
Danbury, CT 06810
(203) 792-1460

Yardney Electric Corp.
82 Mechanic Street
Pawcatuck, CT 02891
(203) 599-1100

9. Lithium-Metal Sulfide Battery

Argonne National Laboratory
Building 205
9700 South Cass Avenue
Argonne, IL 60439
(312) 739-7711

P.R. Mallory & Co., Inc.
Laboratory for Physical Science
Northwest Industrial Park
Burlington, MA 01803
(914) 591-7000

Gould, Inc.
40 Gould Center
Rolling Meadows, IL 60008
(312) 640-4400

G.M. Research Laboratories
Warren, MI 48090
(313) 556-5000

Inco Research and Development Center
Sterling Forest
Suffern, NY 10901
(914) 753-2761

Exxon Research and Engineering Co.
Exxon Research
Box 45
Linden, NJ 07036
(201) 474-2270

EIC, Inc.
55 Chapel Street
Newton, MA 02158
(617) 965-2710

Eagle-Picher Industries
P.O. Box 47
Joplin, MO 64801
(417) 623-8000

Admiralty Materials Laboratory
Holton Heath, Poole,
Dorset, ENGLAND

Atomics International Division
of Rockwell International
Energy Systems Group
8900 DeSoto Avenue
Canoga Park, CA 91304
(213) 341-1000

Catalyst Research Corporation
Research Department
1421 Clarkview Road
Baltimore, MD 21209
(301) 296-7000

10. Sodium-Sulfur Battery

BBC Brown, Boveri & Co., Ltd.
6900 Heidelberg 1
GERMANY

Chloride Silent Power, Ltd.
Runcorn, Cheshire,
ENGLAND

Britsh Railways Board
Research & Development Divison
British Rail Technical Centre
Derby, ENGLAND

DOW Chemical, USA
2800 Mitchell Drive
Walnut Creek, CA 94598
(415) 944-2000

Ford Motor Company
Ford Aerospace & Communications Corp.
Ford Road
Newport Beach, CA 92663
(313) 337-7755

General Electric Co.
G.E. Corporate R&D Center
P.O. Box 8
Schenectady, NY 12301
(518) 385-2011

TRW Space Systems Group
TRW, Inc.
One, Space Park
Redondo Beach, CA 90278
(213) 536-1500

Owens-Illinois, Inc.
P.O. Box 187
Vineland, NJ 08360
(609) 692-4606

General Motors Corporation
G.M. Research Laboratories
Warren, MI 48909
(313) 556-5000

11. Calcium-Metal Sulfide Battery

Argonne National Laboratory
Building 205
9700 South Cass Avenue
Argonne, IL 60439
(312) 972-4544

D. Lead-Acid Battery

1. General Description

The lead-acid battery, first manufactured in 1859, is the most well-developed and the most widely-used electrochemical energy storage technology. Over 25 million kWh of lead-acid battery capacity are produced annually in the United States.

In lead-acid batteries, the positive electrode consists of lead dioxide (PbO_2) and the negative electrode consists of porous metallic lead. Both active materials are mechanically supported on grids made of lead or lead alloy. These grids serve as current collectors for the positive and negative plates. A separator, usually made from cellulose, rubber, or fiberglass, is used between each positive and negative plate to electrically insulate one from the other, while permitting electrolyte to pass between the plates. The electrolyte in which the plate separator assembly is immersed is sulfuric acid (H_2SO_4).

The chemical reaction on which the lead-acid battery is based is:

$$PbO_2 + Pb + H_2SO_4 \underset{\text{charge}}{\overset{\text{discharge}}{\rightleftharpoons}} PbSO_4 + 2H_2O$$

The open circuit voltage per cell depends upon the initial concentration of sulfuric acid, temperature, and state of charge. Under normal conditions, the cell open circuit voltage is 2.08 volts.

During discharge, the positive plate is changed from lead dioxide into lead sulfate ($PbSO_4$). At the negative plate, the porous lead is oxidized into lead sulfate. The sulfuric acid is diluted during discharge. During charging these processes are reversed.

Lead-acid batteries are currently used for three general applications:

(a) Automobile starting, lighting, and ignition (SLI)

(b) Industrial traction (e.g., fork-lift trucks), golf carts, and other off-road vehicle propulsion

(c) Stationary batteries for emergency power, in buildings, telephone systems, and automatic protection systems in power plants. The propulsion battery used in diesel submarines falls into this class.

Considerable research and development effort is being directed toward improving the performance of lead-acid batteries so that they can serve two future applications:

(a) Electric-vehicle propulsion for on-road passenger vehicles

(b) Electric power plant load leveling or peak shaving.

The performance goals for these two applications differ considerably. The DOE goals for the electric vehicle battery are:

(a) Energy density = 40 Wh/kg

(b) Peak power density = 100 W/kg for 15 seconds

(c) Battery life of 800 cycles, assuming average discharge time of 3 hours (the C/3 rate) and 8 hours charging time

(d) Capital cost = $67/kWh by 1986

(e) Energy efficiency = 60 percent.

The goals for a utility load-leveling battery are:

(a) Battery life of 2,500 deep discharge (5 hour) cycles

(b) Battery cost of $25 to $50/kWh

(c) Battery cost of less than $35/kWh for a 5-hour battery.

Firms engaged in this research and development, much of which is supported by the U.S. Department of Energy and the Electric Power Research Institute, include: Gould Industrial Battery Division, the C&D Prestolite Division of Eltra, Exide, and Westinghouse Electric Co. (R&D Center). Many other manufacturing companies are conducting privately supported lead-acid battery development.

2. Production Cost and Selling Price

The present selling price of lead-acid batteries now in production is about $60 per kWh for golf-cart batteries, about $125/kWh for fork lift truck batteries, and about $190/kWh for deep discharge, photovoltaic system batteries (1).

The HAI projected selling price of improved lead-acid deep discharge batteries, assuming mass production, is $72/kWh (±20%). This projection is based on the assumption that lead from used batteries will continue to be recycled.

3. Battery Life

The cycle life of lead-acid batteries in current production ranges from about 200 deep discharge cycles for golf-cart batteries, to about 1,800 discharge cycles for heavy-duty industrial traction batteries.

Battery life is dependent upon both operations and design. Deep discharging batteries significantly shortens their cycle life (see Figure II-2). Also, rapid charging reduces battery life by causing irreversible changes in the structure of the active materials of the battery. Batteries designed with a considerable excess quantity of active materials (and therefore lower energy density) tend to have longer cycle lives. The battery life is lengthened because a smaller percentage of the active materials (lead and lead dioxide) is consumed in the discharge reaction.

The C&D division of Eltra is planning to manufacture a lead-acid battery specifically designed for photovoltaic applications. It claims a 10-year life if the average depth of discharge is 10 percent, and a 5 to 7 year life if average depth of discharge is 80 percent (4). Gates Energy Products is now marketing a sealed lead-acid battery rated at 600 cycles or 5 years if discharged to 60 percent and charged for 16 hours per cycle.

C&D and Exide have developed concept designs for utility load-leveling batteries capable of 2,500 cycles, and Westinghouse has established 5,000 cycles as a goal for its advanced lead-acid load-leveling battery (5).

The most recent tests on lead-acid batteries being developed for electric vehicles (conducted by Argonne National Laboratory) have demonstrated cycle lives of approximately 250 deep discharge cycles (reported at the Electric and Hybrid Vehicle Conference - June 1979).

4. Failure Mechanism

The primary problem with lead-acid batteries is corrosion of the positive electrode grid. Other problems are overheating of the battery when charged too rapidly, and loss of active materials during normal operation (i.e., the discharge reaction is not completely reversed during charge).

High charging rate, or overcharging, causes electrolysis of some of the water in the electrolyte. This water loss also can lead to overheating.

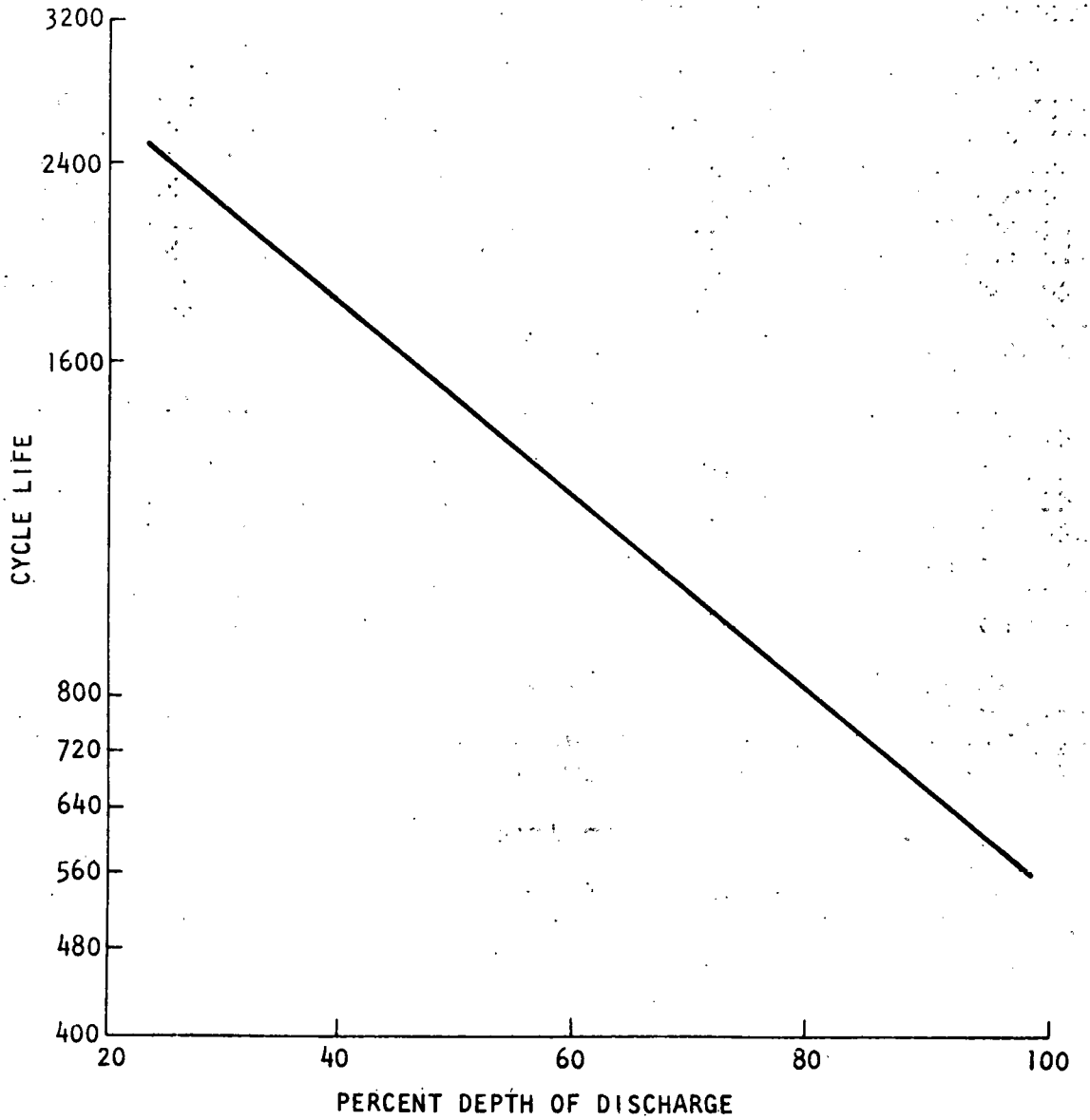

Figure II-2. Cycle Life Vs. Depth of Discharge of Lead-Acid Batteries

If the battery temperature drops below freezing when in the discharged state, the electrolyte can freeze, rupturing the battery case.

5. Reliability

If charging is properly controlled, the electrolyte level is maintained and the battery is operated in its optimal temperature range, the lead-acid battery is highly reliable.

6. Energy Efficiency

Energy efficiency is highest at low discharge rates. The energy efficiency of current-production lead-acid batteries is approximately 75 percent at a 5 hour rate.

The Exide "charge-retaining battery" is claimed to be 83 percent efficient at the 100 hour rate, but 15 percent efficient at the 10 hour rate (4). Gould's "improved golf cart battery" will have an efficiency of 80 percent (2). The Westinghouse state-of-the-art lead-acid load-leveling battery has an efficiency of 75 percent, but 80 percent is projected for the Westinghouse advanced load-leveling battery (3).

7. Maintenance Requirements and Costs

Some small-capacity lead-acid batteries are maintenance free. Maintenance for larger batteries involves checking electrolyte, adding water when necessary, and washing down the batteries periodically (2 to 4 months). Westinghouse estimates the annual maintenance cost for a lead-acid load-leveling battery facility at $0.37 per kWh for the state-of-the-art battery and $0.18 per kWh for the advanced battery (3).

8. Voltage/Current Characteristics

Figure II-3 shows the voltage per cell over the charge and discharge portions of a normal cycle. Figure II-4 shows the effect of higher discharge rates on voltage:

(a) The open circuit voltage is usually given as 2.1 volts/cell

(b) Charge cut-off voltage is 2.6 to 2.7 volts/cell

(c) Discharge cut-off voltage is 1.6 to 1.7 volts/cell.

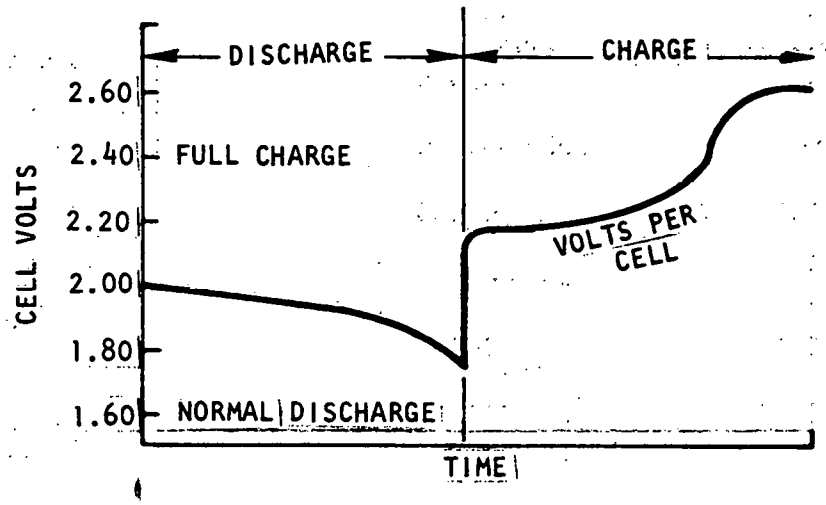

Figure II-3. Typical Voltage Characteristics During a Constant-Rate Discharge and Recharge - Lead Acid Batteries (9)

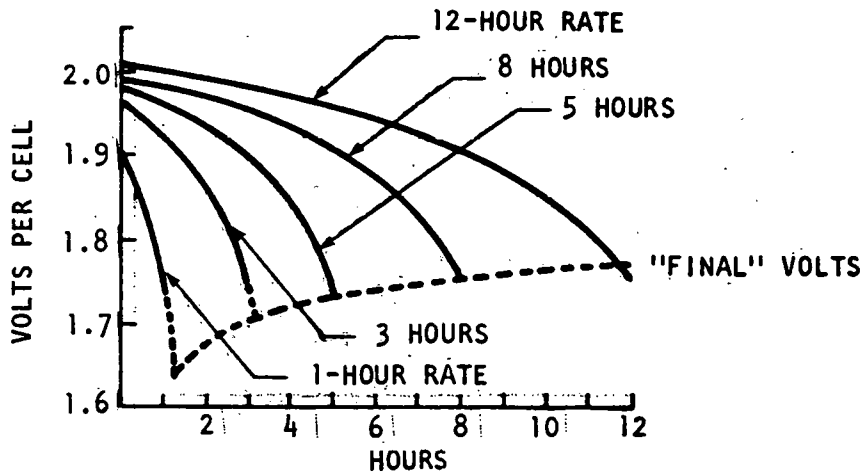

Figure II-4. Effect of Discharge Rate on Voltage Profile - Lead-Acid Batteries (9)

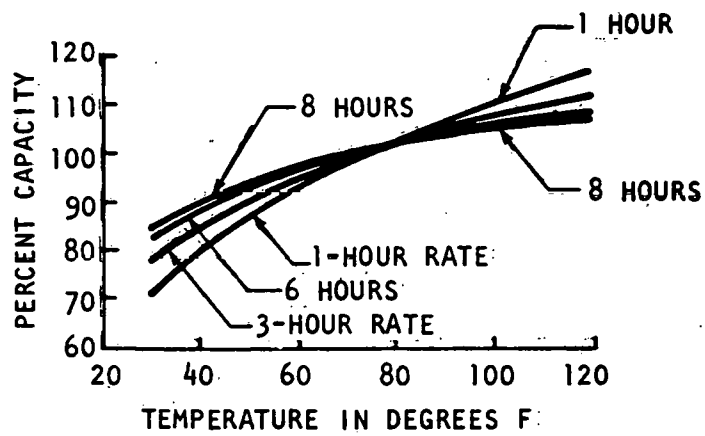

Figure II-5. Effect of Temperature on Capacity (77°F = 100%) Lead-Acid Batteries (9)

9. Charging Characteristics

Most currently available lead-acid batteries require a minimum of 4 hours charging time. Charging at too high a rate causes gassing-electrolysis of water in the electrolyte. Gassing is normal in lead-acid batteries at about 2.3 volts/cell. Excessive charge rate also causes internal heating.

At least one type of sealed lead-acid cell made by Gates, less than 60 Wh in capacity, can be fast charged in less than 1 hour. Most maintenance-free lead-acid batteries require about 20 hours to fully charge. Several methods can be used to charge most lead-acid batteries:

(a) The two-step constant-current method. A current of C/5 amperes (C = the rated capacity in Ah) is applied until battery voltage is 2.4 volts/cell. Charging current is then lowered to about C/20 until battery voltage is 2.5 to 2.6 volts/cell.

(b) Taper method. As the battery voltage increases during charging, the current is gradually decreased.

(c) Float charging. A constant voltage of about 2.2V is maintained at the battery terminals. In partial float charging, a voltage of 2.4V/cell would be used (as in automobile SLI batteries)

(d) Trickle charging. A continuous constant-current method used to maintain a battery in standby service in fully charged condition. A current of 50 to 100 mA/100 Ah capacity is generally used, charging voltage is 2.15 volts/cell.

10. Self-Discharge Rate

The self-discharge rate for lead-acid batteries depends upon the electrolyte concentration, the type of lead alloy used, and the age of the battery and temperature. Self-discharge rate for antimony-lead batteries is about 15 percent per month at 25°C. The C&D (Eltra) photovoltaic storage battery which uses lead-calcium grids has a self-discharge rate of less than 1 percent per month (4). The lead-calcium grid offers the advantages of minimizing water loss, and high charging efficiency.

The Gates sealed lead-acid cell now on the market has a self-discharge rate of 6 to 8 percent per month.

11. Operating Temperature

The variation of battery capacity with temperature is shown in Figure II-5. Although capacity increases somewhat at temperatures above 25°C (the reference temperature for battery rating), continuous operation at high temperature reduces cycle life by increasing grid corrosion.

12. Energy and Power Density

The best electric vehicle lead-acid batteries now available (in prototype) have energy densities of 35 Wh/kg (63 Wh/liter) at the C/3 discharge rate and can deliver 90 W/kg for 15 seconds when 50 percent discharged (E&HV Conference, June 1979). The energy density of golf-cart batteries is 26 Wh/kg at the C/3 rate.

Figure II-6 shows the relationship between specific energy and specific power for three types of lead-acid batteries now in production and the electric vehicle batteries now in development.

13. Materials Availability

Lead and lead oxide constitute 63 percent of the mass of the common lead-acid battery (i.e., 21 kg of lead per kWh of capacity, assuming 30 Wh/kg). While lead is not a scarce resource (the U.S. consumes over 1.3 billion kg of lead per year), its price has fluctuated significantly in recent years. Also, the U.S. imports more than half the lead ore it consumes. Lead is now recycled from used lead-acid batteries.

Other material requirements per kWh of capacity are:

(a) Antimony = 1.6 kg

(b) Arsenic = 0.04 kg.

14. Environmental, Health, and Safety (6)

The lead-acid battery operates at ambient temperatures. The only safety hazard associated with the lead-acid battery is the possibility of spillage of H_2SO_4 in case of battery rupture.

Sulfuric acid, by chemical reaction, is a moderate fire hazard. It is a powerful oxidizer and can ignite upon contact with combustibles. When heated, it emits highly toxic fumes. It will react exothermally with water or steam and can react

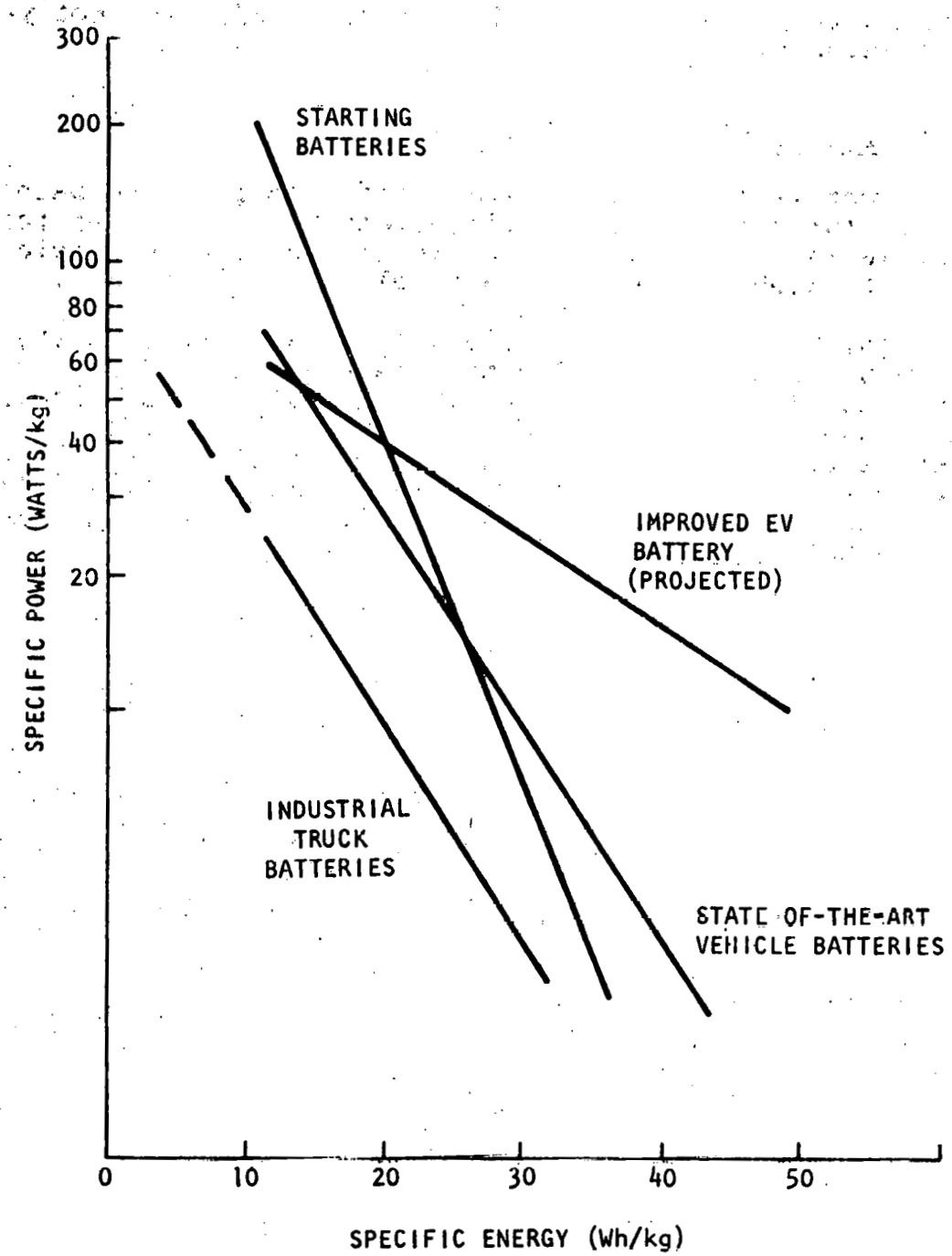

Figure II-6. Specific Energy (Wh/kg) Characteristics of Batteries for Electric Vehicles (2)

with oxidizing or reducing materials. Battery manufacturers feel that the problem of acid spills can be solved with a proper battery case design. Design standards have not yet been developed.

15. Availability

Commercially available lead-acid batteries are being used now for photovoltaic applications. The DOE long-term objective is to increase the cycle life of the lead-acid battery to 3,000 cycles for photovoltaic applications.

Also, the Electric Vehicle Act of 1976 requires the government to purchase and demonstrate 2,500 electric vehicles by 1981 and 7,500 more between 1981 and 1984. Most of these will probably use the lead-acid battery. Improved golf cart batteries are expected to be available in 1980. By 1981, the DOE expects some of its contractors to have pilot lines for the manufacture of 20 to 30 kWh capacity battery banks for test evaluation.

E. Nickel-Iron Battery

1. General Description

The nickel-iron battery, invented by Thomas Edison, has been used commercially for more than 50 years. Although the manufacturing technology for this battery is well developed, it has been largely displaced by the market for lead-acid batteries, which are less expensive. Nickel-iron batteries are still widely used in the U.S.S.R. and Eastern Europe.

The electrochemical reaction for the nickel-iron battery is:

$$Fe + 2NiO(OH) + H_2O \underset{\text{charge}}{\overset{\text{discharge}}{\rightleftharpoons}} Fe(OH)_2 + 2Ni(OH)_2$$

$$E_o = 1.37 \text{ volts}$$

The cathode is nickel oxyhydroxide, NiO(OH). The anode is iron, usually in the form of metallic iron sponge or iron-powder. The electrolyte consists of potassium hydroxide (KOH) and water, with a small addition of lithium hydroxide

(LiOH). Unlike the lead-acid battery, the electrolyte does not take part in the chemical reaction, but serves to transfer chemical oxygen ions from cathode to anode during discharge.

Conventional nickel-iron batteries are constructed using both cathode and anode materials in the form of finely ground powder encased in perforated nickel-plated steel tubes or packets. Most of the development work is being directed toward improved electrode design. The principal companies engaged in nickel-iron battery development are Westinghouse Electric Company, Eagle-Picher, Inc., Exide, and the Swedish National Development Company.

Westinghouse is using an iron electrode of composite structure and a nickel electrode made by electro-precipitation of an active compound on a fiber-metal grid substrate. The largest prototype Ni-Fe battery made by Westinghouse is 22.7 kWh. Eagle-Picher is using a sintered nickel electrode.

2. Production Cost

Current pilot plant manufacturing costs for nickel-iron batteries range from $145/kWh to $484/kWh, depending on size and specific requirements (7). Westinghouse predicts that mass production costs can be lowered to approximately $82/kWh, if its development effort is successful (4). Also, a salvage credit of $4/kWh for recycling the nickel is possible (4).

3. Battery Life

One of the principal advantages of nickel-iron batteries is their long cycle life, even under deep discharge. Westinghouse has achieved 1,600 deep discharge cycles (60 to 80 percent depth of discharge) and lifetimes of more than five years before their experimental nickel-iron batteries degrade to 80 percent of original capacity (8).

4. Failure Mechanisms

The principal failure mechanism on cycling is the loss of capacity in the nickel electrode (8).

5. Reliability

Conventional nickel-iron batteries have been found to be rugged and highly reliable (9). Quantitative data on reliability are not available.

6. Energy Efficiency

The energy efficiency of nickel-iron batteries varies with discharge rate. At the one hour rate (C/1), it has been reported as 48 percent; at the five hour rate (C/5), it is 63 percent; for very slow discharge rate (C/100), it has achieved 70 percent energy efficiency.

7. Maintenance

Maintenance requirements are similar to those for lead-acid batteries. They include periodic cleaning and the addition of water. Water addition can be completely automated for a large nickel-iron battery.

8. Voltage/Characteristics

Figures II-7 and II-8 show the charge and discharge voltage profiles for the nickel-iron battery for four different rates. The charge cut-off voltage is 1.75 volts/cell. Discharge cut-off voltage is 1.0 volts/cell. Open circuit voltage is 1.37 volts (4).

9. Charging Characteristics

The minimum recommended charging time for nickel-iron batteries is 2 hours (e.g., the C/2 rate). Charging at a higher rate raises the temperature of the battery and can lead to excessive water consumption or cell damage. The nickel-iron battery can be float charged at 1.55 volts/cell and a current of 5 mA per amp-hour of capacity (e.g., C/200 rate) (4).

10. Self Discharge

The self-discharge rate for nickel-iron batteries under development by Westinghouse is approximately 5 percent of rated capacity per day (4).

11. Operating Temperature

The nickel-iron battery operates best in the temperature range 15° to 27°C. It has a poor low-temperature performance, especially at high discharge rates, as indicated below (9):

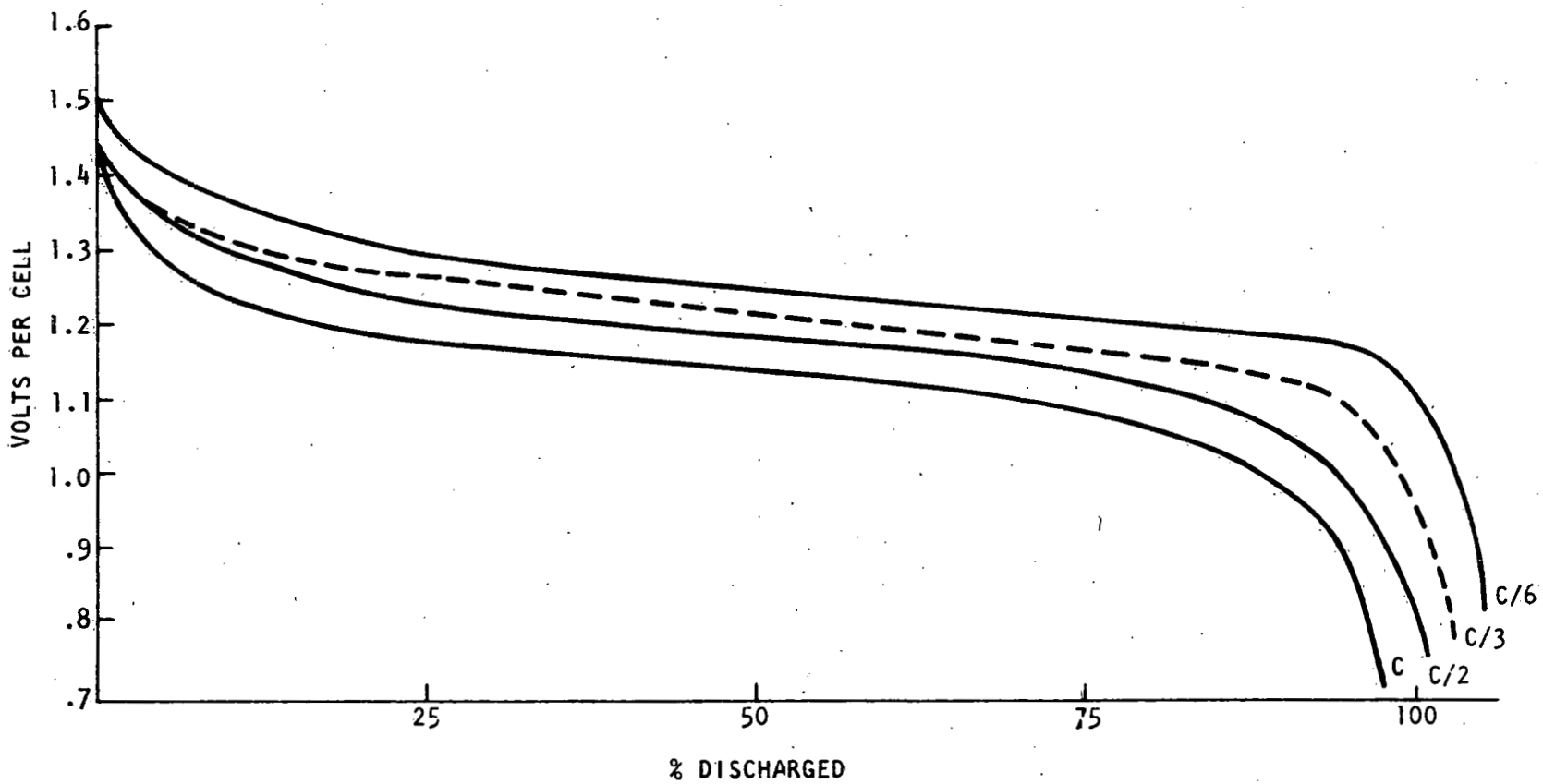

Figure II-7. Predicted Discharge Characteristics of Nickel-Iron Batteries (4)

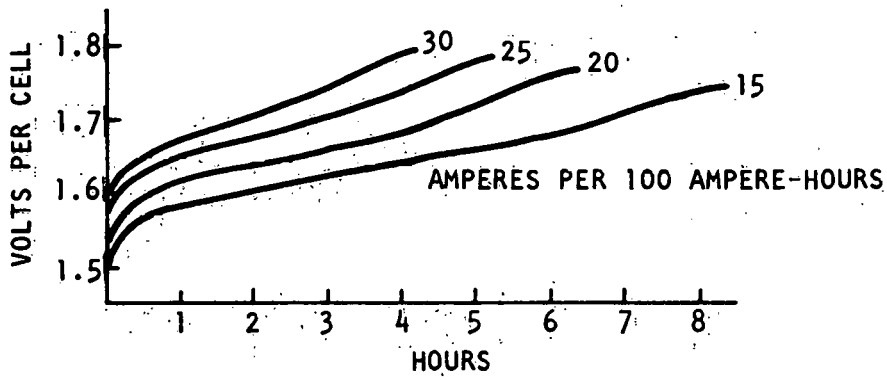

Figure II-8. Typical Charging Voltages for Nickel-Iron Batteries at Various Current Rates (9)

At 7°C Capacity is Reduced by:	When Discharged
80%	C/1
40%	C/2
20%	C/4

12. Energy and Power Densities

Energy density decreases with increasing discharge rate (8):

Energy Density (Wh/kg)	Discharge Rate
50	C/6
45	C/3
37	C/2
25	C

The specific energy density of 50 Wh/kg corresponds to a volumetric energy density of 96 Wh/liter. The nickel-iron battery can deliver sustained power of 20 W/kg; its peak power density is 130 W/kg (7).

13. Material Availability

The only material of questionable availability required for the nickel-iron battery is nickel (approximately 3.2 kg per kWh of capacity). U.S. nickel (mine) production was approximately 12,700 metric tons in 1979. Primary nickel consumption in the United States was 182,700 metric tons. However, because the prime suppliers of nickel to the United States are Canada and Australia, nickel is not considered a critical or scarce material.

14. Environmental, Health, and Safety

The manufacture of nickel-iron batteries may pose an occupational health hazard due to airborne nickel (TLV is 1 mg/m^3). Control technology is not well developed for airborne nickel. In addition, nickel and nickel salts have demonstrated toxic effects on plants and certain species of fish. This has implications both for the manufacture and disposal of nickel-iron batteries.

The primary safety hazard in operating nickel-iron batteries is the generation of hydrogen gas during battery charging. Approximately 28 liters (1 ft^3) of hydrogen are

generated for each 63 Ah of overcharge. Proper venting of this hydrogen is necessary because hydrogen poses a fire hazard when its air concentration is 4 percent.

A secondary safety hazard is the possible spillage of potassium hydroxide electrolyte should the battery short circuit, overheat, and consequently rupture. This spillage could lead to a fire.

15. Development Cost

The cost of the current DOE program to develop a nickel-iron electric vehicle battery is estimated at $7 to $8 million.

16. Availability

The nickel-iron battery has been commercially manufactured in the United States, but has been largely displaced by lead-acid and nickel-cadmium batteries. It is more widely used in Europe and the U.S.S.R.

F. Nickel-Zinc Battery

1. General Description

The nickel-zinc battery is in its developmental phase and must achieve several milestones before it can be commercialized. The two major problems are separator stability and zinc electrode shape change. As separators fail and the zinc electrode changes shape and loses capacity, the life of the battery quickly deteriorates. It is expected that these problems will be overcome and that nickel-zinc batteries will compete with lead-acid batteries in the near future because both the energy and power densities of the nickel-zinc battery exceed the capabilities of the lead-acid battery.

The electrode reactions of the cell are:

$$\text{Positive:} \quad NiOOH + H_2O + e^- \rightleftharpoons Ni(OH)_2 + OH^-$$

$$\text{Negative:} \quad Zn + 2OH^- \rightleftharpoons ZnO + H_2O + 2e^-.$$

The complete cell reaction is:

$$2NiOOH + H_2O + Zn \rightleftharpoons 2Ni(OH)_2 + ZnO.$$

The nominal voltage for this reaction is 1.63 volts per cell. Higher voltages are achieved by connecting individual cells in series.

A nickel-zinc battery is composed of a case, plates, separators, and electrolyte. The active materials in the battery are the positive plate, made primarily from nickel hydroxide; the negative plate, made from zinc; and the electrolyte, which is a potassium hydroxide solution.

The case is generally a plastic or rubber container. Polypropylene is the favored substance for cases because it is light, chemically inert, and strong, but any material that is nonporous and resistant to the electrolyte may be used.

The positive electrode (plate) is made from a nickel substrate with a nickel oxyhydroxide (NiOOH) pressed onto it. The substrate may be sintered to make it physically stronger, yield higher discharge rates, and give it a longer life expectancy.

The negative electrode (plate) is made from zinc. Additives or binders provide mechanical strength needed in the cycling of the battery. Trace materials are added to the zinc to stabilize the shape of the zinc electrode.

Separators that are used in commercial nickel-zinc batteries consist of various materials such as cellulosic membranes and polypropylene films. None of these will stand up in the nickel-zinc cell environment. Separators which will hold up in the cell environment and withstand more than 500 operating cycles are being developed. These separators may be organic or inorganic, and must have microporous membranes and low resistivity.

The electrolyte currently being used in nickel-zinc cells is potassium hydroxide. The electrolyte generally has a 30 to 45 percent concentration which varies with the charge state of the battery. The battery will require periodic addition of water to make up losses caused by electrolysis. The electrolyte does not react with the electrodes during charging and discharging.

Current development of the nickel-zinc battery is directed specifically toward electric vehicle applications. This market requires both a high energy density and a cycle life of at least 300 deep discharge cycles.

The companies involved in research and development work on nickel-zinc batteries are:

Energy Research Corporation Gould, Inc. Yardney Electric Company General Motors Corporation Research and Development	}	Under Contract to DOE

2. Production Cost

Labor and materials costs have been estimated for the manufacture of 25 kWh capacity nickel-zinc batteries. These estimates range from $34 to $39 per kWh, assuming production of 100,000 batteries per year, and $59 to $81 per kWh for a 1,000 battery-per-year production level (10). The most likely projected price for nickel-zinc batteries is $55/kWh (±30%).

3. Battery Life

In October 1979, General Motors reported that it had achieved 300 discharge cycles on a full-scale prototype nickel-zinc battery under development for electric vehicles. Previously, the best cycle life reported had been 270 discharges on a 400 Ah cell (C/5 discharge rate to 80 percent depth of discharge) (10).

4. Failure Mechanisms

Nickel-zinc batteries have two major problems:

(a) Separator failure due to breakdown at high temperatures or penetration by zinc dendrites

(b) Loss of capacity at the zinc electrode due to redistribution of the zinc (and shape change of the zinc electrode) during cycling.

5. Reliability

No data available.

6. Energy Efficiency

The energy efficiency of nickel-zinc batteries that have been tested ranges from 60 to 70 percent (10,11).

7. Maintenance

The nickel-zinc battery requires periodic addition of water to make up for water lost by electrolysis during charging. No maintenance cost data are available.

8. Voltage/Current Characteristics

The voltage profiles during discharge and charge for a 400 Ah cell are shown in Figures II-9 and II-10.

Open circuit voltage is 1.75 V/cell
Charge cut-off is 2.2 V/cell
Discharge cut-off is 1.15 V/cell.

9. Charging Characteristics

A 17 percent overcharge is recommended (11). The charging process is exothermic and care must be taken to cool the battery to avoid damage.

10. Self-Discharge Rate

No data are available on the self-discharge rate for nickel-zinc batteries.

11. Temperature

Operation at ambient temperature is recommended.

12. Energy and Power Density

Energy density is approximately 69 Wh/kg (140 Wh/liter) at the C/3 discharge rate. Projected substained power density is 23 W/kg, and projected peak power density is 150 W/kg.

13. Scarce Materials

The nickel-zinc battery requires approximately 5.4 kg of nickel per kWh of capacity. Nickel is a relatively expensive metal.

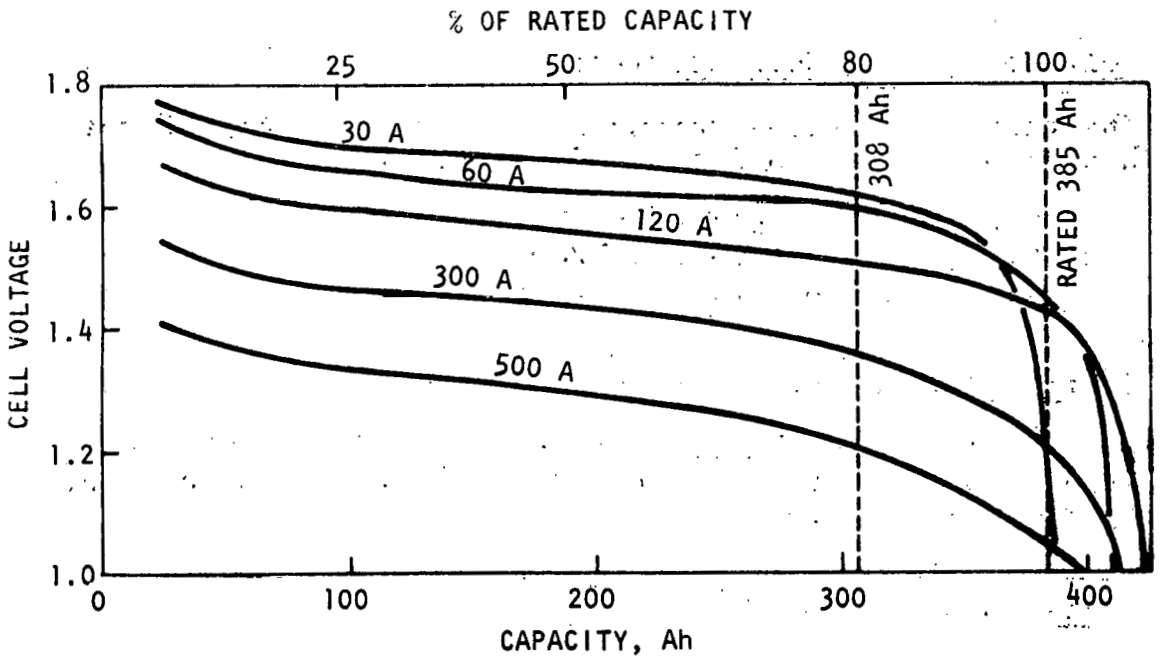

Figure II-9. Typical Discharge Characteristics for the Nickel-Zinc Battery

Design B/Rated Capacity - 385 Ah at 3 to 6 Hour Rates
(95 percent of Actual 406 Ah to 1.3 V)(10)

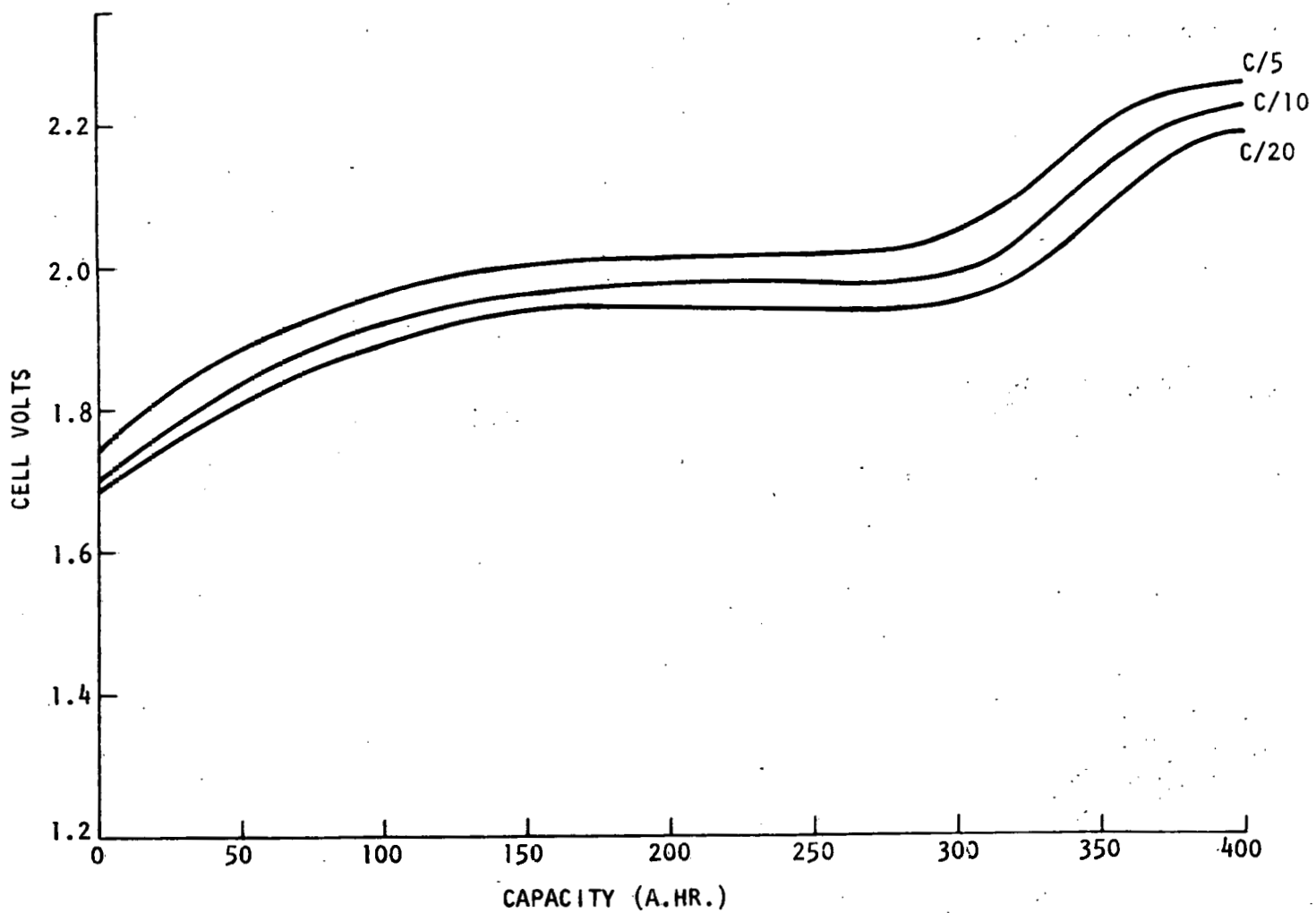

Figure II-10. Typical Charge Characteristics for the Nickel-Zinc Battery

14. Environmental, Health, and Safety

Adequate ventilation is required since hydrogen is evolved during charging. The following potential environmental and safety impacts are associated with the manufacture and disposal of nickel-zinc batteries.

Nickel and nickel salts have demonstrated toxic effects on plants (especially citrus) and certain species of fish. The extent of these effects is unknown; control techniques have not been determined.

The manufacture of battery material results in an air pollutant with known occupational health implications (TLV for airborne nickel = 1 mg/m^3; for zinc-chloride = 1 mg/m^3; for zinc-oxide = 5 mg/m^3). Control technology is unknown.

Nickel carbonyl is a known carcinogen. Clinical and epidemiological data indicate that nickel-containing compounds have caused extensive morbidity in man. The specific chemical forms must be determined for toxicity studies. The extent to which nickel carbonyl will be produced as a by-product of battery manufacture is unknown. Control procedures are unknown. More information will be required as materials are more extensively handled.

G. Redox Flow Battery

1. General Description

Redox is a term used to describe a variety of possible electrochemical storage systems which use the oxidation and reduction of two fully soluble electrochemical couples for charging and discharging. The reactions take place between ions that can exist in two or more different valency states. The reactants which have received the most attention are acidified iron and chromium solutions. The Redox reactions for this couple are described by the formulas:

$$Fe^{+3} + e^- \underset{\text{charge}}{\overset{\text{discharge}}{\rightleftharpoons}} Fe^{+2}$$

$$Cr^{+2} \underset{\text{charge}}{\overset{\text{discharge}}{\rightleftharpoons}} Cr^{+3} + e^-$$

Figure II-11 shows how this Redox system operates. The majority of the reactant solutions, which are chlorides of iron (cathode fluid) and of chromium (anode fluid), are stored in tanks external to the power conversion section (also called the cell stack) where the reaction takes place. The electrodes in the cell stack are inert. The cell stack also contains a selective membrane between each pair of electrodes. Chloride ions are exchanged across this membrane between the two half cell reactions, but not iron or chromium ions.

The Redox energy storage system has several attractive features:

(a) Storage capacity and power output can be independently sized. (This is an advantage that all flow batteries have over fixed electrolyte batteries.)

(b) Moderate operating conditions permit the use of plastic construction materials.

(c) The Redox battery has a very long estimated cycle life and calendar life since the electrodes are inert and should not degrade with cycling. Permanent capacity loss is due only to membrane crossover of chromium ions.

(d) Internal voltage regulation is possible by connecting or disconnecting cells in series.

The primary drawback of the Redox flow battery is that its very slow reaction rates result in low power and energy densities. For this reason, only stationary energy storage applications are envisioned.

The principal organization engaged in Redox research and development is the NASA Lewis Research Center in Cleveland, Ohio.* Subcontractors to NASA are Ionics, Inc., which is working on ion exchange membranes; Giner, Inc., which is developing improved electro catalysts; and United Technologies, Inc., which is performing cost estimates.

The Redox flow battery is considered to be in the exploratory stage of development. The test results to date have been obtained on Redox systems of up to 200 W capacity (an 18-cell stack using 300 cm^2 cells).

**Information in this section was provided by researchers at NASA Lewis Research Center.*

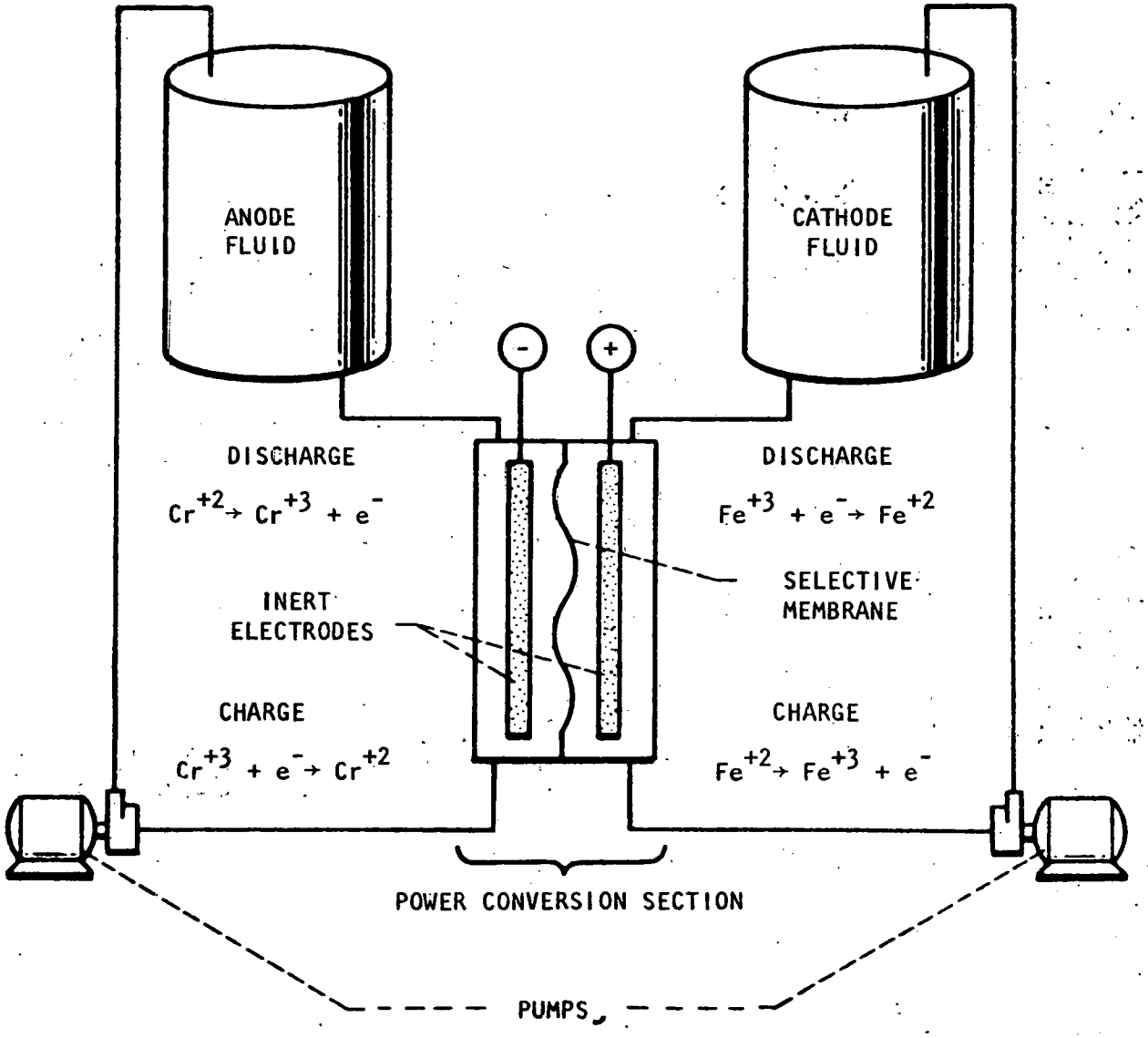

Figure II-11. Two-Tank Electrically Rechargeable Redox Flow Cell (45)

2. Production Cost

Since power output and storage capacity (energy) can be independently sized, the cost of a Redox battery must be expressed as two components -- a cost per unit power ($/kW) and a cost per unit energy ($/kWh) (see Section I - Definition of Parameters). According to NASA Lewis Research Center, the production costs of a 10 kW - 40 hr Redox system (400 kWh capacity) are projected to be $162 per kW and $21 per kWh. Total cost per kWh would therefore be $24 per kWh ($162/40 + $21). This projection assumes substantial reduction in the cost of several components. Based on current costs of existing components used in prototypical Redox systems, the production costs range from $300 to $615 per kW, and $14 to $40 kWh. Power-related cost is sensitive primarily to membrane cost per cm^2 and power density, expressed in watts per cm^2. Energy-related costs are sensitive primarily to the cost of chromium.

3. Life

There is no known inherent cycle life limitation in the Redox flow battery (NASA L.R.C.). Electrodes have been cycled for 5,000 cycles, between 10 percent and 90 percent depth of charge, with no degradation. Test results on complete batteries are not yet available. Calendar life is limited only by membrane cross diffusion. It is estimated that in 20 years the battery will lose 25 percent of its original capacity by cross diffusion.

4. Mechanisms of Failure

The primary failure mechanisms of the Redox battery are membrane or pump failure.

5. Reliability

Reliability is limited by the membranes and pumps. Quantitative estimates are not available.

6. Energy Efficiency

Prototype Redox flow batteries have demonstrated an energy efficiency of 65 percent. It is expected that efficiency can be boosted to 75 percent in full-scale systems (NASA L.R.C.).

7. Maintenance Requirements

Rebalancing to assure that all cells in the stack are at equal states of charge can be completely automated and performed continuously during battery operation. The manual maintenance operations are:

(a) Maintaining the pumps

(b) Replacing membranes and electrodes (frequency unknown)

(c) Replacing anode and cathode fluids once every 15 to 20 years.

8. Voltage/Current Characteristics

Open circuit voltage: 1.18 volts/cell

Charge cut-off: 1.25 volts/cell

Discharge cut-off: 0.85 volts/cell

Figures II-12 and II-13 show voltage and current as functions of time for charging and discharging. It is expected that the discharge voltage curve can be flattened by use of trim cells which would be switched into the circuit as the battery discharges. Figure II-13 shows the variation of voltage with current density.

9. Charging Characteristics

The Redox flow battery should be charged at a constant voltage of 1.25 volts/cell. A 10 kW-40 hour battery would require approximately 32 hours to fully charge.

10. Self Discharge Rate

0.003 percent per day.

11. Temperature Range

20 to 80°C.

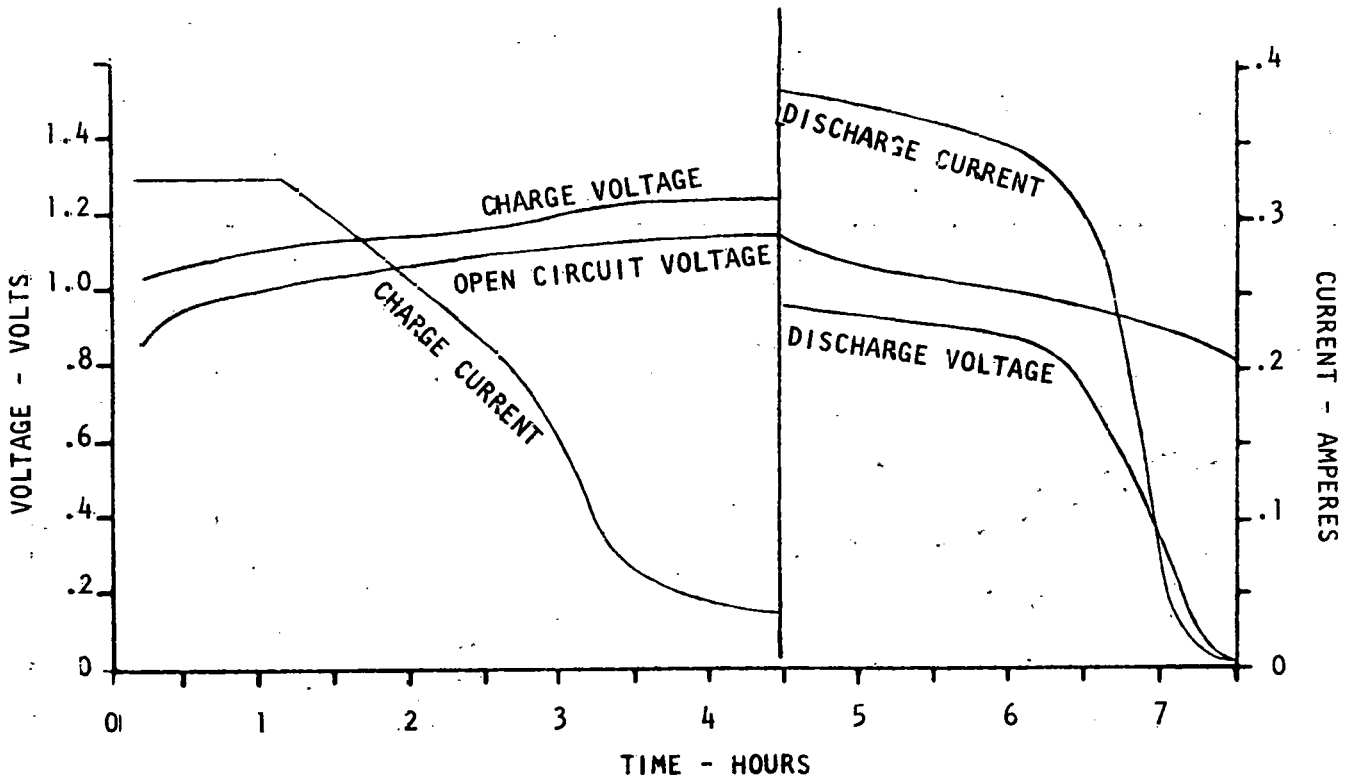

OCV = 1.5V

Figure II-12. Redox Cell with Open Circuit Voltage (Volts/Cell)(45)

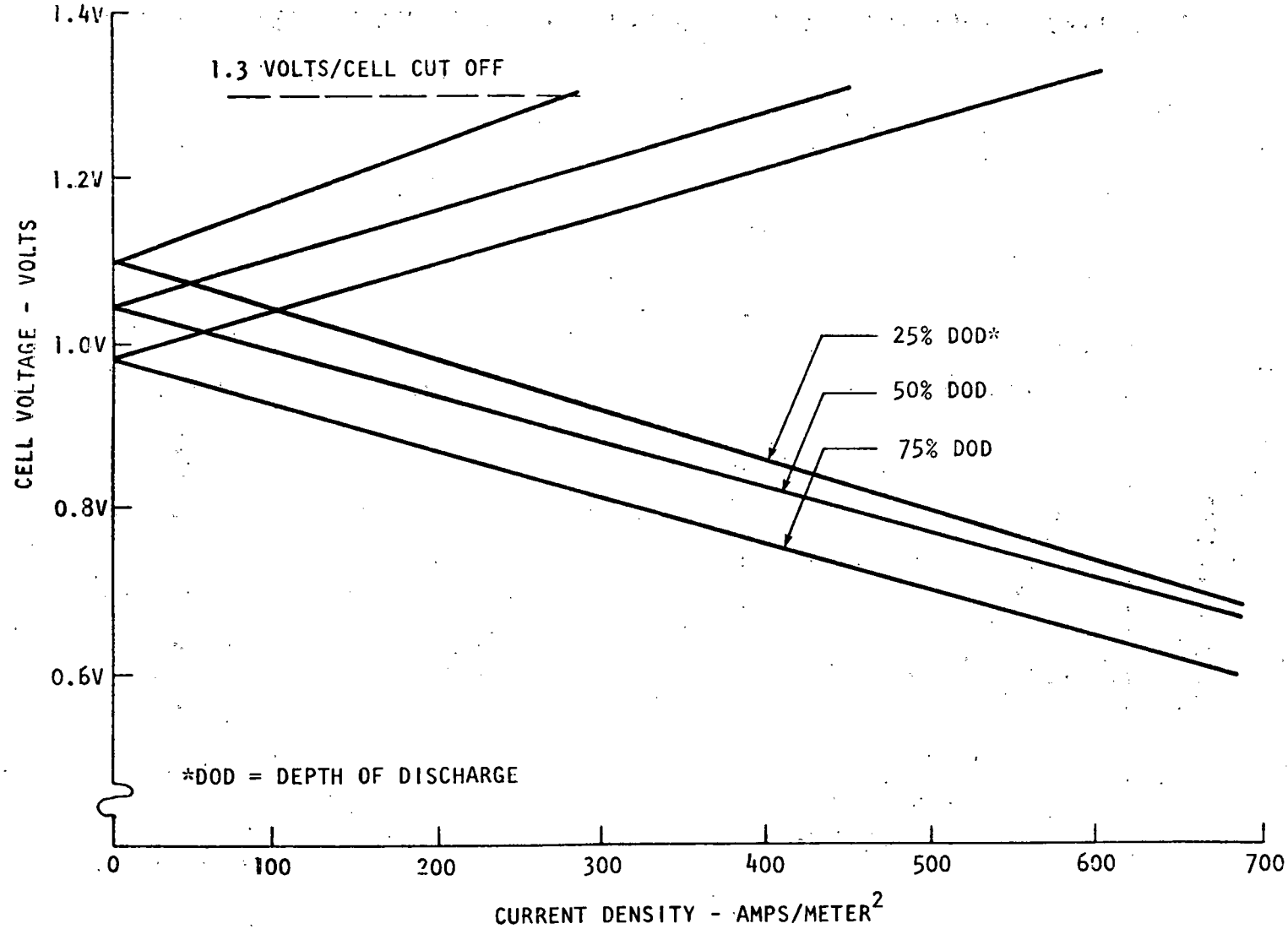

Figure II-13. Variation of Voltage with Current Density (45)

12. Energy and Power Densities

The energy density of a chromium/iron Redox couple-using 1.0 molar solutions is 4.3 Wh/kg, or 6.5 Wh/liter. The energy density is considerably lower than that of lead-acid batteries, which have energy densities of approximately 35 Wh/kg. Energy density is not a function of discharge rate. Power density is generally measured in W/m^2. Currently, at 50 percent discharge, Redox flow batteries have achieved 290 W/m^2. The development goal for solar photovoltaic energy storage application is 484 W/m^2. Specific power at full charge would be 0.122 W/kg (0.164 W/liter); at 80 percent discharged, it would be 0.106 W/kg.

13. Scarce Materials

The Redox flow battery being developed by NASA Lewis Research uses chromium chloride (10.6 kg/kWh) and gold (approximately 540 mg/kW - as an electrode catalyst). The chromium requirement is 2.2 kg per kWh. Almost all of the one million metric tons of chromite (the chromium ore) consumed in the United States annually is imported. World chromite production in 1976 was 9.5 million tons. The major producers are South Africa and the U.S.S.R. Annual U.S. consumption of gold by industry, dentistry, and the arts is approximately 140,000 kg. More than two-thirds of the gold ore refined in the United States is imported. While both chromium and gold are scarce materials, the small quantity of gold required for battery manufacture does not present a problem. The amount of chromium required may, however, pose a problem.

14. Environmental, Health, and Safety

The Redox battery does not pose any major health or safety problems. It is an ambient temperature battery and does not contain any hazardous substances.

15. Availability

The NASA Lewis Research Center is now constructing a 2 kW-5hr (i.e., 10 kWh) Redox flow battery. It is predicted that the Redox flow battery will be available for use in photovoltaic applications (such as a remote village) in 1984.

H. Zinc-Chlorine Battery

1. General Description

The zinc-chlorine battery is an aqueous electrochemical system in which a circulatory electrolyte carries the chlorine reactant. The chlorine reacts on an inert electrode and chlorine gas, which is released during charging, and stored externally from the reaction cell as a frozen hydrate. Zinc is electroplated on the inert electrode during charging, and is electrolytically dissolved into the zinc chloride electrolyte during discharge (see Figure II-14).

The cell reaction is:

$$Zn\ (solid) + Cl_2\ (gas) \underset{\text{charge}}{\overset{\text{discharge}}{\rightleftharpoons}} ZnCl_2\ (aqueous)$$

$$E_o = 2.12\ \text{volts/cell}$$

The chlorine storage reaction is:

$$Cl_2\ (gas) + xH_2O \rightleftharpoons Cl_2 \cdot x\ H_2O \quad (solid)$$

x varies between 6 and 10.

Since this storage reaction requires that heat be removed, the zinc-chlorine battery contains a refrigeration system. The zinc-chlorine battery is being developed by Energy Development Associates (EDA), a subsidiary of Gulf and Western Co. Both electric vehicle and load-leveling applications are envisioned.

2. Production Cost

The projected mass production cost is esimated by EDA at $30 to $40/kWh, assuming a production rate of 25,000 batteries/yr. Projected cost of the 50 kWh electric vehicle battery is $33/kWh (12). A load-leveling battery is projected to cost $28/kWh (13). The estimated cost of power-related components is $128/kW; energy storage-related costs are approximately $14/kWh (12).

3. Life

A 1.7 kWh cell has been cycled 1,050 times and is still on test (EDA). Cycle testing of 50 kWh modules (containing

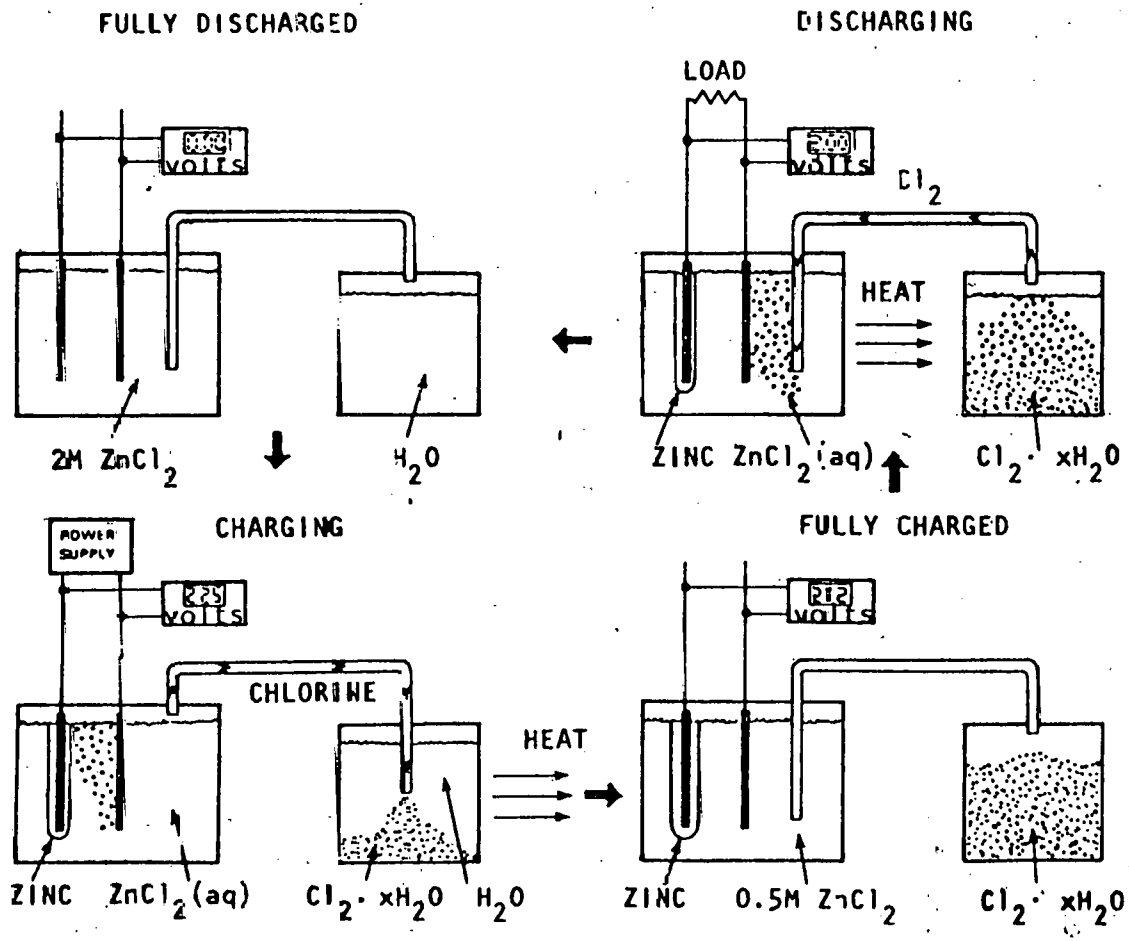

Figure II-14. Schematic Diagram of the Zinc-Chlorine Battery's Operation (13)

60 cells) has demonstrated 60 cycles without failure. EDA claims that there is no inherent calendar life limitation.

4. Failure Mechanisms

Mechanical components -- pumps, seals, valves, and the refrigeration system -- present the major potential for failure. Other failure mechanisms are deterioration of the graphite electrodes and electrical shorting caused by zinc dendrite formation.

5. Reliability

The complexity of the plumbing and control systems may present a reliability problem. Quantitative data are not available.

6. Energy Efficiency

The zinc-chlorine battery has demonstrated a coulombic efficiency of 73 percent, and a voltaic efficiency of 84 percent, for an overall energy efficiency of 60 percent.

7. Maintenance Requirements

Pump and valve maintenance will be required, but the frequency has not yet been determined. Westinghouse estimates the annual maintenance cost of the zinc-chlorine battery to be $0.73/kWh (14).

8. Voltage/Current Characteristics

Open circuit: 2.11 volts/cell

Charge cut-off: 2.28 volts/cell

Discharge cut-off: 1.92 volts/cell

Figure II-15 shows voltage as a function of current density. The discharge voltage curve is very constant over time.

9. Charging Characteristics

The zinc-chlorine battery should be charged at constant current to full capacity. Maximum recommended charging current density is 33 mA/cm^2. Minimum charging time is 3

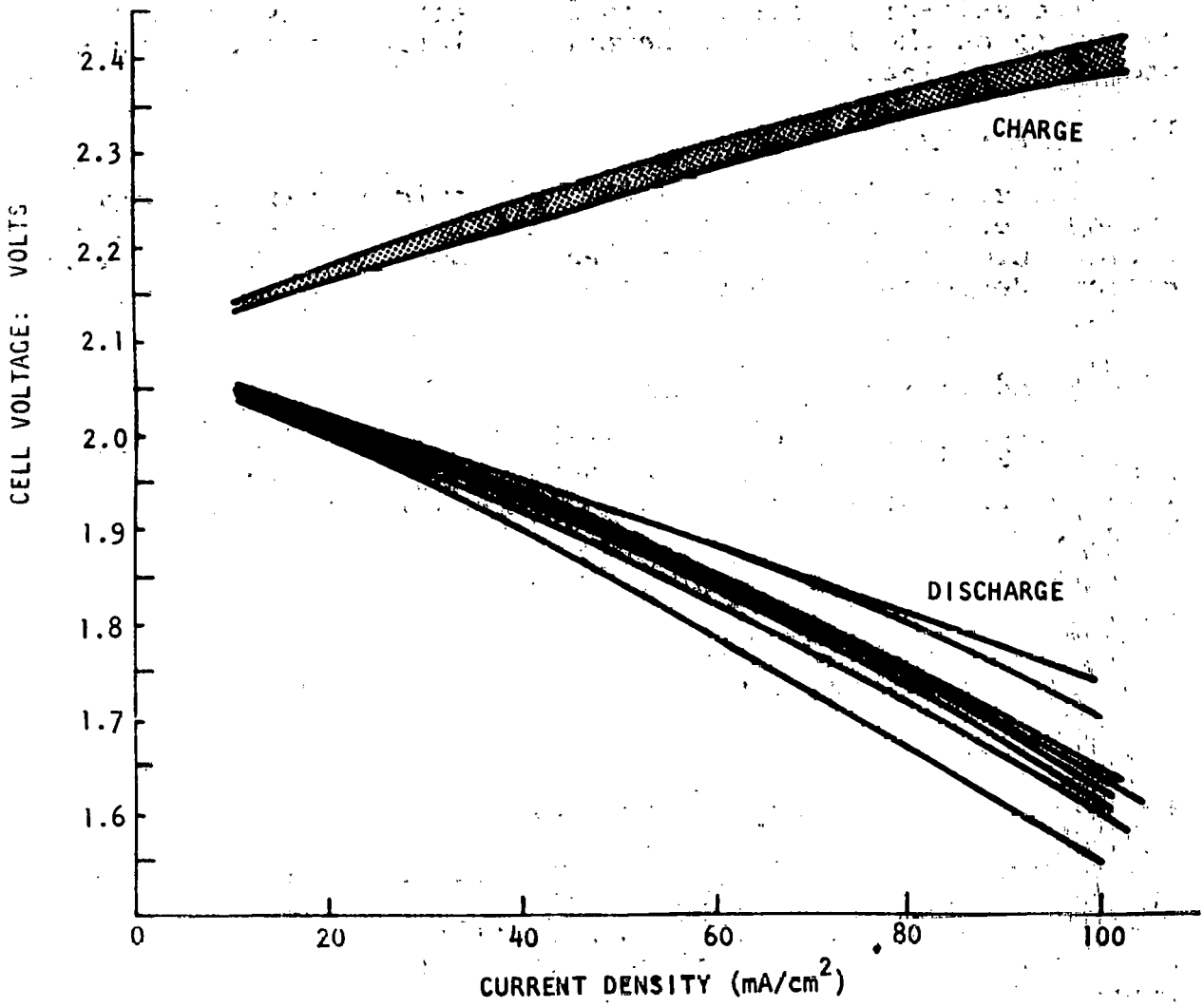

Figure II-15. Typical Cell Current/Voltage Profiles of a Zinc-Chlorine Battery (13)

hours. The battery must periodically be fully discharged to completely strip the zinc from the substrate. The frequency has not yet been determined, but may be as often as every cycle.

10. Self-Discharge Rate

The self-discharge rate is 5 percent per day or less, depending on the level of thermal insulation on the hydrate storage container.

11. Temperature

The zinc-chlorine battery has a maximum operating temperature of 60°C during discharge. Charging requires that the stored chlorine hydrate be cooled to about 5°C. The chlorine hydrate decomposes at 9.6°C (15).

12. Energy and Power Density

Energy density is approximately 70 Wh/kg at a current density of 40 mA/cm^2 (13). A sustained power density of 30 W/kg has been achieved (13). A peak power density of 100 W/kg is possible (7).

13. Scarce Materials

The zinc-chlorine battery uses no scarce materials.

14. Environmental, Health, and Safety

Approximately 5 liters of free chlorine gas are present in the gas space of a 50 kWh battery. The chlorine gas is maintained at a pressure of -5 psi (below atmospheric). This gas presents only a minimal danger in the event of battery rupture.

The worst possible accident with the zinc-chlorine battery would be chlorine gas leakage from the chlorine hydrate storage vessel. The battery contains approximately 0.7 kg of chlorine hydrate per kWh of capacity when fully charged. A large quantity of chlorine gas could be released only if the containment vessel ruptured and the refrigeration system failed simultaneously. The rate of chlorine release would then depend on the ambient temperature (higher temperatures cause faster chlorine evolution). Only 1 ppm of chlorine in the atmosphere is needed to reach a toxic level.

Another toxic substance contained in the electrolyte of the zinc-chlorine battery is thallium chloride; however, only about 2 g are used per kWh of capacity.

15. Availability

A 4.8 MWh load-leveling plant is scheduled to be evaluated at the Battery Energy System Test (BEST) facility operated by Public Service Electric and Gas Company (New Jersey) in June 1981. A 50 kWh electric vehicle battery is scheduled for demonstration in an electric van in the spring of 1980. Pilot plant-manufactured commercial batteries are projected to be available in 1982.

Full-scale commercial availability of stationary zinc-chlorine batteries is projected for June 1984.

16. Development Cost

The development cost for the next five years is estimated at $35 million.

I. Zinc-Bromine Battery

1. General Description

The zinc-bromine battery is similar to the zinc-chlorine battery in that it uses a circulating aqueous electrolyte and stores the halogen (in this case bromine instead of chlorine) external to the cell stack. An important difference is that the zinc-bromine battery stores the bromine in a "polybromide" phase by using an organic complexing agent. Figure II-16 depicts the operation of this battery.

The zinc-bromine battery contains two distinct electrolyte circulation paths separated by a micro-porous membrane. During charging, metallic zinc is electroplated onto the negative electrode and bromine gas is liberated from the zinc bromide electrolyte. The bromine remains dissolved in the electrolyte and is circulated through the storage vessel where it is removed by the organic complexing agent.

During discharge, zinc is oxidized, going from the metallic to ionic phase, and bromine gas from the storage vessels circulates via the electrolyte to react in the cell stack with the zinc.

The zinc-bromine battery is under development by Gould Laboratories (for load-leveling application), Exxon Research and Engineering Company (for electric vehicles and load leveling) and by Eco, Inc. (a noncirculating battery for portable tools). The largest zinc-bromine battery built to date is 8 kWh.

Two chemical reactions are reported for the zinc-bromine battery:

(Exxon) Zn (solid) + Br_2(gas) $\underset{\text{charge}}{\overset{\text{discharge}}{\rightleftharpoons}}$ $ZnBr_2$ (aqueous)

E_o = 1.85 volts

(Gould) and $Zn_{(s)} + Br_3^-(aq) \underset{\text{charge}}{\overset{\text{discharge}}{\rightleftharpoons}} Zn^{++}(a) + 3Br^-(aq)$

The formulas differ because Gould and Exxon use different bromine storage agents.

Both electrodes are made of carbon-felt. The negative is designed for planar flow (e.g., flow of electrolyte parallel to the surface). The positive electrode is porous and designed to allow the electrolyte to circulate through it. The advantages of the zinc-bromine battery are:

(a) A flat voltage profile

(b) Chemically inert electrodes

(c) Circulation of the electrolyte simplifies control of electrolyte temperature and composition

(d) All the materials are readily available.

2. Production Cost

Projected mass production-scale costs range from $45/kWh to $70/kWh (Exxon). Gould estimates $50/kWh.

3. Life

Gould reports that a 64 Wh two-cell battery has been cycled over 600 times (5-hour rate, deep discharge), and that a 3.2 Wh experimental cell has been cycled 1,900 times (16). Cells have been tested for over 10,000 hours without failure.

Exxon reports 250 cycles on 0.25 kWh cells.

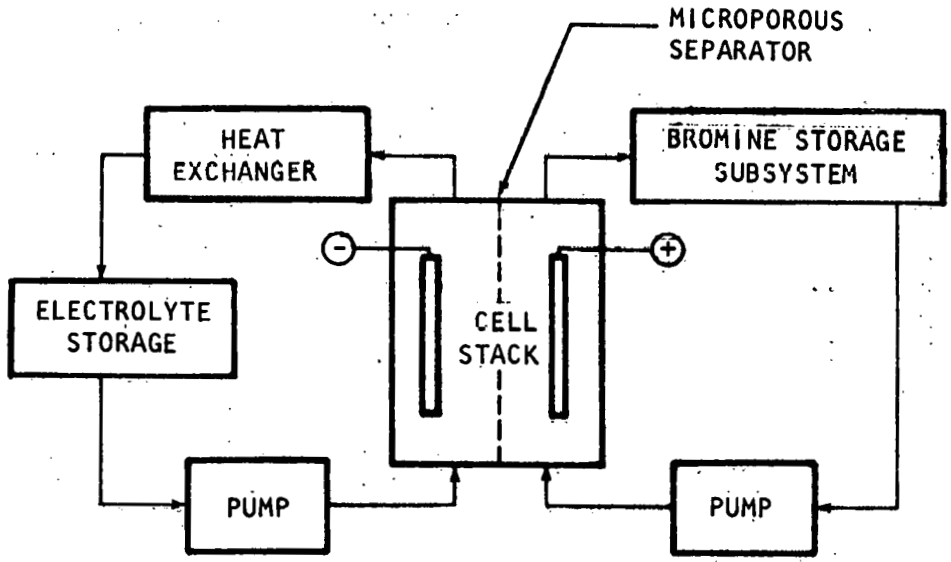

Figure II-16. Schematic of the Zinc-Bromine Battery (16)

4. Failure Mechanisms

Failure modes for the zinc-bromine battery are:

(a) Internal shorting due to formation of dendrites at the zinc electrode

(b) Pump failure

(c) Plastic creep or elongation (long-term materials stability has not yet been determined)

(d) Electrode corrosion in the noncirculating electrolyte battery (Eco, Inc.).

5. Reliability

Reliability is limited by the two electrolyte pumps and the seals.

6. Energy Efficiency

An energy efficiency of approximately 70 percent is projected. Tests of the Gould 1.28 kWh battery indicate efficiencies of 40 to 50 percent due to lower than expected voltaic efficiencies (16). Exxon has reported a coulombic efficiency of 85 percent and a voltaic efficiency of 83 percent for an energy efficiency of 71 percent on 500 Wh batteries.

7. Maintenance Requirement

Exxon's zinc-bromine battery must be completely discharged every 50 to 100 cycles. The Gould load-leveling battery is expected to require complete discharging at least once every five cycles. In addition, periodic maintenance on pumps is required. No maintenance cost estimates are available.

8. Voltage/Current Characteristics

Open circuit voltage: 1.75 to 1.78 volts/cell

Charge cut-off: 1.95 to 2.0 volts/cell

Discharge cut-off: 1.0 to 1.3 volts/cell

Figure II-17 shows discharge voltage as a function of current density. Figure II-18 shows the voltage profile for a 5-hour charge, 5-hour discharge cycle at current density of 20 mA/cm^2.

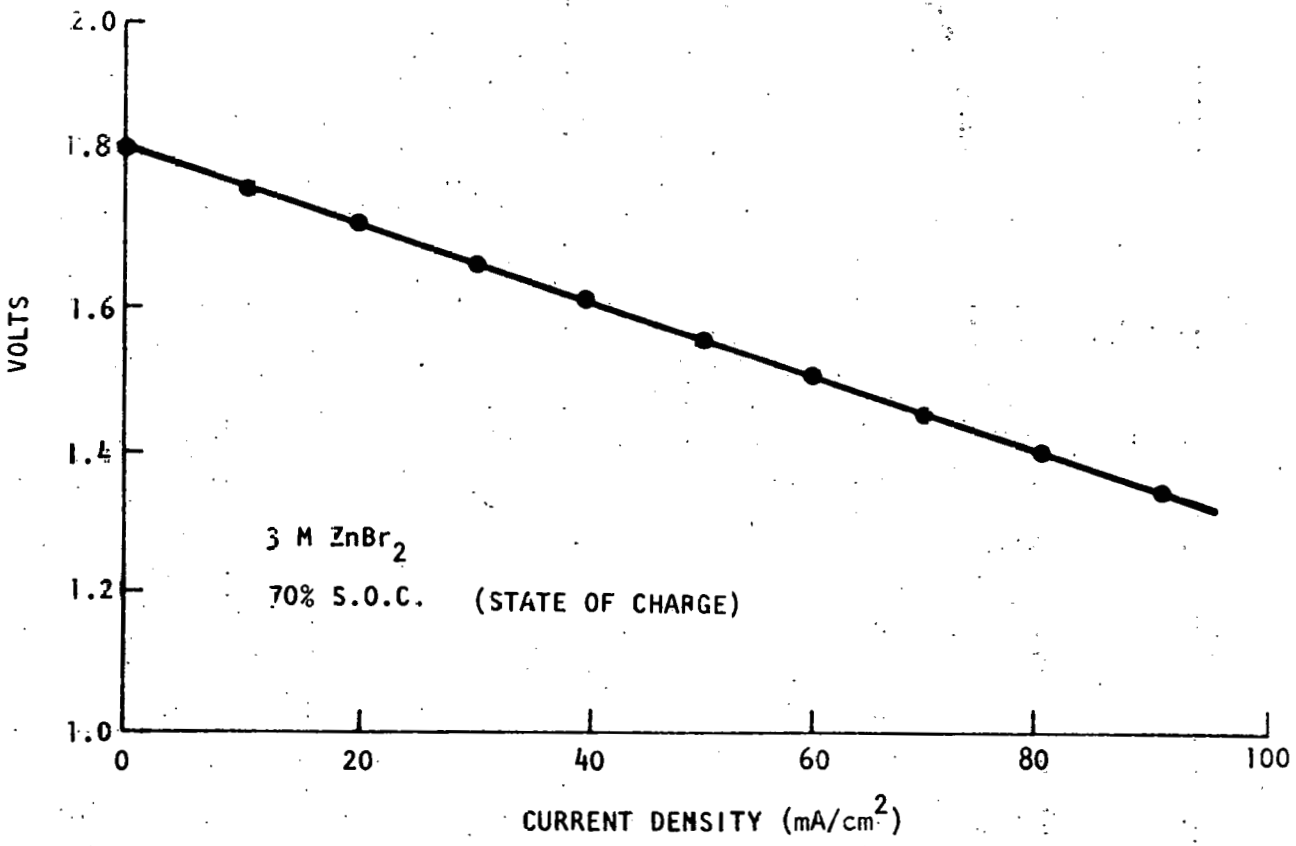

Figure II-17. Voltage Vs. Current Density for the Zinc-Bromine Battery (46)

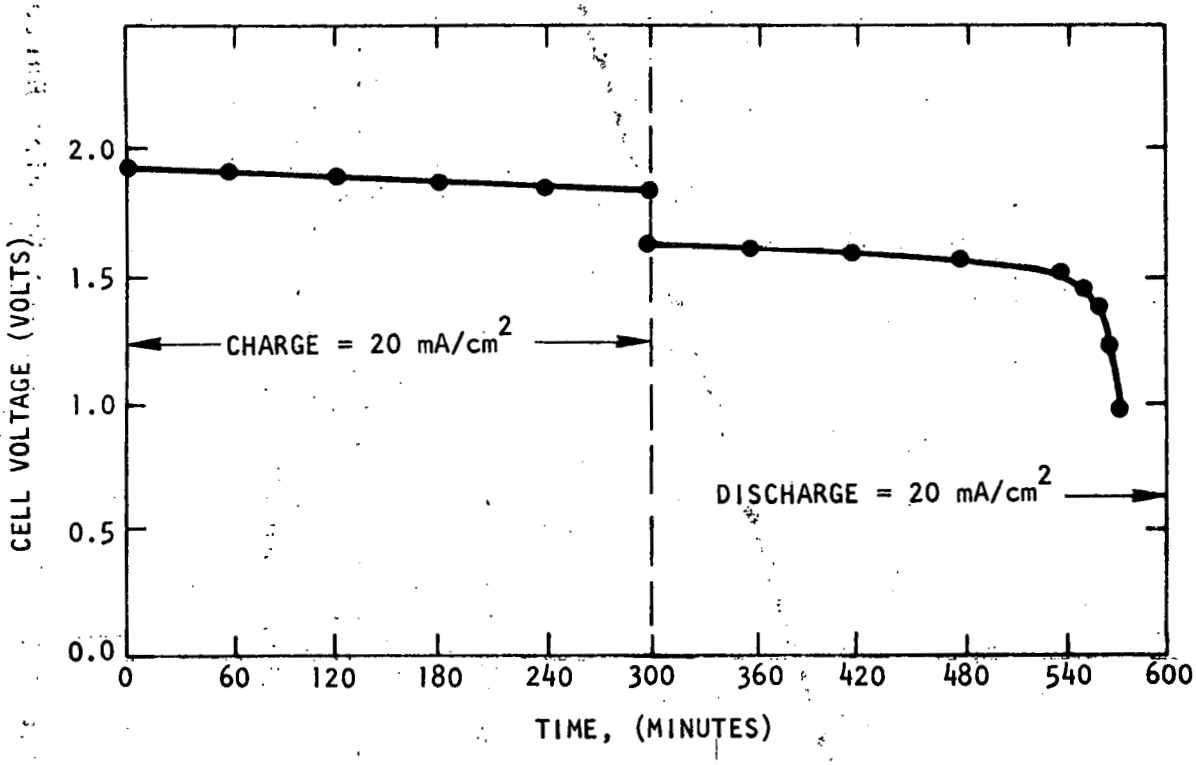

Figure II-18. Voltage During Charge and Discharge for the Zinc-Bromine Battery (46)

9. Charging Characteristics

Exxon recommends charging at constant current until the voltage equals 2 volts. The shortest charging time for a 20 kWh battery is 1 hour. Maximum recommended charging current density is 60 mA/cm^2.

The Gould battery is designed for a 5-hour charging time.

10. Self-Discharge Rate

Gould reports less than 1 percent per day.

Exxon reports less than 0.1 percent per day.

Eco reports approximately 30 percent per day.

11. Temperature

20 to 60°C.
50 to 60°C is optimal.

12. Energy and Power Density

Gould reports an energy density of 40 Wh/kg for discharge rates of C/3 and slower. Exxon reports an energy density of 65 to 80 Wh/kg at the C/3 discharge rate, and 75 to 85 Wh/kg at the C/10 rate. Eco reports an energy density of 66 Wh/kg at the C/3 rate.

The Gould battery has a power density of 25 W/kg, both at full charge and 80 percent discharge. The Exxon battery has a power density of 80 to 90 W/kg at full charge and 70 to 80 W/kg at 80 percent discharge. Eco claims 66 W/kg at full charge and 60 W/kg at 80 percent discharge.

13. Scarce Materials

The Gould battery uses approximately 0.3 grams of ruthenium per kWh of battery capacity as an electrode catalyst.

14. Environmental, Health, and Safety

Bromine gas is toxic in the free state. The zinc-bromine battery uses approximately 2 kg of Br_2 per kWh of capacity;

however, most of the bromine is stored in the polybromide phase, where it is relatively innocuous. Moreover, the volatility at room temperature is relatively low.

15. Availability

The Gould and Exxon batteries are expected to be commercially available between 1988 and 1990.

16. Development Cost

Development cost for the zinc-bromine battery is estimated to be $50 million over the next eight years (7).

J. Hydrogen-Chlorine Battery

1. General Description

The hydrogen-chlorine battery is a continuous feed flow battery which, in its discharge mode, is similar to the fuel cell. Hydrogen and chlorine gases, each stored externally, are fed to the cell stack, where they react to form hydrogen chloride gas.

The reaction is:

$$H_2(g) + Cl_2(g) \underset{\text{charge}}{\overset{\text{discharge}}{\rightleftharpoons}} 2\ HCl\ (aq)$$

$$E_o = 1.33 \text{ volts/cell}$$

The hydrogen chloride is circulated as an aqueous solution which also carries unreacted chlorine gas. The cell stack consists of hydrogen electrodes which are fabricated from platinum catalyzed graphite, chlorine electrodes composed of nitric acid treated graphite, and membrane separators. NAFION, a commercially available ion exchange membrane, is used. Figure II-19 illustrates the H_2-Cl_2 operation.

Brookhaven National Laboratory is the principal organization involved in hydrogen-chlorine battery research and development. Supporting work is being performed by Gould, Inc., General Electric Corporation, Energy Development Associates, and Bechtel Corporation.

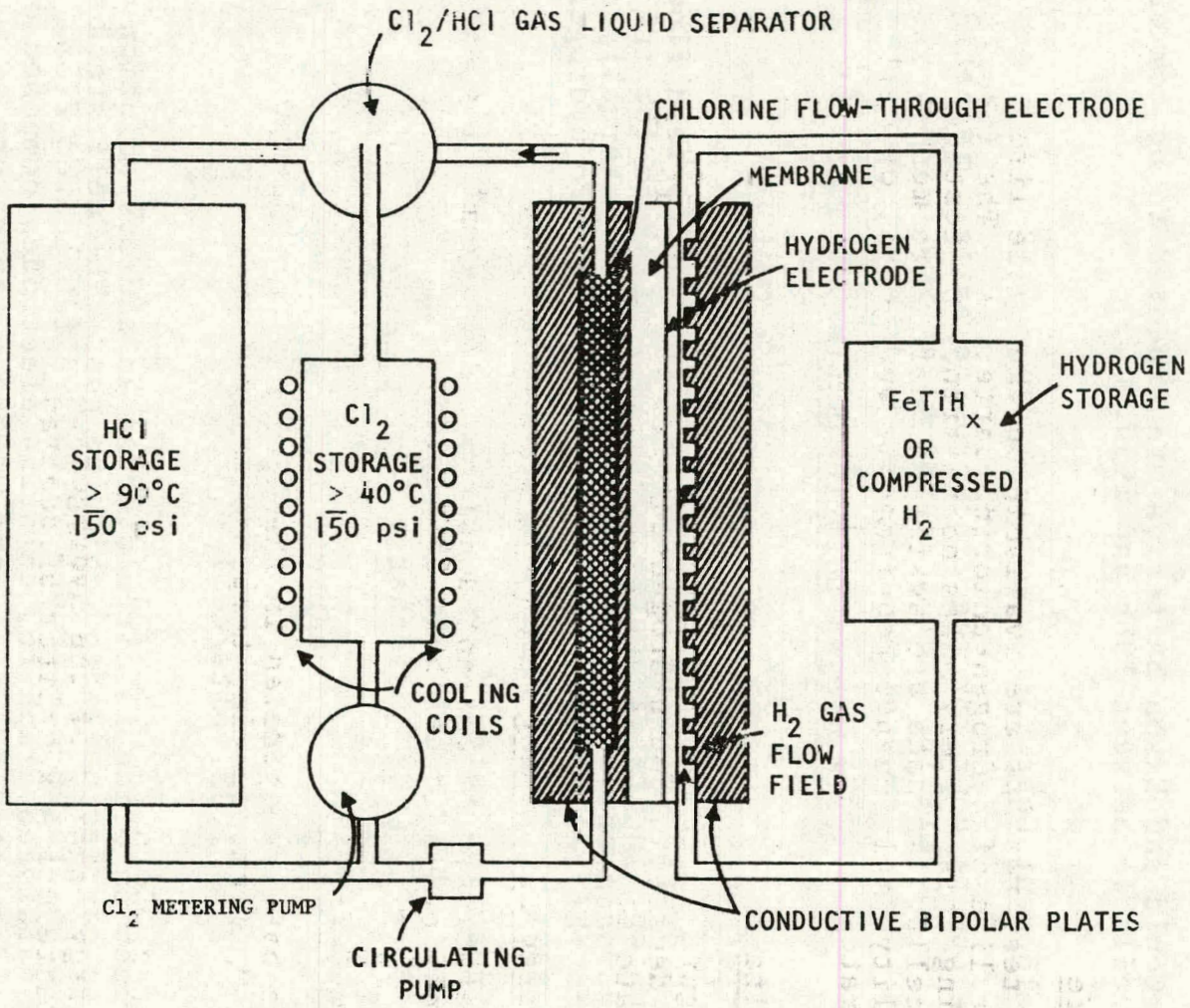

Figure II-19. Hydrogen-Chlorine Energy Storage System (BNL) (41)

2. Production Cost

Based on a conceptual design study for a 20 MW load-leveling plant, the capital cost of a hydrogen-chlorine battery would range from $41 to $60/kWh. The lower value is for a 10-hour storage cycle; the higher is for a 5-hour cycle.

3. Life

No test results are available on the cycle life or calendar life of hydrogen-chlorine batteries. The literature describing this battery makes no reference to testing of actual cells. No data are available on failure mechanisms, reliability, maintenance requirements and costs, or self-discharge rates.

4. Voltage

Figure II-20 shows the variation of cell voltage with current density. The hydrogen-chlorine battery is expected to operate at a current density of 270 mA/cm^2.

5. Energy Efficiency

Operating at a current density of 270 mA/cm^2, its energy efficiency at would be about 65 percent.

6. Temperature

The battery operates in the temperature range of 20 to 100°C. Optimum charging temperature is 35°C.

7. Energy Density

Energy density of the hydrogen-chlorine battery is approximately 1.4 kWh/liter of reactant.

8. Power Density

Power density is approximately 140 W/liter.

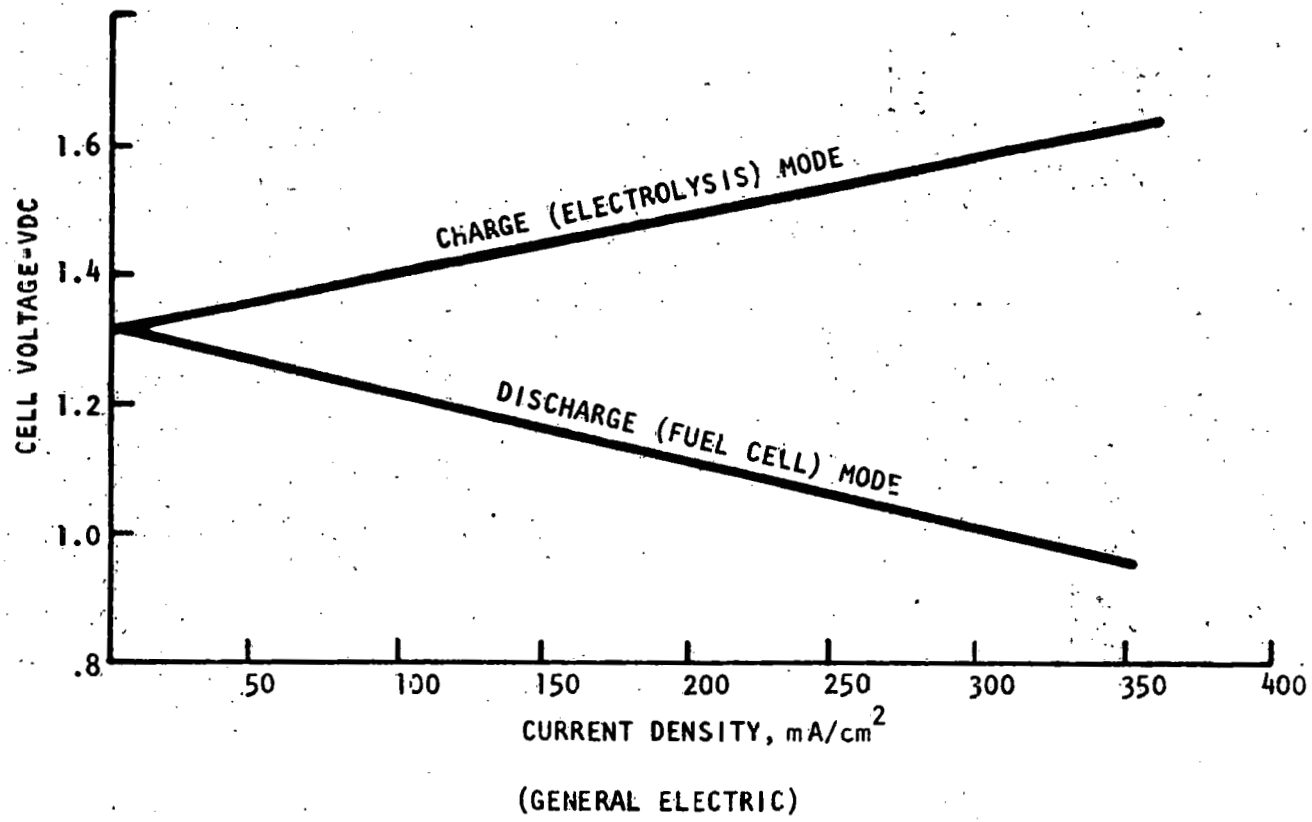

Figure II-20. Voltage vs. Current Density for the Hydrogen-Chlorine Battery (41)

9. Scarce Materials

Platinum is used as an electrode catalyst. The minimum quantity required per kW of capacity is yet to be determined.

10. Environmental, Health, and Safety

One proposed method for storing the hydrogen is as a compressed gas at 2,000 psi. Rupture of the containment vessel would pose a fire hazard. Other possible safety problems are the potential leakage of chlorine gas (also to be stored at high pressure).

11. Availability

The hydrogen-chlorine battery is in the exploratory stage and is not expected to be commercially available until sometime in the 1990s.

12. Development Cost

Approximately $800,000 was spent on this battery in each of the past two years.

K. Nickel-Hydrogen Battery

1. General Description

The nickel-hydrogen battery was originally developed for military and commercial satellite applications. Its advantages are high reliability, long cycle life, and built-in overcharge protection. The nickel-hydrogen cell consists of a cell stack contained within a sealed pressure vessel. The cell stack is made up of a series of positive electrodes (electrochemically impregnated nickel hydroxide) and negative electrodes (Teflon-bonded platinum supported within a fine mesh nickel screen). Between each negative and positive electrode is an electrolyte-impregnated separator, made of asbestos or polypropylene. Potassium hydroxide is used as the electrolyte. During charging, hydrogen gas is evolved at the negative electrode. The hydrogen is contained within the space of the pressure vessel surrounding the cell stack. When completely charged, the hydrogen pressure is about 500 psi. On discharge, hydrogen is recombined with the nickel oxyhydroxide to form nickel hydroxide.

The electrochemical reactions for the nickel hydrogen battery are:

$$NiO(OH) + \frac{1}{2} H_2 \underset{\text{charge}}{\overset{\text{discharge}}{\rightleftharpoons}} Ni(OH)_2$$

$$E_o = 1.45 \text{ volts}$$

When overcharged, oxygen is evolved, but it immediately combines with hydrogen gas at the negative electrodes to form water.

Development of nickel-hydrogen batteries for military applications is being conducted by the Aeropropulsion Laboratory at Wright-Patterson Air Force Base in Cleveland and by the U.S. Army Electronics Command at Fort Monmouth, New Jersey. COMSAT Laboratories and Eagle-Picher Industries are working on nickel-hydrogen batteries for satellite applications. The Navigation Technology Satellite 2, launched in late 1976, contained a 640 Wh nickel-hydrogen battery consisting of 14 cells. The Union Carbide Battery Products Division and Yardney Electric Company are both working on a small nickel-hydrogen battery for the consumer market.

2. Production Cost and Selling Price

Eagle-Picher Industries is now manufacturing nickel-hydrogen batteries on a custom-ordered basis, primarily for satellite power systems. Eagle-Picher estimates that a nickel-hydrogen battery can be mass produced for terrestrial applications for $150 to $300 per kWh. Hittman Associates has independently estimated the projected selling price for nickel-hydrogen batteries at between $180 and $250/kWh.

3. Life

Cycle testing on 50 Ah nickel-hydrogen cells has shown that these cells have cycle lives of more than 2,000 cycles. Some cells have undergone more than 2800 cycles without severe degradation of performance (18). The only effect prior to failure has been a gradual voltage reduction (19). Eagle-Picher has been able to obtain 10,000 cycles at 80 percent depth of discharge.

4. Failure Mechanism

The primary failure mechanism observed is a drying of the separator caused by absorption of electrolyte by the nickel hydroxide electrode. This effect is due to the cyclic expanding and contracting of the nickel electrode.

This problem can be minimized by constructing a nickel electrode with a lower level of $Ni(OH)_2$ loading, so that more electrolyte is initially present in the electrode pores (19).

5. Reliability

The fact that nickel-hydrogen batteries are now being used for satellite missions of several years attests to the high reliability of this battery.

6. Self-Discharge

The nickel-hydrogen battery loses approximately 20 percent of capacity in the first 24 hours. After 72 hours it has been observed to lose 40 percent of capacity (20, 18).

7. Operating Temperatures

The optimal temperature range is 0 to 10°C. The battery can be operated up to 25°C. Higher temperatures diminish battery capacity and efficiency.

8. Energy and Power Density

The energy density of the nickel-hydrogen battery is 66 Wh/kg at discharge rates of C/5 and lower (20). At the C/2 rate it is 45 Wh/kg (19). At the 5C rate, energy density falls off to around 38 Wh/kg. A power density of 300 W/kg has been measured (20).

9. Energy Efficiency

The energy efficiency declines with increasing temperature. Below 20°C, efficiency is between 60 and 66 percent. At 30°C, energy efficiency is approximately 30 percent (18).

10. Maintenance

No manual maintenance is required.

11. Voltage/Current Characteristics

See Figures II-21 and II-22.

12. Charging Characteristics

The nickel-hydrogen battery can be charged at very high rates of up to 5C. Pressure, voltage, and temperature are all good indicators of the battery's state of charge. The preferred method for terminating battery charging is to use pressure as the indicator.

13. Scarce Materials

Currently available nickel-hydrogen batteries require 0.37 kg of platinum per kWh of capacity. Research is underway to substitute palladium for the platinum. Approximately 4 g of palladium would be needed per kWh of capacity. The nickel-hydrogen battery also uses 2.9 kg of nickel hydroxide per kWh of battery capacity.

14. Environmental, Health, and Safety

When completely charged, hydrogen pressure in the sealed vessel is about 500 psi.

15. Availability

The nickel-hydrogen battery is currently available on a custom-order basis.

L. Zinc-Ferricyanide Hybrid Redox Battery

1. General Description

The zinc-ferricyanide battery, a type of Redox flow cell under development by the Lockheed Missile and Space Company, uses the following two half-cell reactions:

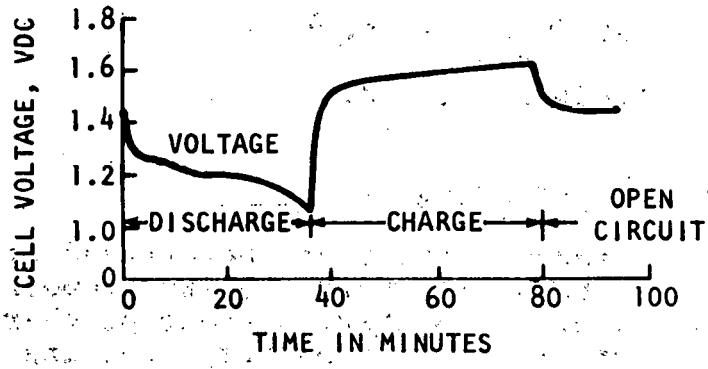

Figure II-21. Voltage During Charging and Discharging - 50 Ah Nickel-Hydrogen Cell (20)

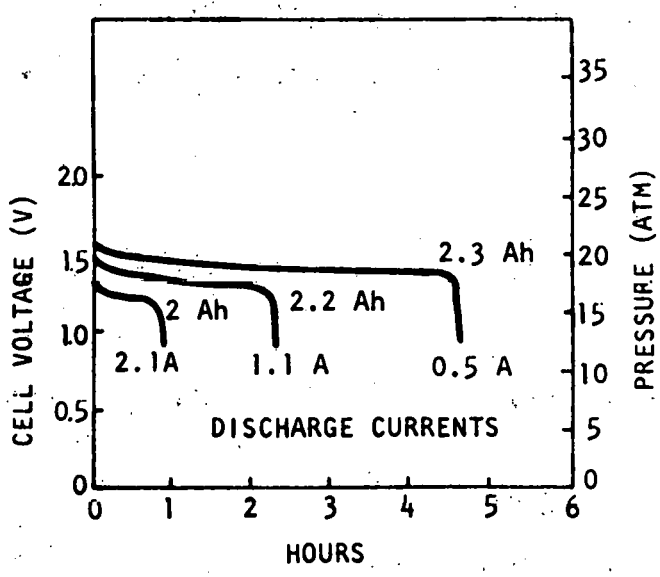

Figure II-22. Discharge of D Size Nickel-Hydrogen Cell at Different Loads (2.5 Ah Capacity)(20)

$$ZnO_2^{-2} + 2H_2O + 2e^- \underset{\text{discharge}}{\overset{\text{charge}}{\rightleftharpoons}} Zn + 4OH^-$$

$$Fe(CN)_6^{-3} + e^- \underset{\text{discharge}}{\overset{\text{charge}}{\rightleftharpoons}} Fe(CN)_6^{-4}$$

Open circuit voltage is 1.86 volts. This battery uses potassium hydroxide or sodium hydroxide as an electrolyte. It is still in the exploratory stage. Operational data are based on testing of a 3.6 watt cell.

2. Capital Cost

Based on the conceptual design of a 10 MW-8.5 hour load-leveling battery, capital costs of $230/kW and $32/kWh are projected.

3. Life

The 3.6 W cell has been cycled 650 times. No data are available on failure mechanisms, reliability, maintenance requirements, self-discharge rate, or environmental effects.

4. Energy Efficiency

An efficiency of 70 percent is projected for full-size batteries. Energy efficiencies of 90 percent have been observed in the 3.6 W cell.

5. Voltage/Current Characteristics

See Figures II-23 and II-24.

6. Operating Temperature

The zinc-ferricyanide battery operates in the temperature range of 25 to 50°C.

7. Energy and Power Density

Nominal energy density is 15.3 Wh/kg. Power density is 0.19 W per cm^2 of cell area.

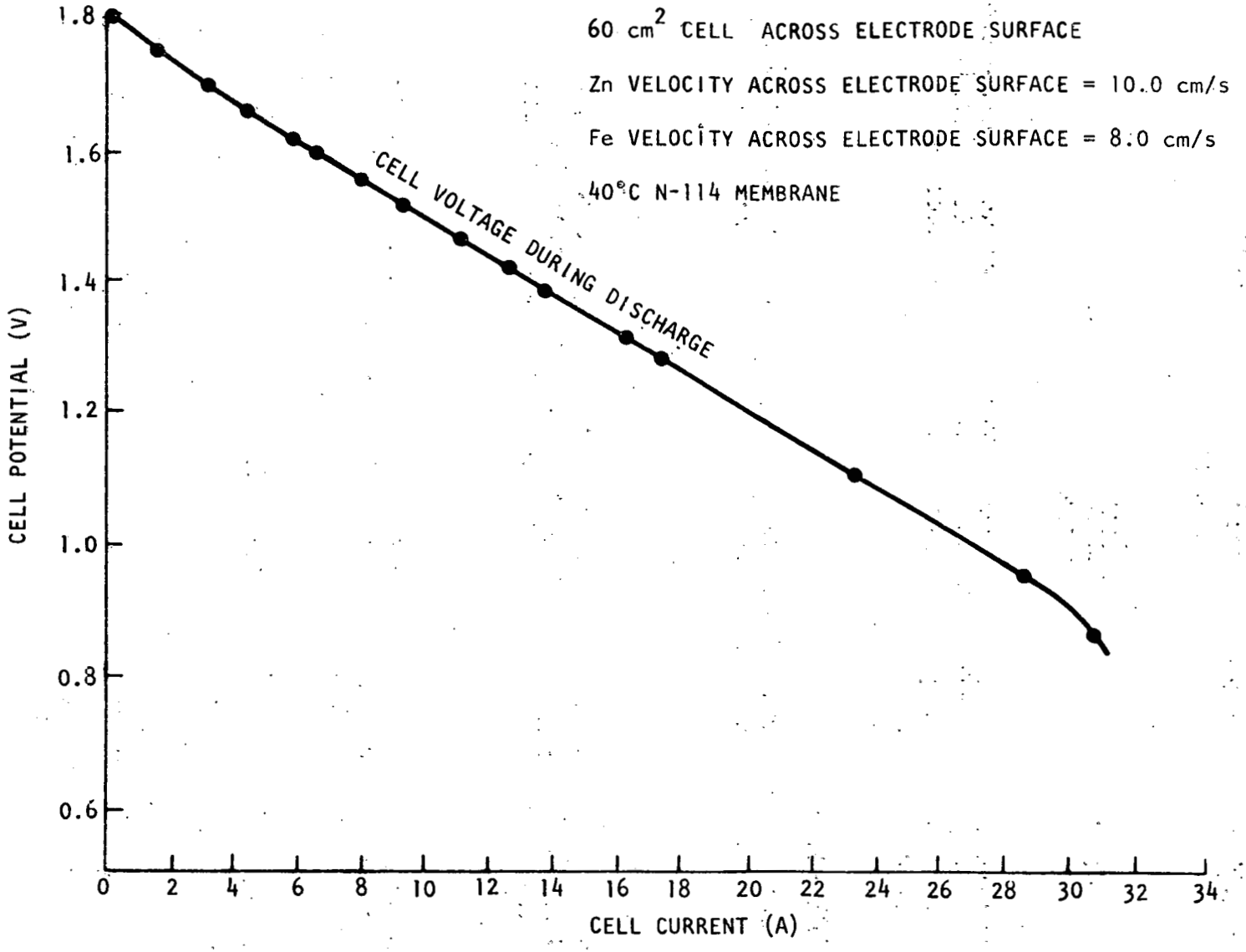

Figure II-23. Zinc-Ferricyanide Hybrid Redox Battery Voltage (44)

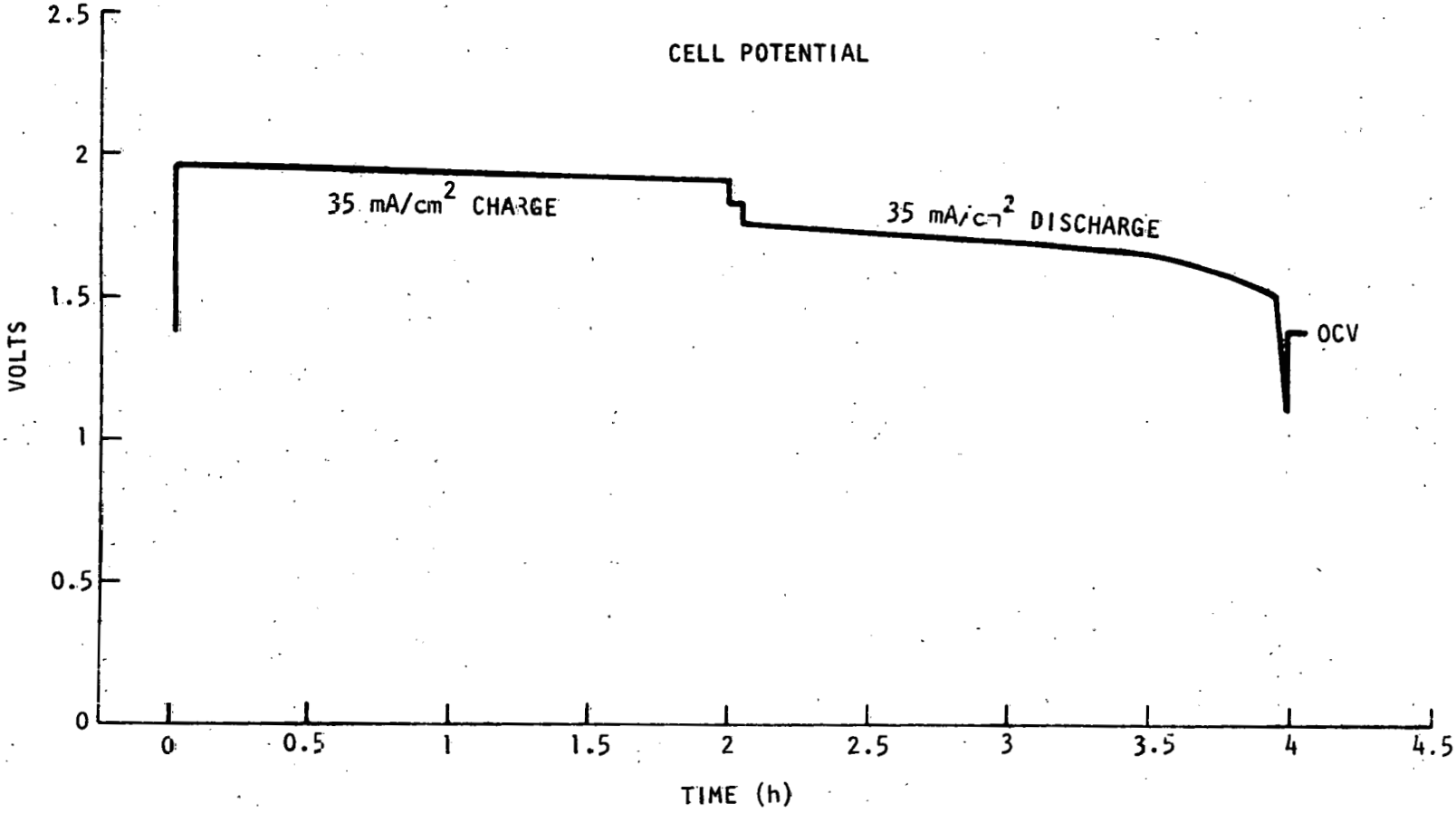

Figure II-24. Cell Voltage During Charging and Discharging for Zinc-Ferricyanide Hybrid Redox Battery (44)

8. R&D Schedule

An 85 W multicell battery is scheduled to be built in 1980, and a 600 W, 10-cell battery is scheduled for testing in 1984. Further development would depend on the evaluation of these small-scale test batteries.

M. Lithium-Metal Sulfide Battery

1. General Description

The lithium-metal sulfide cell employs solid electrodes and a molten salt electrolyte. The negative electrode is composed of a lithium alloy containing either aluminum or silicon, in the form of a porous matrix. The positive electrode is a metal sulfide, also in the form of a porous matrix. The predominant metal used is iron, either as FeS or FeS_2. Nickel has been tested as a substitute for iron, but its higher costs outweigh the marginal performance improvements achieved. Titanium is being tested as an additive to the FeS_2 anode because of its role in decreasing the ohmic resistance of the electrode. Early tests using titanium as a replacement for iron ended with many mechanical problems leading to short circuiting during the first few cycles of operation. The electrolyte employs a mixture of LiCl and KCl eutectic salts with a melting point of about 352°C. A non-eutectic electrolyte enriched in LiCl has been developed which allows battery operation at temperatures near 500°C and increases active material utilization of the positive plate by about 40 percent at the four-hour rate. This is achieved by eliminating the formation of a solid phase ($LiK_6Fe_{24}S_{26}Cl$) caused by interaction between the FeS electrode and potassium in the eutectic electrolyte (21). The basic cell reaction for the lithium-metal sulfide battery system is:

$$2\ Li + MS_n \rightleftharpoons Li_2S + MS_{n-1}$$

M represents the metal component, which is usually iron

n can equal either 1 or 2

Table II-2 shows the cell reactions and open-circuit voltages for the lithium-metal sulfide systems currently under development.

TABLE II-2. CELL REACTIONS AND OPEN-CIRCUIT VOLTAGES

Battery Type	Cell Reaction	OC Voltage
LiAl-FeS	$2LiAl + FeS \rightleftarrows Li_2S + Fe + 2Al$	1.33
LiAl-FeS_2	$4LiAl + FeS_2 \rightleftarrows 2Li_2S + Fe + 4Al$	1.76, 1.33
LiSi-FeS	$Li_4Si + 2FeS \rightleftarrows 2Li_2S + 2Fe + Si$	1.65
LiSi-FeS_2	$Li_4Si + FeS_2 \rightleftarrows 2Li_2S + Fe + Si$	2.05, 1.65

A LiAl-FeS cell is shown in Figure II-25 (22). The largest LiAl-FeS_x unit that has been laboratory tested to date is a 2.5 kWh cell (24). LiSi-FeS_x cells up to 1 kWh have been laboratory tested and a prototype 2.5 kWh cell was constructed in 1978. The research and development organizations and manufacturers currently working on high-temperature lithium-metal sulfide battery systems include:

Argonne National Laboratory
Atomics International Division of Rockwell International
Catalyst Research Corporation
Exide
Eagle-Picher Industries, Inc.
Electric Power Research Institute
General Motors Corporation
Gould, Inc.
P.R. Mallory & Company, Inc.
Admiralty Materials Laboratory, Dorset, England

2. Production Cost and Selling Price

The projected production costs and selling prices of the various lithium-metal sulfide battery systems are shown in Table II-3. These values are based on the assumed production volumes shown for each system.

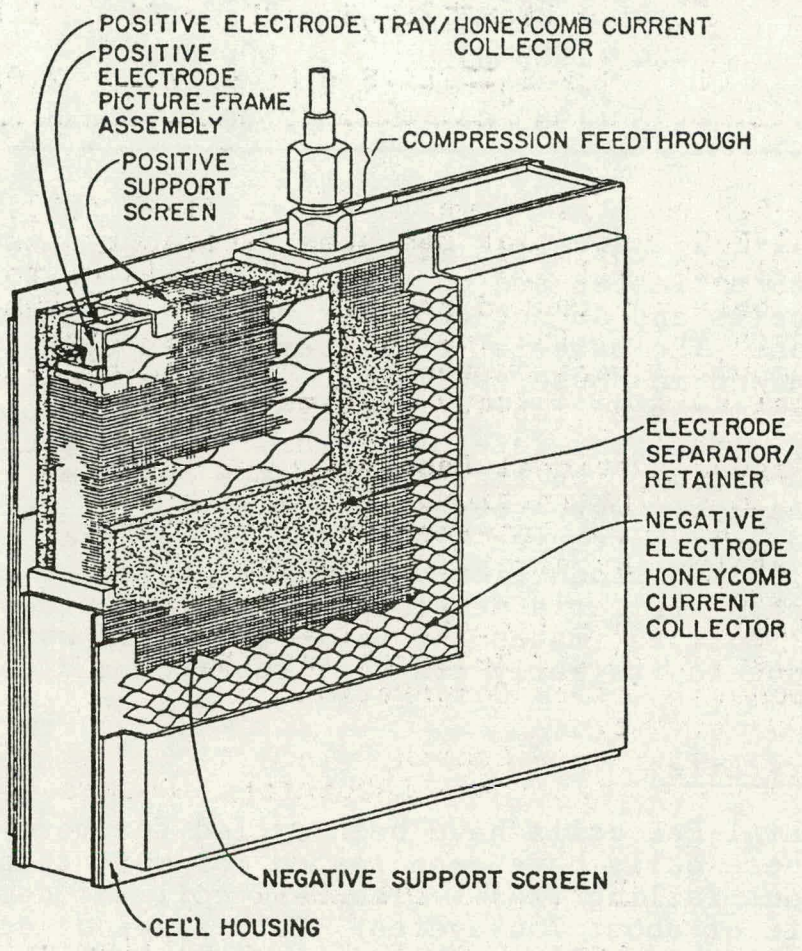

Figure II-25. LiAl-FeS Cell (22)

TABLE II-3. COST PROJECTIONS FOR LITHIUM-METAL SULFIDE CELLS

Battery Type	Cost $/kWh	Annual Production Volume	Source
LiAl/FeS	55-65 (1980 $)	10-100 MWh	(24)
LiAl/FeS_2	60-70 (1980 $)	20-300 kWh	(24)
LiSi/FeS	~34 (1980 $)	1000 MWh	(25)
	~26 (1980 $)	2500 MWh	(25)

The LiAl-FeS estimates are selling price projections. The LiSi-FeS estimates are materials and labor cost projections for cells and do not consider profit or equipment depreciation. The material costs were based upon suppliers' information and in-house estimates. Fabrication costs were based on estimates of fabrication time for each component and an industry-wide labor rate of $15/hr. Assembly costs were based on the assumption that labor rates and time requirements for assembly were roughly the same as those for automobile lead-acid batteries (25). A selling price of $34/kWh for the 2,500 MWh production volume was projected using the cost-estimating criteria developed by A.D. Little for EPRI in 1976 (25). Cost estimates for LiSi-FeS_2 cells were not available due to its early stage of research and development.

3. Battery Life

Some LiAl-FeS cells have been cycled for more than 1,000 cycles. These cells have been tested for more than 8,000 hours without failing (24). The FeS_2 cell has demonstrated a cycle life of about 750 cycles. Both types of cells experience less than a 10 percent decline in capacity (26). The charge and discharge rates used in life testing were 40A and 70A, to a 1.0 V cut-off, for the FeS cells. However; cycle life declines to several hundred cycles for bicells and multiplate cells. Life testing of LiSi-FeS cells resulted in a cycle life of several hundred cycles (25). For LiSi-FeS_2 cells, a cycle life of more than 250 deep discharge cycles has been achieved (7). The LiSi-FeS_2 cells have been tested for more than 5,000 hours.

4. Failure Mechanism

The primary mechanism of failure for all of the lithium-metal sulfide battery systems under investigation is short circuiting caused by extrusion of active material from the positive electrode. In addition, in the LiSi-FeS_x cells, silicon transfers from the alloy to the ferrous substrate at high temperatures (550°C).

5. Reliability

For all lithium-metal sulfide cells, large cells would be better for utility applications, but due to the high short-circuit failure rate (per unit of cell capacity, per cycle), very large cells would have to be replaced more frequently (27). Due to the cycle life problems associated with multicell batteries, reliability for these battery systems is low.

6. Energy Efficiency

The energy efficiency for LiAl-FeS_x batteries is 75 to 85 percent (24). The energy efficiency for the LiSi-FeS battery is 69 to 77 percent (25). The LiSi-FeS_2 battery has an energy efficiency in the range of 60 to 90 percent (7).

7. Maintenance

Maintenance requirements for all of the lithium-metal sulfide systems include checking the performance, inspecting connections, servicing the cooling air system, charging as required to provide the desired capacity on the next discharge, and replacing defective cells. The cell temperature must be monitored and means should be provided for maintaining the design operating range. The estimated annual O&M cost for LiAl-FeS and LiSi-FeS battery systems is $.73/kWh (14). This estimate is based on a 500 kWh plant size. It does not include replacement costs.

8. Voltage/Current Characteristics

Table II-4 shows the voltage characteristics of the various lithium-metal sulfide systems under investigation.

TABLE II-4. LITHIUM-METAL SULFIDE CELL VOLTAGE CHARACTERISTICS

Battery Type	Open Circuit Voltage (V)	Charge Cut-Off Voltage (V)	Discharge Cut-Off Voltage (V)	Source
LiAl-FeS	1.33	1.6	.9-1.0	24
LiAl-FeS_2	1.76, 1.33	2.2	1.0	28
LiSi-FeS^2	1.65	1.8	.9	4
LiSi-FeS_2	2.05, 1.65	2.15	1.0	4

Voltage vs. capacity curves for charging and discharging of each of the systems under consideration are shown in Figures II-26 through II-29.

9. Charging Characteristics

Although the LiAl-FeS_x cells are relatively insensitive to charging schedule changes, cells cannot tolerate any overcharge without a permanent loss of capacity (11). Differences in capacities of cells in series will therefore disrupt the charging process. The use of current bypasses for each cell is being investigated to alleviate this problem. Presently, charging uses current-limited constant potential followed by low-current equalization of each cell. Present charging times are 6 to 8 hours (24). LiSi-FeS_x cells are charged using a cell equalization system to adjust the charging current for taper charging each cell individually (24). These cells have a maximum charge rate of C/5 (4).

10. Self-Discharge Rate

LiAl-FeS_x cells have a self-discharge rate of less than 1 percent of rated capacity a day (24). LiSi-FeS_x cells have a self-discharge rate of 7 to 8 percent of capacity per day (4). Due to the thermal storage capacity of the battery insulation and housing, there is no energy input requirement to maintain the operating temperature of lithium-metal sulfide systems during day-to-day operation. For idle periods of two days or more, a resistance heating unit operates to maintain the battery above 420°C.

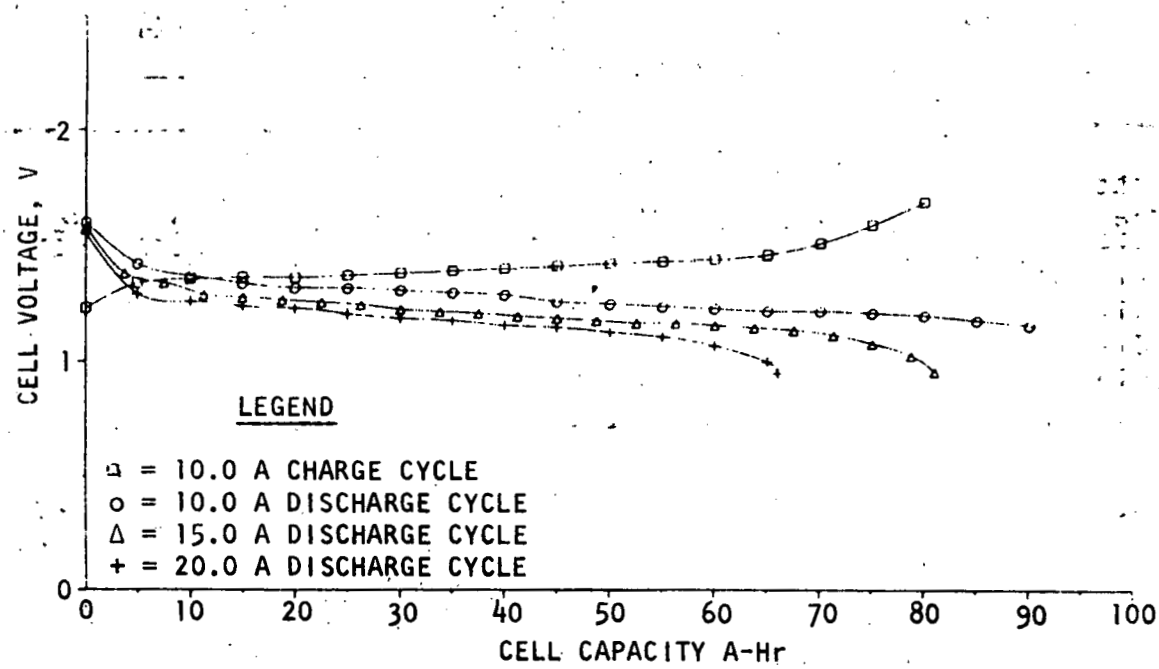

Figure II-26. Voltage vs. Capacity Curves for LiAl-FeS Cell (28)

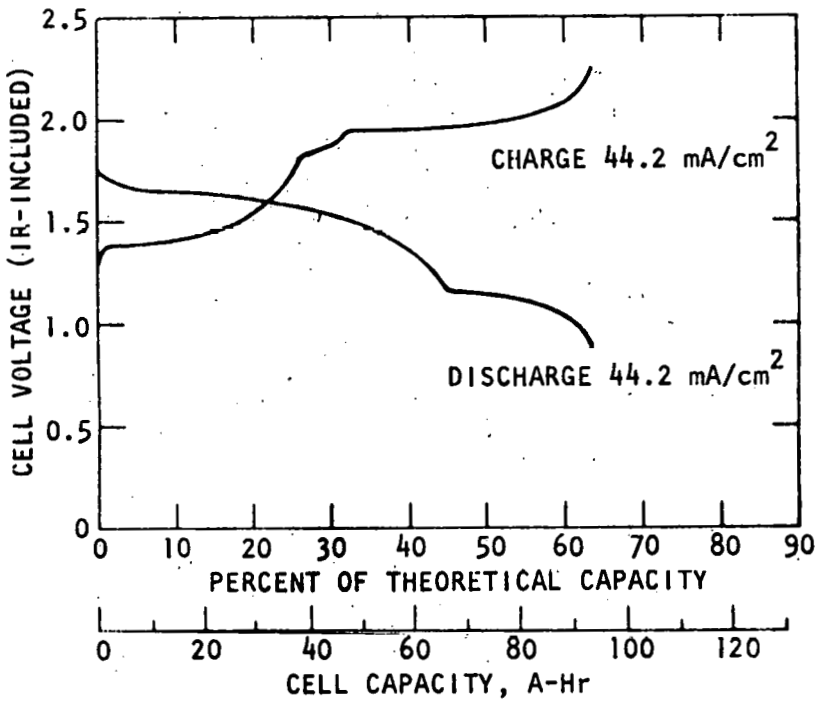

Figure II-27. Voltage vs. Capacity Curves for LiAl-FeS_2 Cell (28)

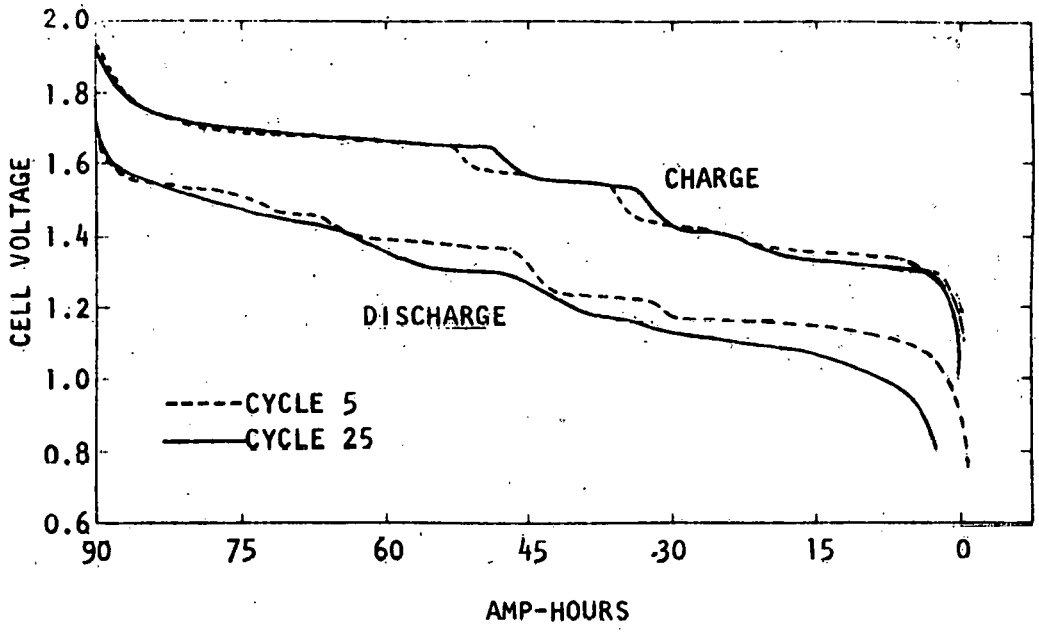

Figure II-28. Charge-Discharge Curves for the LiSi-FeS Cell at Cycle 5 and 25 (25)

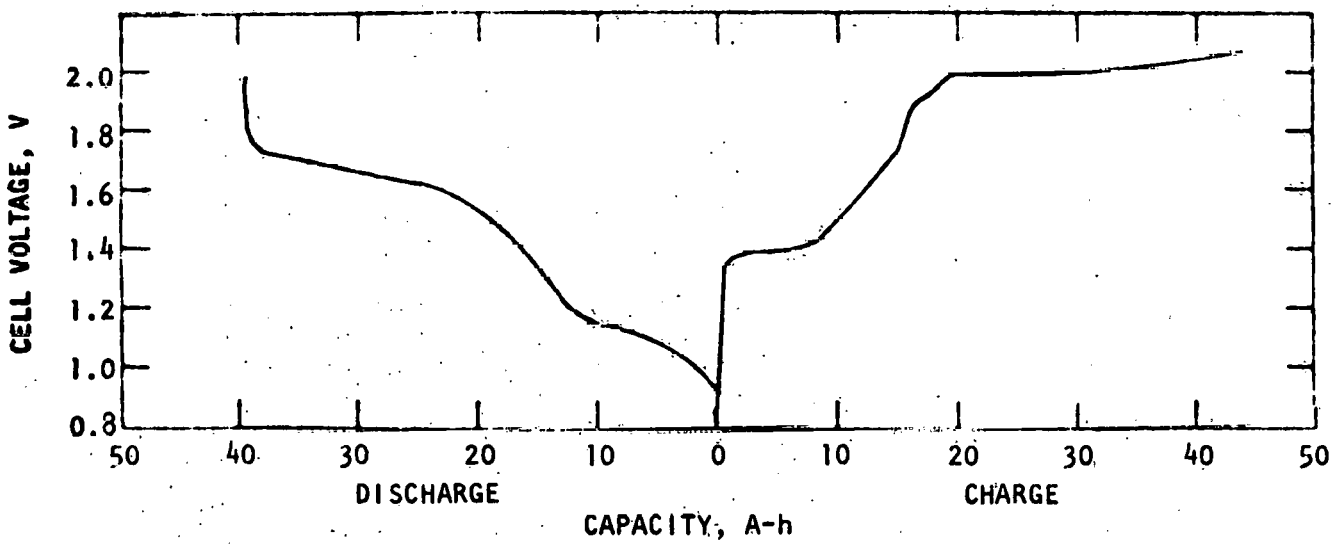

Figure II-29. Voltage vs. Capacity Curves for the LiSi-FeS_2 Cell (7)

11. Operating Temperature

The operating temperature range for LiAl-FeS_x battery systems is 425 to 500°C, and 400 to 500°C for LiSi-FeS_x systems.

12. Energy and Power Densities

Table II-5 shows the energy and power densities at various discharge rates for the various lithium-metal sulfide cells under consideration.

TABLE II-15. LITHIUM-METAL SULFIDE CELL ENERGY AND POWER DENSITIES

	Energy Density Wh/kg			Power Density W/kg		
	C/3	C/5	C/10	100% Charge	50% Charge	Source
LiAl-FeS	70	80	90	140	70	(26)
LiAl-FeS_2	80	95	100-115	180	100	(22,26)
LiSi-FeS^2		54	65-80		N/A	(25)
LiSi-FeS_2	120 at C/4				30 at C/4	(7)

NOTE: N/A = Data not available.

13. Scarce Materials

Lithium is the major scarce material used in these battery systems. About 0.45 kg of lithium are required per kWh of battery capacity. The United States consumes approximately 4,400 metric tons of lithium annually. Most is produced domestically. A recycling potential exists for lithium. The value of recovered lithium would be about $5 to $10/kWh.

14. Environmental, Health, and Safety

Lithium is a toxic substance which could be released in an accident. In addition, the high operating temperatures pose a possibility of burns and fire hazards in the event of battery housing rupture. Possible reaction products could be explosive hydrogen gas and toxic H_2S (14). Aside from thermal pollution, this system appears to have few adverse environmental effects (14).

15. Commercial Availability

The LiAl-FeS_x systems are expected to be commercially available by 1990, with a prototype in operation by 1986. A

prototype LiSi-FeS_x battery system is expected to be in operation by 1980, with commercial production in the early 1980s.

16. Research and Development Risks

Research and development risks for the lithium-metal sulfide high-temperature battery systems are projected to be high due to the existence of several significant technical problems (14). Major advances required include the development of an economically viable separator material, the development of a reliable long-life feedthrough, and improvements in the negative and positive current collectors (14). There are no available figures on the development costs associated with these technical problems. While budget estimates are only available for up to two years, the research and development program is projected to continue beyond 1986.

N. Sodium-Sulfur Battery

1. General Description

Sodium-sulfur batteries are divided into two categories according to the type of electrolyte used. The electrolyte for one of the batteries is composed of a solid β-alumina ceramic; the other battery employs a hollow glass fiber electrolyte. Both batteries use molten positive and negative electrodes. The Na-S-glass cell uses the glass tube electrolyte to separate the liquid sodium anolyte and the liquid sulfur-sodium polysulfide catholyte (29). This is shown in Figures II-30 and II-31.

The Na-S-β-alumina cell employs a similar cell configuration and uses the same anolyte and catholyte as the Na-S-glass cell, as shown in Figure II-32.

Solid electrolytes are ionic conductors which allow the sodium ions to flow between the electrodes. The basic cell reaction, similar for both cell types, is:

$$2Na + S \underset{\text{charge}}{\overset{\text{discharge}}{\rightleftharpoons}} Na_2S$$

The largest Na-S-glass unit that has been tested is a 30 kWh battery built by Dow Chemical Company. The largest Na-S-β-alumina units tested have been an 0.3 kWh cell and a 150 kWh multicell unit, both built by Chloride Silent Power, Ltd., of England. The manufacturers and organizations involved in research and development of those battery types are:

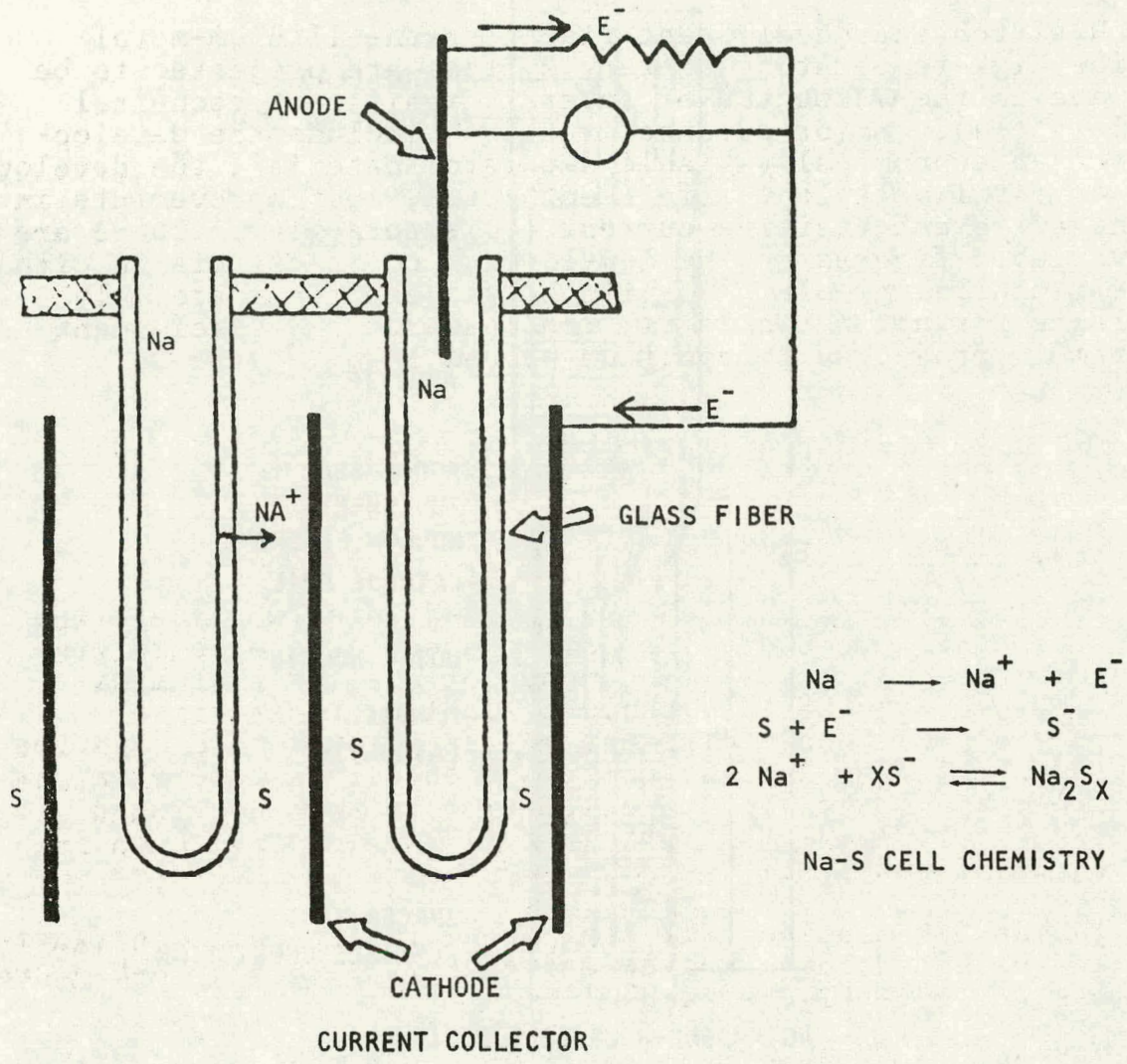

Figure II-30. Schematic Diagram of Sodium-Sulfur Glass Fiber Cell (30)

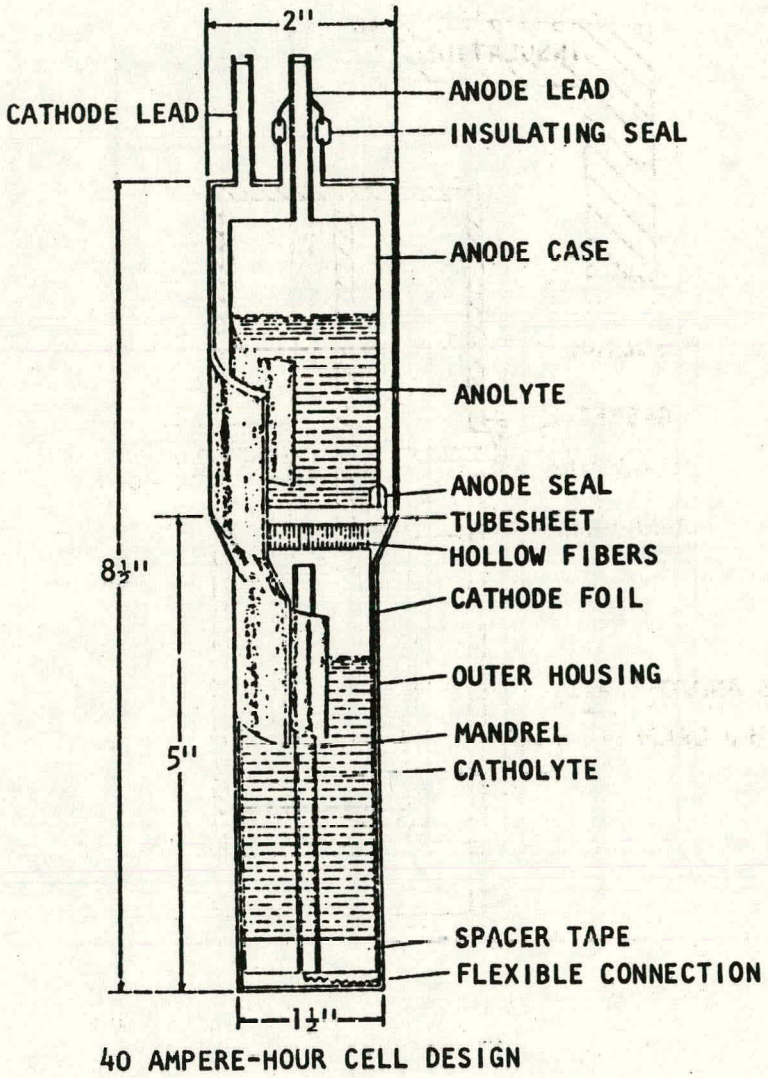

Figure II-31. Cross-Sectional View of a Sodium-Sulfur Glass Fiber Cell (30)

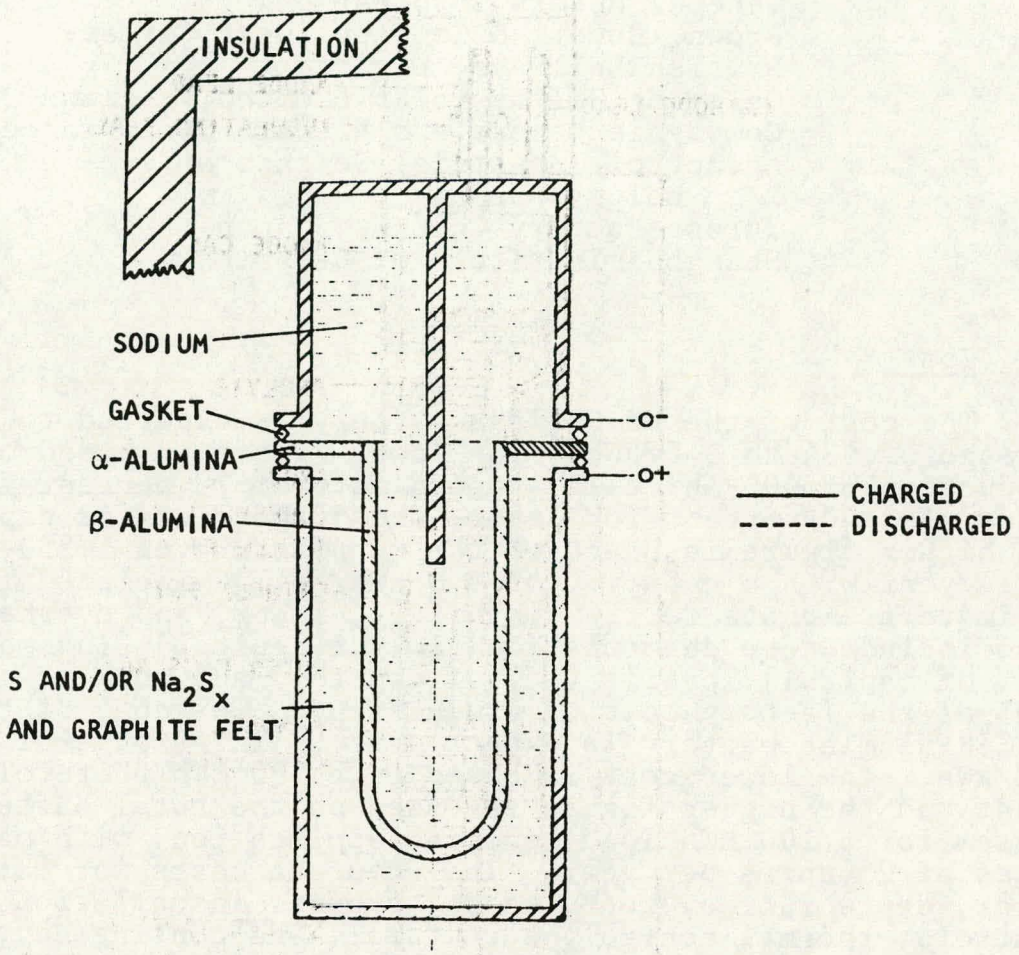

Figure II-32. Cross-Section of a Sodium-Sulfur-β-Alumina Cell (43)

Dow Chemical Company
EIC Corporation
Exide
Exxon Research & Engineering Company
Ford Aerospace & Communications Corporation
General Electric Company
General Motors Corporation
Brown, Boveri & Company, West Germany
British Railways, England
Chloride Silent Power Limited, England
Compagnie Generale d'Electricite, France
Agency of Industrial Science & Technology, Japan
Yurasa Battery Company, Japan
Shanghai Institute of Ceramics

2. Cost

The cost of the Na-S-glass battery is expected to be in a range of $34 to $46/kWh. The lower figure is based on the production of 400 Ah cells and consists of 25 percent for materials, 40 percent for labor, and 35 percent for capital. The higher figure is based on the manufacture of 1,250,000 cells/year with a capacity of 0.8 kWh/cell. Included in the estimate are costs for raw materials, labor, and overhead. Also included are depreciation (10% of capital), income tax (15% of capital), profit (15% of capital) and working capital (30% of the factory cost of production). The cost of the Na-S-β-alumina battery is expected to be in a range of $43 to $52/kWh. The lower cost is based on a 500 MWh photovoltaic plant and the higher figure is based on the total battery system for a 100 MWh load-leveling application, with manufactures of 25 units per year. Included are costs for materials, labor, depreciation, rent, taxes, profit, installation, controls, thermal control, structural, and contingency.

3. Battery Life

The battery life of Na-S-glass cells appears to be inversely related to cell size. Cells with a capacity of 0.5 Ah have life cycles of about one year at a 30 percent depth of discharge and 3,800 cycles for several months at a 90 percent depth of discharge (30). 5 Ah cells cycled to a 26 percent depth of discharge at a 13-hour discharge/8-hour charge rate had a life of over 375 cycles in 88 days (26), and cells with a capacity of 138 Ah cycled to a 10 percent decrease in capacity at a 7-hour charge/4-hour discharge rate had a life of 250 cycles (33). The Na-S-β-alumina battery cells have shown cycle lives of 1,200 to 1,500 cycles. Cells with a capacity of 16 Ah have been tested to 1,200 cycles and

10,000 hours at a 7-hour charge and 5-hour discharge rate (33). Cells with a capacity of 80 Wh have been tested to 1,500 cycles and 8,000 hours at a C/5 charge and C/2.5 discharge rate to a 100 percent depth of discharge (34); 200 Wh cells have been tested to 1,800 cycles (40).

4. Failure Mechanism

The major failure mechanism of the Na-S-glass cells is the fracture of the glass fiber electrolyte tubes, caused by either impurities in the sodium or the cooling of the electrodes. Another major problem is the penetration of high-purity sodium through the glass seal into the sulfur electrode (14). Failure mechanisms of the Na-S-β-alumina cells are fracture of the ceramic tube due to cooling of the electrodes, corrosion of the sulfur container, and penetration of the glass seal by the sodium anolyte.

5. Reliability

Problems with thermal expansion, glass seal degradation, and over-discharge mechanical stress resulting from the formation of solids result in moderate reliability for these battery systems (14).

6. Energy Efficiency

The energy efficiency of the Na-S-glass cell is about 84 percent (14). The Na-S-β-alumina cell has an efficiency range of about 75 to 80 percent measured at a 7-hour charge and 4-hour discharge rate (32,35). The efficiency of this battery system is highly dependent upon the rate of charge and discharge.

7. Maintenance

Annual operation and maintenance costs for these battery systems are estimated to be $.73/kWh for the Na-S-glass system and $.55/kWh for the Na-S-β-alumina system (14). Procedures include temperature monitoring and control, cell equalization and replacement, and cooling air equipment servicing. In addition, maintenance of safety equipment is required for these systems.

8. Voltage Characteristics

Voltage characteristics for these battery systems are shown below:

	Na-S glass	Na-S-β-Alumina
Open circuit voltage	2.1 volts	2.1 volts
Charge cut-off voltage	2.8	2.4
Discharge cut-off voltage	1.8	1.6

Charge/discharge voltage curves are shown in Figure II-33 for a Na-S-glass battery.

Current-voltage curves and voltage vs. time curves are shown for charging and discharging of Na-S-β-alumina batteries in Figures II-34 and II-35.

9. Charging Characteristics

Little information is available on charging voltage and current regulation requirements. For Na-S-glass batteries, a maximum charge rate of 2C has been used. A taper charge at constant voltage will probably be used for cell equalization. For Na-S-β-alumina batteries, a maximum charge rate of C/5 has been recommended. These cells will not tolerate overcharge, so some type of equalization system is necessary. Although charging requirements have not been fully investigated for these batteries an equalization system will have to be built into the battery or battery cells will have to be charged individually.

10. Self-Discharge Rate

For both types of Na-S batteries, the self-discharge rate is equal to zero.

11. Temperature

The operating temperature range for both battery systems is 300 to 400°C. Parasitic losses during charging and discharing are expected to maintain the battery at its operating temperature during use.

12. Energy and Power Densities

Little information is available on energy and power density of Na-S-glass cells and batteries. Energy density

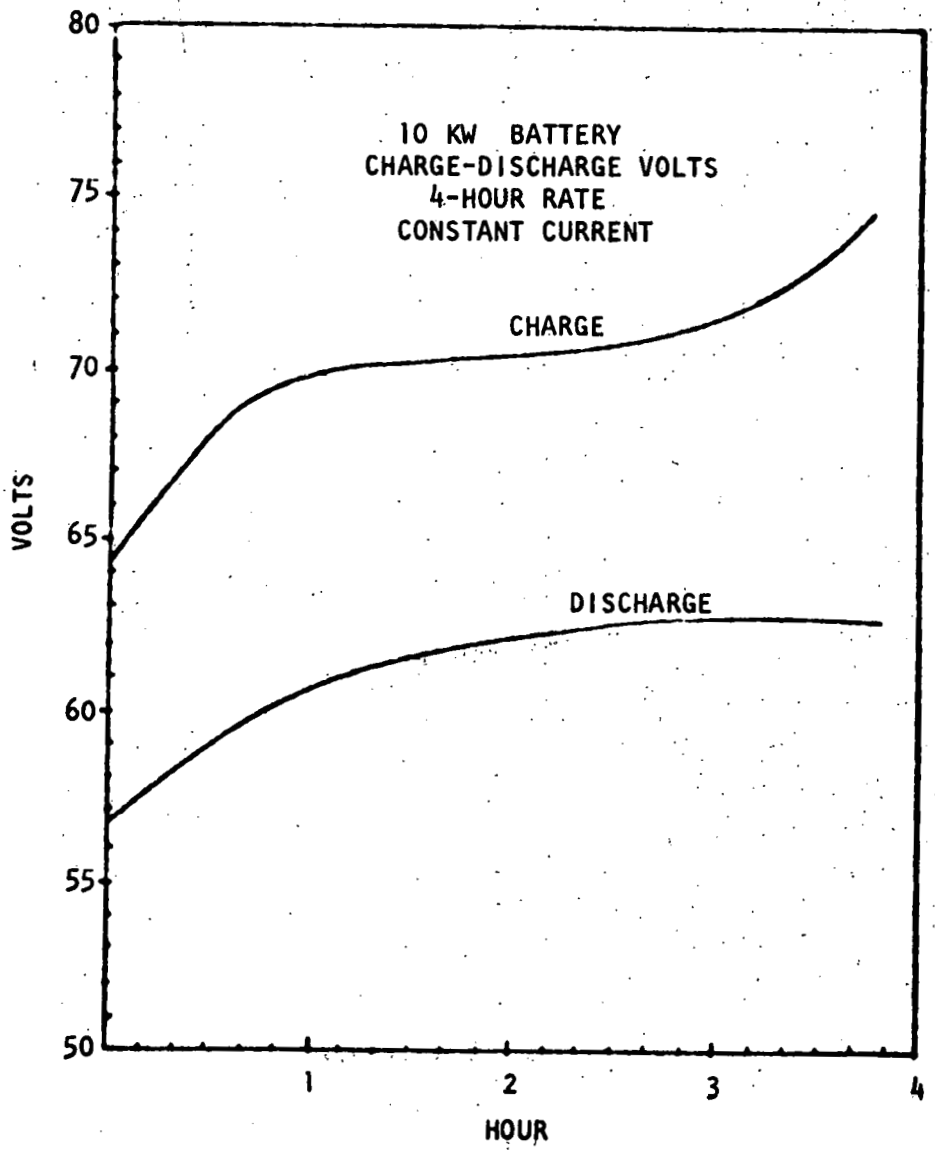

Figure II-33. Charge/Discharge Voltage Curve for a Sodium-Sulfur Glass Electrolyte Battery (30)

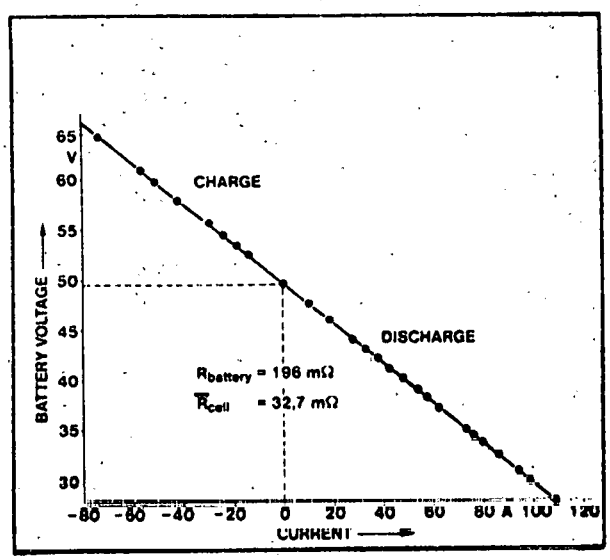

Figure II-34. Current Voltage Curve for Sodium-Sulfur-β-Alumina Cell

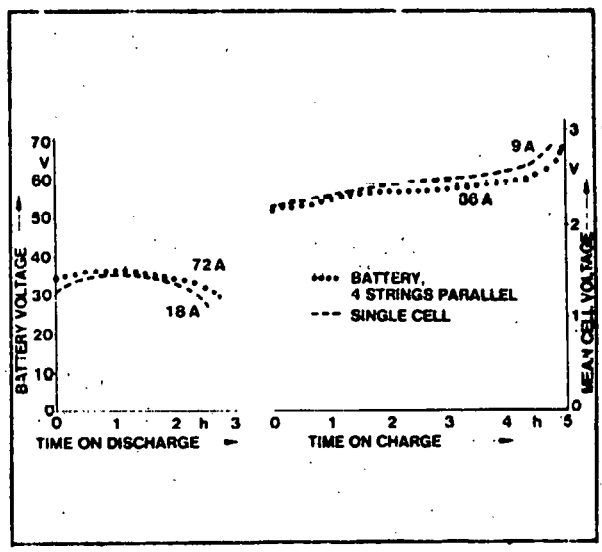

Figure II-35. Charge/Discharge Voltage Curve for a Sodium-Sulfur-β-Alumina Cell (42)

has been estimated at 270 Wh/kg in cells and 200 Wh/kg in batteries (36). Calculations based on nominal dimensions of cells of 20, 50, and 400 Ah capacities, at an operating voltage of about 2V, result in energy volume densities of about 150, 230, and 300 Wh/l, respectively (4). These values correspond to energy weight densities of about 95, 150, and 195 Wh/kg. Energy densities for Na-S-β-alumina cells are about 80 to 90 Wh/kg (11,32). Power densities are about 120 W/kg at full charge and 80 percent discharge, with a peak power occurring near the C discharge rate (34).

13. Materials Availability

No scarce materials are used in fabricating these battery systems; sodium and sulfur are abundant and inexpensive.

14. Environmental, Health, and Safety

Environmental, health, and safety considerations include danger of reactions between large quantities of sodium and sulfur, or reaction of sodium with air or water during cell rupture. At moderate temperatures, sodium can react spontaneously with air and emit toxic sodium oxide fumes. The reaction with moisture is exothermic and evolves hydrogen. Also, sulfur will burn in air at moderate temperatures, emitting toxic fumes of SO_x. Sulfides will also react in air and hydrogen sulfide will form in the presence of moisture or acids. Also, chemical burns can occur when sodium or sulfur comes in contact with the skin, and SO_2 is a dangerous eye irritant. In addition, the hot air generated during operation requires ventilation, which can contribute to thermal pollution.

15. Commercial Availability

The Na-S-β-alumina battery system will probably not be commercially available until after 1984. A prototype battery is scheduled to be tested at the BEST facility in the early 1980s. The battery system will probably be available for use in photovoltaic systems at the time of its commercial availability. The Na-S-glass battery system is scheduled to be tested at the BEST facility in 1985, with commercial availability following.

16. Research and Development Risk

There is a high research and development risk with both of the Na-S battery systems, due to the operating problems encountered with the glass seals and the solid electrolyte.

No data were available on associated development costs. The R&D program is expected to continue until commercialization in about 1984. The funding level for DOE-supported programs in this area was about $5 million in 1979 and $6 million in 1980.

O. Calcium-Metal Sulfide

1. General Description

The calcium-metal sulfide cell, which is in the exploratory research stage, employs solid electrodes and a molten salt electrolyte. Two negative electrodes made of intermetallic compounds have been developed which show great potential for use as the cathode. The first electrode, a bimetallic compound of calcium and silicon, has a very high theoretical capacity of 3.63 Ah Ca per gram of Si (37). However, discharging to low levels in cells, using these electrodes, causes excessive corrosion of the current collectors. This problem is eliminated when cells are prevented from discharging completely, but there is loss in the theoretical specific energy density of about 15 percent. The other negative electrode under investigation is an intermetallic compound of calcium, magnesium, and silcon. This electrode has a theoretical capacity approaching 2 Ah Ca per gram of Mg_2Si and has demonstrated the best overall performance of all the electrodes tested (37). The positive electrodes under consideration for use as the anode in a calcium-metal sulfide cell are either iron or nickel sulfide. The results of extensive testing of all the electrodes indicate that the use of a calcium silicon cathode and an iron sulfide anode provides the highest performance. Additional testing is underway to improve the performance of the positive electrode and determine the optimum electrolyte composition. Currently a quarternary eutectic system of lithium, sodium, calcium, and barium is used to form the electrolyte. The overall reaction of this Ca_2Si-FeS_2 cell is shown in the following chemical reaction:

$$2Ca_2S + FeS_2 \xrightleftharpoons{4e^-} CaSi_2 + 2CaS + Fe + Ca \qquad Vo = 1.65V$$

The largest unit tested to date is a 0.16 kWh cell at Argonne National Laboratory, where the work on calcium-metal sulfide batteries is currently being conducted.

2. Cost

The costs of manufacturing this battery are unknown at this time due to its early stage of development. Hittman Associates has estimated the projected selling price at between $32 and $40/kWh.

3. Battery Life

These cells have been tested for a cell life of 120 cycles or 2,500 hours (38).

4. Failure Mechanism

The main mechanism of failure is mechanical shorting. In addition, excessive corrosion of the current collectors occurs during discharge to low levels.

5. Reliability

No data are available on the reliability of this battery system due to its early stage of development.

6. Energy Efficiency

The energy efficiency is rated at 70 percent based on testing performed at ANL (38).

7. Maintenance

Because this battery system is in the exploratory stage, maintenance requirements and costs have not been determined.

8. Voltage/Current Characteristics

The open circuit voltage of the Ca_2Si-FeS_2 cell is 1.65V (37). The charge and discharge cutoff voltages and voltage curves are not available for this battery system.

9. Charging Characteristics

Due to the exploratory nature of the R&D of this battery system, charging voltage, current regulation requirements, and minimum charging time are not available.

10. Self-Discharge

The self-discharge rate has not been measured.

11. Operating Temperature

The operating temperature range is 450 to 500°C (38).

12. Energy Density

The calcium-metal sulfide battery system has a theoretical energy density of about 1,800 Wh/kg (26). The specific energy capacities of a cell for discharge rates of C/5 and C/25 are 42 Wh/kg and 78 Wh/kg, respectively (38). At a cell density of about 3 kg/l, the energy volume densities are 126 Wh/l and 234 Wh/l, respectively (38). Power density values were not available.

13. Materials Availability

There are currently no scarce materials used in fabrication of this battery system. All materials are widely available at low cost.

14. Environmental, Health, and Safety

Safety considerations have to do with the high operating temperature of this battery system. A cell rupture could cause a serious fire if the high temperature solids and liquids come in contact with flammable materials. These solids and liquids could also pose a serious health problem if contacted by people.

15. Availability

The laboratory testing of a prototype multi-cell battery is expected to occur about 1986. If tests are successful, the battery is expected to be commercially available by around 1990.

16. Development Costs

Due to the early stage of research, the developmental costs of the battery are not known at this time.

P. References

1. Ciprios, G., W. Erskine, Jr., and P.G. Grimes. Redox Bulk Energy Storage System Study, Volumes: 1 and 2. NASA-Lewis Research Center, January and February 1977.

2. Gould Incorporated. State-of-the-Art Lead-Acid Vehicle Batteries. Rolling Meadows, Illinois: Prepared for Argonne National Laboratory, August 26, 1977.

3. Feduska, W., et al. Energy Storage for Photovoltaic Conversion, Volumes 1, 2, and 3. Prepared for U.S. Energy Research and Development Administration by Westinghouse R&D Center, September 1977.

4. Bechtel Corporation. Final Report on Battery Storage Performance Requirements for Terrestrial Solar Photovoltaic Power Systems. August 1977.

5. Argonne National Laboratory. Proceedings of the Symposium and Workshop on Advanced Battery Research and Design. March 22 to 24, 1976.

6. U.S. Department of Energy. Environmental Development Plan for Energy Storage Systems, FY78, ERDA.

7. U.S Department of Energy. Battery Technology: An Assessment of the State of the Art. Prepared by TRW, Inc., under Contract No. EX-76-C-10-3885, March 27, 1978.

8. Roberts, R. Status of the DOE Battery and Electrochemical Technology Program, MTR-8026. Mitre Corporation, September 1979.

9. Hedderson, George W. "Batteries." In: Standard Handbook for Electrical Engineers, Donald G. Fink, ed. McGraw-Hill, 1968.

10. Gould Incorporated. Develop Nickel-Zinc Battery Suitable for Electric Vehicle Propulsion. Rolling Meadows, Illinois: Prepared for Argonne National Laboratory, 1977.

11. Hamilton, William. Prospects for Electric Cars, Final Report. General Research Corporation, March 15, 1978.

12. Catherino, H. et al. Cost Analysis of 50 kWh Zinc-Chlorine Batteries for Mobile Applications. Prepared for U.S. Department of Energy, by Energy Development Associates, January 1978.

13. Energy Development Associates. Flow Battery Project Review: The Zinc Chlorine Battery. July 17 to 18, 1979.

14. Pittman, P. F. Conceptual Design and Systems Analysis of Photovoltaic Power Systems, Volume I. Prepared for U.S. Energy Research and Development Administration by Westinghouse Electric Corporation, April 1977.

15. Argonne National Laboratory. Development of Lithium/Metal Sulfide Batteries at Argonne National Laboratory: Summary Report for 1977. March 1978.

16. Putt, R. A. "A Zinc Bromine Battery for Energy Storage." In: Proceedings of the 14th Intersociety Energy Conversion Engineering Conference, American Chemical Society, August 1979.

17. Behrin, E., et al. Energy Storage Systems for Automobile Propulsion. Lawrence Livermore Laboratory, December 15, 1977.

18. Lear, John W. "Nickel Hydrogen Cell Characterization and Simulated Low Earth Orbit Cycling." In: Proceedings of the 14th Annual Intersociety Energy Conversion Conference.

19. Dunlop, J. D., G. Van Ommering, and M. W. Earl. "NiH_2 Battery Flight Experiment." In: Power Source 6: Research and Development in Non-Mechanical Electrical Power Sources, Proceedings of the 10th International Symposium, Brighton, September 13 to 16, 1976, pp. 231-247.

20. Giner, J., and J. D. Dunlop. "The Sealed Nickel-Hydrogen Secondary Cell." J. Electrochem. Soc.: Electrochemical Science and Technology, January 1975, Volume 122, No. 1, pp. 4-11.

21. Martino, J. J. et al. "Development of Li-Al/FeS Cells with LiCl-Rich Electrolyte." Prepared for Symposium on Battery Design and Optimization, Pittsburgh, Pennsylvania, October 1978.

22. Nelson, P. A., A. A. Chilenskas, and R. K. Steunenberg. "Lithium-Iron Sulfide Batteries for Electric Vehicles." The Fifth International Electric Vehicle Symposium, October 1978.

23. Symons, P. C. and M. J. Hammond. Evaluation of a 1-kWh Zinc Chlorine Battery System, Interim Report. September 1976.

24. Chilenskas, A. A. Questionnaire response.

25. Sudar, S., et al. Development of Lithium-Metal Sulfide Batteries for Load Leveling. Atomics International, July 1977.

26. U.S. Energy Research and Development Administration. Engineering Study of a 20 MW Lead-Acid Battery Energy Storage Demonstration Plant, ERDA-E (04-3)-1205. Prepared by Bechtel Corporation, San Francisco, October 1976.

27. Zivi, S. M., et al. "Battery Engineering Problems in Designing an Electrical Load Leveling Plant for Lithium/Iron Sulfide Cells." In: Proceedings of the 14th Intersociety Energy Conversion Engineering Conference, American Chemical Society, 1979.

28. Steunenberg, R. K. Lithium-Aluminum Metal Sulfide Batteries. Argonne National Laboratory, March 1977.

29. Anand, J. N. "Dow Sodium-Sulfur Battery for Energy Storage." Presented at the 14th Intersociety Energy Conversion Engineering Conference, American Chemical Society, 1979.

30. Levine, C., and J. Anand. "The Sodium-Sulfur Battery with Glass Electrolyte." In: Proceedings of the Symposium on Load Leveling, Electrochemical Society, Inc., October 1977.

31. Birk, J. R., and N. P. Yao. Proceedings of Symposium on Load Leveling. Electrochemical Society, Inc., October 1977.

32. Bridges, D. W., R. W. Minck, and D. G. Poquette. "Reproducibility and Performance of Large Prototype Na/S Cells." In: Proceedings of the 14th Intersociety Energy Conversion Engineering Conference, American Chemical Society, 1979.

33. Chatterji, D., et al. "Sodium-Sulfur Battery Development at General Electric." In: Proceedings of the Symposium on Load Leveling. Electrochemical Society, Inc., October 1977.

34. Fischer, W. Questionnaire response. Brown, Bouveri, Inc., Heidelberg, F.R.G.

35. Lazennec, Y. Improvements of Electrolyte and Seal Technology for Sodium-Sulfur and Sodium Antimony Trichloride Load-Leveling Batteries. Electric Power Research Institute, June 1977.

36. Lindsley, E. F. "Exotic New Batteries - More Miles for Electric Cars." Popular Science, February 1979, pp. 78-83, 158.

37. Preto, S. K., et al. "Calcium/Iron Sulfide Secondary Cells." Prepared for the meeting of the Electrochemical Society, Philadelphia, Pennsylvania, May 8 to 13, 1977.

38. Preto, Sandra. Argonne National Laboratory. Questionnaire respondent.

39. Personal communication between Lee E. Miller (Eagle-Picher Industries) and Amitava Podder (HAI), March 1980.

40. Sudionu, J.L. British Railways. Questionnaire response.

41. Srinivasan, S., R. Yea, and A. Beaufrere. "Hydrogen-Halogen Energy Storage Systems: Preliminary Feasibility and Economic Assessment." ERDA Contractors Coordination Meeting, January 1977.

42. Fischer, W., et al. "Sodium-Sulfur Batteries for Peak Power Generation." In: Proceedings of the 14th Intersociety Energy Conversion Engineering Conference. American Chemical Society, 1979.

43. Fischer, W., et al. "Recent Advances in Na-S Cell Development - A Review, 1978." Journal of Power Sources, Volume 3, No. 4, December 1978, Elsevier Sequoia S.A., Lausanne, Switzerland.

44. Adams, G.B. and R.P. Hollandsworth. "Rechargeable Alkaline Zinc/Ferricyanide Redox Battery." In: Proceedings of DOE Battery and Electrochemical Contractors' Conference (U.S. DOE), December 10-12, 1979.

45. Thaller, Lawrence H. Recent Advances in Redox Flow Cell Storage Systems, DOE/NASA 1002-79/4. Prepared for 14th Intersociety Energy Conversion Engineering Conference, American Chemical Society, 1979.

46. Exxon Research and Engineering Company. "Zinc-Bromine Battery System." Summary of Information presented at the Department of Energy - Division of Energy Storage Systems Flow Battery Project Review. Sheraton Potomac Inn, Rockville, Maryland, July 17-18, 1979.

III. DATA BASE ON POWER CONDITIONING EQUIPMENT

A. Terminology

Current-Fed - The source is constrained to be a constant current generator. It is an AC source as viewed by the parallel connected AC system and delivers real power only.

Voltage-Fed - The source is constrained to be a constant voltage source. It is a conventional generation voltage source and is capable of supplying reactive as well as real power.

Self-Commutation - The act of commutation can be performed wholly within the inverter.

Line-Commutation - The kVA required for commutation is provided by the AC system or reactive elements connected at the equipment's AC terminals.

Buck-Boost DC/AC Converter - Two inverters series connected at the DC terminals, in which variations in DC and AC voltages are accomplished by adjusting the delay angle on the controllable inverter from inversion end-stop (full boost) at the maximum DC, minimum AC voltage, to rectification end-stop (full buck) at minimum DC, maximum AC voltage.

Buck DC/DC Converter - Produces a DC voltage which is lower than that of its source.

Boost DC/DC Converter - Produces a DC voltage which is higher than that of its source.

Buck-Boost DC/DC Converter - Buck and boost converters connected in series.

Complementary Inverter - Uses two inverters, each delivering one-half of the total power. One is self commutated and the other is line commutated.

Chopper Inverter - Matches the DC source voltage to the inverter's DC terminal voltage. Reduces the need for power factor connection.

Inverter - A device for converting direct current into alternating current.

Transformer - Used to transfer electric energy from one or more circuits to one or more other circuits. Transfer occurs without change in frequency but usually with changed values of voltage and current.

Ripple - The AC component in the output of a DC power supply, arising within the power supply from incomplete filtering or from commutator action in a DC generator.

Comparator - An electronic instrument that measures a quantity and compares it with a precision standard.

Filter - A network that transmits alternating currents of desired frequencies while substantially attenuating all other frequencies.

Rectifier - A device for converting alternating current into direct current.

B. Definition of Power Conditioning

A power conditioning unit is one of the subsystems required in a photovoltaic electric system, as indicated in Figure III-1. The power conditioner may include any or all of the functions shown, depending on the specific application. A power conditioner may serve a DC load or an AC load and may be designed for autonomous or non-autonomous operation. In the case of a non-autonomous operation, an auxiliary energy source such as a utility line or a generator is required. In many cases, the power conditioning unit controls the performance of the other subsystems with which it interfaces. A power conditioner essentially serves the following three functions (2):

(1) Transmission of usable power to the load upon demand - This includes control of output voltage and transfer function for either-or operation. Additionally, for AC systems, this includes DC/AC inversion and phase angle control.

(2) Management and control of power generated by the photovoltaic array - Allows for load shedding, automatic startup and shutdown, maximum power tracking, battery charge and discharge control, and connection of array strings to DC bus in response to load demand.

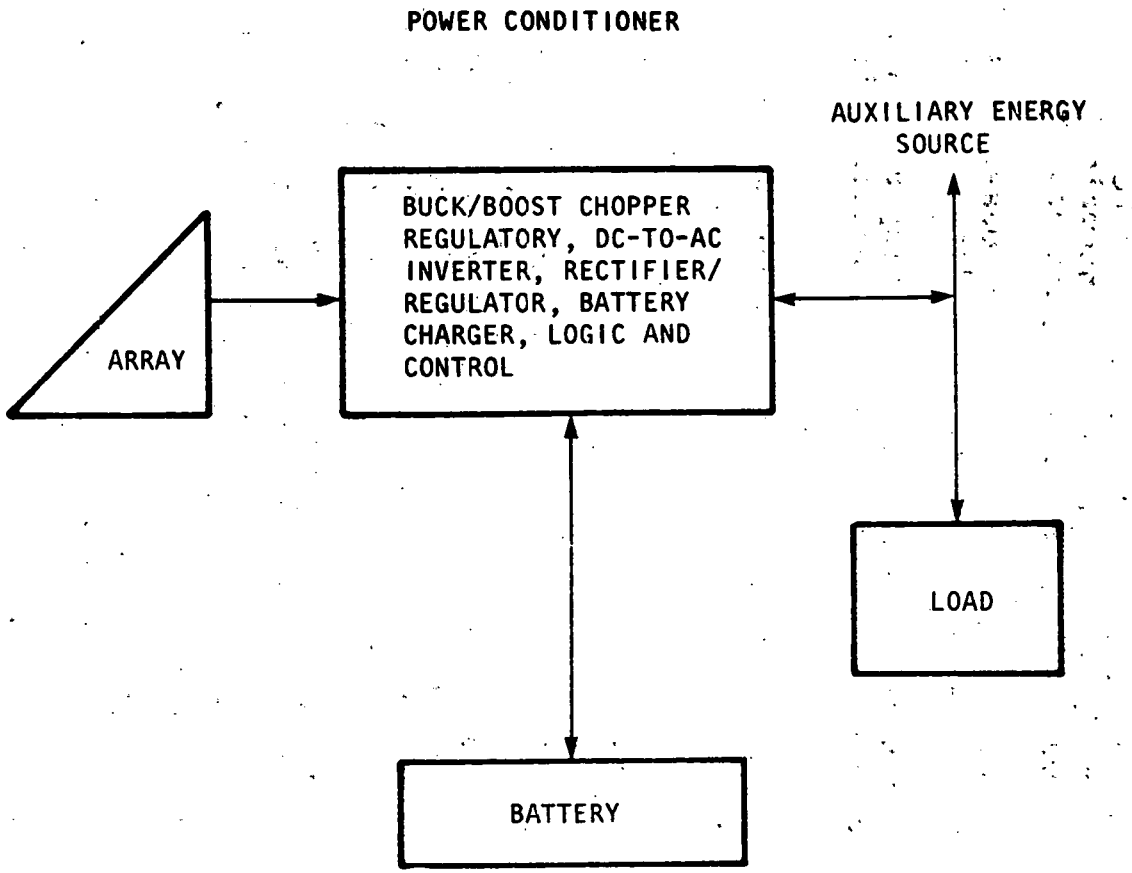

Figure III-1. Definition of Functions Performed by Power Conditioner Subsystem (1)

(3) Protection of the overall system - Provides fault protection and clearing. Additionally, for non-autonomous AC systems, this includes synchronizing power output to utility grid and system isolation during failure of the utility system.

The equipment required to perform the power conditioning function consists of DC smoothing components, switching elements, DC current interrupter, harmonic filters, commutating circuit auxiliaries, capacitors for power factor correction, and transformers (3).

Power conditioners must meet the following operational requirements:

(1) Withstand network disturbance without presenting an additional fault to the network

(2) Clear internal faults due to malfunction

(3) Operate independent of the AC system when supplying power to AC loads

(4) Bring on-line a system with isolated operation capability independent of the AC power system when supplying power to AC loads

(5) Switch equipment instantaneously from charging to discharging the storage medium

(6) Provide voltage support and system stability.

Power conditioners must meet the following utility interface requirements (3):

(1) Provide good power factor

(2) Limit harmonic injection into the utility system

(3) Operate over the usual range of network voltage and frequency tolerances

(4) Operate over the normal ranges of voltage unbalance for a 3-phase system.

(5) Tolerate load, line, and/or generator faults on the network without presenting an additional fault condition.

The source interface requirements are as follows:

(1) Clear DC faults

(2) Maintain ripple current and voltage within the source's capability to bear them.

The internal requirements of the power conditioner are as follows:

(1) Survive network disturbance without presenting an additional fault condition

(2) Clear internal faults

(3) Withstand momentary inrush, e.g., motor starting.

A power converter controls the mixing of solar and utility power and maximizes the utilization of solar power. A power conditioner also performs the following functions:

(1) Handles variable input current, input voltage, ambient temperature, and output load.

(2) Matches power quality with utility in case of non-autonomous operation

(3) Prioritizes power usage

(4) Maximizes power drawn from the solar system.

C. Description of Power Conditioning Parameters

1. Capital Cost and Availability

The cost of power conditioning equipment is dominated by conventional components such as the inductor, capacitor, and transformer, not by their active semiconductor devices. Even when array costs drop to $.50/W, the array cost is still the dominant portion of the capital cost of a photovoltaic system. Should the array cost fall to the $.10 to $.20/W range, the power conditioner capital cost would become a significant portion of the total photovoltaic system capital cost.

The cost per kW for converters decreases with an increase in power level. Also, the cost per kW at any given power level varies, depending on equipment design and manufacturer. Most of the power conditioners available today are of smaller capacities (50 kVA). The larger units have to be specially ordered and there is a lead time before the unit can be manufactured. Availability on a large scale will

depend on future market penetration. At present, there are only a few firms that manufacture smaller units as "off-the-shelf" items. More manufacturers are expected to be attracted to production of power conditioners as the market develops and, hence, the units will be more readily available. All costs in this section are in 1980 dollars.

2. Efficiency

The efficiency of a power conditioner is defined as the ratio of the output power delivered to the input power. Efficiency is one of the most important factors in a conversion system; losses contribute to the operating cost. While full-load loss is the major concern, part-load loss must be considered when selecting a power converter. Losses are contributed to not only by the active switching components but also by the associated passive components such as transformers, filters, power factor correction capacitors, and DC reactors.

The current-fed schemes, because of the I^2R behavior of the bulk of their losses, show little variation in efficiency as the load is reduced. Voltage-fed schemes and the high-frequency link schemes show increased percentage losses with decreasing load. This is due to the fixed losses of some of their constituent functions.

Full- and part-load losses increase with decreasing DC source voltage. This has two causes: (1) the increase in the percentage losses of the smaller passive components, and (2) the increase in the percentage loss of active devices and their ancillaries.

Figures III-2 and III-3 show full-load efficiency versus DC voltage curves using thyristors and transistors, respectively (4). These curves were obtained for a single-phase bridge, self-commutated inverter. The efficiency decreases somewhat as the voltage is reduced to 150V and falls rapidly if the voltage level is further reduced.

Figure III-4 shows efficiency as a function of inverter output. The efficiency remains at a high level even at very low loadings. This requirement is unique to photovoltaic applications, in which the power available from the array is frequently less than peak power rating.

Since the efficiency of converters decreases at part-load conditions, it may be necessary for the power conditioning units to include provisions for switching to the utility line when low levels of power are demanded regularly. Also,

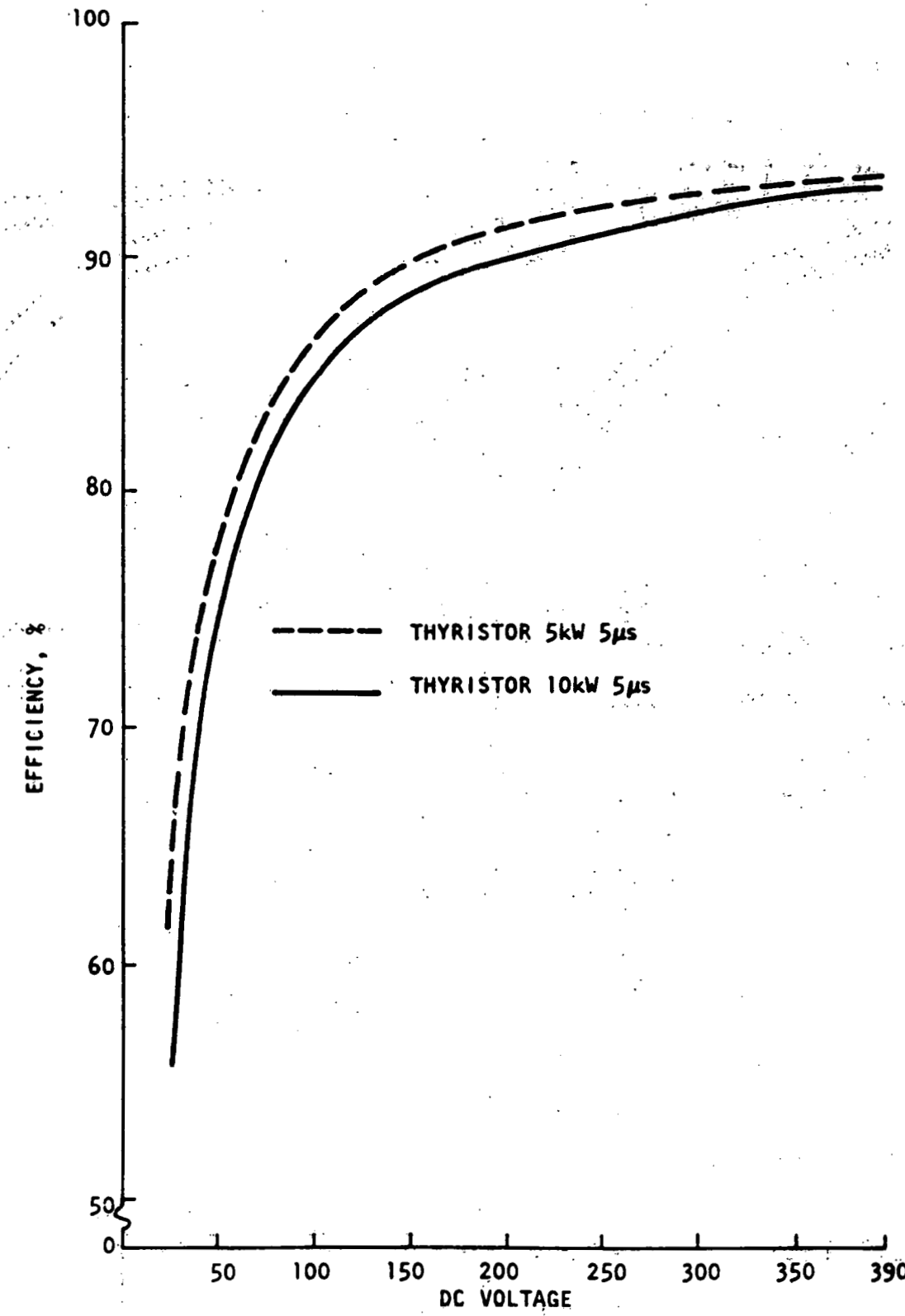

Figure III-2. Full Load Efficiency Versus DC Voltage for Thyristors (Top of Charge)(4)

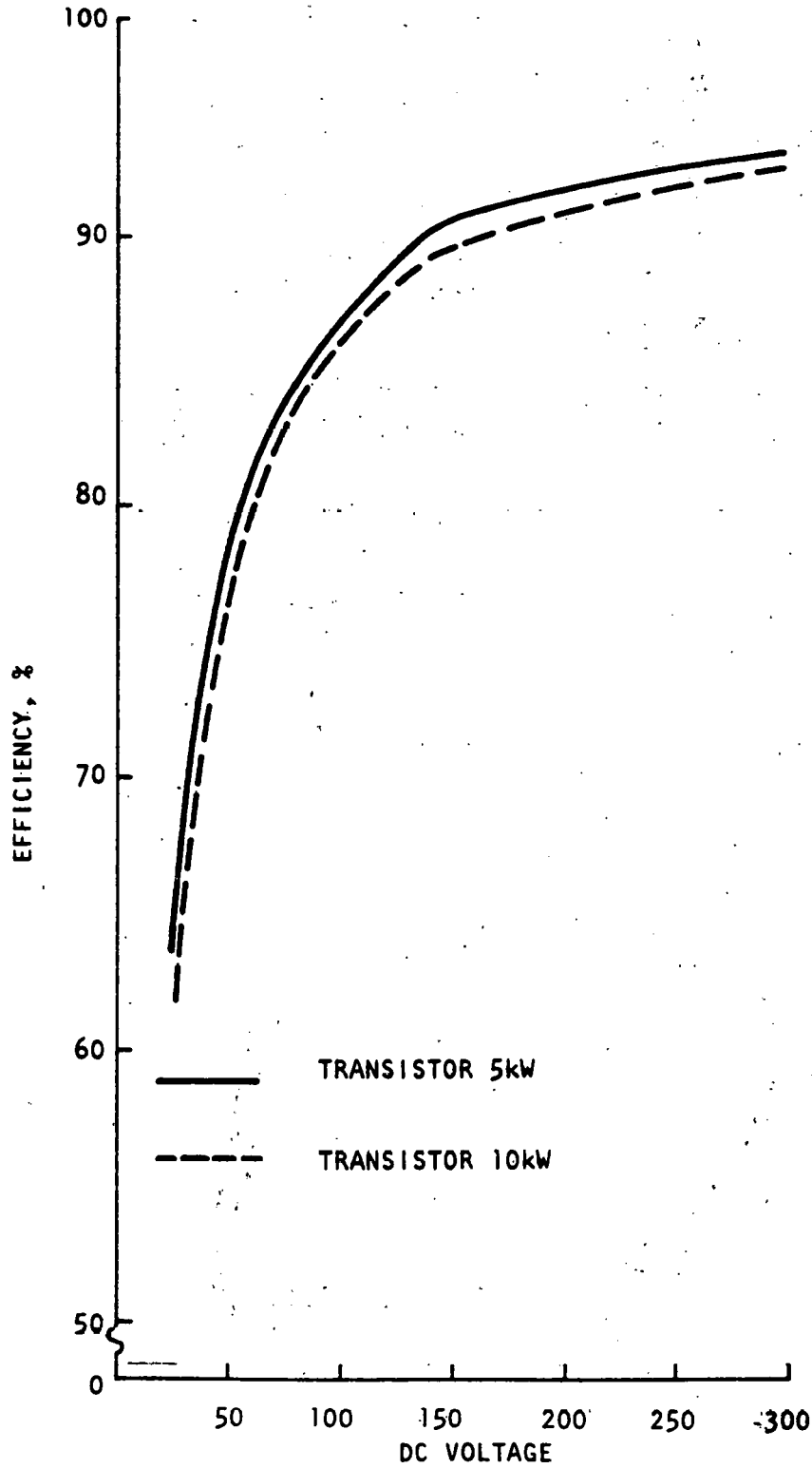

Figure III-3. Full Load Efficiency Versus DC Voltage for Transistors (Top of Charge)(4)

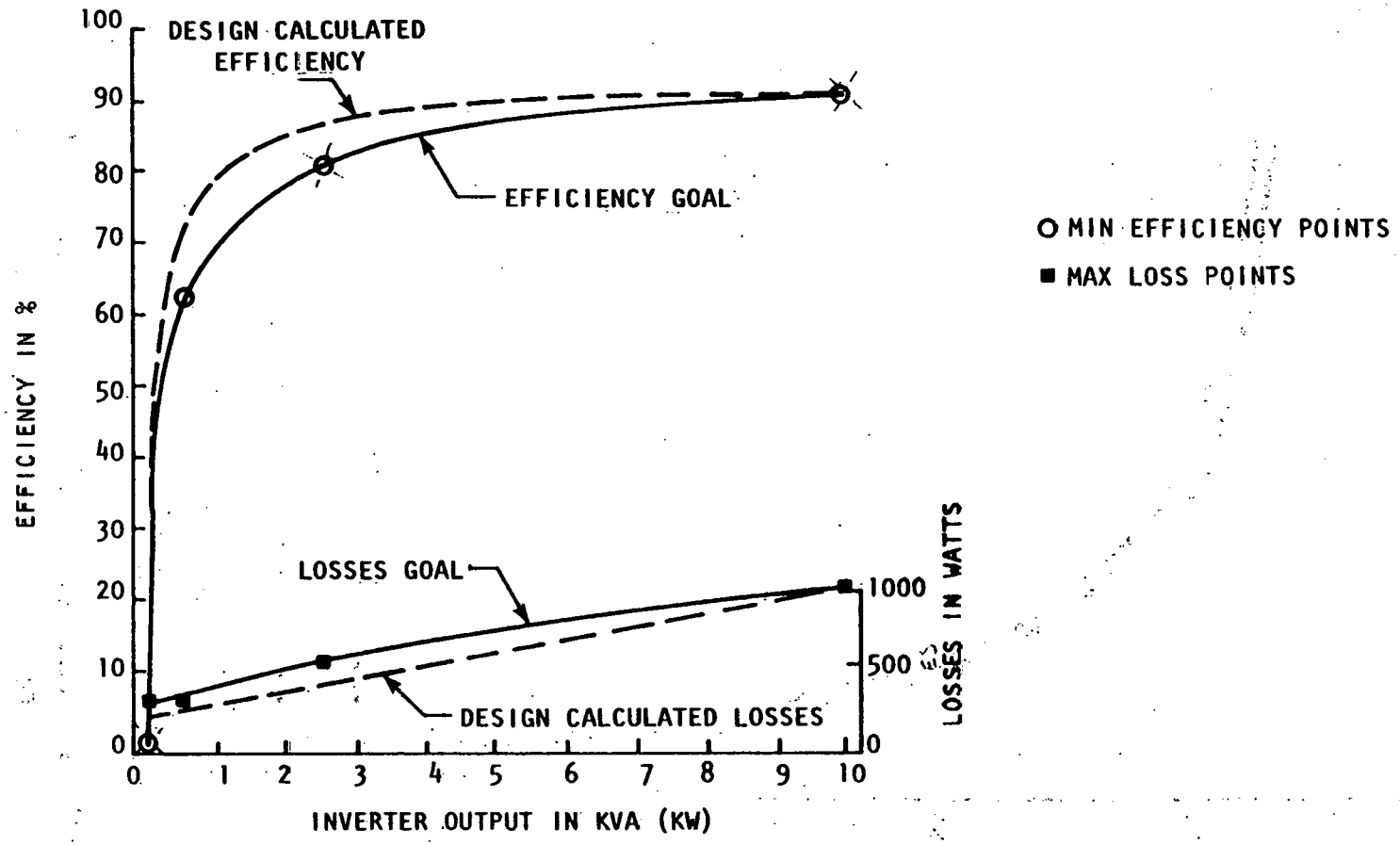

Figure III-4. Efficiency and Losses for a 10 kVA Self-Commutated Inverter (8)

the use of two smaller converters may be more efficient in certain applications; only one unit will operate at part load and both units will operate at full load (6).

Current-fed conversion systems generally possess full-load efficiencies ranging from 92 to 94 percent at low power levels and 95 to 97 percent for high power levels (MW region). Their ratio of fixed losses to resistive losses is less than unity and, hence, the maximum efficiency point exists at less than full load. Efficiencies are equal to or greater than their full-load performance at fractional loadings (7).

Voltage-fed conversion systems typically have full-load efficiencies of 90 to 96 percent. Their ratio of fixed losses to resistive losses is more than unity. Efficiency therefore decreases as the load is reduced. DC/DC converters have similar part-load behavior. A full-load efficiency of 97 to 99 percent has been observed for units running at modest switching rates, and full-load efficiencies of 65 to 75 percent have been observed in low-power, high-frequency ranges (7).

3. Harmonic Content

The AC line current of a static converter is nonsinusoidal and can be resolved into fundamental and harmonic components. Total harmonic distortion is the total nonlinear distortion in which undesired harmonics of a sinusoidal input signal are generated because of nonlinearity in the circuit.

The harmonic content of the AC waveform supplied to the utility must be reasonably low so that it does not disrupt the utility system. Although the harmonic tolerance levels in utility systems are not known, it is well understood that harmonic distortion can be a problem. In one application, total harmonic distortion was limited to 5 percent with a maximum of 3 percent for any single harmonic (9).

4. Power Factor

Power factor can be expressed as the ratio of active current to the total current. It can also be defined as the ratio of kW to the total kVA. The power factor may be lagging or leading, depending on the direction of both magnetizing kilovar and kilowatt flow. The power factor that the utility system receives from the power conditioner, if uncorrected, can vary over a wide range. The variation is dependent on the thyristor conduction/extinction angle. Capacitors are normally employed to improve the power factor.

5. Power Rating

Power can be rated in terms of input and output. The output power is obviously lower than the input power because of the losses. Power conditioner ratings are usually expressed in terms of continuous ratings and short-term ratings. The continuous power rating represents the power that the unit can withstand continuously, whereas the short-term power rating represents the power that the unit can withstand for a short period of time. The short-term rating is very important in applications in which motors are used. Power conditioners should be capable of handling motor inrushes, which can last up to a few seconds, depending on the mechanical load present at starting.

6. Input Voltage

The input voltage of a power conditioner is specified as the normal input operating voltage range and maximum input voltage. A solar array generates a voltage that varies during the day. The voltage generated depends on the solar insolation; hence, the power conditioner must be capable of handling the variable input voltage. A power conditioner is rated for a specified DC voltage range.

The maximum input voltage determines the maximum DC voltage that the power conditioner can withstand.

7. Output Voltage

The output voltage can be DC or AC, depending on the application. The voltage level desired at the output depends on the application. Some of the common AC output voltages are 240/120V, 1 Ø; 208/120V, 3 Ø; 480/277V, 3 Ø. Some of the common DC output voltages are 12V, 48V, 90V, and 180V.

8. Life

Life expectancy is the period of time over which the power conditioner will perform the functions for which it was designed. Designs which maximize unit life are desirable. Solid-state conversion equipment can be used, employing conservative and proper construction techniques to increase the life. However, the cost of the power conditioner increases as the life expectancy increases.

9. Environment

A power conditioner is generally rated for a specific temperature and humidity range. Depending on the application, temperature and humidity may play an important role in the selection of a power conditioner. Operating a power conditioner beyond its rated temperature and humidity tends to decrease the life expectancy of the unit.

10. Physical Characteristics

Physical characteristics include size and weight. Depending on the application, the size and weight may become important factors in the selection of power conditioners. Transformers contribute significantly to the size and weight of power conditioners.

11. Reliability

Reliability of a power conditioner is usually expressed as the mean time between failures in hours. The data available on the mean time between failures (MTBF) in power conditioners for photovoltaic applications are based on theoretical calculations, not on practical testing. The power conditioners, however, use off-the-shelf devices whose reliability data are available and are based on actual testing. Reliability can be increased by employing standby redundancy or parallel redundancy. The cost premium for redundancy can be quite high; however, it is an extremely effective way to increase reliability. Another way to increase reliability is to create series or parallel redundancy in the thyristor valve strings.

The reliability needed for photovoltaic applications is high, especially in remote scenarios. Reliability can be increased through the use of solid-state conversion equipment, conservative design, and proper construction techniques.

12. Maintenance and Repair

Power conditioning equipment generally does not require much maintenance. Since no long-term experience results are available on power conditioners for photovoltaic applications, it is extremely difficult to assess the maintenance cost. Repair may be needed in case there is a failure of the units. Depending on the application, some power conditioners may have to be repaired quickly, and hence, standardized repair procedures are necessary. Repairs can be made either

at the site or by the manufacturer, depending on the complexity of the failure and the availability of replacement parts.

D. Types of Power Conditioning Units

Power conditioning units can use DC/AC conversion or DC/DC conversion, depending on the type of load. All power conditioning equipment can be divided into two classes: current-fed and voltage-fed. Another class of DC/AC inverters is the high-frequency link type. The current-fed types can be line-commutated, forced-commutated, buck-boost, complementary, or chopper types. The voltage-fed types can be line-commutated, forced-commutated (phase-angle control or conduction-angle control), or complementary.

Figure III-5 is a simplified schematic of a current-fed converter. Current-fed converters have the following characteristics (7,10,11):

(1) The source is constrained to be a constant current generator.

(2) Commutation is achieved by transferring the current flow from one output line to the other.

(3) The system is capable of delivering real power only.

(4) The DC voltage at the sending end cannot be rapidly controlled. DC interrupters with high speed ratings should be used.

(5) The thyristors are exposed to the full impact of the transients caused by the system.

(6) The system operates at a generally poor lagging power factor.

(7) The system is susceptible to commutation faults engendered by AC line faults.

(8) At the AC terminals, the system acts as a harmonic current generator.

(9) The system requires reversing switchgear to permit battery charging from the AC supply.

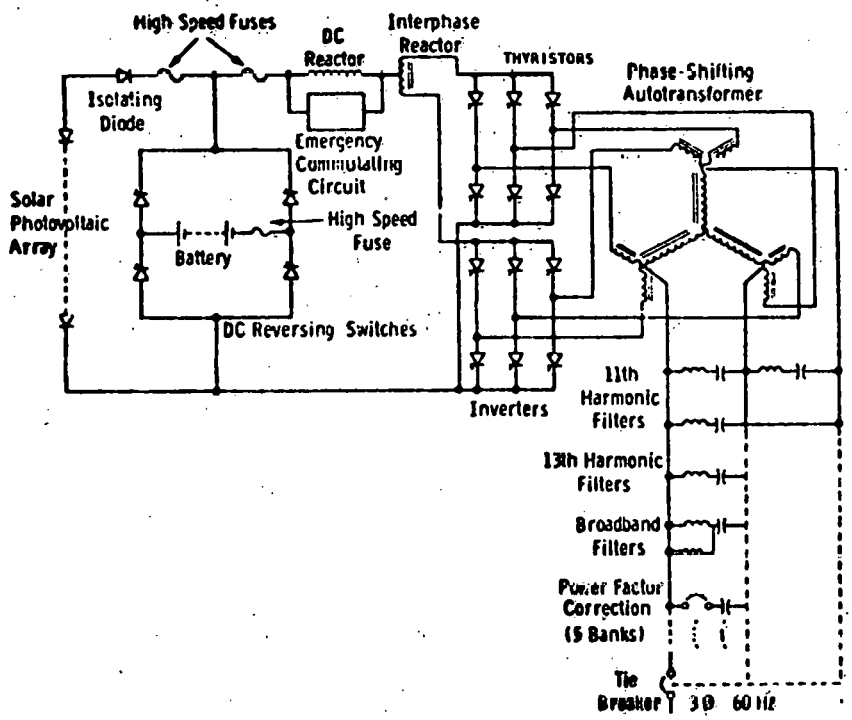

Figure III-5. Elementary Schematic of Current-Fed Power Conversion Arrangement (1)

(10) The system is inexpensive.

(11) For low power levels, efficiencies range from 92 to 94 percent at full load. For MW ranges, efficiencies range from 95 to 97 percent at full load. The maximum efficiency can be obtained by operating the system at less than full load.

(12) At the AC interface, VAR demand is controlled independently of the converter and its control.

(13) At the DC interface, power flow is controlled by the adjustment of the phase-delay angle.

Figure III-6 shows the basic circuit design of a voltage-fed power converter. The basic operating principle is to switch the DC voltage to the AC terminal with suitable alterations of polarity. The system generates an output wave which is a reasonably close approximation to the sinusoidal AC system voltage to which the converter's AC terminals are connected.

If the switching operations are performed according to Figure III-6a, a three-phase AC power will be produced at the output terminals. Figure III-6b shows the shape of the AC wave form for the three phases. These are 6-pulse voltages, containing fundamental and harmonic components. The harmonics can be filtered using suitable filters and the required AC voltage can be obtained by suitable transformers.

The following are characteristics of voltage-fed converters (7,10,11):

(1) The source is limited to constant-voltage types.

(2) Commutation is achieved by transferring the voltage connection of an output line from one DC bus to the other.

(3) The system is capable of delivering real as well as reactive power.

(4) Interruption techniques are complicated since there is no inductance in the DC loop. Fuses are therefore the only type of interrupting device that can be used.

(5) The voltage safety factor is difficult to determine.

(6) Efficiencies range from 90 to 96 percent at full load, the higher end for higher power units. Efficiency decreases as load decreases.

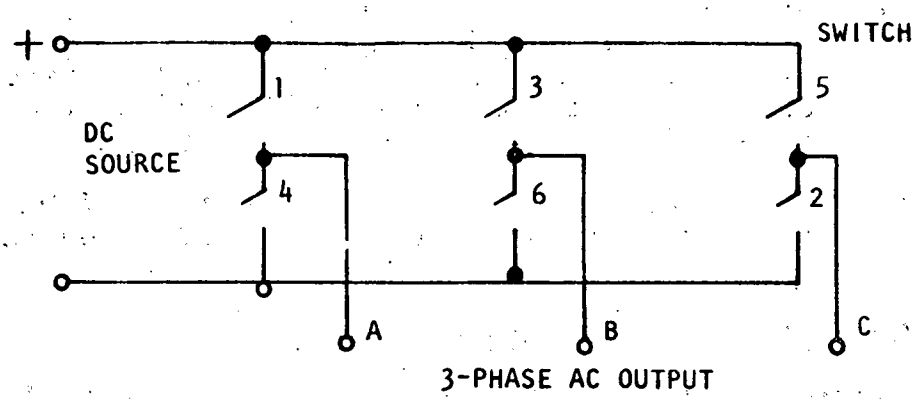

Figure III-6. Basic Circuit Design of a Voltage-Fed Power Converter (5)

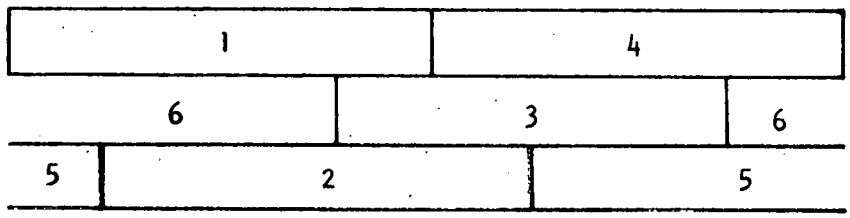

Figure III-6a. Switching Operation of the Power Converter Shown in Figure III-6 (5)

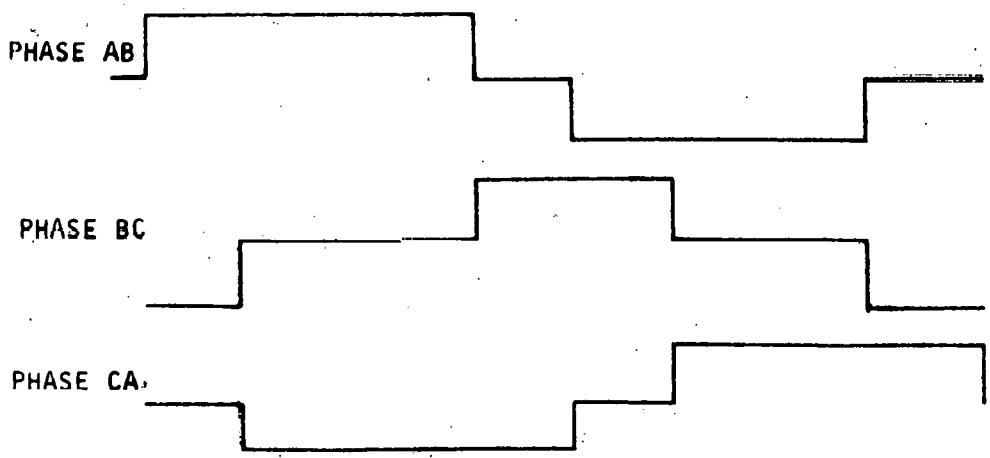

Figure III-6b. AC Output of the Circuit Shown in Figure III-6 (5)

(7) At the AC interface, the magnitude of the AC voltage must be controlled independently of DC-side conditions if control of the VAR demand is needed. Real power flow is controlled by adjusting the phase of this voltage with respect to AC supply.

(8) At the DC interface, direct control of DC interface parameters is neither possible nor required.

1. Current-Fed Line-Commutated Inverter

Figure III-7 is a schematic of a current-fed line-commutated inverter. For this kind of inverter, a system of low-impedance voltage must be present at the AC terminals to allow for the line commutation of current from one thyristor to the other. Also, the fundamental component of the current delivered by the inverter system should lead the system voltage. At its input terminals, the system acts as a unidirectional-current, bidirectional-voltage system. The main advantage of this type of inverter is its simplicity. Its drawbacks are the poor power factor and dependence upon the AC system voltage for successful operation (10).

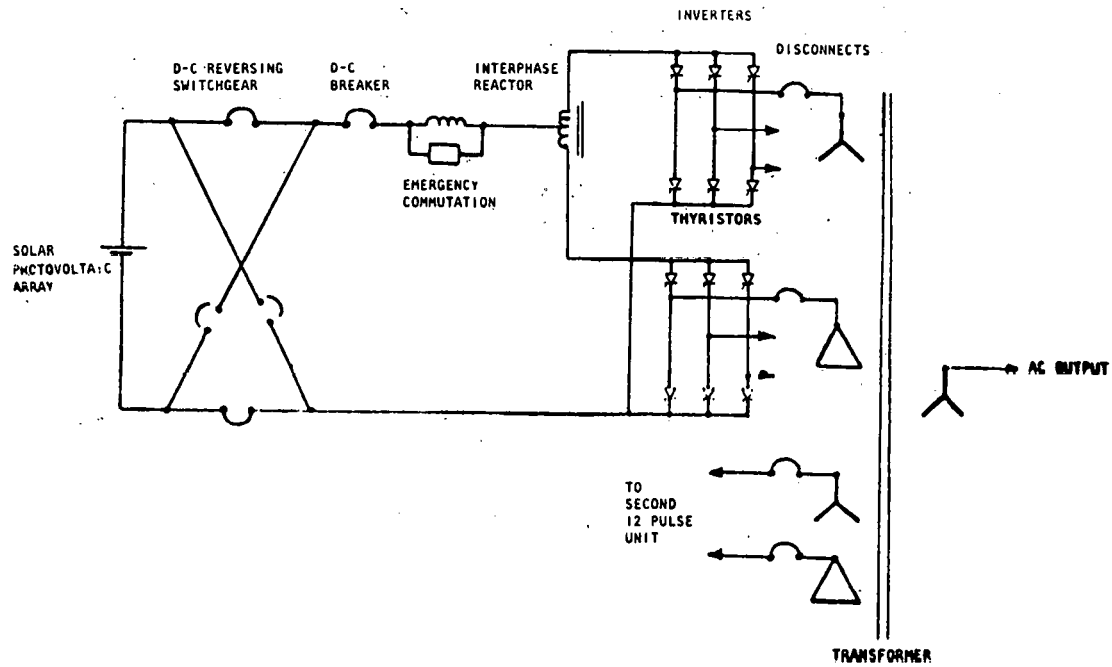

Figure III-7. Schematic of a Current-Fed Line-Commutated Inverter (10)

2. Current-Fed Forced-Commutated Inverter

Figure III-8 shows the schematic of a current-fed forced-commutated inverter. The system operates at unity power factor and the voltage is controlled by adjusting the conduction angle. The DC terminal voltage is alternated between a selected line voltage and zero. The latter is obtained by allowing the current to freewheel through any two devices in series across the DC terminals (5). The main advantage of this type of system is its independence of AC system voltage and its capability to operate at unity power factor.

3. Current-Fed Line-Commutated Buck-Boost Inverter

Figure III-9 shows the schematic of a line-commutated buck-boost inverter. The poor power factor of a simple line-commutated inverter can be improved by using two inverters, as shown in Figure III-9. In this type of arrangement, one inverter operates at a fixed angle and, thus, delivers the best power factor. The other inverter accommodates variation of the AC and DC voltages; hence, the requirement for power factor correction is minimized (10).

4. Current-Fed Complementary Inverter

Figure III-10 is a schematic of a current-fed complementary inverter. The system uses two inverters, each delivering one-half of the total power requirement. One of the inverters is line commutated and draws lagging quadrature current; the other is forced commutated and draws leading quadrature current. This results in a unity power factor to the system. The power factor correction requirement is greatly reduced and is less than the requirement for simple line-commutated types.

5. Current-Fed Chopper Inverter

If the system reactance is low, the power factor of a simple line-commutated inverter operating continuously at the inversion end stop is good. To operate in this mode, the inverter's DC terminal voltage should be a prescribed irrational multiple of the AC system voltage under all conditions. In a forced-commutated thyristor chopper, the DC source voltage is matched to the inverter's DC terminal voltage by a DC commutating circuit, thus reducing the need for power factor correction. This type of inverter is less efficient and more expensive than the simple line-commutated types (5).

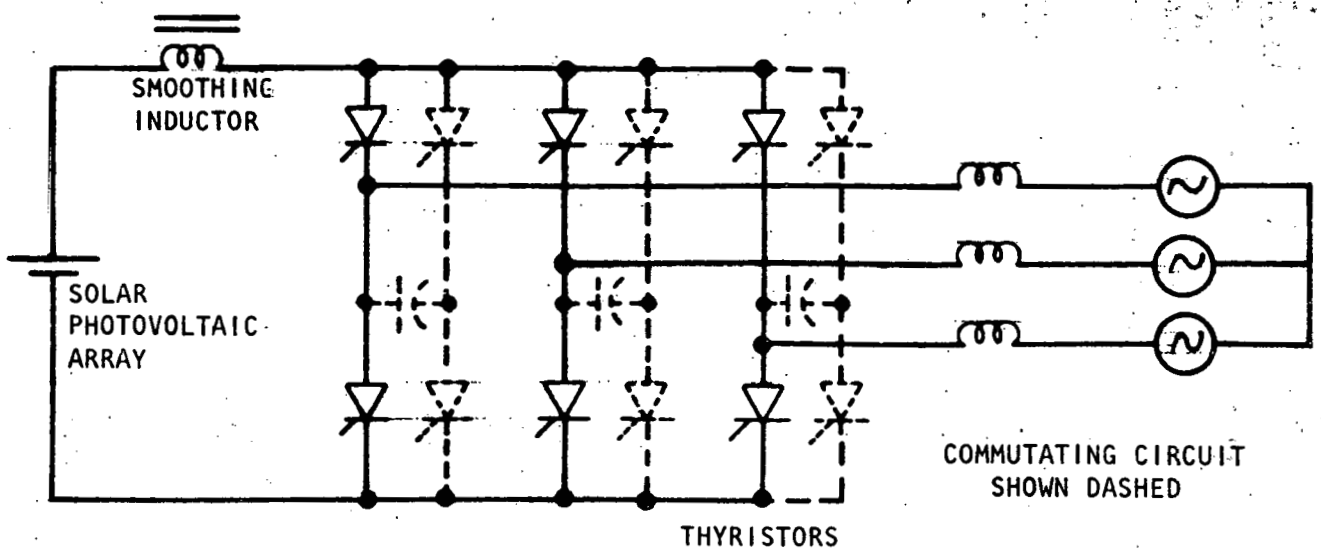

Figure III-8. Schematic of a Current-Fed Forced-Commutated Inverter (5)

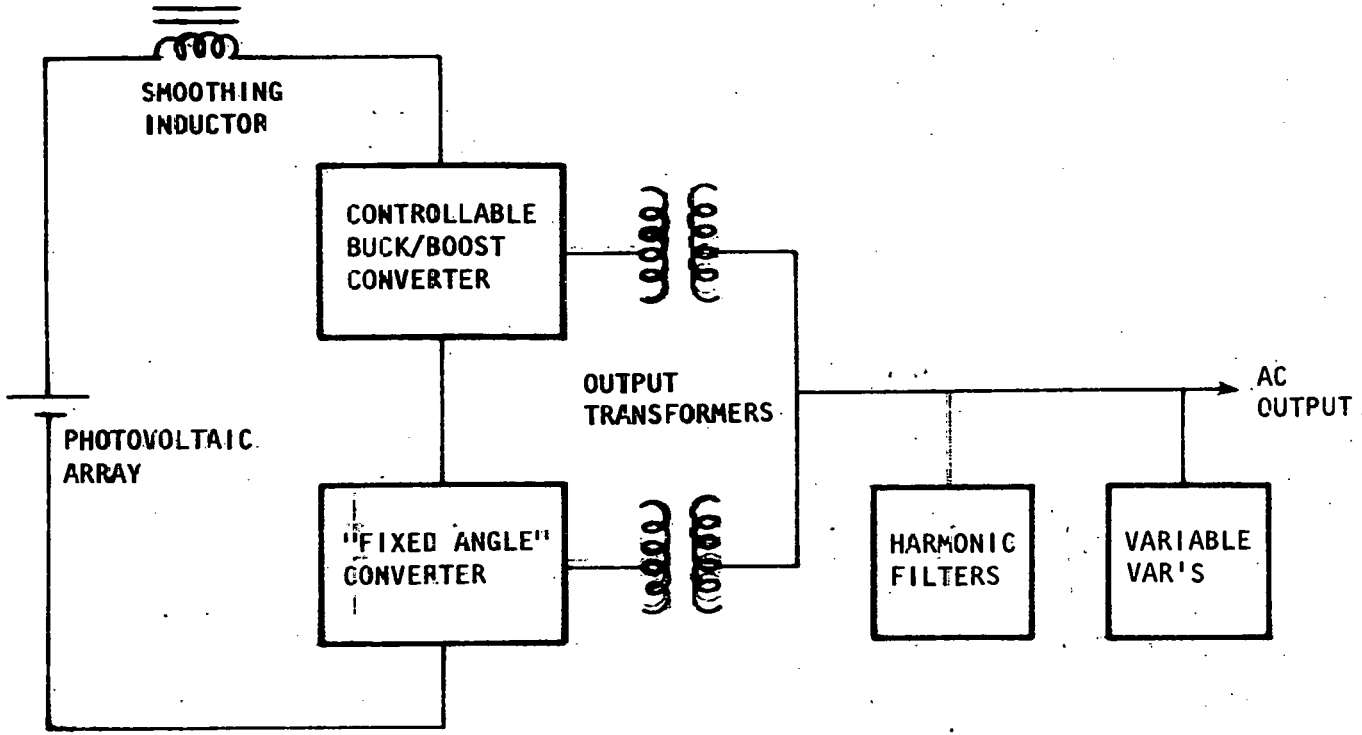

Figure III-9. Schematic of a Line-Commutated Buck-Boost Inverter (5)

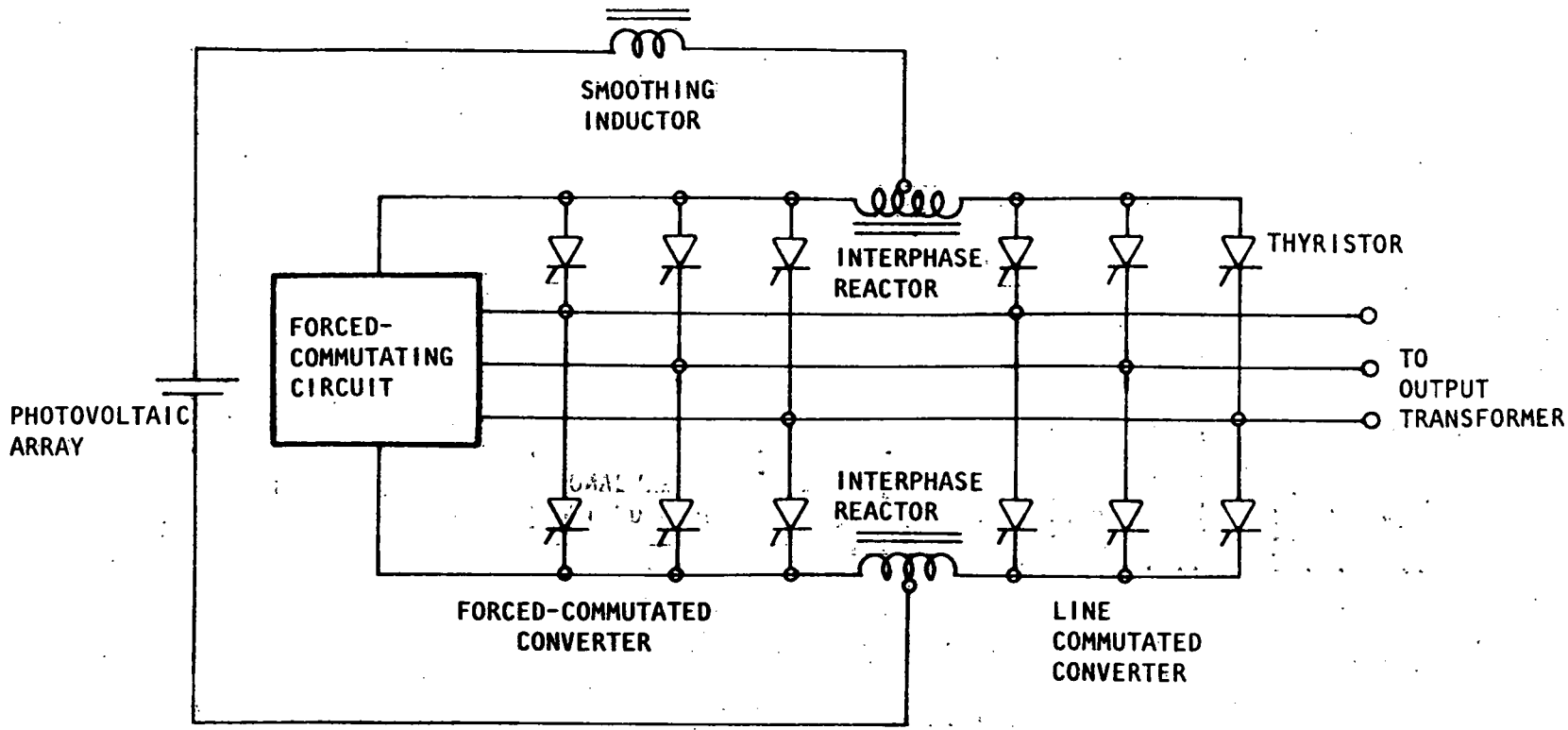

Figure III-10. Schematic of a Current-Fed Complementary Inverter (5)

6. Voltage-Fed Line-Commutated Inverter

Figure III-11 shows the schematic of a voltage-fed line-commutated inverter. Line commutation is achieved through adjustment of the magnitude and phase of the inverter output voltage relative to the DC source voltage. This system represents a lagging VAR loading on the AC system.

7. Voltage-Fed Forced-Commutated Inverter

Figure III-12 shows the components of a voltage-fed forced-commutated inverter. Its major advantage is that it does not depend on AC system voltage and controllable power factor. Also, this type of inverter can operate under isolated conditions. At the AC terminals, it acts as a harmonic voltage generator. It can present any desired quadrature current demand to an AC system to which it is connected. This system works efficiently when DC storage is required. This type of inverter is frequently used in uninterruptible power supply systems. It introduces a high level of ripple on the DC bus. The active switching devices that may be used include transistors, gate-controlled switches, or gate-assisted turn-off devices. These are more expensive than the current-fed types. There are two methods of output voltage control:

(a) Conduction-angle voltage control - Figure III-13 presents the basic arrangement of a voltage-fed conduction angle control forced-commutated inverter. The voltage is controlled by varying the conduction angle of the output wave.

(b) Phase-angle voltage control - Figure III-14 represents the basic arrangement of a voltage-fed phase-angle control forced-commutated inverter. This system uses two inverters and sums the output voltages. Any desired output from a DC input may be obtained with this type of arrangement.

8. Voltage-Fed Complementary Inverter

Figure III-15 is a schematic of a voltage-fed complementary inverter. Two voltage-fed inverters are used in a complementary fashion. One operates as a line-commutated type and runs at a leading power factor, whereas the other operates as a forced-commutated type and runs at an equal lagging power factor. The resultant power factor is unity. Voltage is controlled by shifting the individual voltage reactors by equal but opposite angles about the resultant output voltage vector. The disadvantages of this system are

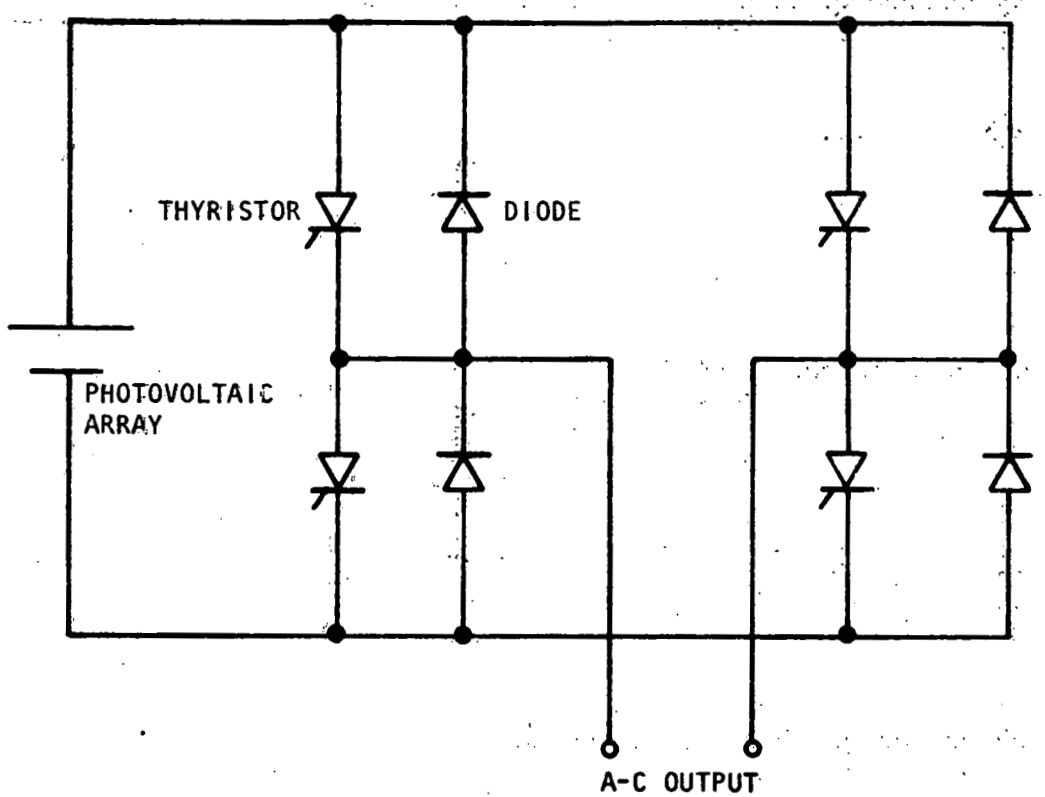

Figure III-11. Schematic of a Voltage-Fed Line-Commutated Inverter (5)

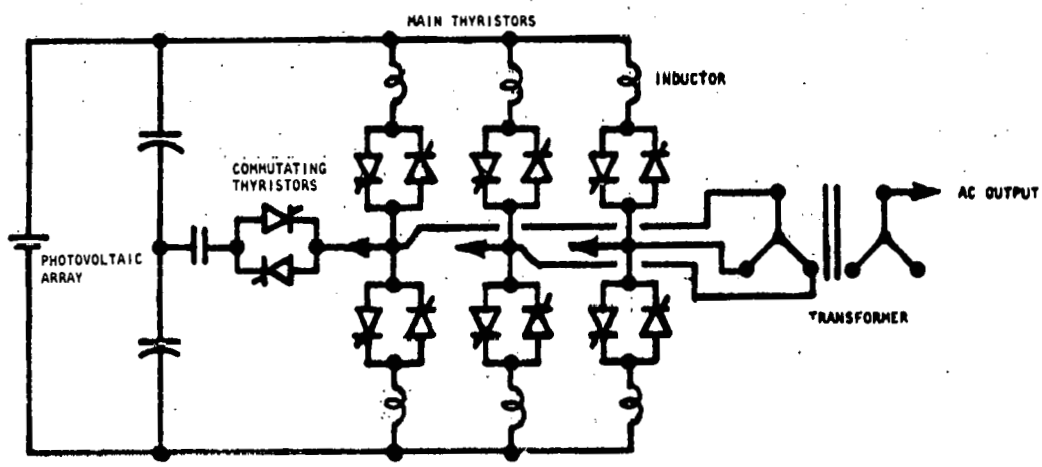

Figure III-12. Schematic of a Voltage-Fed Forced-Commutated Inverter (11)

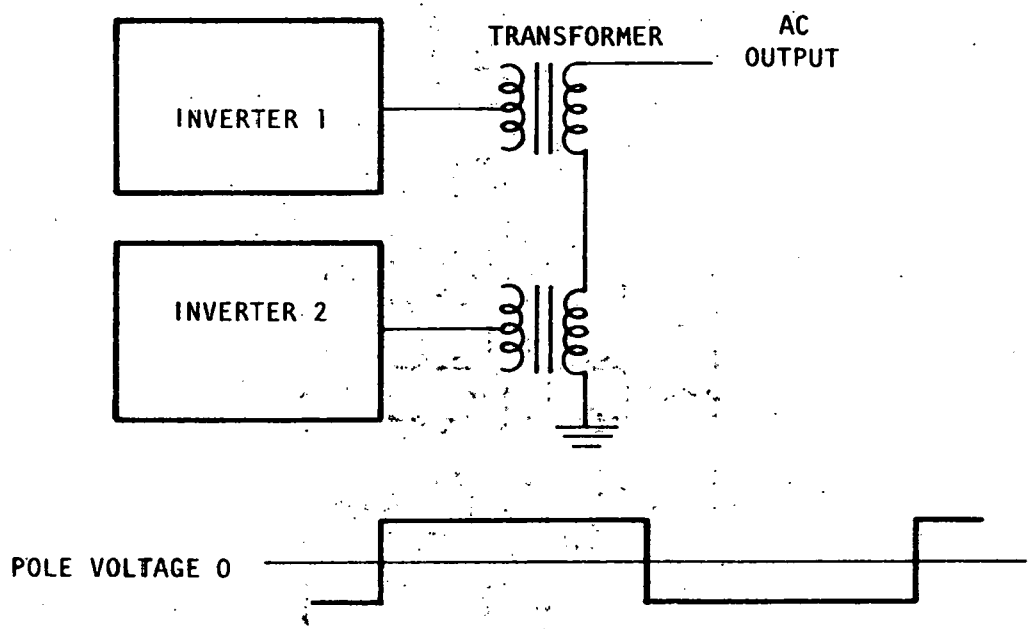

Figure III-13. Phase-Angle Controlled Voltage-Fed Inverter (12)

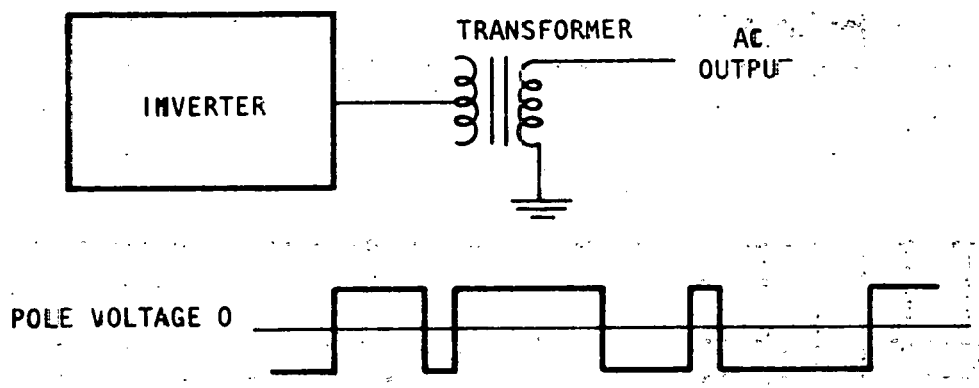

Figure III-14. Conduction Angle Controlled Voltage-Fed Inverter (12)

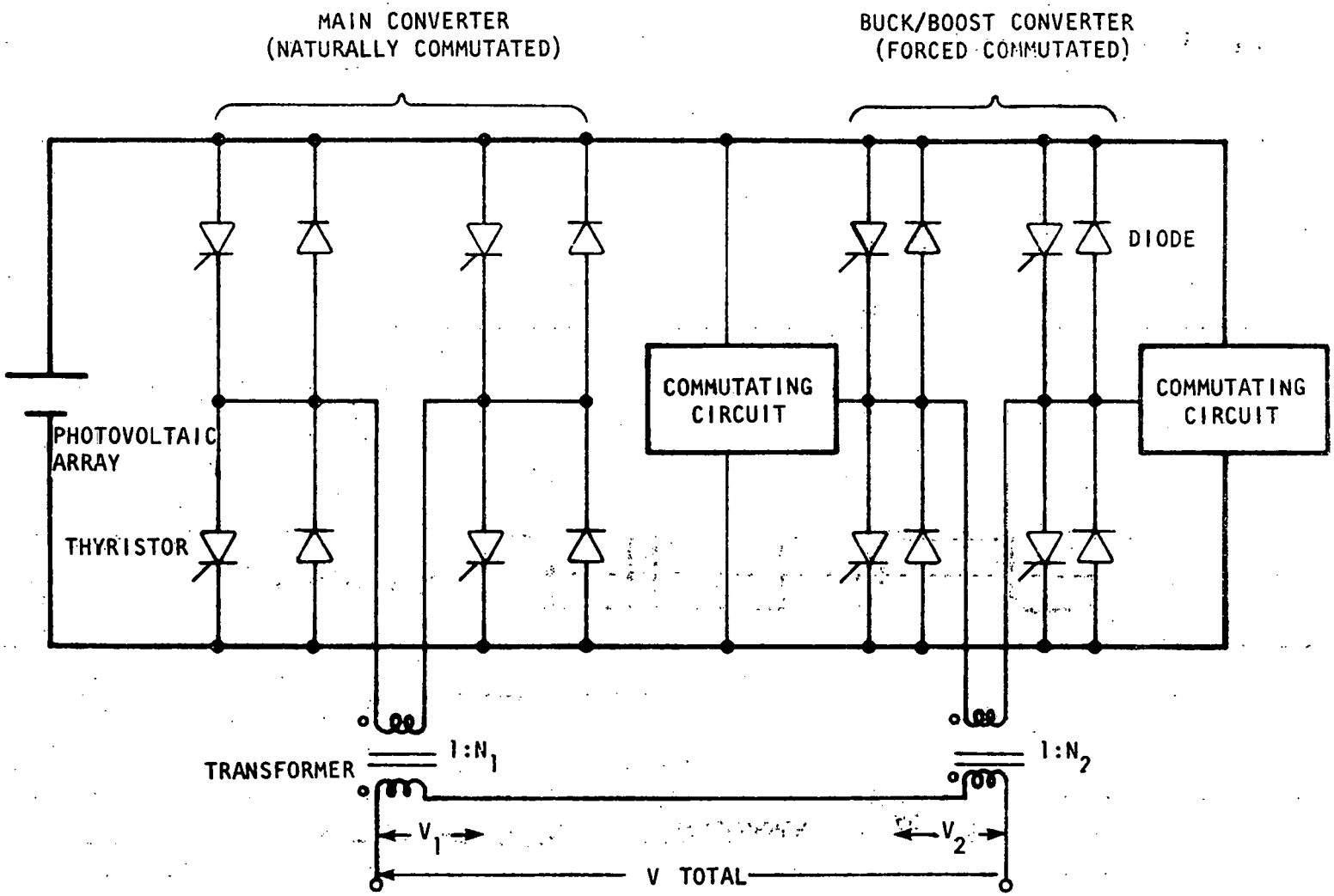

Figure III-15. Schematic of a Voltage-Fed Complementary Inverter (5)

the loss of control range and the need to insure that circuit conditions are appropriate for line commutation in one-half of the inverter (5). The major advantage of this type of inverter over a voltage-fed forced-commutated inverter is that only one-half of the scheme in the former type is forced-commutated.

9. High-Frequency Link Scheme

Figure III-16 shows an inverter that uses a high-frequency link scheme. The system consists of a cascade arrangement of a line-commutated current-fed inverter and a line-commutated cycloconverter with a high-frequency link at the cascade connection. A line-commutated cycloconverter produces a sinusoidally changing average output voltage with superposed ripple. It draws a lagging quadrature current from its AC source, regardless of the direction of the power flow. The line-commutated inverter supplies sinusoidal output voltage and the cycloconverter produces a lower-frequency sinusoidal AC output to the load.

Power is transferred from the DC source through the inverter and the cycloconverter to the load. The link tank circuit meets the commutating lagging quadrature current demands of both inverter and cycloconverter and supplies the harmonics of the current from the inverter and the distortion components of the current from the cycloconverter. It maintains a sinusoidal set of voltages to provide line commutation for the thyristors in the inverter and the cycloconverter (10).

The high-frequency link produces internally the voltages needed for line commutation of the thyristors and presents current source loading of the DC side and voltage source capabilities at the AC terminals (10).

10. DC/DC Converters

Figures III-17, III-18, and III-19 are diagrams of various kinds of DC/DC converters. These types of inverters are required when power has to be fed to a DC load. DC/DC converters are derived from DC/AC-AC/DC converters by degenerating the AC terminal set and supply to DC. These types of converters can be either current-fed or voltage-fed as shown in Figures III-17 and III-18, respectively. The combined version is shown in Figure III-19. A simple DC/DC converter is a single quadrant device, and must be forced commutated. The arrangement in Figure III-17 can only produce a DC voltage level which is lower than that of its source. It produces high source ripple currents, however. The arrangement

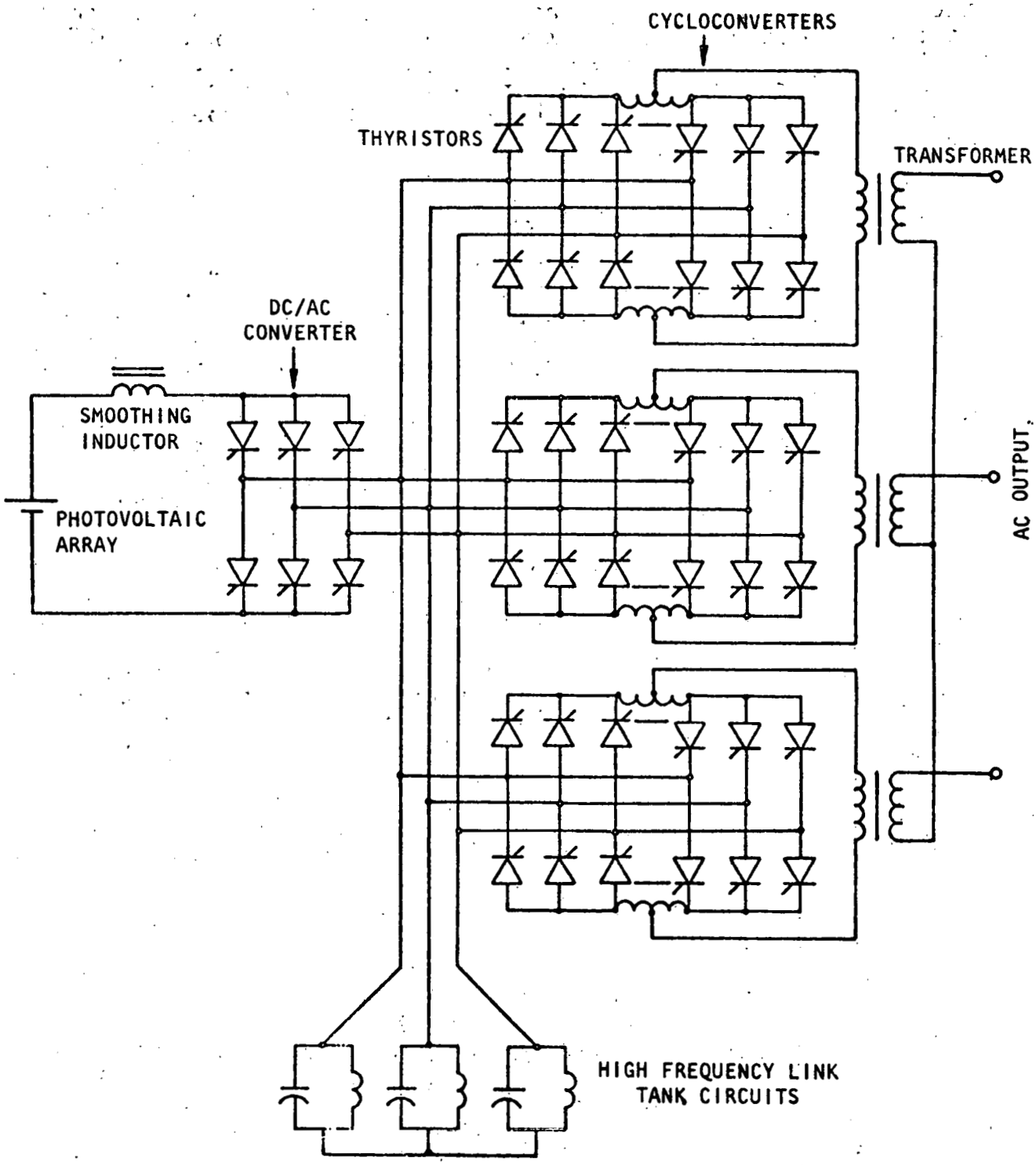

Figure III-16. Schematic of a High-Frequency Link-Type Inverter (5)

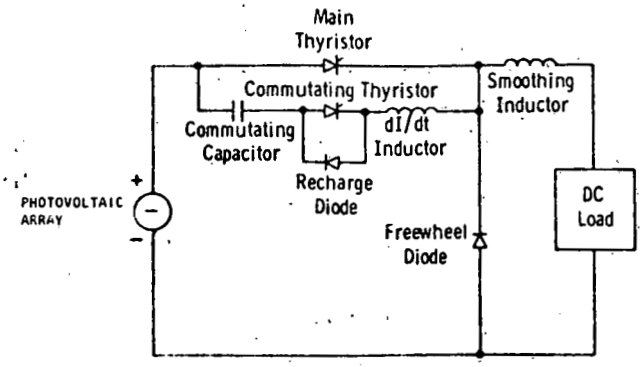

Figure III-17. "Buck" (Current-Fed) DC/DC Converter (7)

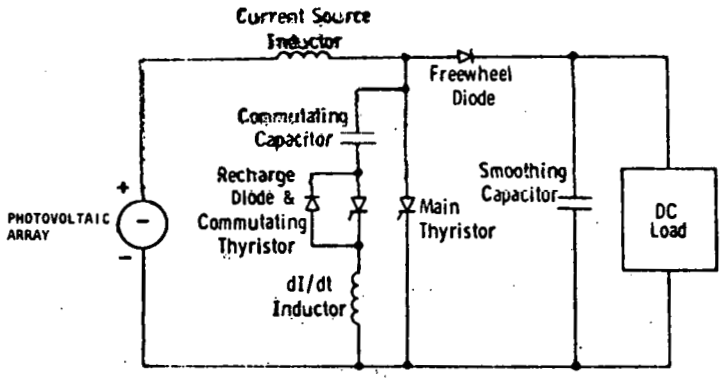

Figure III-18. "Boost" (Voltage-Fed) DC/DC Converter (7)

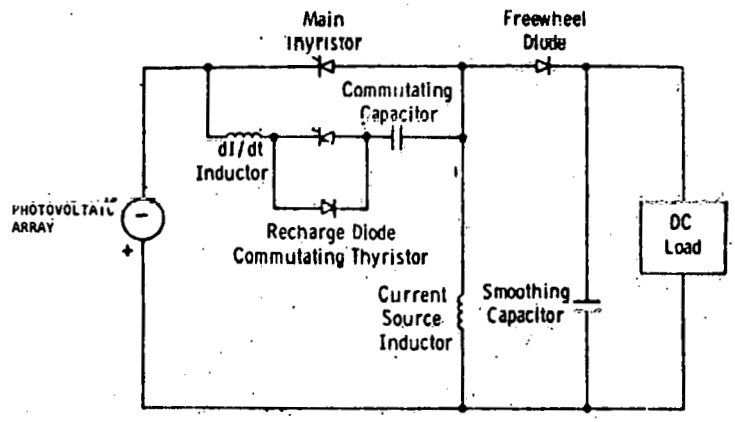

Figure III-19. "Buck-Boost" DC/DC Converter (7)

in Figure III-18 produces a DC voltage level which is higher than that of its source and produces high-load ripple currents. The arrangement in Figure III-19 produces high ripple currents for both load and source.

DC/DC converters range in voltage from a few watts to a few megawatts. DC voltages range from a few volts to about 3 kV (7). For low-power and low-voltage applications, transistors are used, whereas for high power applications, thyristors are used.

E. Device Technology Projections

The major problem in power conditioning equipment design is reducing capital cost, as well as operation and maintenance costs. Power conditioning equipment manufacturers claim that they can easily meet the present DOE goals on the cost of power conditioners and that, if they receive enough orders, they can easily produce them. Even if solar panel costs fall to $.50 per watt, panel cost still plays a dominant role in determining the capital cost. But if the panel costs fall to $.10 per watt, the power conditioner cost becomes a significant portion of the total capital cost. For the current-fed types, higher current and voltage devices will improve the situation at high power levels, whereas voltage-fed and DC/DC types need faster switching devices with greater tolerance of current and voltages (7).

The power conditioner circuit cost is influenced by the passive components, i.e., the commutation inductor and capacitor, and the semiconductor devices. All other items contributing to the overall cost are not related to the circuit choice. Device cost is a very small fraction of the total conversion system cost. Even if the device costs are zero, the system cost will be reduced by no more than 10 percent (12).

The price of semiconductors has been observed to drop as the market expands, but for labor-intensive and raw-material-rich passive components, it is extremely difficult to assume that the cost will decrease appreciably in the near future. Also, it is unlikely that semiconductor prices will decrease indefinitely. However, as production technology matures, the use of automation systems and the increase in sales of fast-switching silicon devices will further reduce the prices of semiconductor devices (13). Actually, the price of the passive components will determine the price of the complete power conditioner.

Passive components contribute significantly to the losses. Transformers and inductors in power converters contribute substantially to the losses; hence, future efforts to increase the efficiency of transformers will be important. The use of amorphous magnetic materials to manufacture transformers and inductors will reduce core losses. It can be expected that advances in thyristor technology will occur and that high-voltage thyristors will be available. The losses can be minimized by using higher voltage ratings.

For the past 15 years, fast switch development has lagged behind conventional device development. With a particular silicon slice, blocking current and voltage ratings suffer when compared to conventional devices. With the increase in the slice size, the number of defects per slice increases. It is very difficult to obtain a high production rate for fast switches as slice defects increase. The importance of di/dt, dv/dt and stored charge has led to the use of more sophisticated device geometries. For these reasons, production rates have suffered. Hence, as long as silicon is used as a semiconductor device, these problems will remain (12).

Silicon diameter has been growing steadily over the past 20 years. Diameters of up to 67 mm (2.64 in.) are available today. The increase will continue, but probably at a slower rate (12).

About five years ago, devices were rated at no more than 600 volts. Today, 2,500-volt devices are very common. Slice edge processing is a big obstacle to higher voltage-rated devices. Since the problem is in the process itself, high-voltage devices will probably not be manufactured for some time.

For the fast switch devices, di/dt, dv/dt, stored charge and recovery time are the parameters of major importance in equipment design. Improvement in recovery time has been slow over the years, but it is expected that recovery time will improve in the future. It may, however, be difficult to increase the di/dt and dv/dt ratings for fast large devices (12).

For forced-commutated applications, gate-assisted turn-off thyristors, transistors, and gate-controlled switches are suggested to replace thyristors. However, replacement of thyristors with these devices is not expected for high-power applications in the near future (12).

The 1980 ratings for forced-commutated thyristors are up to 5,000 volts and 3,000 amperes rms and 77 mm (3.03 in.) chip sizes. More development is expected in other power

semiconductors and basic thyristor types including gate turn-off and gate-assisted turn-off thyristors, reverse-conducting thyristors, and high-power triacs (14). For utility-related applications, transistors cannot match the capabilities of thyristors. Transistors are not expected to be fully competitive in the near future. Gate-assisted turnoff thyristors might replace thyristors in forced-commutated applications.

Figure III-20 shows predicted improvements in thyristor characteristics (14), based on manufacturers surveyed by United Technologies Corporation. Device improvements are referred to a benchmark thyristor. The continued improvement in thyristor characteristics will give the power conditioner designer the following options:

(1) Higher current and voltage ratings will reduce the need for the series connection of thyristors and allow use of few bridges in parallel.

(2) Reduction of turn-off time will allow decrease of commutation circuit components and losses.

(3) Reduction of components will reduce labor cost and increase reliability.

(4) Reduction of thyristor components will reduce loss due to reduced voltage drop.

The need for a high-speed commutation circuit is apparent. It will require more experimental work and system analysis (5).

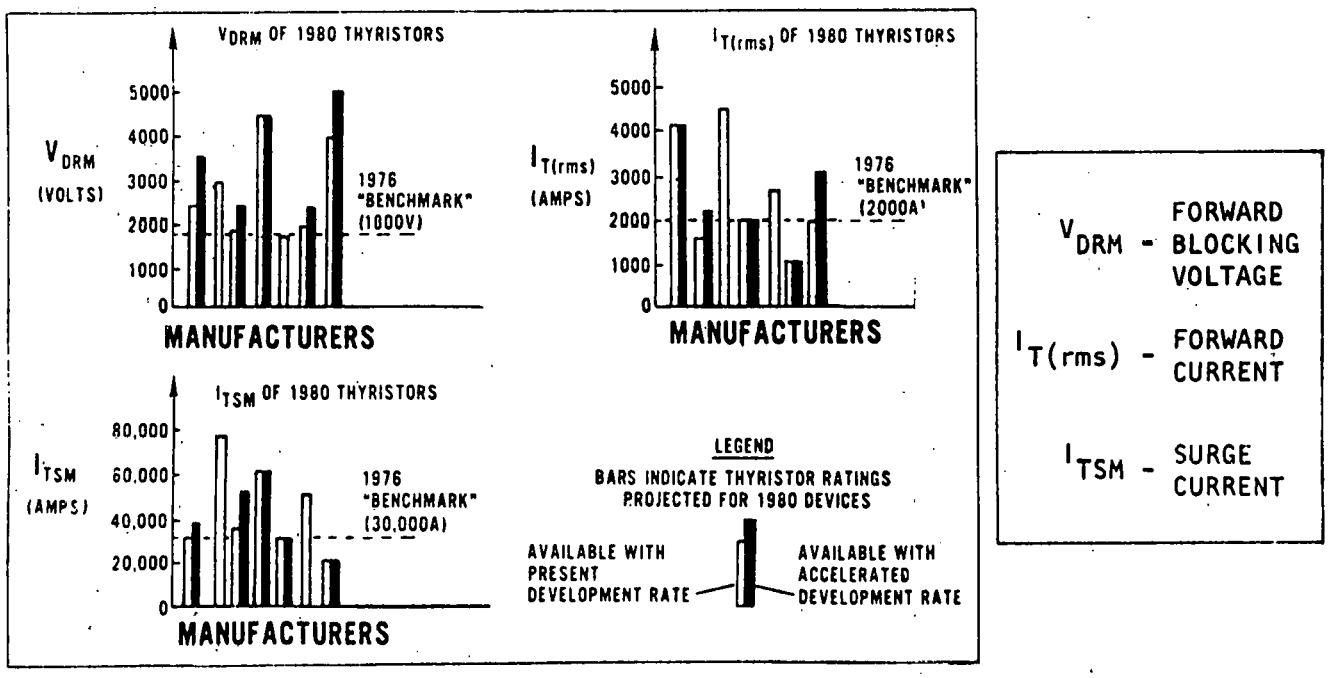

Figure III-20. Projection of Thyristor Characteristics (14)

Future development of high-speed DC breakers is needed. These breakers should withstand more fault interruptions. This could eliminate static DC fault clearing circuits, thus reducing costs (5).

Power factor correction is also needed, especially in schemes in which connection to a utility line is required. Special surge arresters installed at the AC terminals could minimize some of the problems associated with power factor correction requirements.

New circuit designs are expected to evolve. A strong relationship exists between improved circuit design and improved semiconductor and magnetic devices. New circuit designs will exploit innovations in device performance. New types of analytical techniques and digital computer applications will make possible optimum circuit designs and components, which will improve circuit performance. Also, increased use of microprocessors will result in more reliable power conditioners.

New technology is anticipated in the following areas (15):

(1) Power Circuit Design

- New commutation circuits
- New topologies
- Use of active filters
- New computer-aided analytical techniques to determine circuit performance reliability and cost/performance/reliability trade-offs.

(2) Semiconductor Power Devices

- Improved transistors
- Improved thyristors
- Gate-assisted turn-off thyristors
- Gate turn-off thyristors
- Power field effect transistors.

(3) Magnetic Devices

- New transformers using amorphous magnetic materials
- New inductors using amorphous magnetic materials.

(4) Logic and Control

- Advanced microprocessors
- Improved power device modifications

- Improved output regulation
- Data logging
- DC self-diagnostics
- Unified power conditioner and system control in smaller systems
- Unified power conditioner and system self-diagnostics in smaller systems
- Fault annunciation and indication.

F. Power Conditioner Manufacturers and Developers

1. Introduction

There are a number of power conditioner manufacturers, but most of them do not have experience with photovoltaic systems. An extensive search was made for the manufacturers of power conditioners. Ten manufacturers of power conditioners for solar photovoltaic applications were identified. It is expected that as the market develops, more manufacturers will be attracted to the production of these systems. Table III-1 presents a summary of the characteristics of power conditioning equipment by manufacturers. The following is a list of the manufacturers and developers who are developing power conditioners for photovoltaic systems:

Windworks, Inc.
Route 3, Box 44A
Mukwonago, WI 53149
(414) 363-4088

Abacus Controls, Inc.
P.O. Box 893
Somerville, NJ 08876
(201) 526-6010

AiResearch Company of California
2525 West 190th Street
Torrence, CA 90509
(213) 323-9500

Westinghouse Electric Corporation
Aerospace Electrical Division
P.O. Box 989
Lima, OH 45802
(419) 224-0121

TABLE III-1. SUMMARY OF THE CHARACTERISTICS OF POWER CONDITIONING EQUIPMENT BY MANUFACTURER

MANUFACTURER	CHARACTERISTICS						
	Efficiency	Cost	Max Input Voltage	Minimum Input Voltage	Normal Input Operating Voltage Range	Output Frequency	Output Voltage
Windworks	96% max -1Ø 98% max -3Ø	$350-$800 per kW	213.6V DC for 240V AC systems	No Minimum	0-500V	60 cycles	120V AC 240V AC 480V AC
Abacus	90% max	$1,200-$1,525 per kW	310V DC	190V DC	200-300V DC	50, 60 cycles	240/120V AC 208V AC 480V AC
AiResearch	93% max	ND	600V DC	ND	200-300V DC	60 cycles	480/277V
Westinghouse	92% max	$600 per kW	350V DC	200V DC	200-300V DC	60 cycles	208/120V AC 480/277V AC
Soleq	93% max	$750-$2,440	ND	ND	10.5-140V DC	60 cycles	240V AC 120V AC
Delta	95% max	$150-$1,000 per kW	650V DC	ND	200-500V DC	60 cycles	480/277V AC 75-500V DC
United Technologies	89.5% max	ND	ND	ND	130-240V DC	60 cycles	208V DC
Elgar	89% max	$2,600 per kW	ND	ND	21-60V	60, 50 cycles	115V AC 230V AC

ND = No data available

TABLE III-1. SUMMARY OF THE CHARACTERISTICS OF POWER CONDITIONING EQUIPMENT BY MANUFACTURER (Continued)

MANUFACTURER	CHARACTERISTICS						
	Output Power	Total Harmonic Distortion	Power Factor	Reliability (MTBF)	Life	Lead Time on Orders	Operation Mode
Windworks	2 kW-100 kW	ND	ND	ND	ND	8-20 weeks	Utility
Abacus	4 kW-60 kW	4%	0° lead to 0° lag	30,000 hrs	Indefinite	13-18 weeks	Utility & Stand Alone
AiResearch	20-250 kW	<5%	>.90	20,000 hrs	10-20 years	12-18 months	Utility
Westinghouse	62.5 kW	<5%	0.9 lead -0.7 lag	--	20 years	10 months	Utility & Stand Alone
Soleq	2 kW - 60 kW	5%	ND	10,000 hours	30 years	8-12 weeks	Stand Alone
Delta	60-400 kW	<3%	ND	20,000 hrs	20 years	6-9 months	Stand Alone & Utility
United Technologies	48.8 kVA	<15%	.85	ND	ND	29 weeks	Stand Alone & Utility
Elgar	.6 kW-1 kW	5-10%	ND	15,000-30,000 hrs	ND	2-8 weeks	Stand Alone

ND = No data available

Soleq Corporation
5969 North Elston Avenue
Chicago, IL 60646
(312) 792-3811

Delta Electronics Control Corporation
2801 South East Main Street
Irvine, CA 92714
(714) 546-4731

United Technologies Corporation
Power Systems Division
Box 109
South Windsor, CT 06074
(203) 727-2264

Elgar Corporation
8225 Mercury Court
San Diego, CA 92111
(714) 565-1155

Cyberex, Inc.
7171 Industrial Park Blvd.
Mentor, Ohio 44060
(216) 946-1783

Nova Electric
263 Hillside Avenue
Nutley, NJ 07110
(201) 661-3434

The following is a list of power conditioners used in various photovoltaic applications experiments:

Application	Operated by	PCU Mfr.	KVA Rating
Irrigation Pumping Mead, Nebraska	MIT-Lincoln	Nova	22.5 (3x7.5)
Park Headquarters Nat. Bridges, Utah	MIT-Lincoln	Cyberex Nova	50 5 (UPS)
Radio Station Bryan, Ohio	MIT-Lincoln	Nova	5
Test Facility Lexington, Mass.	MIT-Lincoln	Abacus	6
Test Facility Arlington, Texas	UT-Arlington MIT-Lincoln	Windworks	8

Application	Operated by	PCU Mfr.	KVA Rating
Radar Facility Mt. Laguna, Calif.	DOD-Meradcom	Delta	60
Mississippi County Community College Blytheville, Ark.	TEAM	Delta	300
NW Mississippi Junior College Senatobia, Miss.	-----	TBD (RFQ)	3x50 1x2
DC Application Schuchuli Village Arizona	NASA-Lewis	NASA-Lewis	3.5 kW
Remote Village Upper Volta, Africa	NASA-Lewis	NASA-Lewis	1.8 kW
Village Power System Saudi Arabia	SERI	TBD (RFQ)	350

NOTE: TBD - To be Determined
RFQ - Request for Quotation
UPS - Uninterruptible Power System

2. Windworks Power Conditioner

a. Background. Windworks is presently manufacturing current-fed line-commutated DC/AC power conditioners. These units can operate only in parallel with a utility. At present they are manufacturing single-phase units rated at 4 kW and 8 kW and 3 Ø units rated at 20 kW, 40 kW, 50 kW, and 100 kW. Single-phase units rated up to 15kW and three-phase units rated up to 1.5 MW will be available in the future. While the 3 Ø systems are capable of supplying unbalanced 3 Ø loads, it is not desirable to operate in that mode because it will inject harmonics into the utility line (16).

b. Operating Principle. The Gemini synchronous inverter, when interposed between a variable voltage DC source and an AC source, converts the DC power to AC at standard line voltages and frequencies. In operation, all the available DC power is converted to AC. If more power is available from the solar arrays than is needed by the load, the excess power can be fed to the utility AC line. If less power is available from the solar arrays than required by the load, the difference is provided by the utility AC line. Thermal, chemical, or

electrical energy storage may be added to the system. When storage is used, controls are available which will monitor the net power demand from the AC lines and direct the excess power to the storage system.

Automatic tracking units have been developed which can utilize the highest output by varying the array loading.

The technology of the inverter is derived from solid-state industrial drive circuitry. The inverter operates on the principle of synchronous inversion.

In operation, the control circuit of the inverter senses the instantaneous AC line voltage and connects the solar array to the utility AC line during that portion of each sine half-wave when the voltage produced by the array is greater than the utility voltage. Power flows from the higher to the lower voltage. When the utility voltage exceeds the array voltage, the control circuitry disconnects the two sources. The inverter then waits until the beginning of the next half-cycle before reconnecting the two sources.

Figure III-21 shows how current pulses are fed into the line. The magnitude of the pulse is dependent on the amount of power that is being fed into the line, while the duration depends on the relative voltages of the two sources. Note that the current is negative when the voltage is positive, indicating that the array is feeding power to the utility.

c. Basic Subsystems. The basic subsystems consist of the following:

(1) Metering circuitry

(2) Control electronics

(3) Power electronics

(4) Magnetic control.

The metering circuitry consists of panel meters, the current sensing shunt, and the selector-switch test circuitry. The metering circuit is used to program the inverter for specific load demand curves. During normal operation, it monitors system performance.

The control electronics are contained in a regulator printed circuit board. The firing of the SCRs is controlled by this circuitry. The power electronics consist of silicon-controlled rectifiers, the optical firing circuit board (isolates control circuitry from power circuitry), filter, and fuses. The power electronics transfer power from the DC source to the AC source.

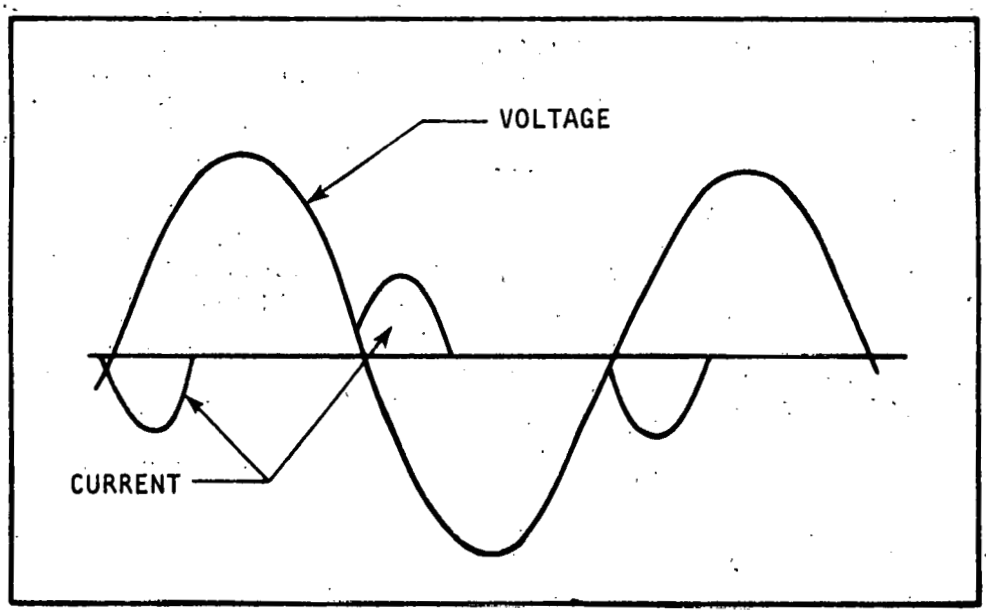

Figure III-21. Voltage and Current Waveform from a Gemini Inverter (17)

The magnetic control consists of the DC contactor and the on/off switch. It connects the DC source to the inverter during normal operation. If AC power fails, the contactor opens its contacts and disconnects the DC source from the AC lines.

d. Specifications. The following are specifications of Windworks inverters suitable for photovoltaic applications (17):

Input	Specification
Maximum Voltage	213.6V DC for 240V AC system 106V DC for 120V AC system
Minimum Voltage	No Minimum
Normal Operating Range	0-100V DC for 1 Ø systems 0-200V DC for 1 Ø systems 250V DC for 3 Ø systems 500V DC for 3 Ø systems
Output	
Voltage	120V AC 240V AC 480V AC
Power	2 kW, 4 kW, 8 kW, 15 kW for 1 Ø systems 20 kW, 40 kW, 50 kW, 100 kW for 3 Ø systems
Efficiency	97% at rated load for 1 Ø systems 96% at rated load for 3 Ø systems 97% at 50% load for 1 Ø systems 95% at 50% load for 3 Ø systems (exclusive of optional filters and transformers)

Physical Characteristics

Size	17.8 cm x 30.5 cm x 45.7 cm (7"x12"x18") for 4 kW, 1 Ø units 20.3 cm x 35.6 cm x 55.9 cm (8"x14"x22") for 8 kW, 1 Ø units 0.91 m x 1.22 m x 0.34 m (3'x4'x13-1/2") for 15 kW, 1 Ø units 0.91 m x 1.22 m x 0.34 m (3'x4'x13-1/2") for 20 kW-100 kW, 3 Ø units

Weight	12.3 kg	(27 lbs) for 4 kW, 1 Ø systems
	25.5 kg	(56 lbs) for 8 kW, 1 Ø systems
	90.9 kg	(200 lbs) for 20 kW, 3 Ø systems
	113.6 kg	(250 lbs) for 40 kW, 3 Ø systems
	136.4 kg	(300 lbs) for 50 kW, 3 Ø systems
	159.1 kg	(350 lbs) for 100 kW, 3 Ø systems

Protection	Fuses in AC line Fuses in DC circuit Contactor in DC circuit Surge suppressors
Meters	DC Ammeter Voltmeter AC and DC power indicator for lights

The following options are available:

(1) Interface filters: If the DC source is of low impedance, an inductive or an inductive/capacitive filter may be required. Air core reactors and electrolytic capacitors are normally used.

(2) Maximum power tracker: Automatic power tracking circuitry can be built in. The tracker seeks the operating level which results in the maximum power conversion from the array.

(3) Isolation transformers: When DC source voltage is too low or too high with respect to AC line voltage or for applications requiring grounding of the DC source, isolation transformers can be provided.

(4) DC field supplies: If shunt-wound generators are used, the field supply can be built into and controlled by the inverter.

The following are new products that will be available in the future:

(1) AC/DC wattmeters: Watthour meters and VAR meters will be available for various ratings. The meters will be available with analog or digital readouts. Meter error is less than 1 percent of full scale for frequencies up to 1,000 Hz.

(2) Load management hardware: An AC dumping circuit is presently under development which dumps the surplus generated power to a non-critical load instead of feeding back to the utility. A DC-dumped circuit is also under development which allows storage of surplus DC energy in a battery system. When the battery reaches a minimum charged state and sufficient power is not available from the arrays to meet the load, the system automatically shuts down. Batteries can also be charged from the AC line with little additional circuitry.

e. Maintenance, Repair, and Warranty. Windworks inverters are guaranteed for one year. The factory representatives do not recommend any spare parts and long-term maintenance contracts are available. For repair of the power conditioning units, the smaller units must be shipped to the factory, whereas for the larger units the factory is notified. The factory representatives will then make site visits and perform the necessary repair work (16).

f. Cost and Availability. The list prices for the single-phase power conditioners are as follows (17):

Power Conditioners

Power Capacity (kVA)	Input Voltage (VDC)	Maximum Current (Amps)	Output Voltage (VAC)	List Price ($)
2	100	20	120	1,075
4	200	20	240	1,050
4	100	40	120	1,850
8	200	40	240	1,825
15	200	75	240	3,900

Filters

Power Capacity (kVA)	Maximum Current (Amps)	Inductance (mH)	List Price ($)
4	20	20	475
8	40	10	590
15	100	5	850

Field Protection Circuit: $40

Special Enclosure Cabinets: Basic Enclosure: $100
End Cover, Louvered: $30

The lead time on orders for the single-phase units up to 80 kW is 4 to 8 weeks. For the three-phase units up to 100 kW, 16 to 20 weeks of lead time are anticipated. For larger sizes, longer lead times can be expected (16).

g. Test Results by Wisconsin Electric Power Company. Table III-2 shows results of tests conducted by Wisconsin Electric Power Company on a single-phase Gemini Inverter at various power loadings and for various AC loads. The performance of three-phase systems is much better than that of the single-phase systems because higher DC voltages may be used for the three-phase systems.

TABLE III-2. TEST RESULTS OF 2KW AND 6KW INVERTERS (17)

	Gemini Output: 2kW			Gemini Output: 6kW		
	No Load	Res Load	Res Cap Load	No Load	Res Load	Res Cap Load
LINE						
AC volts	235	232	233	238	235	235
AC Amps	14.3	14.0	7.5	37.5	28.3	20.0
kVA	3.36	3.25	1.75	8.93	6.65	4.70
kW	-2.035	1.925	1.935	-5.93	-1.90	-1.90
kVAR	2.84	2.709	0.125	6.559	6.231	3.612
LOAD						
kW	0	3.927	4.00	0	4.015	4.015
GEMINI						
DC Volts						
Input	190.8	190.5	190.6	180.0	180.6	180.4
DC Amps						
Input	12.2	12.2	12.2	35.5	35.5	35.5
Output kW	2.03	2.047	2.057	6.0	6.0	6.0

Res = Resistive
Cap = Capacitive

h. Test Results at The DOE/LeRC Photovoltaic Systems Test Facility. At the DOE/LeRC photovoltaic systems test facility, an 8-kW single-phase current-fed line-commutated

inverter developed by Windworks has been tested in a photovoltaic power system. The inverter operates in parallel with the utility line. The utility can accept power or provide power and acts as a virtual energy storage system.

Figure III-22 is a simplified block diagram of the inverter in a photovoltaic system. Figure III-23 depicts the inverter and typical current and voltage waveforms. The inverter consists of an 8-kW thyristor bridge, a series inductor, a shunt capacitor, and a 15-kVA transformer. During the first half-cycle of the AC voltage waveform, thyristors A and B are turned on. At $90° < \omega t = \gamma < 180°$, turn-on occurs and current conduction stops at 180°. The thyristors C and D are turned on at $\gamma + 180°$ and conduction continues up to 180°. This process continues and AC current is generated at the output of the inverter. The AC current output is harmonically distorted. The output current lags the voltage and the AC system must supply the reactive volt-amperes to compensate for the leading current output (18).

Figure III-24 indicates AC output voltage and current waveforms for 200V and 25 amps input to the inverter, and with an input capacitance of 30,000 μF and input inductance of 20 MHz. For the current waveform, the form factor was 1.24, distortion factor was 1.04, and total harmonic distortion was 0.28. For the voltage waveform, the form factor was 1.11, distortion factor was 1.00, and total harmonic distortion was 0.03. The voltage waveform is almost a sine wave and its total harmonic content is small. However, the output current waveform has higher harmonic content.

During initial operation, capacitance was needed to prevent the cyclical momentary collapse of solar array voltage when inverter peak current greatly exceeded the current available from the array. Figure III-25 shows efficiency and power factor as a function of shunt capacitance and inductance. By increasing the shunt capacitance and inductance, both efficiency and power factor are increased.

Figure III-26 shows efficiency as a function of input current and reciprocal of DC input voltage. Maximum efficiency was attained at about half the rated power of the inverter. At 200V DC input voltage, the peak efficiency was 88 percent at half-rated inverter input power and 82 percent at 15 percent rated power.

Figure III-27 shows the power factor as a function of DC input voltage and input current. The power factor ranged from 36 to 72 percent and lagging reactive volt-amperes were required from the utility line. The maximum attainable power factor was determined to be 77 percent at 208V input voltage and 40 amps input current. Power factor also increased with increases in input voltage and current.

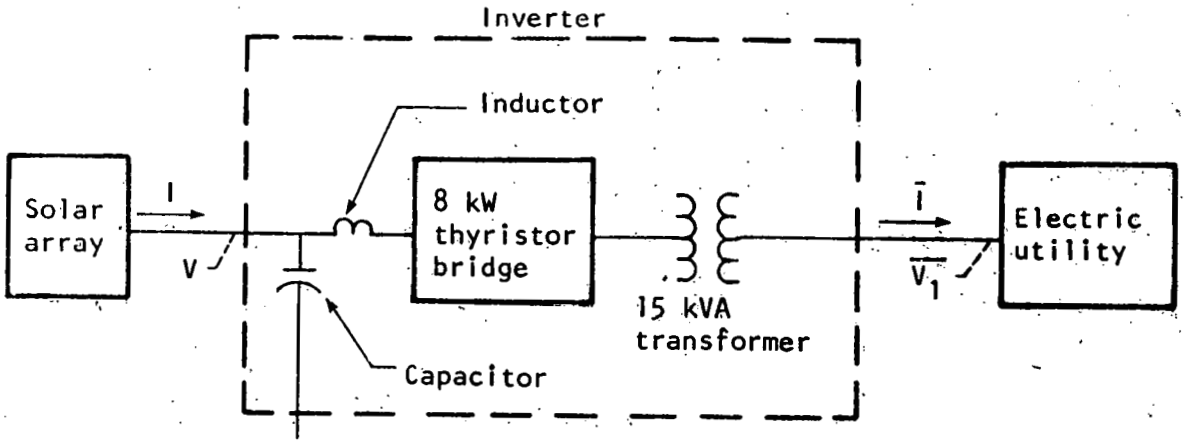

Figure III-22. A Single-Phase Line-Commutated Inverter in a Photovoltaic Power System (18)

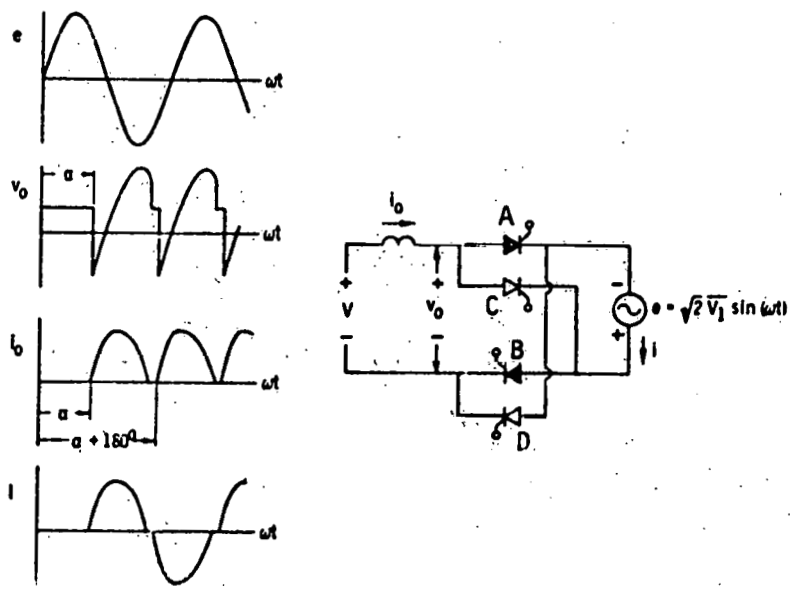

Figure III-23. A Single-Phase Line-Commutated Inverter and Typical Current and Voltage Waveforms (18)

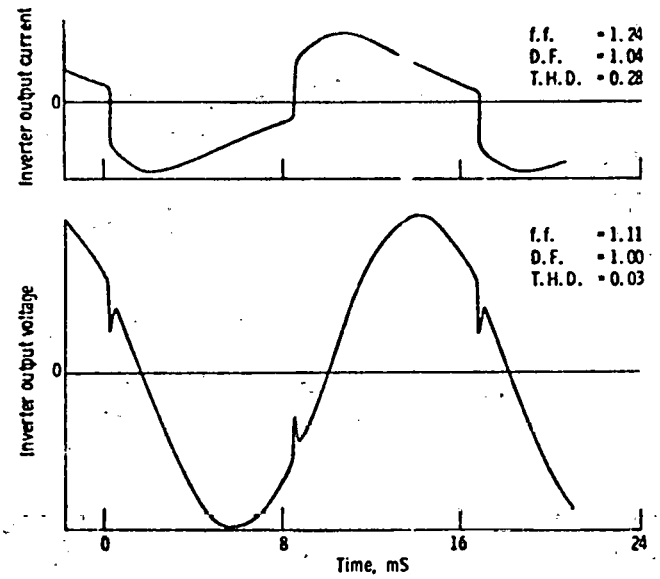

Figure III-24. Output Current and Voltage Waveforms for 25 A and 200 V Input to the Single-Phase Line-Commutated Inverter (30,000 μF Shunt Capacitance and 20 mH Series Inductance)(18)

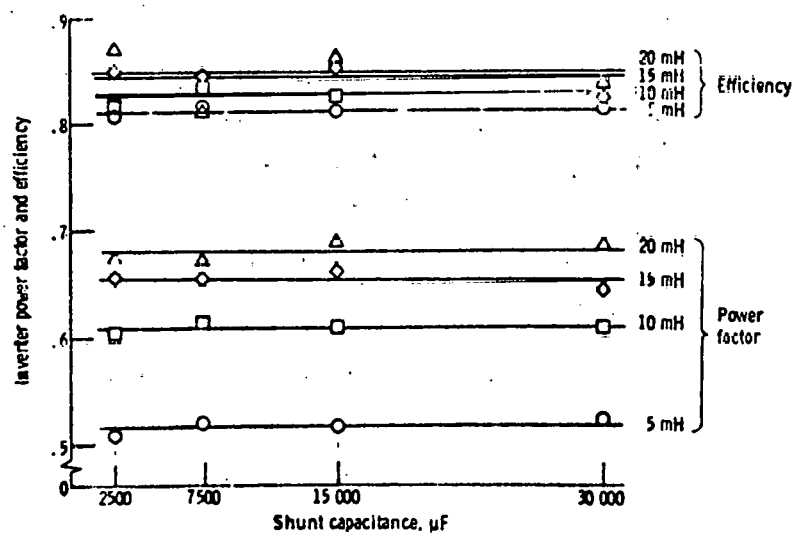

Figure III-25. Effect of Input Capacitance and Inductance on Efficiency and Power Factor of the Single-Phase Line-Commutated Inverter for 24 A and 200 V Input Conditions (18)

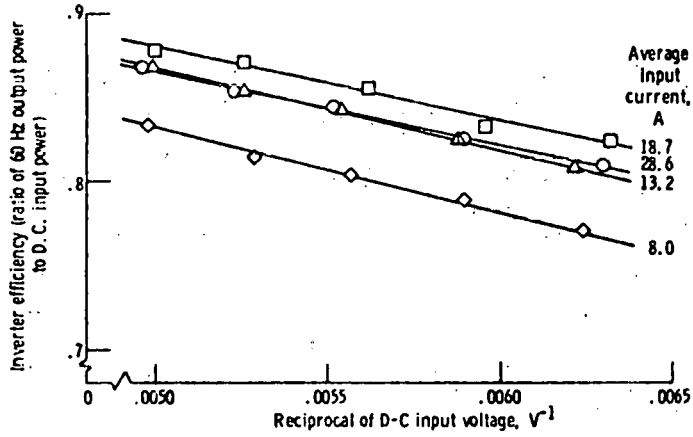

Figure III-26. Effect of Input Voltage and Current on Efficiency of the Single-Phase Line-Commutated Inverter: Filter Capacitance 30,000 μF and Inductance 20 mH (18)

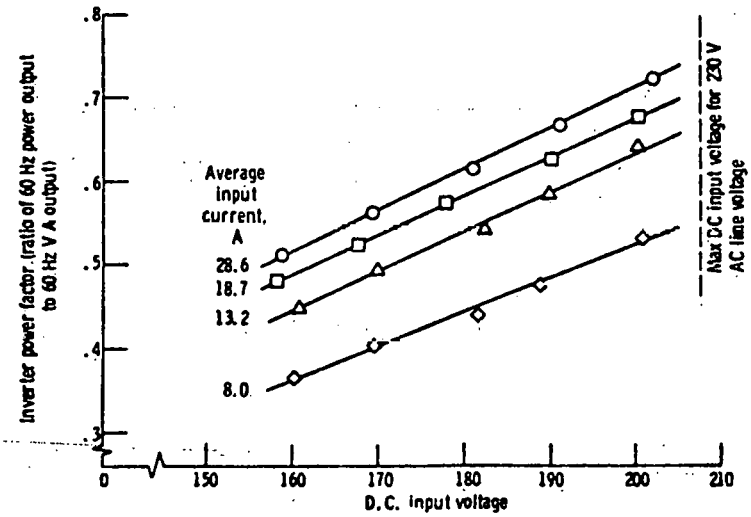

Figure III-27. Effect of Input Voltage and Current on Power Factor of the Single-Phase Line-Commutated Inverter: Filter Capacitance 30,000 μF and Inductance 20 mH (18)

3. Abacus Controls, Inc. Power Conditioners

a. Background. Abacus Controls, Inc., is presently manufacturing forced-commutated DC/AC power conditioners using transistors. These units have the capability of operating in stand-alone or utility interface modes. At present they are manufacturing units rated at 4 kVA to 10 kVA, 1 Ø. These 1 Ø units can be connected in combination to produce 3 Ø units. The 3 Ø units can operate with unbalanced 3 Ø loads. 3 Ø units are available in 30 kVA and 60 kVA ratings. Abacus Controls, Inc., is currently developing a low-cost 10 kVA inverter for Sandia Laboratories, after which they intend to commercially produce inverters rated up to 50 kVA. The larger units are expected to be available in 1980 (19).

b. Principle of Operation. The Abacus Controls AC power source uses digital sine wave synthesis technology. Digital sine wave synthesis applies digital techniques to convert DC to AC (Figure III-28). Switching power circuits, digital filtering, and three-phase pulse patterns stored on a memory IC provide the AC power source. A pulse pattern for a sine wave is stored on an integrated circuit menory. Amplitude of the voltage is controlled by changing the dwell time at zero volts in the stored pulse pattern. The pulse pattern has harmonics of the fundamental frequency above tenth, which are filtered by the LC filter. The low-order harmonics are eliminated digitally; no bulky filters are needed. A current limit signal overrides the voltage feedback signal during overload conditions. When the overload is removed, the system automatically returns to voltage-regulated output. No tuning filters are required for switching and, hence, operation into zero lag or zero lead power factor does not damage the AC power source.

c. Specifications. The following are specifications of Abacus Controls, Inc., inverters suitable for photovoltaic applications (20):

Input	Specification
Maximum voltage	310V DC
Minimum voltage	190V DC
Normal operating range	200-300V DC
Output	
Frequency	50,60
Voltage	240/120V AC, 1 Ø 208V AC, 3 Ø 480V AC, 3 Ø or as required

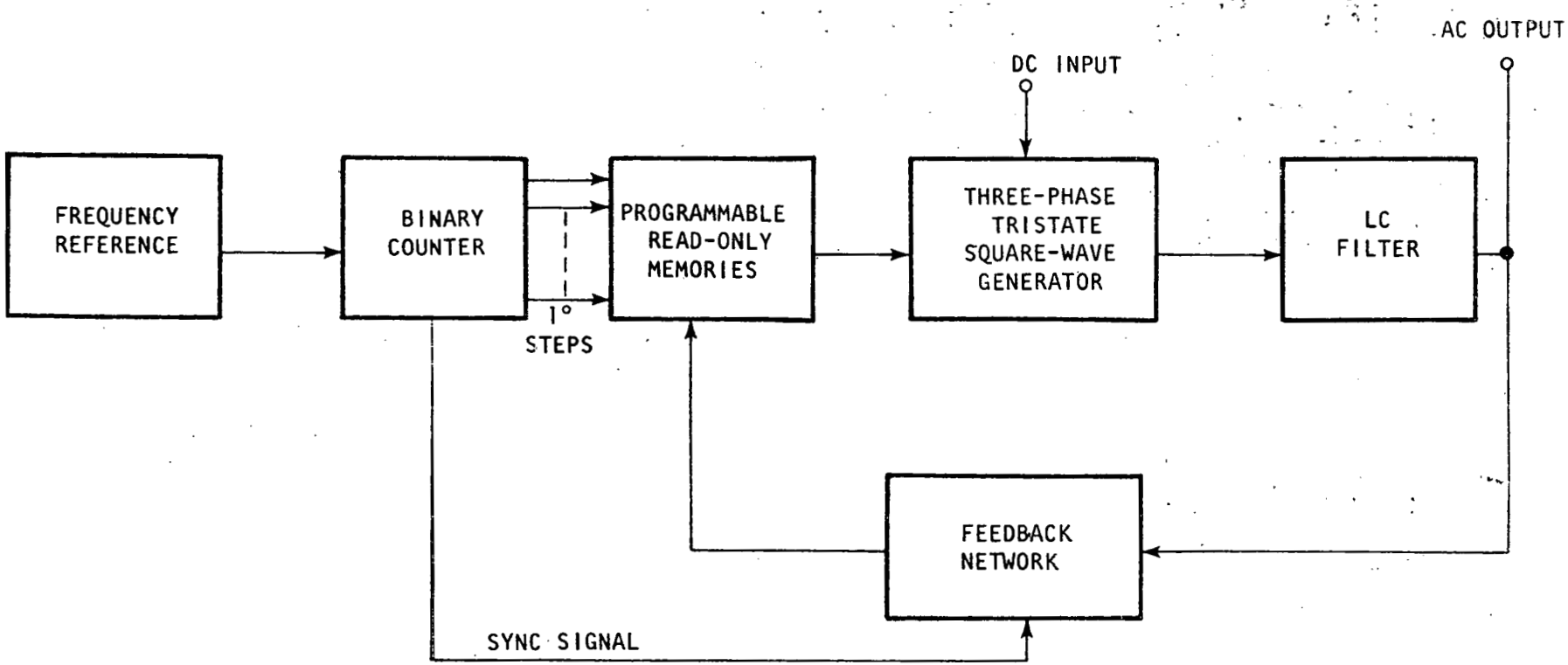

Figure III-28. Block Diagram of the Digital Sine Wave Synthesis Technology (20)

Power	4 kVA, 6 kVA, 10 kVA for 1 Ø units 30 kVA, 60 kVA for 3 Ø units
Short-term rating	125% of continuous rating for 10 seconds
Efficiency	90% for full load to 25% load
Total harmonic distortion	4%
Power factor	0° Leading to 0° lagging
Reliability (mean time between failures)	30,000 hours
Life	Indefinite

Physical Characteristics

Size
1.2 m x .61 m x .61 m (48"x24"x24") for 4 kVA and 6 kVA 1 Ø
1.83 m x 0.66 m x .76 m (72"x26"x30") for 10 kVA, 1 Ø

Weight

109 kg	(240 lbs)	for 4 kVA, 50 ~, 1 Ø
105 kg	(230 lbs)	for 4 kVA, 60 ~, 1 Ø
182 kg	(400 lbs)	for 6 kVA, 50 ~, 1 Ø
177 kg	(390 lbs)	for 6 kVA, 60 ~, 1 Ø
245 kg	(540 lbs)	for 10 kVA, 50 ~, 1 Ø
236 kg	(520 lbs)	for 10 kVA, 60 ~, 1 Ø

Environment

Operating temperature range: 0 to 40°C (32 to 104°F)

Protection

Stand-alone operation	Short circuit Under-over voltage in output Overcurrent in output
Utility tie operation	Short circuit Under-over voltage in output Overcurrent in output Utility voltage high-low in dication Out of synchronization Solar system cutoff due to utility failure

Options	Maximum power tracker, capability to return AC power to utility lines (future), meters

d. Cost and Availability. The approximate list price is $6,100 for the 4 kVA units, $8,500 for the 6 kVA units, and $12,000 for the 10 kVA units (21). The lead time on orders for units rated 10 kVA or less is 13 to 16 weeks, whereas for the large units, 16 to 18 weeks is anticipated (21).

e. Repair, Maintenance, and Guarantee. The standard units have a one-year warranty limit. The spare parts recommended are the active components, e.g., printed circuit cards, big power semiconductors, etc. For repair of the power conditioning units, the smaller units are shipped to the factory, whereas for the larger units the factory is notified. The factory representatives then make site visits (20).

f. Contract with NASA-LeRC. A contract was awarded to Abacus Controls, Inc., for the design and fabrication of a 10 kVA forced-commutated inverter suitable for photovoltaic application. Major operating features of the inverter include:

(1) High efficiency both at full load and light loads

(2) Stand-alone and utility connection capability

(3) Provision for external control of the operating power level when connected to the utility system

(4) Use of off-the-shelf technology.

The input voltage of the inverter is 200 to 300V DC and the output voltage is 240V AC. Single-phase design performance goals are as follows:

(1) An inverter capable of withstanding 150 percent of peak load for one minute and 125 percent for 15 minutes.

(2) Losses of less than 250 watts at no load and less than 1,100 watts at full load.

(3) Harmonic distortion of less than 5 percent. Figure III-29 shows the efficiency and losses as a function of inverter output. Efficiency remains at a high level even at low loadings.

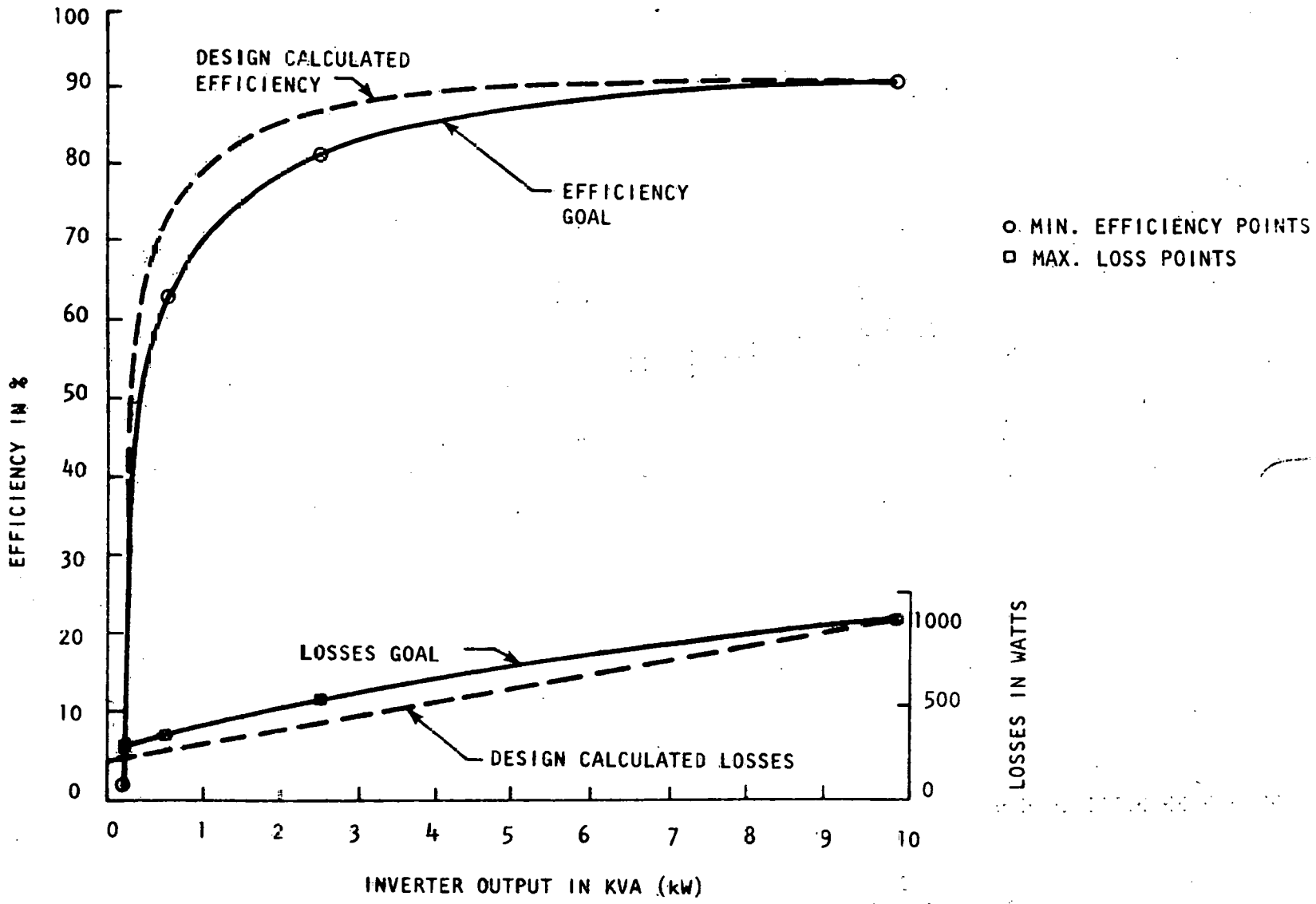

Figure III-29. 10 kVA Self-Commutated Inverter Goals for Efficiency and Losses (21)

g. Current Contracts with Sandia Laboratories. Current Abacus Controls contracts with Sandia Laboratories for the development of power conditioning units are as follows:

(1) Abacus Controls 10 kVA "Sunverter"

(2) Abacus 10 kVA Advanced Design.

Figure III-30 is a block diagram of the Sunverter. The following are the characteristics of the Sunverter (2):

Rating: 10 kVA

Output: 60 Hz, 1 phase, 240V AC

Input: 200-300V DC

Type: Dual bridge, transistor, digitally synthesized

Efficiency: Greater than 90% at full load

Total harmonic distortion: Less than 5 percent

Utility tie: Automatically synchronized with line

Additional:

- Improved version of NASA/LeRC unit
- Operates stand-alone or utility tie
- Automatic start-up and shut-down
- Maximum power tracker

Figure III-31 is a block diagram of the Abacus advanced-design 10 kVA power conditioner. The unit has the following characteristics:

Rating: 10 kVA

Output: 60 Hz, 1 phase, 240V AC

Input: 200-300V DC

Type: Conventional SCR bridge followed by controlled ferroresonant transformer

Efficiency: 54% at 5% load
84% at 25% load
92% at 100% load

Total harmonic distortion: Less than 2 percent

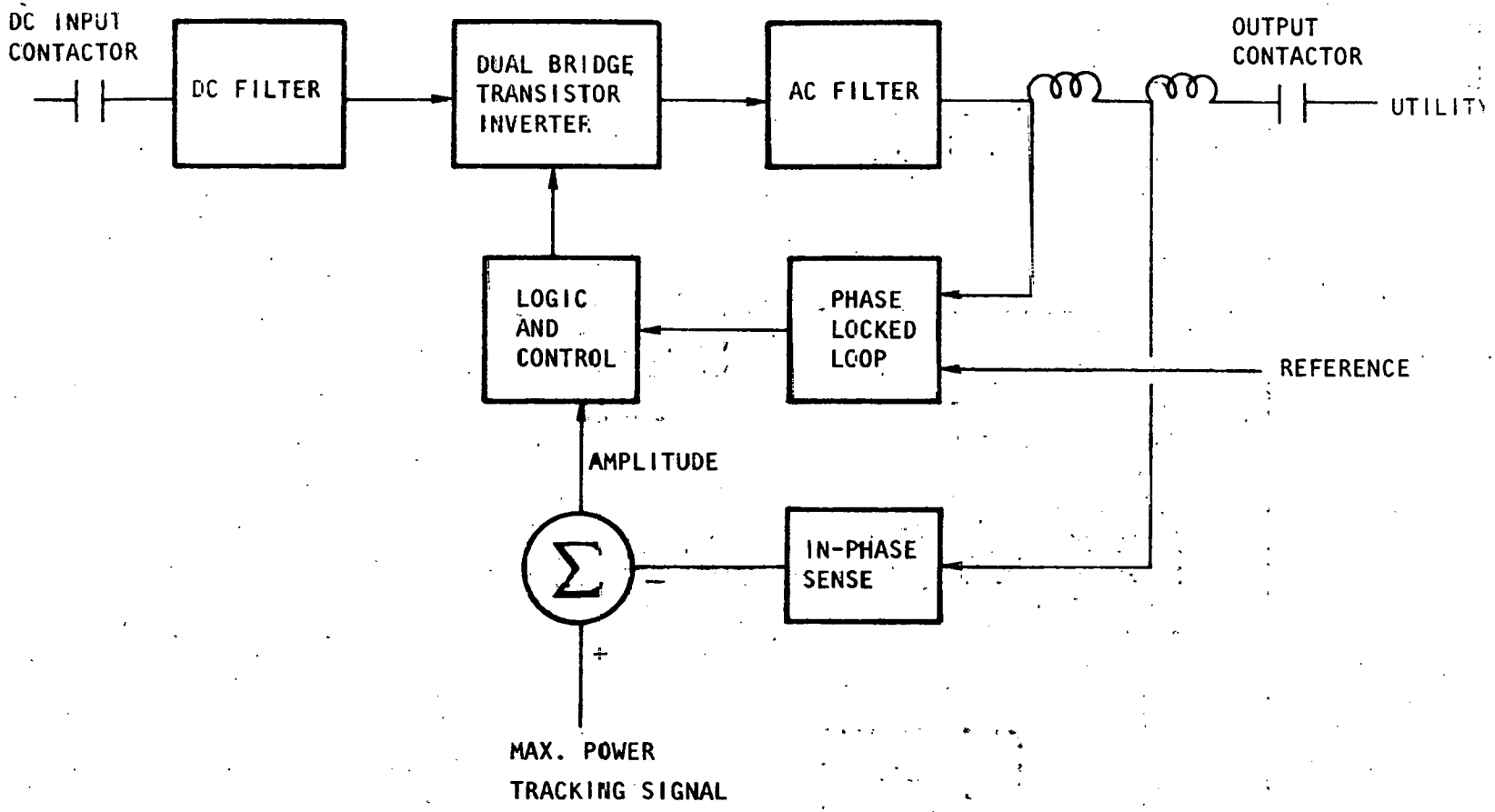

Figure III-30. Abacus "Sunverter" Power Conditioning Unit (2)

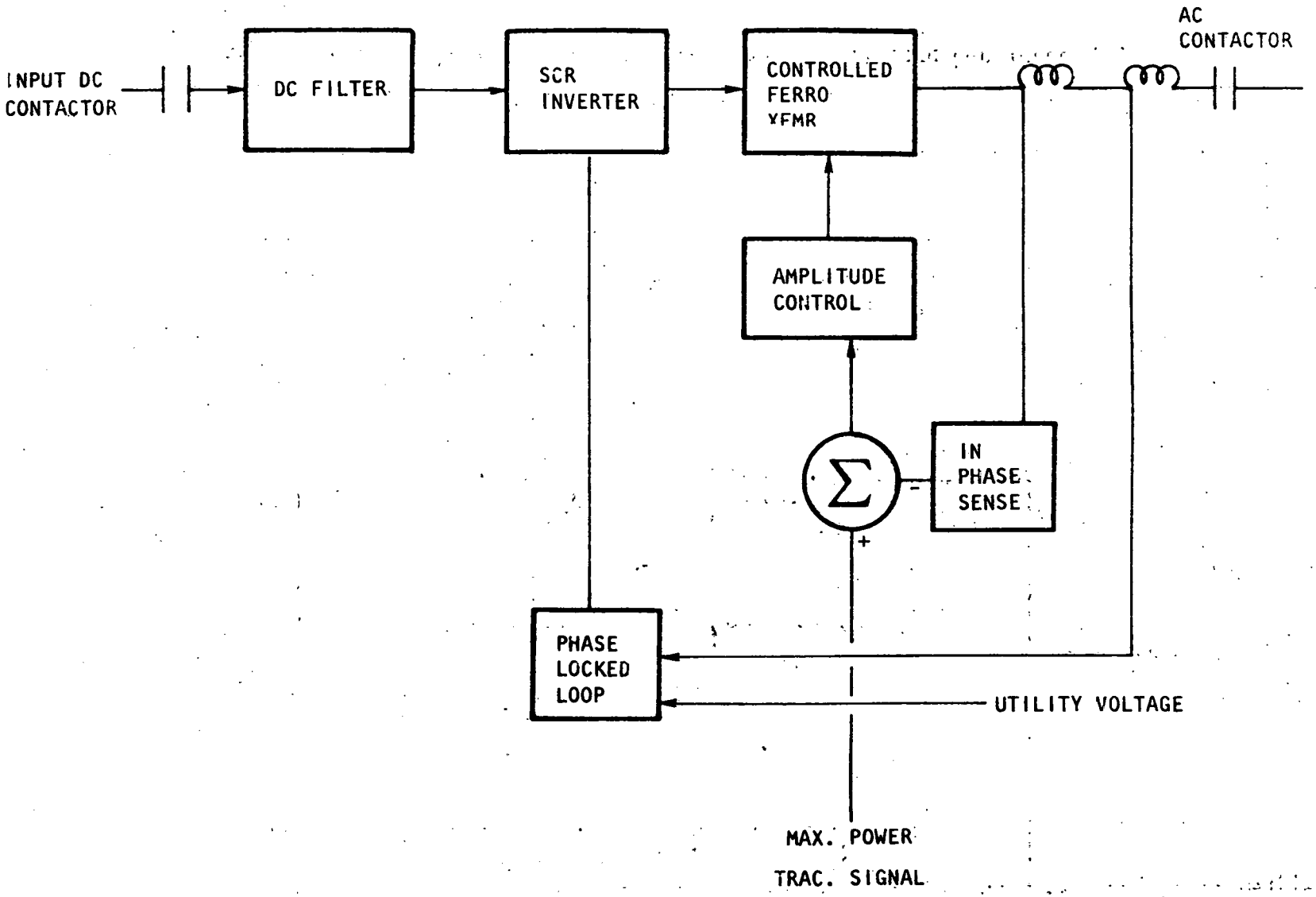

Figure III-31. Abacus Advanced Design 10 kVA Power Conditioning Unit (3)

Utility tie: Automatically synchronized with line

Additional:

- Operates only in parallel with utility
- Automatic start-up and shut-down
- Maximum power tracker

4. Elgar Corporation Power Conditioners

a. Background. The Elgar Corporation has been involved in the manufacture of AC power supplies since 1965. They are currently manufacturing a line of low-power-output, forced-commutated inverters specifically designed for use with solar photovoltaic cells, fuel cells, and windmill generators. This alternative energy source line of inverters is designed to provide AC power from a DC source. The inverters operate in a stand-alone mode and are not intended for operation in parallel with utility lines. Elgar's line of inverters is available in two basic types: a High-Inrush series and a Precise series. The Precise series offers ±2 percent output voltage regulation, while the High-Inrush series offers inrush currents of up to four times rated steady-state output. Both series are currently available in two power sizes: 0.6 kVA and 1 kVA, both of which are available with a choice of two nominal input voltages -- 24V DC or 48V DC. Output voltage is the standard 115V AC at 60 Hz. Both the High-Inrush series and the Precise series can be obtained in the optional 230V AC, 50 Hz output voltage range.

Original equipment manufacture (OEM) packages are available. For OEM applications of at least 50 pieces, Elgar will adapt their line of alternative energy supply inverters to power levels from .1 kVA to 3 kVA in form factors designed to fit specific application needs. Elgar is also considering manufacturing some larger units in the alternative energy supply line of inverters in the near future.

b. Operating Principle. Elgar's inverter circuitry uses power transistor switches capable of switching high-current DC through a low forward impedance by means of a magnetics design which delivers a control pulse to the base of each transistor used. Figure III-32 is a simplified block diagram of a 48V DC input, 1kVA high inrush series inverter. A DC input filter is provided to eliminate transients. The control circuit contains the electric circuit board and magnetics which control the turning on and off of the solid-state switches. This results in the waveform A-B. The inverter output filter smooths out these rectangular pulses

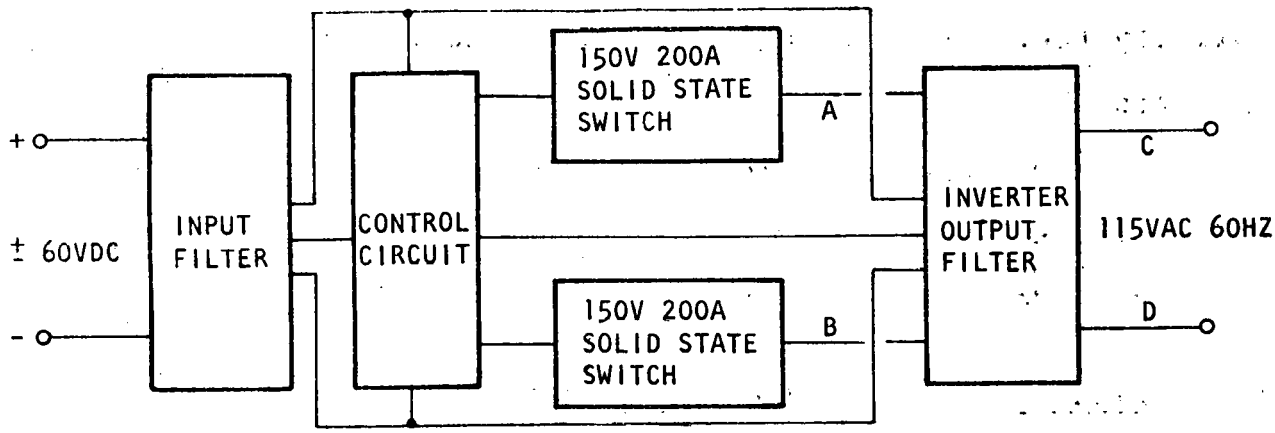

a. Simplified Block Diagram of 1KVA 48 VDC Nominal Input High-Inrush Series Elgar Inverter

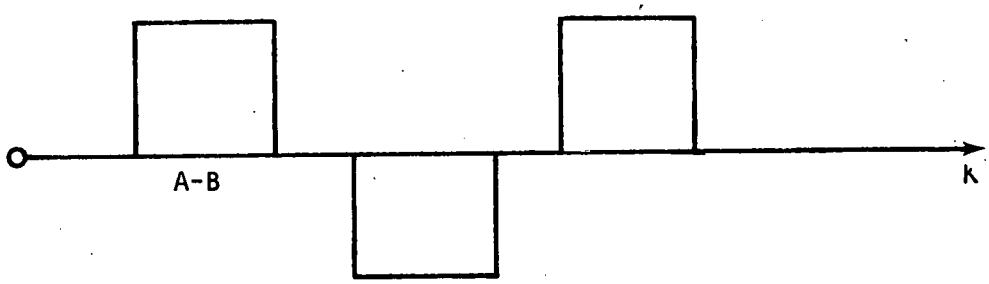

b. Output Waveform at Points A-B

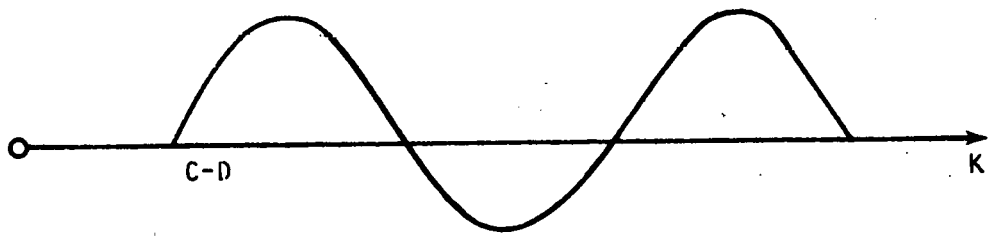

c. Final Output Waveform at Points C-D

Figure III-32. Simplified Block Diagram of an Elgar Inverter (22)

into the 60 Hz 115V AC sine wave, as shown in the waveform C-D which has a total harmonic distortion of 10 percent or less.

c. Specifications (22).

(1) General Specifications.

Input Voltage Ranges: 21-30V DC for nominally 24V DC models, 42-60V DC for nominally 48V DC models.

Input Ripple: 3% maximum

Efficiency: At 85-100% of rated load:

24V DC models: 84% typical
82% minimum

48V DC models: 89% typical
86% minimum

Output Rating: Full VA rating at 0.6 lead

Output Rating Regulation:

High-inrush series: ±5% full range of input line with a fixed resistive load, 95-130V AC for full input voltage range and all load conditions, including motor load startup.

Precise Series: ±2% line, load, and temperature.

Output Frequency Stability: ±0.5%

Operation Temperature: -10 to 60°C (+14 to 140°F)

Relative Humidity: 0 to 95 percent

Operating Altitude: Sea level to 3,048 m (10,000 feet)

Storage: -20 to 71°C (-4 to 160°F), sea level to 12,469 m (40,000 feet)

Protection: Output-electronic current limit; input fuse

Remote Control: The inverter may be operated by remote control.

(2) Detailed Specifications. Detailed specifications are shown in Table III-3.

d. Other Features. The Elgar inverter series for alternative energy sources are housed in convection-cooled, weatherproof packages suitable for outdoor installations at temperatures up to 60°C (140°F). All the models in this series may be mounted in any axis and, hence, are suitable for drawer, floor, or wall applications.

e. Maintenance, Repair, and Warranty. Elgar inverters have a one-year warranty on parts and labor. Inverters shipped to the factory will be serviced free of charge during the warranty period. Field service is provided but the customer must cover travel and living expenses of repair personnel. There are no spare parts recommended. Maintenance contracts are available on customer equipment which is out of warranty (23).

f. Cost and Availability. The Elgar power conditioning units for alternate energy sources are available for $2,600 per kW. Maintenance costs are estimated to average $100 annually after the warranty period. The 48V DC nominal input voltage units are available for delivery two weeks after the order is placed, while the 24V DC nominal input voltage units are available eight weeks after an order is placed (23).

5. Soleq Corporation Power Conditioners

a. Background. Soleq Corporation is presently manufacturing two types of voltage-fed forced-commutation type inverters. The Soleq "B" sine wave inverter and the Soleq windmill inverter are both designed for DC/AC stand-alone or master/slave operation. The units are not intended for operation in parallel with utility lines. At present, the Soleq windmill inverter is available in 1 Ø units, rated 1.5, 3, and 6 kVA. The Soleq "B" sine wave inverter is available in 1 Ø units, rated 2, 4, and 8 kVA. Both units are identical in their parameters of performance and principle of operation. The Soleq "B" inverter uses the less-expensive vented-rack panel-construction and is available at a lower cost. Soleq has expressed an interest in selling 1 Ø units in sizes up to 200 kVA and 3 Ø units in sizes up to 500 kVA if there is a demand (24).

TABLE III-3. DETAILED SPECIFICATIONS OF ELGAR POWER CONDITIONERS (22)

	High-Inrush Series				Precise Series			
Rating	600VA	600VA	1000VA	1000VA	600VA	600VA	1000VA	1000VA
Input VDC	21-30	42-60	21-30	42-60	21-30	42-60	21-30	42-60
Output VAC	115,230	115,230	115,230	115,230	115,230	115,230	115,230	115,230
Output Frequency, Hz	60,50	60,50	60,50	60,50	60,50	60,50	60,50	60,50
Minimum Available Starting Current, A	21	21	35	35	N/A	N/A	N/A	N/A
Overcurrent Set Point, A	15.7	15.7	26	26	6.5	6.5	11	11
Output Distortion, %THD, maximum	10	10	10	10	5	5	5	5
MTBF, hours	25,00	30,000	20,000	25,000	20,000	20,000	15,000	20,000
Physical Size LxWxD, in.	.46x.43x.18	.46x.43x.18	.56x.43x.18	.46x.43x.18	.18x.48x.48	.18x.48x.48	.36x.48x.48	.18x.48x.48
Physical Size, LxWxD, cm.	18x17x7.25	18x17x7.25	22x17x7.25	18x17x7.25	7x19x19	7x19x19	14x19x19	7x19x19
Weight, Kg	29.5	27.3	34.5	31.8	31.8	29.5	43.2	36.4
Weight, lbs	65	60	76	70	70	65	95	80

THD - Total harmonic distortion

MTBF - Mean time between failures

b. Operating Principle. Figure III-33 shows a simplified block diagram of a Soleq power conditioning unit. The power control observes the output amplitude delivery from the array. It senses the DC voltage and cuts off when the voltage level exceeds a specified voltage range. The control logic senses the AC current and amplitude and the DC voltage and current, and performs the on-off control function of the power control. The power control shuts off the power in case of any abnormality in the system and restarts automatically when normal mode is restored. The uninterruptible power supply retains the power during motor starting. The transient recovery circuit rectifies the overshoot during transition from full-load to no-load operation and feeds back the power to the DC power source. The transistor drive inverts the DC voltage and can be either push-pull type or bridge type. The waveshaper and isolator consist of a transformer and a filter. The AC waveform obtained by inversion is filtered to eliminate unnecessary harmonics and transformed to a usable voltage level. The crystal time base, drive logic, and regulated driver act as a frequency controller and prevent the transistors from going into unnecessary saturation.

c. Specifications. The following are specifications of the Soleq windmill inverter (25):

Capacity	Nominal Input Voltage	Input Operating Range	Output Voltage
1.5 kVA, 1 Ø	12V DC	10.5-15V DC	120V AC ±3%
	24V DC	21-30V DC	120V AC ±3%
	32V DC	28-40V DC	120V AC ±3%
	64V DC	56-80V DC	120V AC ±3%
	112V DC	98-140V DC	120V AC ±3%
3.0 kVA, 1 Ø	24V DC	21-30V DC	120V AC ±3%
	32V DC	28-40V DC	120V AC ±3%
	64V DC	56-80V DC	120V AC ±3%
	112V DC	98-140V DC	120V AC ±3%
6.0 kVA, 1 Ø	24V DC	21-30V DC	240V AC CT ±3%
	32V DC	28-40V DC	240V AC CT ±3%
	64V DC	56-80V DC	240V AC CT ±3%
	112V DC	98-140V DC	240V AC CT ±3%

Output Frequency: 60 Hz ±0.01%

Power Capacity: Continuous - 1.5 kVA, 3 kVA, and 6 kVA
Short term - 3 kVA, 6 kVA, and 12 kVA (for 2 seconds)

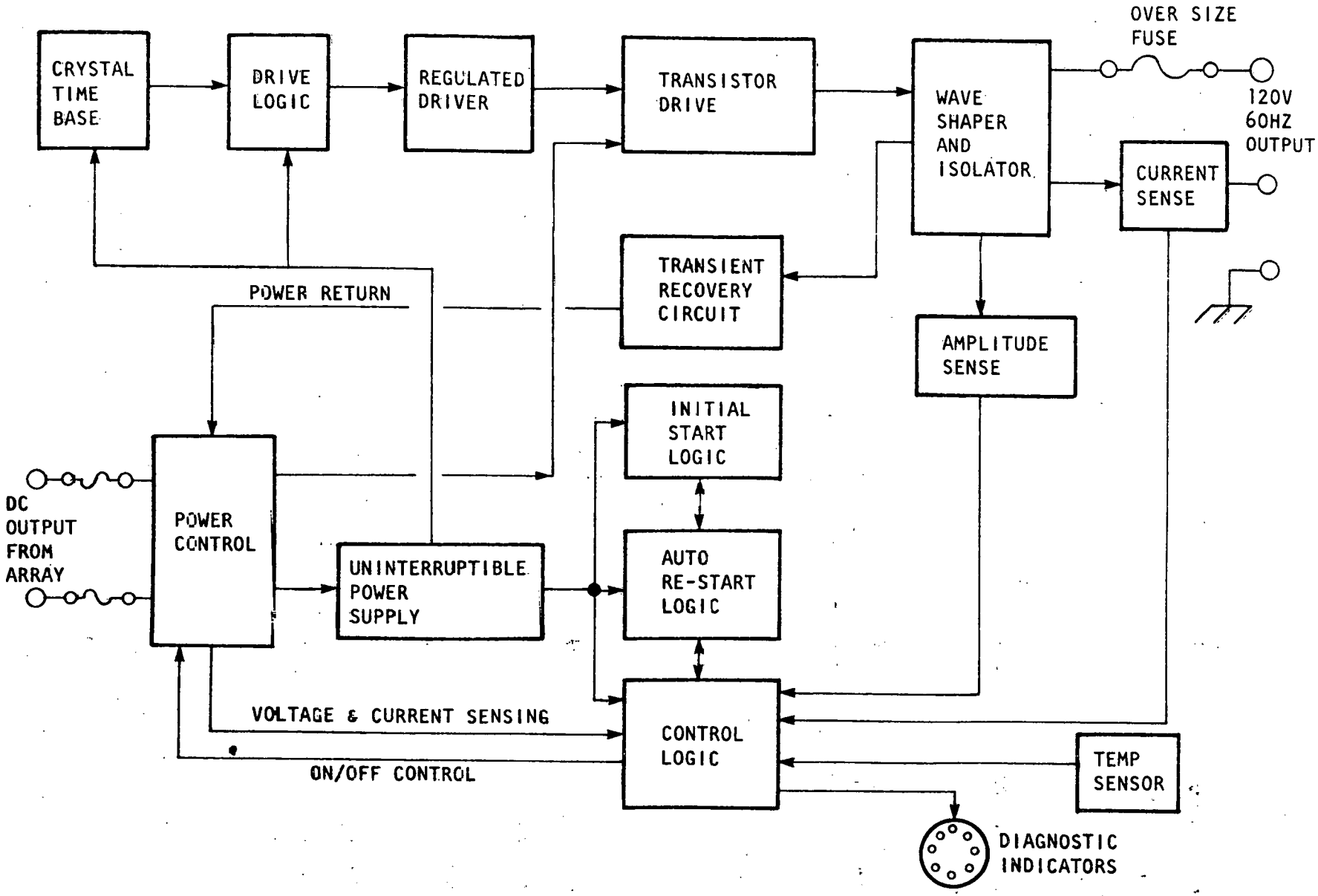

Figure III-3. Block Diagram of a Soleq Power Conditioner (25)

Efficiency	1.5 kVA Unit	3 kVA	6 kVA
Full load	88%	90-93%	90%
50% load	81.5%	80%	85%
25% load	68.4%	60%	
1.5% load	50%	50%	

Total Harmonic Distortion: 5%

Mean Time Between Failures: 10,000 hours

Unit by Rated Capacity	Mechanical Dimensions	Weight
1.5 kVA	0.43 m x 0.43 m x 0.76 m (17"x17"x30")	114 kg (250 lbs)
3.0 kVA	0.51 m x 0.43 m x 0.76 m (20"x17"x30")	148 kg (325 lbs)
6.0 kVA	0.76 m x 0.43 m x 0.76 m (30"x17"x30")	239 kg (525 lbs)

Operating temperature: -30 to 50°C (-22 to 122°F)

Storage Temperature: -30 to 85°C (-22 to 185°F)

The following are specifications of the Soleq "B" sine wave inverter (25):

Capacity	Nominal Input Voltage	Input Operating Range	Output Voltage
2 kVA	12V DC	10.5-15V DC	240V AC Center Tap (CT) (2x120V)
	24V DC	21-30V DC	240V AC CT (2x120V)
	32V DC	28-40V DC	240V AC CT (2x120V)
	64V DC	56-80V DC	240V AC CT (2x120V)
	112V DC	98-140V DC	240V AC CT (2x120V)

Capacity	Nominal Input Voltage	Input Operating Range	Output Voltage
4 kVA	24V DC	21-30V DC	240V AC CT (2x120V)
	32V DC	38-40V DC	240V AC CT (2x120V)
	64V DC	56-80V DC	240V AC CT (2x120V)
	112V DC	98-140V DC	240V AC CT (2x120V)
8 kVA	24V DC	21-30V DC	240V AC CT (2x120V)
	32V DC	28-40V DC	240V AC CT (2x120V)
	64V DC	56-80V DC	240V AC CT (2x120V)
	112V DC	98-140V DC	240V AC CT (2x120V)

Power Capacity: Continuous - 2 kVA, 4 kVA and 8 kVA
Short term - 4 kVA, 8 kVA and 16 kVA (for 2 seconds)

Efficiency: Approximately 90% at nominal voltage and capacity. Efficiency is somewhat lower for low-capacity and or low-voltage units.

Total Harmonic Distortion: 5%

Mean Time Between Failures: 10,000 hours

Unit by Rated Capacity	Mechanical Dimensions	Weight
2 kVA	0.43 m x 0.62 m x 0.3 m (17"x241/2"x12")	102 kg (225 lbs)
4 kVA	0.43 m x 0.63 m x 0.3 m (17"x241/2"x12")	136 kg (300 lbs)
8 kVA	0.43 m x 0.98 m x 0.3 m (17"x381/2"x12")	227 (500 lbs)

Operating Temperature: -10 to 50°C (14 to 122°F)

Storage Temperature: 40 to 85°C (40 to 185°F)

d. Other Features. The Soleq sine wave windmill inverter and the Soleq "B" sine wave inverter use transis-

torized circuitry to invert DC power into 60Hz AC. Frequency control is provided by quartz crystal oscillators. System protection is provided by self-surveillance logic circuitry which automatically shuts down the power conditioning unit if AC amplitude is too low, DC input voltage goes beyond the rated range, operating temperature is exceeded, or rated output capacity is exceeded for more than two seconds. The basic design prevents output overvoltage.

Loads of twice the rated output can be sustained for up to two seconds, allowing motor start inrush in excess of nominal rating. Soleq windmill inverters are totally enclosed in sealed, fabricated aluminum housing equipment with aluminum radiating fans for the cooling. These weather-tight housings make this model suitable for outdoor applications. The Soleq series "B" inverter uses vented rack-panel construction. This model must be housed in a location that is free of dust and away from explosive or corrosive areas and extremes of temperature and humidity.

e. Cost and Availability. The following cost figures are for catalogue list price in 1979 dollars (25):

Unit Type	Rating	Cost
Soleq windmill inverter	1.5 kVA	$3,664
Soleq windmill inverter	3 kVA	$4,632
Soleq windmill inverter	6 kVA	$6,995
Soleq "B" sine wave inverter	2 kVA	$2,950
Soleq "B" sine wave inverter	4 kVA	$3,371
Soleq "B" sine wave inverter	8 kVA	$5,910

Most catalogue units are either in stock or are available in 8 weeks. Custom design orders can be handled in 12 weeks.

f. Maintenance, Repair, and Warranty. Based on considerable field experience using Soleq inverters, Soleq claims that some of the inverters will last 10 to 20 years or longer without service. Consequently, no spare parts are recommended. Soleq inverters are sold with a one-year material and labor warranty. Maintenance contracts are available on inverters which are out of warranty. For repair, units must be shipped to the factory freight prepaid (24).

6. Delta Electronic Power Conditioners

a. Background. Delta Electronics is presently manufacturing voltage-fed, forced-commutated DC/AC and buck-type DC/DC power conditioners. The DC/AC units can operate in a stand-alone or utility-interface mode; the DC/DC units can only operate in stand-alone applications. Delta Electronics has built power conditioners for systems of from 50 watts to 350 kilowatts. The 3 Ø systems can supply unbalanced 3 Ø loads (26).

b. Operating Principle.

(1) General System. Figure III-34 shows the basic system of power conversion. The array supplies power to the DC/DC converter. The DC/DC converter converts the array voltage to the bus voltage at an efficiency of 95 percent. The buck-type regulator is normally used, but boost types are also available with comparable efficiencies. The DC/AC inverter operates from the battery bus and generates the AC output. More than one inverter may be operated in parallel to increase power or redundancy. The inverters can be operated in parallel with generators or a utility system.

The battery monitoring system senses battery voltage and charge. An undervoltage error signal is generated to turn off the inverters and prevent further battery discharge. An overvoltage error signal is generated to turn the inverter off. Battery temperature is used to adjust the battery float voltage for proper battery use.

(2) DC/DC Converter. Figure III-35 is a simplified block diagram of a DC/DC converter. The converter operates like an automatically controlled "DC Variac." The control circuitry selects the ratio of the input voltage to the output voltage. The control circuitry includes controls for peak power tracking. When the array power is insufficient to supply the inverter load, both the battery and the array supply power to the load. When the power from the array exceeds the load demand and the battery is charged to its full capacity, the controls automatically increase the array voltage and reduce array power output, thus preventing overvoltage of the battery. The filters reduce the ripple on the array and the battery.

(3) DC/AC Inverter. Figure III-36 shows the Delta Electronics inverter. Essentially, it consists of an input contactor, input filter, DC/AC power inverter,

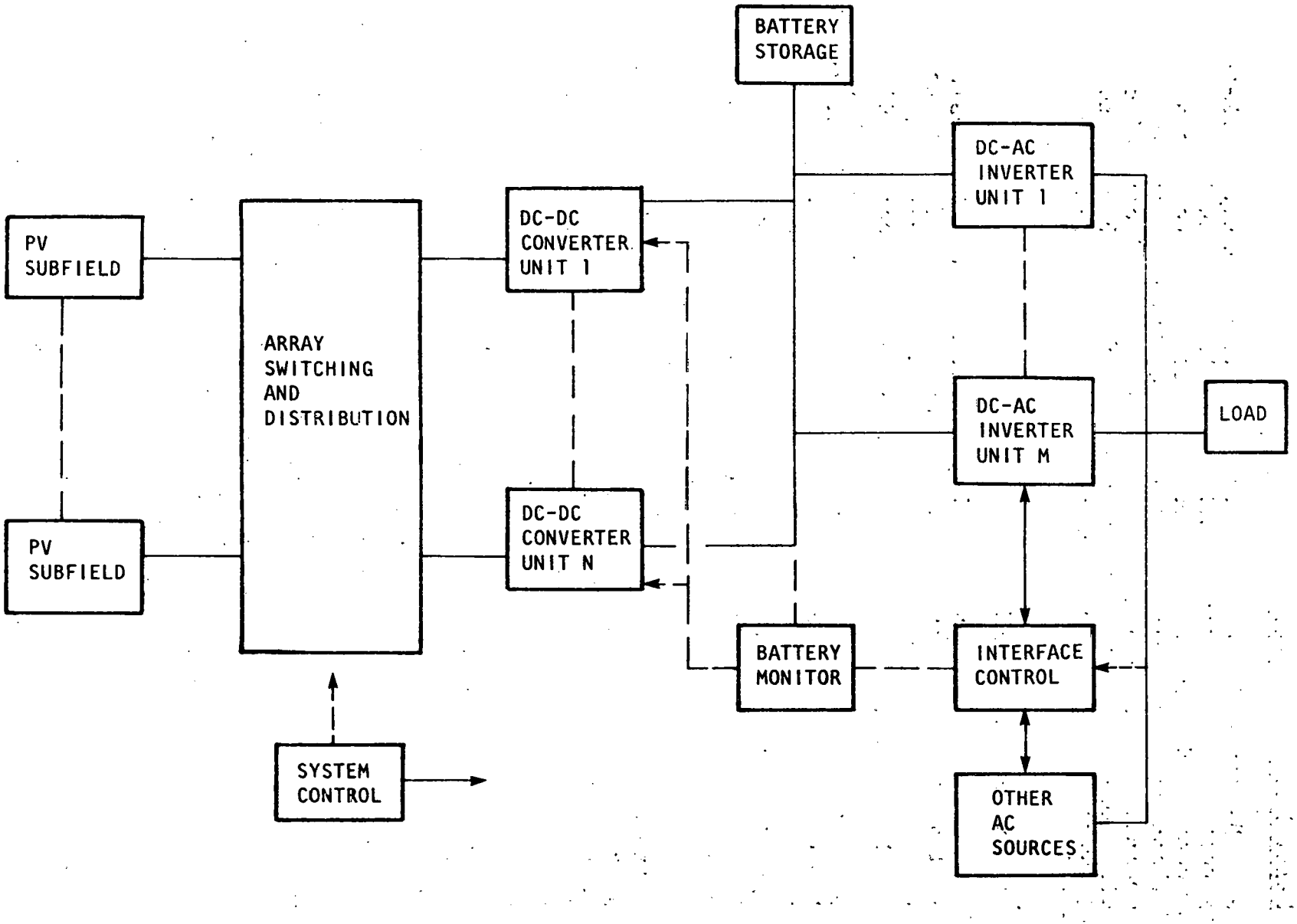

Figure III-34. Photovoltaic Power Conversion with Battery Energy Storage (28)

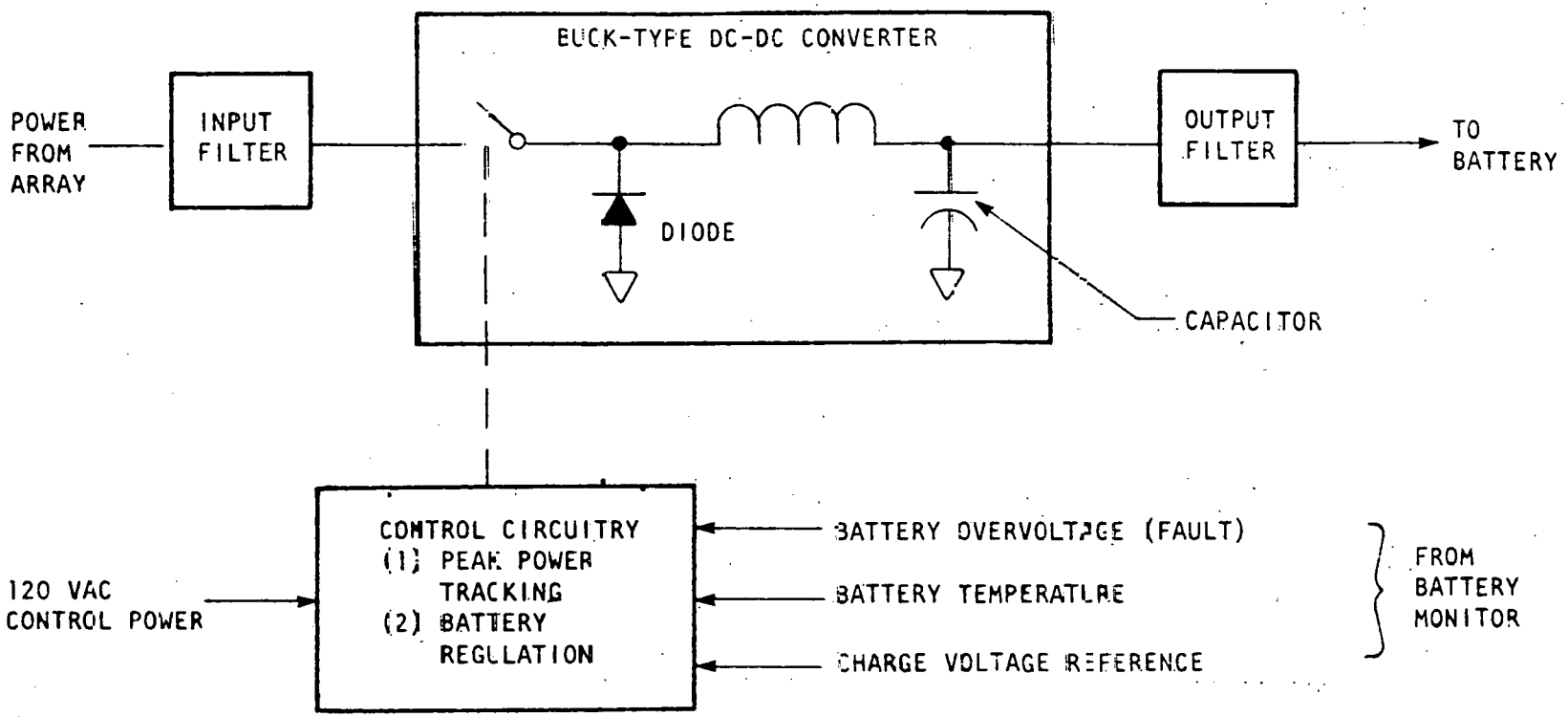

Figure III-35. DC/DC Converter with Peak Power Tracking (28)

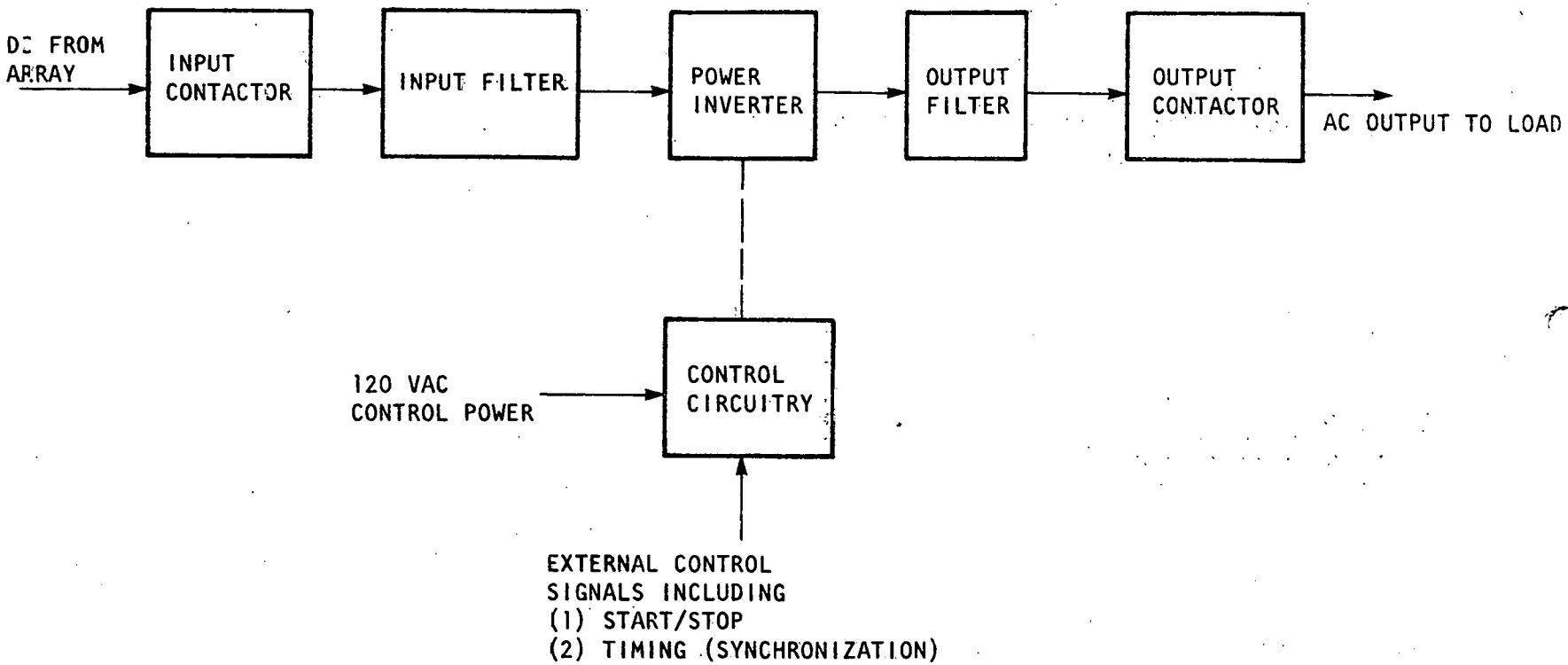

Figure III-36. Simplified Block Diagram of Delta Electronic DC/AC Inverter (28)

output filter, output contactor, and control circuitry. The inverter is self-commutated and voltage-fed. It uses pulse modulation to generate a 3-phase, 12-step sine wave synthesis. The significant harmonics generated are the 11th and 13th and are removed by the output filters. During parallel operation with the utility, the control circuitry responds to information from the system interface control circuitry to assure synchronization and load control. Fault sensing and protection, turning on and turning off of inverters are accomplished automatically.

c. Specifications. Table III-4 specifies typical parameters of the DC/DC and DC/AC inverters. Specifications of other parameters that apply to all DC/AC inverters follow (26):

Parameter	Specification
Total harmonic distortion:	Less than 3%
Temperature:	-10 to +50°C (14 to 122°F)
Humidity:	0-95%
Short-term rating:	150% of continuous kVA rating for 10 seconds
Reliability (mean time between failures):	20,000 hrs for larger units 15,000 hrs for small units
Life:	20 years
Protection:	Overtemperature, blown fuse, grid overvoltage, grid undervoltage, overload, reverse power flow
Meters:	Input power, input voltage, input current, DC link voltage, DC link current, output voltage, output current, output power, output VAR, output kWh, output frequency, running time

The following are specifications of the 60 kW unit (28):

TABLE III-4. SPECIFICATIONS FOR PHOTOVOLTAIC POWER CONVERSION EQUIPMENT FOR USE WITH BATTERY STORAGE (28)

DC/DC CONVERTERS (WITH PEAK POWER TRACKING)

Model	Rated Output Power (kW)	Effic. at Full Power	No Load Losses (W)	Input Voltage Max.	Input Voltage Normal Operation	Output Voltage Range*	Output Voltage Recom. Battery Float	Size WxDxH	Estimated Weight
61250	75	94%	200	400	200-300	175-290	240	91.4 cm x 81.3 cm x 203 cm (36 x 32 x 80)	454 kg (1,000 lb)
61251	125	95%	250	650	300-500	290-500	420	91.4 cm x 81.3 cm x 203 cm (36 x 32 x 80)	680 kg (1,500 lb)
61252	200	95%	350	650	300-500	290-500	420	102 cm x 102 cm x 203 cm (40 x 40 x 80)	1,134 kg (2,500 lb)
61523	400	95%	500	650	300-500	290-500	420	102 cm x 102 cm x 203 cm (40 x 40 x 80)	2,041 kg (4,300 lb)

DC/AC INVERTERS

Model	Rated Output kVA	Effic. at Full Power	No Load Losses (kW)	Load P.F.	Input Voltage Range	Input Voltage Recom. Battery Float	Output Voltage, 3-phase	Size WxDxH	Estimated Weight
61254	60	92%	2.2	0.8-1	180-290	240	480/277	91.4 cm x 81.3 cm x 203 cm (36 x 32 x 80)	2,041 kg (4,500 lb)
61255	100	92%	3.2	0.8-1	290-500	420	480/277	91.4 cm x 81.3 cm x 203 cm (36 x 32 x 80)	2,268 kg (5,000 lb)
61256	350	92%	6.0	0.8-1	290-500	420	480/277	355.6 cm x 102 cm x 203 cm (140 x 40 x 80)	6,124 kg (13,500 lb)

Output voltage must be less than input voltage

Input	Specification
Maximum Voltage	400V DC
Normal operating range, loaded	180-290V DC
Output	
Voltage	480V AC, 3-phase*
Power	60 kW
kVA (stand-alone mode)	75 kVA
kVAR (augmentation mode)	Automatically minimized
Efficiency	
No load losses	2.2 kW
Efficiency at 30 kW	91%
Efficiency at 60 kW	92%
Output current distortion, full load, augmentation mode	3% THD
Output voltage distortion, stand-alone mode	3% THD
Frequency synchronization range, augmentation mode	60±1 Hz
Frequency stability, stand-alone mode	60 Hz ±0.1%
Environment	
Temperature	-10 to 50°C (14 to 122°F)
Humidity	0-95%

**Other voltages are also available.*

d. Cost and Availability. The selling prices of the DC/AC power conditioners are as follows (26):

Size	Price
Residential Unit	$150-200/kW
75 kVA	$1,000/kW
300 kVA	$500/kW

The selling prices of the DC/DC power conditioners are as follows (2):

Size	Price
75 kW	$ 500/kW
300 kW	$ 250/kW.

The lead time on orders of the power conditioners is approximately 6 to 9 months.

e. Repair, Maintenance, and Warranty. The standard units have a one-year warranty limit. The spare parts recommended are the active components, e.g., printed circuit boards. Maintenance contracts are available on a year-to-year basis. The factory needs to be notified for repairs of the power conditioning units. The factory representatives will then make onsite repairs (26).

f. Test Results. Under the sponsorship of the U.S. Department of Energy, Delta Electronic Control Corporation has designed and built a 60 kW photovoltaic power system (27). Tests have been performed on the power conditioner at full power from an array simulator and at half power from a photovoltaic array. Table III-5 shows the test data for the power conditioner. Figure III-37 shows the efficiency as a function of system output power. The power-tracking circuit has tracked the maximum array power to within 99 percent.

During the tests, power was fed to a utility grid. The photovoltaic power system did not cause any observable disturbance to the utility line. The output current from the power conditioner was increased gradually, which minimized disturbance to the utility line at startup. Also, the power conditioner operated properly through a series of grid abnormalities and interruptions. Figure III-38 shows the rate of rise of output current at turn-on with 30 kW array power available.

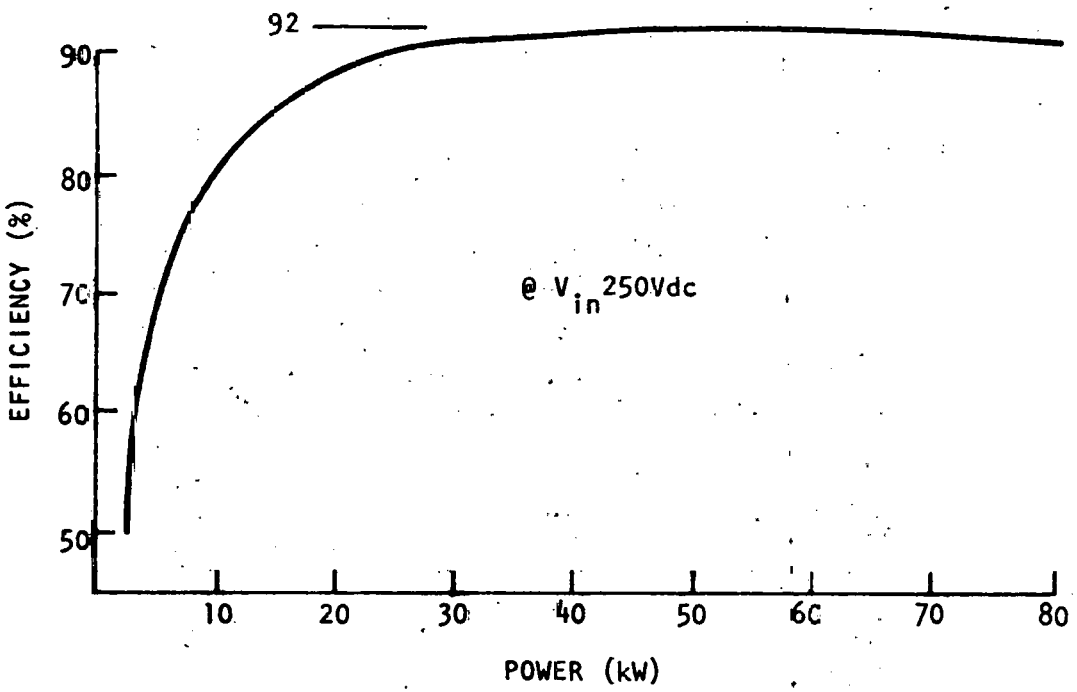

Figure III-37. Delta Electronic Power Conditioner Efficiency (27)

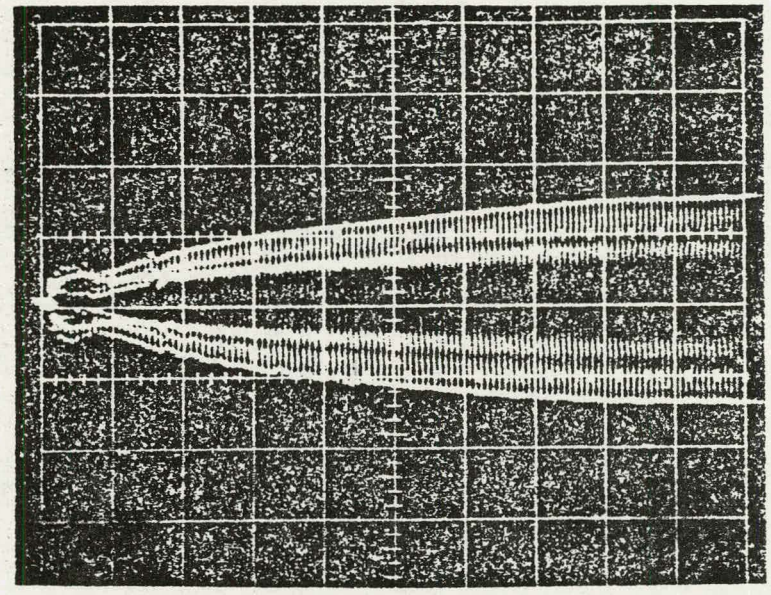

Figure III-38. Rate of Rise of Output Current at Turn-on, 30 kW Array Power Available (27). Horizontal Scale: 0.2 Seconds Per Division Vertical Scale: 25 Amps Per Division

TABLE III-5. TEST DATA FOR THE 60 kW INVERTER (27)

Input	
Operating voltage range	180-290V DC
Maximum input voltage	400V DC
Output	
Rated power	60 kW (75 kVA)
Frequency	60 Hz
Voltage	277/480V AC, three-phase
Efficiency	
At 60kW	90% specified, 92% measured
At 30kW	85% specified, 91% measured
Current dist. (THD) at 60kW	3% specified, 1.5% measured
Power control	Four-quadrant

7. Westinghouse Corporation Power Conditioners

a. Background. Westinghouse has designed and constructed a 62.5 kW, 3-phase, 60-Hertz voltage-fed forced-commutated DC/AC power conditioner. This unit is self cooled by air and can operate with a utility tie as well as in a stand-alone mode. A 5 kVA voltage-fed forced-commutated DC/DC power conditioner and a 10 kVA residential type of current-fed line-commutated DC/AC power conditioner will be available in 1980. The 50 kW unit has the capability to sustain a load unbalance of 15 kW, but the total power drawn by one phase must be limited to one-third of the 50 kW rating (29).

b. Operating Principle. Figure III-39 is a block diagram of the Westinghouse 50 kVA power conditioning unit. The preregulator at the input modifies the input voltage from the solar array to the desired level. The preregulator regulates the voltage by energy storage provided by an inductor and an SCR switching circuit. The inverter inverts the regulated voltage. The inverter consists of six SCR forced-commutated power stages or power poles. These power poles switch at 60 Hz and drive two transformers. Harmonics are neutralized by the vector summation technique and an output voltage waveform is obtained which is free from harmonics up to the 11th.

During parallel operation with the utility, extra inductors are switched into the output to absorb line-to-line voltage and phase difference. PCU supplies the real power to the utility by shifting the phases of the inverter voltages with respect to the utility voltages. The inverter source voltage is modified when control of reactive current flow is desired.

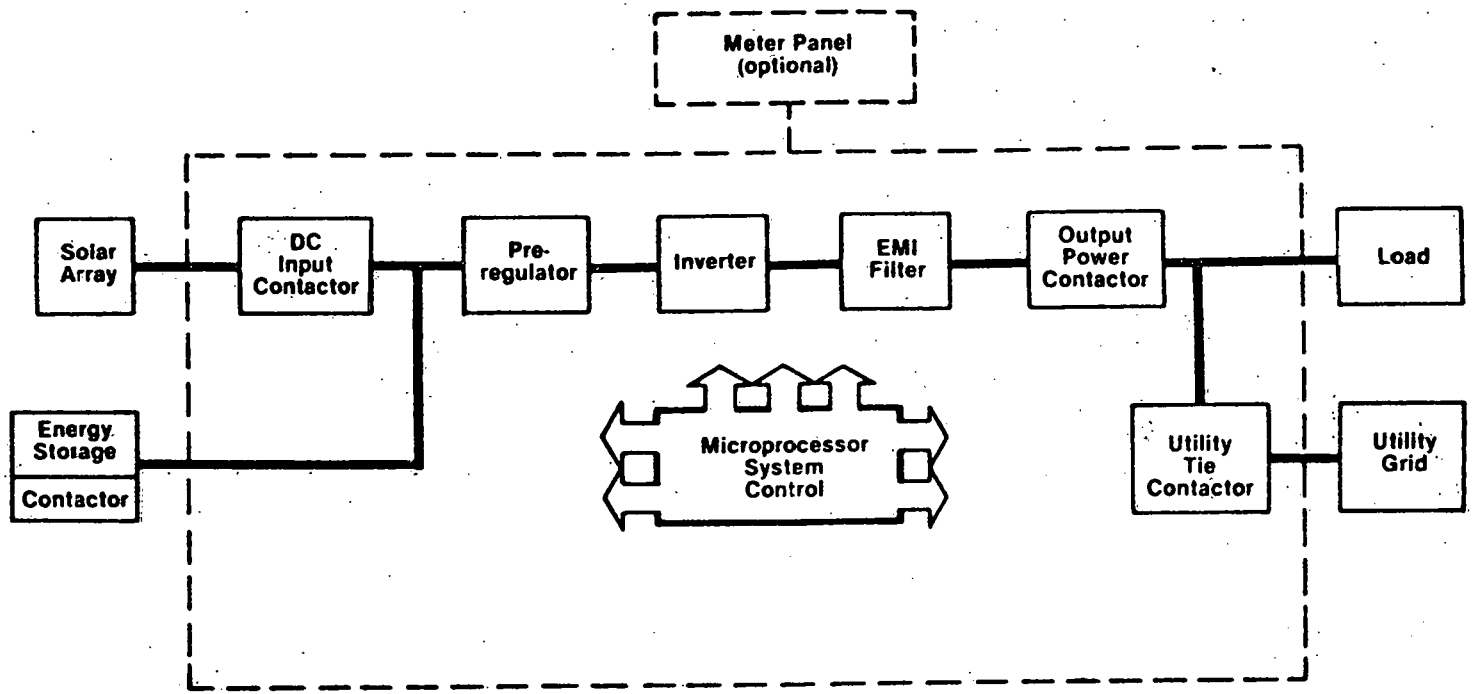

Figure III-39. Block Diagram of the Westinghouse Power Conditioning Unit (30)

The power system controller monitors voltage, current, and frequency. A microprocessor is used to control the contactors and circuit breaker. This system control allows the power conditioner to start and stop automatically, depending on the capability of the solar array. The power system controller is constructed with a microprocessor as the core. In addition to the process hardware, a support development system is used for software/hardware generation and debugging.

The battery charger and battery are accessible only in the manual isolated operation mode. Under this circumstance, the battery charger will operate if the battery is not on-line and the array has more power than that required by the load. After the charging of the battery has been completed, the battery contactor can be closed either manually or automatically. This mode will be maintained until the battery is discharged or the operating mode is changed.

c. Specifications. The following are specifications of the Westinghouse power conditioning unit suitable for photovoltaic applications (30):

Input	Specification
Maximum voltage	350V DC
Minimum voltage	200V DC
Normal operating range	200-300V DC
Output	
Voltage	208/120V, 3 Ø 480/277V, 3 Ø
Power	62.5 kW
Short-term rating	100 kVA for 5 seconds
Efficiency	92% of full load 90% at 50% load 87% at 25% load
Total harmonic distortion	Less than 5%
Power factor	Stand alone-0.9 lead to 0.7 kg
Physical Characteristics	
Size	199.4 cm x 87.6 cm x 76.2 cm (78.5 in. x 34.5 in. x 30 in.)

Weight	816.5 kg (1800 lbs)
Life	20 years
Environmental	
Ambient Temperature	-10° to 45°C (14° to 113°F)
Relative Humidity	96% (non condensing)
Barometric Pressure	790 to 520 mm Hg (31.1 to 20.5 in. Hg)
Protection	Input fuses Output current limiter Over/under voltage protection Abnormal frequency protection
Meters	DC & AC Ammeters DC & AC Voltmeters
Additional	Peak power tracking, Load shed signal on overload, Battery charger control signal, Automatic startup and utility grid paralleling

d. Cost and Availability. The list price for the 62.5 kVA, 3 Ø unit is $38,500 (29). The following are the areas in which significant reduction in component and labor costs are anticipated:

(1) Output capacitors: More economical sizes can be selected.

(2) Cooling fans: Use of fabricated units in high quantities indicates that substantial savings can be achieved.

(3) Microprocessor: As applications increase, the cost will drop.

(4) Automation: Labor cost can be reduced through increased automation.

A mature power conditioner with a high rate of production would probably cost $200 to $250/kVA in 1975 dollars (30). The lead time on order for the 50 kW unit is approximately 10 months (3).

e. Repair, Maintenance, and Warranty. The power conditioner has a one-year warranty limit. The spare parts recommended are the control boards, fuses, and active semiconductors. For repair of the power conditioning units, the factory is notified. The factory representatives will then make onsite repairs (29).

8. AiResearch Manufacturing Company Power Conditioners

a. Background. A current-fed, line-commutated DC/AC power conditioner is being developed by AiResearch Manufacturing Company as a specific design for photovoltaic application, supplying from 20 to 250 kW of three-phase, 60 Hz power into a 480V AC bus. These units are capable of operating with utility tie only (32).

b. Operating Principle. Figure III-40 shows a single-line diagram of the power conditioner. The system consists of two physical modules, the DC module and the AC module. The DC module contains the input disconnect, the input filter section, the inverter, and the control unit. The AC module contains the output transformer, AC filtering, power factor correction capacitors, fuses, and the output disconnect.

The control unit is energized by closing the DC disconnect and the AC fused disconnect switch. The operator depresses the start button to begin operation. The control unit checks the voltage, current, and temperature before delivering power to the AC bus. Power delivery is delayed until the DC current exceeds 10 percent of full-rated current, and the DC voltage must be at least 50 volts. At this time, the power conditioning unit operates at the peak DC power point. The peak-power tracker continues to operate until the current at peak power is less than 5 percent of the rated current.

If the operating voltage drops rapidly below 75 percent of rated voltage before the undervoltage relay has time to respond, shorting of the arrays will occur. If the line voltage remains below 75 percent of rated voltage, the power conditioner will remain in the power-on mode. The unit will function in the operation mode as soon as the line voltage exceeds 75 percent of the rated voltage.

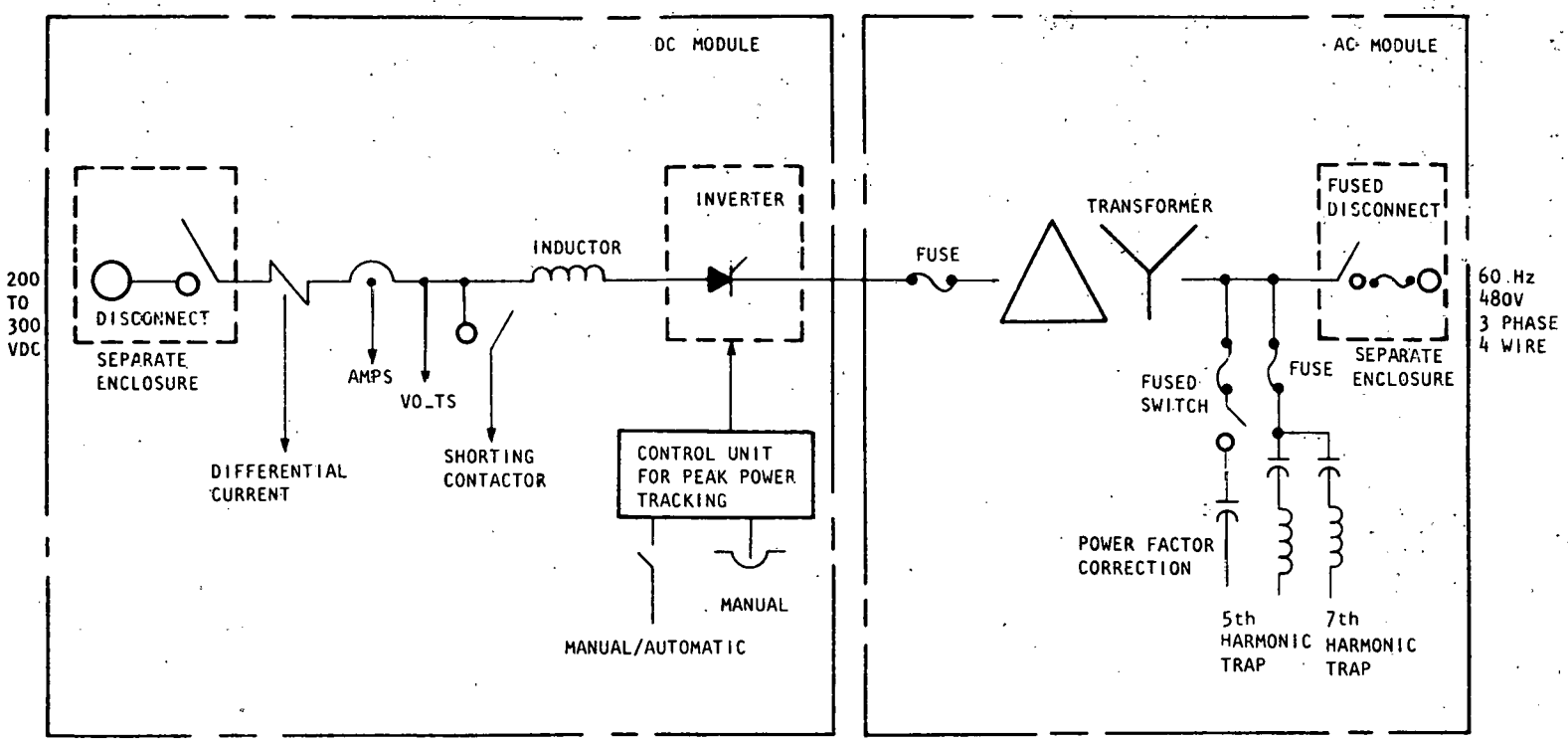

Figure III-40. Single-Line Diagram of the AiResearch Power Conditioning Unit (32)

The peak-power tracking unit can be operated in the automatic or manual mode. In the automatic mode, maximum power is obtained from the array automatically. In the manual mode, the operator adjusts the operating point on the photovoltaic characteristic manually. The harmonic traps provide a shunt path for harmonic currents. Power factor correction is provided by the application of capacitors.

To service the power conditioner, both the AC and the DC disconnect switches must be opened. To place the unit in a standby or power-on mode, the stop push-button is depressed.

c. Specifications. The following are specifications of some of the important parameters of power conditioners (32):

Input	Specification
Maximum voltage	600V DC
Normal operating range	200-300V DC
Maximum rated current	640 Amps DC
Output	
Voltage	480/227V, 3 Ø
Power	20-250 kW
Efficiency	93% at full load 86% at 20% load
Total harmonic distortion	5%
Power factor	.90
Life	10-20 years
Reliability (mean time between failures)	20,000 hrs.

	Specification
Protection	Ground fault, high AC line, low AC line, blown fuse, out of phase, overtemperature
Environment	
Ambient temperature	0 to 40°C (32 to 104°F)
Relative humidity	0 to 95% noncondensing
Altitude	0 to 1,219 m (0 to 4,000 ft)

Meters	Input DC voltage, input DC current, input power, output voltage, output current
Indicators	Overtemperature, DC overvoltage, AC undervoltage, single phase, phase rotation.

d. Cost and Availability. Because of the lack of demand for power conditioners in the photovoltaic market, the manufacturer cannot estimate the cost at the present time. The power conditioners developed by the AiResearch Manufacturing Company are not yet commercially available; however, the manufacturer will accept orders. The lead time is expected to be approximately 12 to 18 months. The standardized units will be available in 1983 (31).

e. Repair, Maintenance, and Warranty. The power conditioners will have a one-year warranty limit. The manufacturer recommends customer purchase of spares for field-removable major subassemblies or components down to the printed circuit board level. For repair of the large power conditioning units, the factory must be notified. The factory representatives will then make onsite repairs. The smaller units, however, have to be shipped to the factory for repair. The company has a worldwide product support organization; hence, maintenance contracts are available. The company can train customer personnel to perform maintenance work and can also accept contracts to do periodic maintenance work (31).

9. United Technologies Power Conditioners

a. Background. United Technologies Corporation, Power System Division, has available on a contract basis a voltage-fed, self-commutated inverter for use in photovoltaic systems. The unit is a 3 Ø, 4-wire device with a rating of 48.8 kVA. The unit's basic design is for stand-alone operation, but it can be modified to operate in parallel with utility lines. United Technologies also builds a multi-megawatt inverter.

These power conditioning units are not catalog items but are available on a contract basis with a 24-week lead time on orders (33).

b. Operating Principle. United Technologies Corporation power conditioning equipment uses the principle of pulse width modulation. It is a two-stage system for the static inversion of DC power to AC power. The first stage is a DC/DC preregulator. The second stage is a voltage-fed, self-commutated inverter.

The DC/DC preregulator supplies a fixed DC voltage to the input of the voltage-fed self-commutated inverter. The inversion process is then accomplished by use of a self-commutated thyristor inverter circuit. The inverter supplies three-phase output to a neutral-forming single-winding transformer to provide a 3 Ø wire output. The unit is designed to follow the power demand of the connected load automatically. System logic is provided by a microprocessor-based system with programmed switching patterns to minimize filtering requirements.

c. Specifications (33). The specifications of the United Technologies power conditioning unit are shown below:

Unit capacity:	48.8 kVA
Short-term capacity:	82 kVA for 5 seconds
Input voltage range:	130-240V DC
Output voltage:	208V line-to-line (3 Ø, 4 wire)
Power factor:	0.85 for continuous rating 0.70 for short-term rating
Full-load efficiency:	89.5%
Efficiency at 50% load:	86.2%
Total harmonic distortion:	15%
Available fault current:	300 amps for line-to-line fault 450 amps for line-to-neutral fault

Physical Characteristics

Dimensions	58.4 cm deep (23") 10.77 cm wide (42") 104.2 cm high (43")
Weight	362.9 kg (800 lbs)
Operating temperature range:	-31.6 to 43.3°C (-25 to 110°F)
Operating altitude range:	Sea level to 1,828.8 meters (6,000 feet)
Relative humidity:	Up to 100% from -17.8 to 37.8°C (0 to 100°F)

d. Other Features. The United Technologies Corporation power conditioning unit was designed with a reliability goal (mean time between failures) of 20,000 hrs and an inverter life target of 20 years.

The unit is capable of supplying loads with up to 30 percent load unbalance, where:

$$\text{Load unbalance} = \frac{\text{Imax-Iave}}{\text{Iave}} \times 100$$

Imax = maximum output current in any phase

Iave = average output current of all phases

The unit is a stand-alone baseline design that can be modified for a utility line parallel interface. The unit is not provided with a "tracking unit," which insures operation of the photovoltaic array on the maximum power locus of its voltage current curve. Such a unit can be added when it is required. The unit is self-protecting and shuts down automatically when the DC source, AC load, or inverter output exceed design limits. In the operational mode, the unit will automatically adjust to the changes in power required by the load. The system is designed for modular replacement of power poles, DC/DC preregulator and logic circuitry.

e. Maintenance and Repair. As previously mentioned, the United Technologies power conditioning unit is not a catalogue item but is available on a contract basis. The availability of maintenance contracts can be negotiated as can the procedure for repair service. Replacement fuses are recommended as spare parts (33).

f. Cost and Availability. The cost of the system is to be negotiated, depending on requirements and quantity. Systems are available on a contract basis with a 29-week lead time on orders (33).

10. NASA's Jet Propulsion Laboratory Power Conditioner

A power conditioner has been developed by NASA's Jet Propulsion Laboratory. The unit has been installed in a house trailer and can supply 3kW of power. The DC input voltage ranges from 130 to 275V DC and the AC output voltage is 110V 60hz. Figure III-41 is a simplified block diagram of the inverter. Power obtained by the solar array is supplied to the load through the main inverter. If the power produced by the array is more than that required by the load, then the excess power is used to charge the battery.

The dynamic-impedance comparator compares the array resistance with the resistance of the impedance comparator. An error signal from the comparator controls the charging current to the storage battery. When the array delivers its

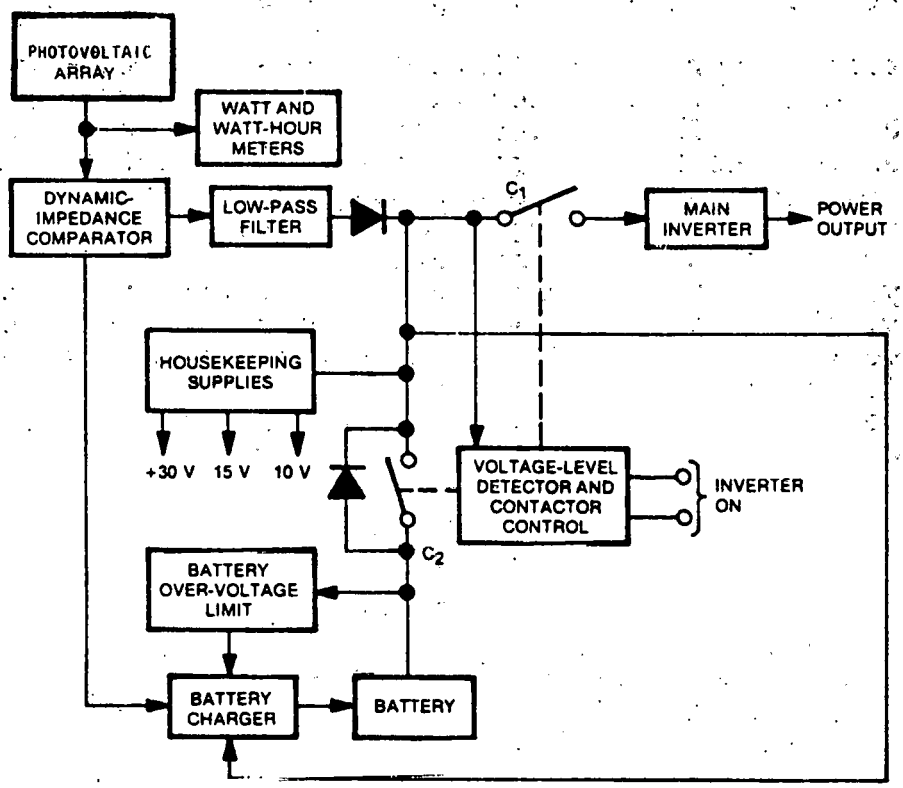

Figure III-41. Simplified Block Diagram of a Power Conditioner Developed by NASA's Jet Propulsion Laboratory (34)

maximum power to the load, no error signal is generated and, hence, the battery is not charged. Generation of a positive error signal indicates an excess of power that can be used to charge the battery. A negative error signal indicates the array power is less than required by the load. In this case, both the array and the battery supply the power.

The battery overvoltage limit disconnects the flow of current to charge the batteries when the battery voltage reaches 170 volts. The voltage level detector and contactor control measures the DC voltage to the main inverter and determines the status of the power supply. If the voltage-level detector senses a voltage above 130 volts, contact C_1 closes and contact C_2 opens and power flows to the load from the battery or the array, whichever is at a higher voltage. If, however, the voltage level detector senses a voltage below 130 volts, contactor C_1 opens, contactor C_2 closes, and the array feeds power to the battery only for charging. The control power needed for the unit is approximately 10 percent of the load.

G. References

1. Pittman, Paul F. "Implications of New Technology on Power Conditioner Design." Workshop on Power Conditioning for Alternative Energy Technologies. Denver, Colorado: May 9-11, 1979.

2. Smith, D.R. "Power Conditioning for Photovoltaics." Workshop on Power Conditioning for Alternative Energy Technologies. Denver, Colorado: May 9-11, 1979.

3. Wood, Peter, et al. "Power Conversion Equipment - A Key Component in New Power System Generation and Storage Concepts." Proceedings of American Power Conference 1976, Vol. 38.

4. Feduska, et al. "Energy Storage for Photovoltaic Conversion, Final Report, Volume III, Residential Systems." Westinghouse Research and Development Center, September 30, 1977.

5. Wood, Peter. "AC/DC Power Conditioning and Control Equipment for Advanced Conversion and Storage Technology." Prepared for EPRI, August 1975.

6. Bechtel Corporation. "Battery Storage Performance Requirements for Terrestrial Solar Photovoltaic Power Systems." Prepared for Argonne National Laboratory under Contract No. 31-109-38-2962, Phase 1D, July 1977.

7. Wood, Peter. "Power Condition for Solar Photovoltaic/ Battery Storage Systems." Westinghouse Electric Corporation. Abstracts of Invited Papers presented at Workshop on Battery Storage for Solar Photovoltaic Systems, Denver, Colorado, January 1113, 1978.

8. Pickrell, R. "10kVA Inverter/Controller." Proceedings of the Semiannual Review Meeting-Silicon Technology Programs Branch - August 23, 1977. Organized by the BDM Corporation for the ERDA. Contract No. EG-77-C-01-7533.

9. Goodman, F.R., Jr. Los Angeles Department of Water and Power. "Power Conditioning Requirements for Application of Nonconventional Energy Technologies in Electric Utility Systems." Workshop on Power Conditioning for Alternative Energy Technologies. Denver, Colorado, May 9-11, 1979.

10. Wood, et al. "Power Conversion Equipment - A Key Component in New Power System Generation and Storage Concepts." Proceedings of American Power Conference, 1976, Vol. 38.

11. Wood, Peter. "Power Conditioning Systems." In: Record of the Photovoltaics Power Conditioning Workshop. Albuquerque: October 13-14, 1976.

12. Wood, Peter. "AC/DC Power Conditioning and Control Equipment for Advanced Conversion and Storage Technology." November 1976.

13. Abbondanti, A. and P. Wood. "A Criterion for Performance Comparison Between High Power Inverter Circuits." Westinghouse Electric Corporation Research Laboratory. IAS, 1975 Annual.

14. Rosati, et al. "AC/DC Power Converter for Batteries and Fuel Cells." Prepared for EPRI by United Technologies Corporation, August 1978.

15. Eltimsahy, et al. "Experimental Investigation of a Solar Cell/Inverter System." Proceedings of the 1977 Annual Meeting of the American Section of the International Solar Energy Society, Volume 1, Sections 14-25. Orlando: June 6-10, 1977.

16. Personal communication between David H. Matsen (Windworks, Inc.) and Amitava Podder (HAI), July 1979.

17. Manufacturer's brochures, Windworks, Inc. Mukwonago, Wisconsin.

18. Stover, John B. "NASA-LeRC Photovoltaic Power System Tests on an 8-Kilowatt Single-Phase Line-Commutated Inverter." February 1978. Prepared for U.S. Department of Energy by NASA-Lewis Research Center, February 1978.

19. Personal communication between George A. O'Sullivan (Abacus Controls, Inc.) and Amitava Podder (HAI), July 1979.

20. Manufacturer's brochures, Abacus Controls, Inc., Somerville, New Jersey.

21. U.S. Department of Energy. "Photovoltaic Tests and Applications Project Progress Report for April 1976-June 1977." NASA-Lewis Research Center, November 1978.

22. Manufacturer's brochures, Elgar Corporation, San Diego, California.

23. Personal communication between Charles Price (Elgar Corporation) and Amitava Podder (HAI), July 1979.

24. Personal communication between S. Ohba (Soleq Corporation) and Amitava Podder (HAI), July 1979.

25. Manufacturer's brochures, Soleq Corporation, Chicago, Illinois.

26. Personal communication between Chuck Jobbinf (Delta Electronic Control Corporation) and Amitava Podder (HAI), July 1979.

27. Svelzie, L.R., Delta Electronic Control Corporation and D.J. Roesler, U.S. Department of Energy. "Operational Characteristics of a 60 kW Photovoltaic System Integrated with a Utility Grid."

28. Manufacturer's published literature. Delta Electronic Control Corporation, Irvine, California.

29. Personal communication between Donald Shireman (Westinghouse Electric Corporation) and Amitava Podder (HAI), July 1979.

30. Stump, et al. Westinghouse Aerospace Electrical Division. "Design and Construction of a 50 kVA Power Conditioning Unit for Photovoltaic Power Systems." Prepared for Sandia Laboratories under Contract No. 07-6940. April 1979.

31. Personal communication between J.W. Main (AiResearch Manufacturing Company) and Amitava Poder (HAI), August 1979.

32. Manufacturer's published literature, AiResearch Manufacturing Company of California, Torrance, California.

33. Personal communication between Joseph King (United Technologies Corporation) and Amitava Podder (HAI), September 1979.

34. "Solar Power Conditioner". NASA's Jet Propulsion Laboratory, Pasadena, California. NASA Tech. Briefs, Spring 1979.

IV. DATA BASE ON SOLAR ARRAYS

A. Definition of Arrays

An array is one of the subsystems required in a photovoltaic electric system, as indicated in Figure IV-1. The array converts solar energy, or radiation, into electricity by grouping photovoltaic cells together. A single photocell produces less than one watt of power at approximatley 0.5 volts. In order to provide power for typical loads, many cells must be grouped together. Accordingly, cells are connected in series and/or in parallel to achieve the voltage and power levels necessary to serve a particular load. The cells are grouped into a module, several of which make a panel. The panels are then mounted into a structure called an array (see Figure IV-2).

B. Description of Solar Arrays

The purpose of a solar array is to convert the solar energy directly into electricity. Although the principle of operation for a photocell is simple, its power generation is dependent upon a variety of complicated relationships. It is these relationships that control the usefulness of the device.

The parameters which affect the performance of the array are: (1) the current, voltage, and power of the cell under both loaded and unloaded conditions; (2) the efficiency of the cell and the array; (3) the frequency or spectral response, which affects the cell output; (4) cell type; and (5) temperature and intensity of the solar radiation or insolation.

In addition to electrical performance, considerations such as cost, maintenance, reliability, and life are important.

1. Current-Voltage-Power

The current, voltage, and power of a photovoltaic array are directly related to each other and can best be expressed graphically. Figure IV-3 shows the output I-V curve of a typical cell.

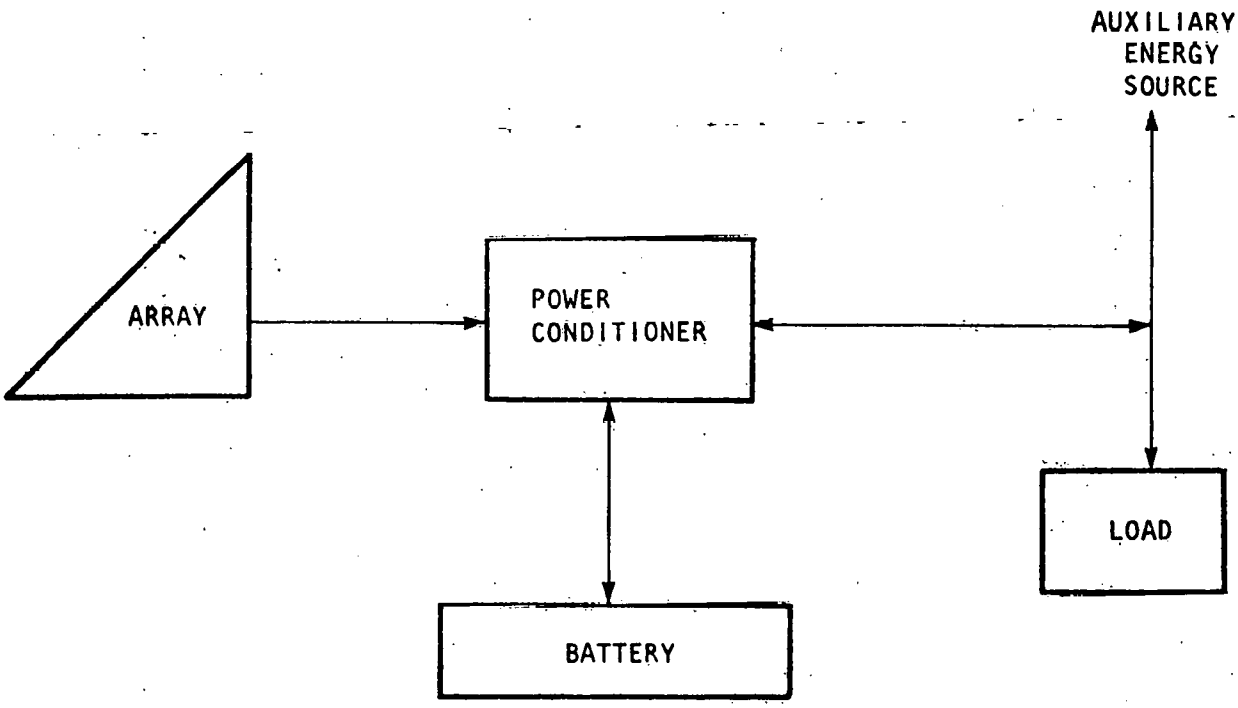

Figure IV-1. Photovoltaic Electric System

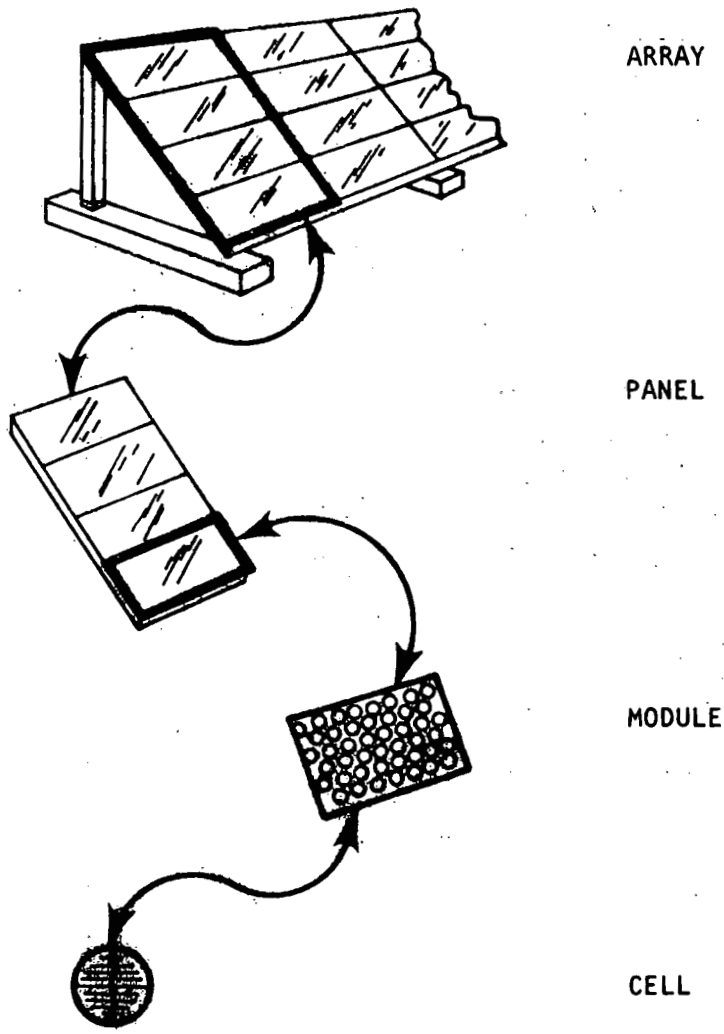

Figure IV-2. Array Nomenclature (1)

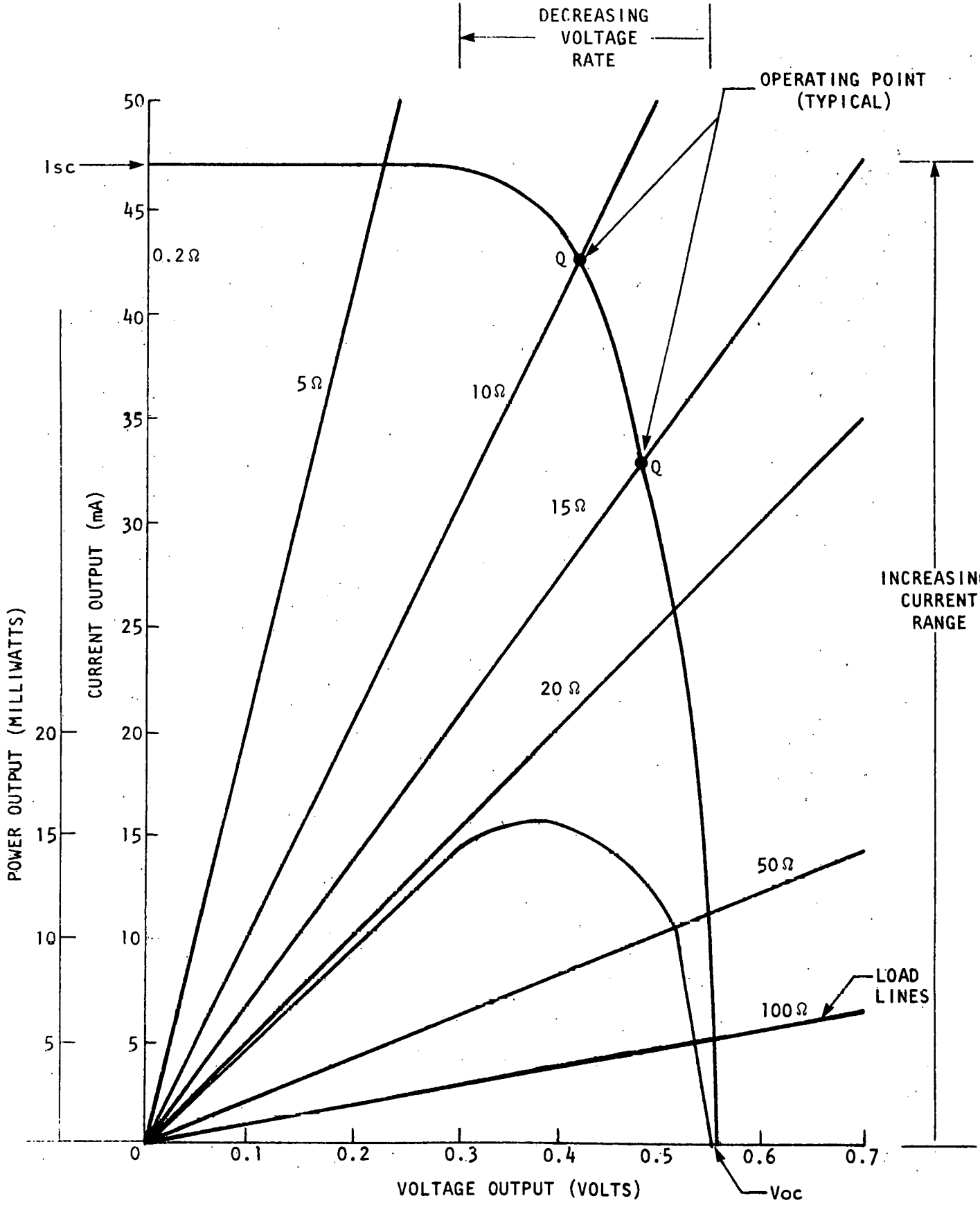

Figure IV-3. Typical Cell-Output Characteristics

As light strikes the cell surface and is absorbed, the cell generates a voltage called the open-circuit voltage (Voc). This is the voltage which appears across the cell with no load connected to it. If a load is connected to the cell, a current will flow. As the load resistance decreases, more current will flow, as is indicated by tracking the decreasing resistance load lines shown in Figure IV-3. As the load resistance decreases, the quantity of current that can be withdrawn from the device levels off and stabilizes at a value of current called the short-circuit current (I_{sc}). The point at which one operates on the output characteristics is determined by the load and is graphically determined by the intersection of the load line with the current-voltage characteristic curve. This point is designated as the operating point, or "Q" point. A closer look at the "Q" point reveals that the voltage at this point is not the open-circuit voltage and the current at this point is not the short-circuit current.

Figure IV-3 shows that the current increases rapidly and then levels off as it approaches the value of the short-circuit current. The output characteristics also show that as the current increases, the voltage decreases. This voltage drop can best be understood by examining the equivalent circuit for a photocell, which is shown in Figure IV-4.

The available power is directly related to the current and voltage at the operating point and is mathematically equivalent to the product of the current times the voltage.

$$P = v_o i$$

Since the power variables are represented by the two axes of the output characteristic curve, constant-power curves can be plotted and superimposed on the output characteristics, as shown in Figure IV-5. It can be seen from the figure that the maximum power that the array can deliver at a specified temperature is at the point where the constant-power curve is tangent to the array output characteristic. In Figure IV-5 this maximum power point, 25°C, is 11 watts at a voltage of 16.2 volts. In order to realize this maximum available power, a load must be selected such that its load line will cross the output characteristic curve.

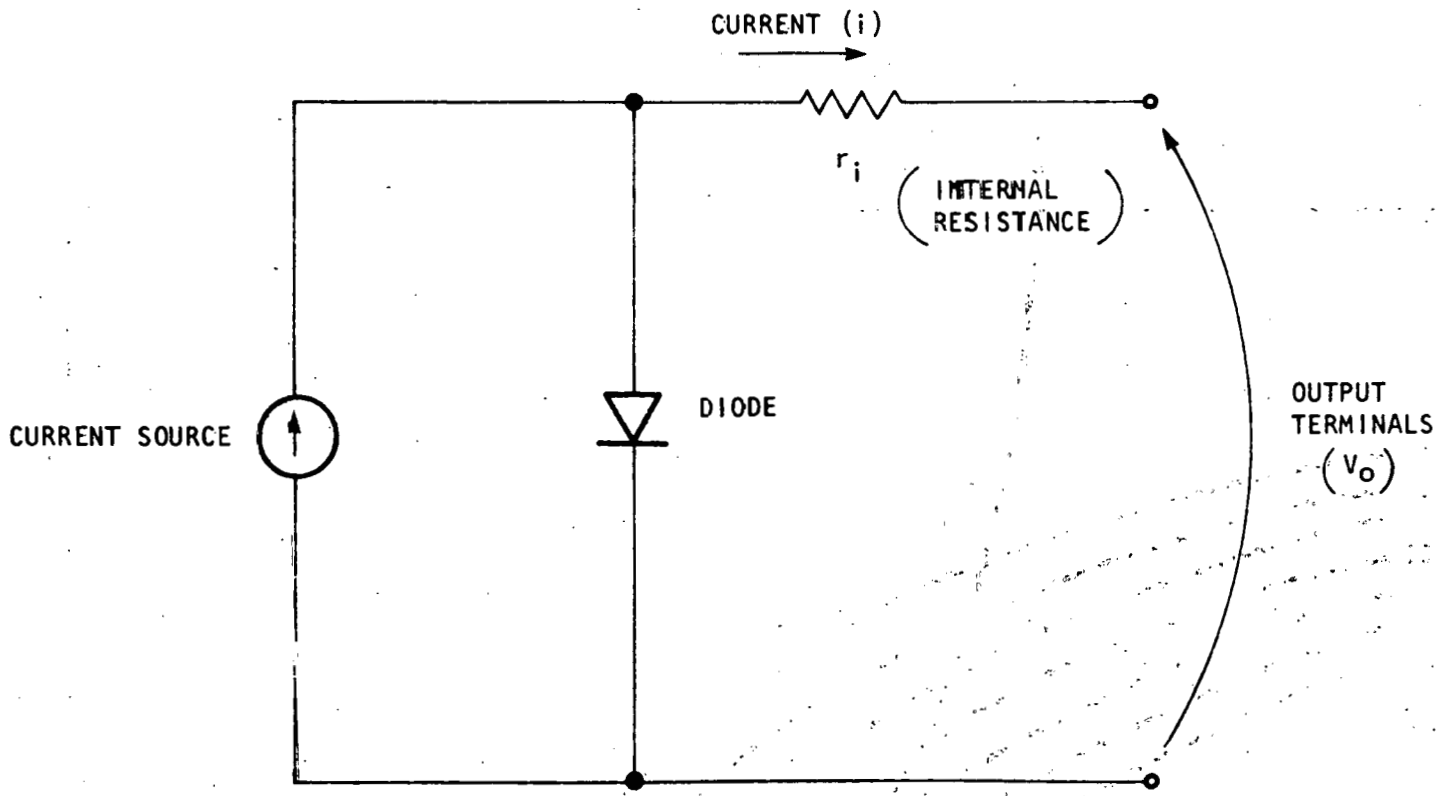

Figure IV-4. Equivalent Circuit for a Photovoltaic Cell

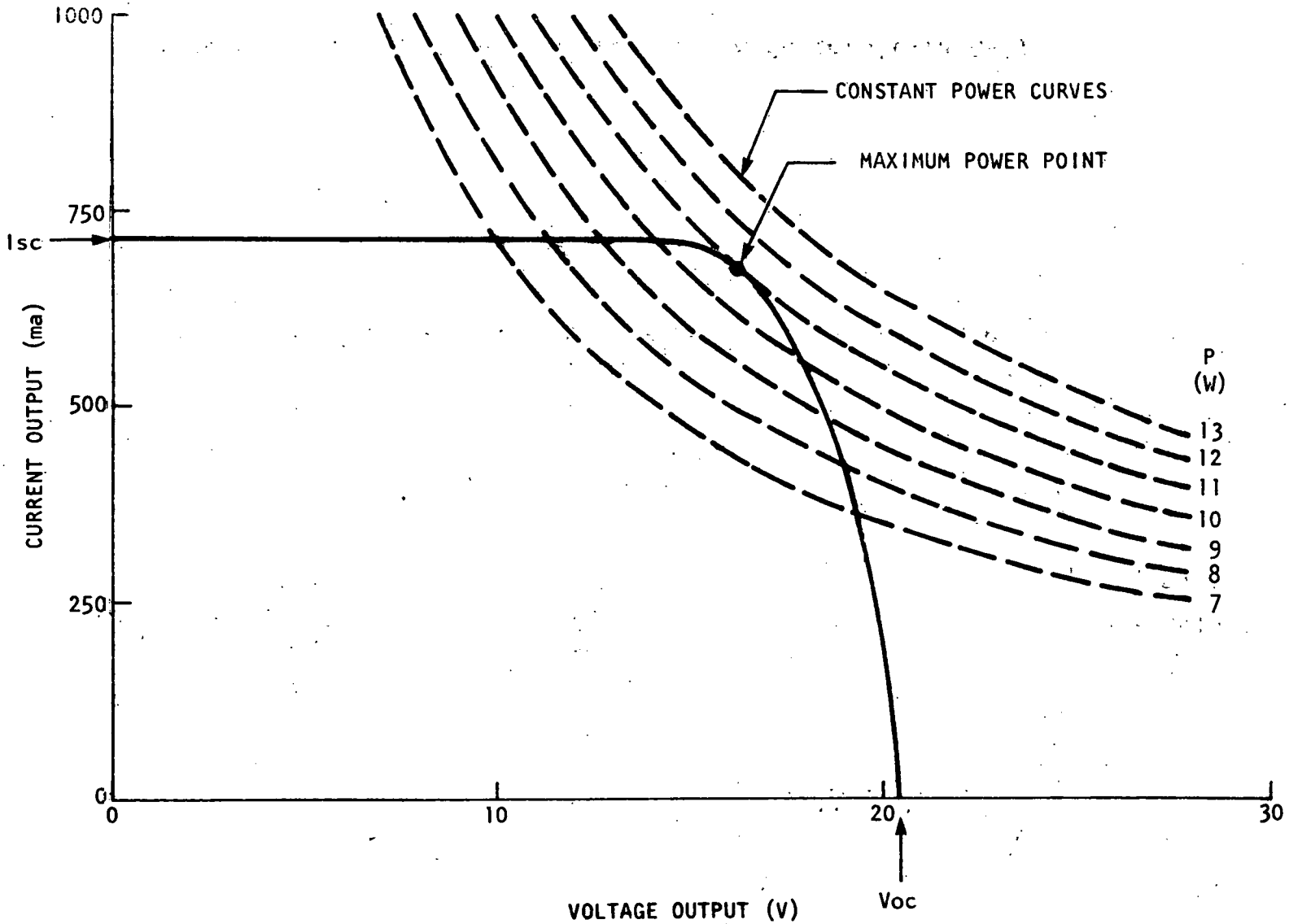

Figure IV-5. Voltage-Current Characteristics of a Photovoltaic Array

2. Efficiency

Cell or array efficiency is the capability of the unit to convert solar radiation to electricity. Although it is a measure of performance, it does not guarantee that the array will operate at its optimal performance level. It is therefore important to use this parameter as a measure of potential performance rather than a guarantee of performance.

Efficiency can be defined as:

$$= \frac{\text{Electrical Energy Output/Unit Area}}{\text{Solar Energy Input/Unit Area}} = \frac{\text{Power Out/Unit Area}}{\text{Power In/Unit Area}}$$

The amount of electrical energy that can be withdrawn from the cell or array is dependent upon the intensity of the solar energy striking the cell, the efficiency of the cell, and the effective area.

When considering the effective area of an array, one must include the surface area of (1) the photocells, (2) the voids between photocells and, (3) the frame and flanges. For this reason, the efficiency of an array is much less than the efficiency of the individual photocells in it. Additional factors which reduce efficiency are encapsulation materials and cell mismatching. Cells are encapsulated to protect them from the environment. The encapsulation material will reflect and absorb some of the incident light and transmit most of it. Only that light which is transmitted reaches the photocell. As a result, the encapsulated cell will be less efficient than the open cell. Although all cells produced in a given manufacturer's production run are made in the same way, each cell is unique. There is some variation in the voltage and current from cell to cell. When these cells are grouped together into an array, the fact that their characteristics may be slightly mismatched causes the array efficiency to be less than the efficiency of the individual cells.

The efficiency equation is used to calculate array efficiency. The solar energy input is generally expressed in terms of the quantity of solar radiation available at the surface of the array and normal to it. As an average figure, the amount of solar radiation available from the sun at sea level, without cloud cover, is 1 kW/m^2 (2) which is equivalent to 100 mW/cm^2. The physical size and power output of the array are available from manufacturer. The efficiency can then be calculated as follows with the aid of Figure IV-6. The solar radiation striking the array is assumed to be 100 mW/cm^2 or 0.1 W/cm^2.

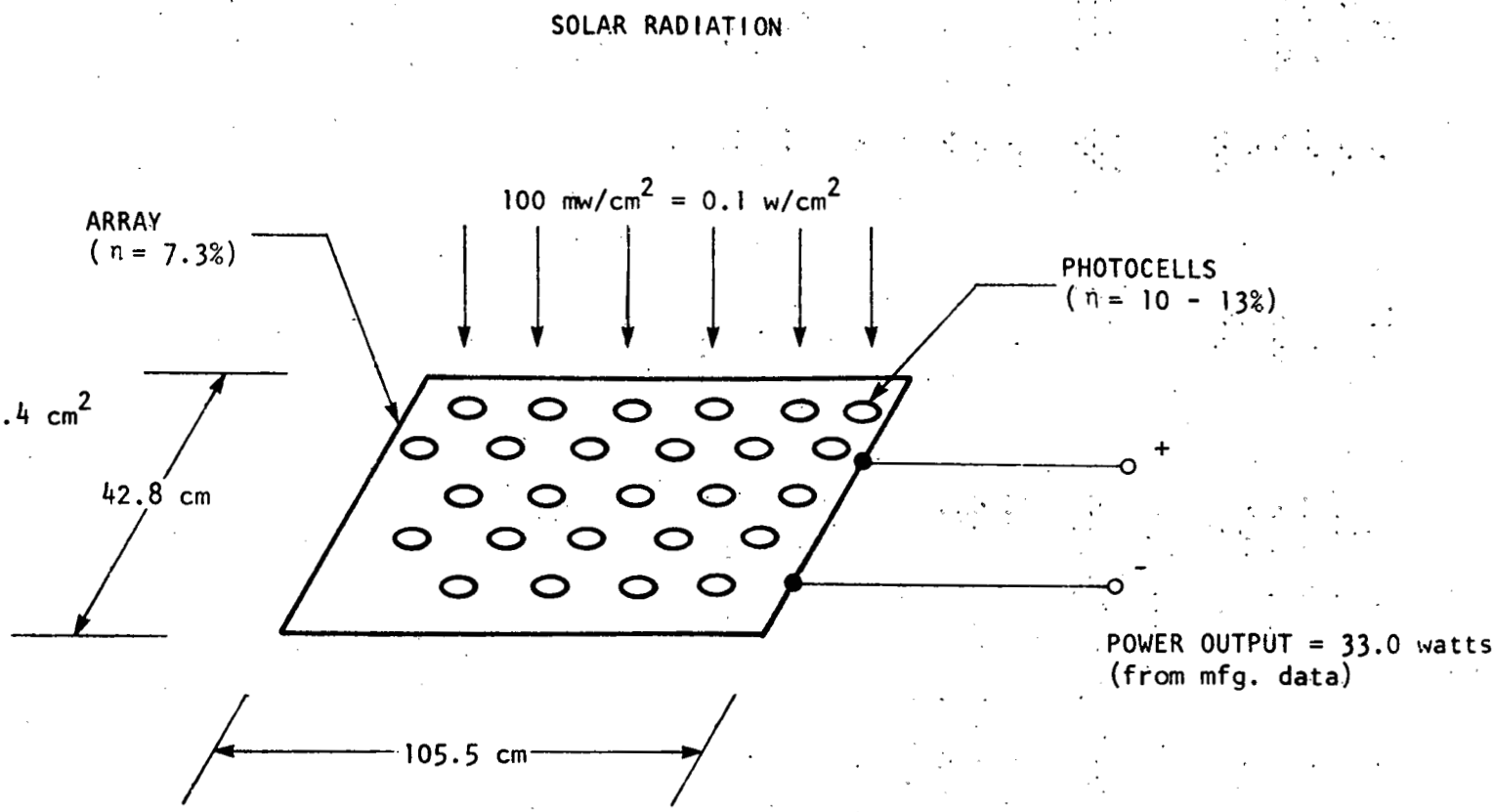

Figure IV-6. Cell vs. Array Efficiency

Example (Figure IV-6):

Solar Radiation x Surface Area = Power In

$0.1\ W/cm^2 \times 4515.4\ cm^2 = 451.54$ watts

$$\text{Array} = \frac{\text{Power Out}}{\text{Power In}} = \frac{33.0\ W}{451.54\ W} = 7.3\%$$

As indicated in Figure IV-6, there is a considerable difference between the cell efficiency and the array efficiency. It is also important to remember that it is the load which determines the operating point. If the load is not properly matched for most efficient operation, the system will operate at a lower efficiency than the array might otherwise provide.

3. Spectral Response

The output of a solar cell is dependent upon two factors: (1) the spectral distribution of the radiation falling on it, and (2) the ability of the solar cell material to absorb those particular wavelengths of radiation. Figure IV-7 shows both the spectral distribution of sunlight and the spectral response of a typical silicon solar cell.

4. Temperature

Photocells are temperature sensitive and their power decreases as the temperature increases. The temperature of the cell surface is the determining factor, not the temperature of the air around the cell. A cell operating in an ambient temperature of 45°C (113°F) with no wind blowing can be expected to have a temperature of between 65°C (149°F) and 70°C (158°F). The cell temperature decreases with increasing wind speed. At a wind speed of 2 mph, for example, the cell temperature would be only about 15°C (59°F) above ambient.

The effects of temperature on the output of the cell are shown in Figure IV-8. As indicated in this figure, when the temperature increases, the open-circuit voltage decreases, but the short-circuit current increases. Figure IV-9 shows the effect of temperature on the output variables. It is apparent that the percent of voltage decrease is much larger than the current increase. Since power is the current-voltage product, one would expect the power to decrease with a temperature rise and Figure IV-9 confirms this.

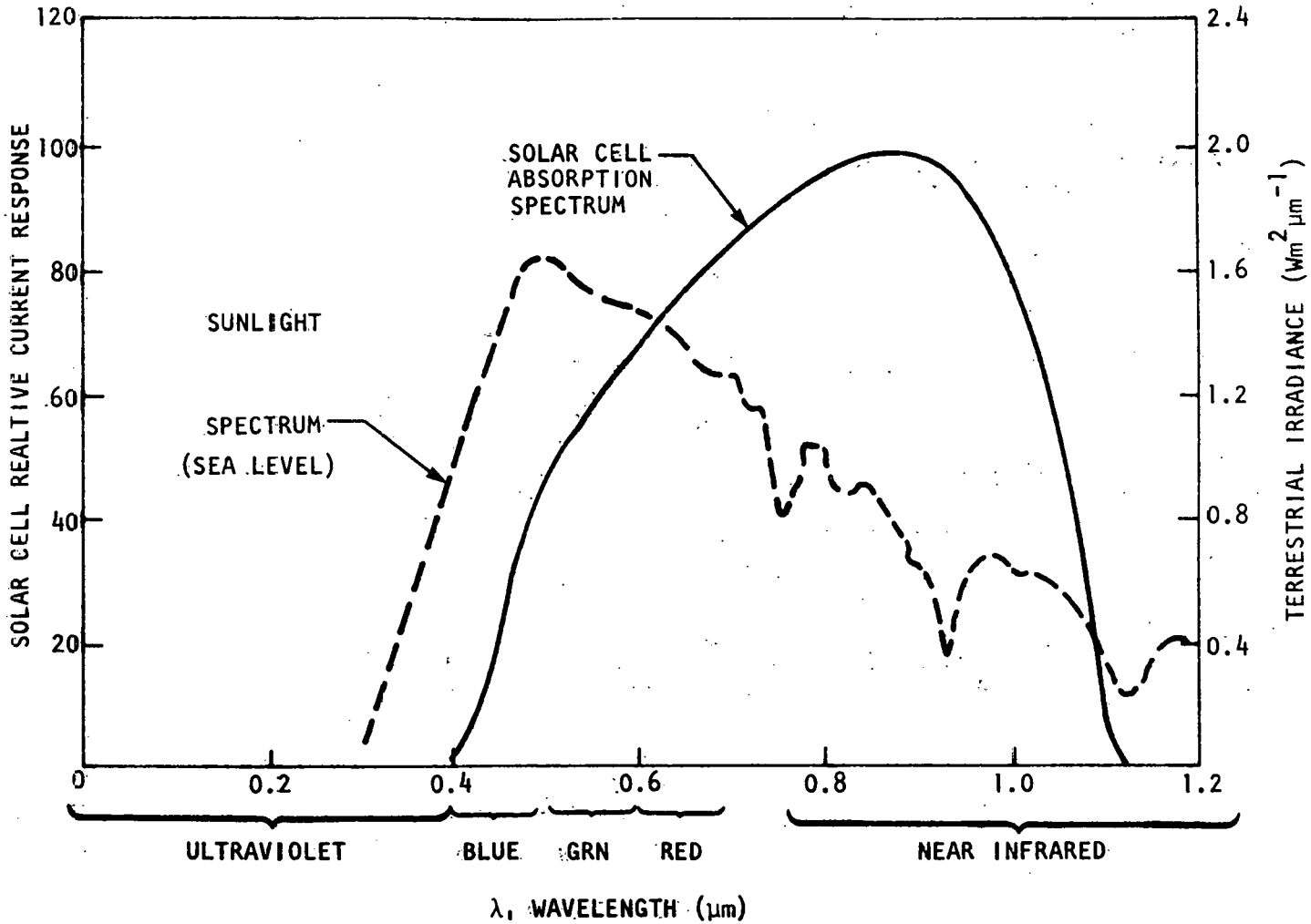

Figure IV-7. Spectral Response Curves for a Silicon Solar Cell

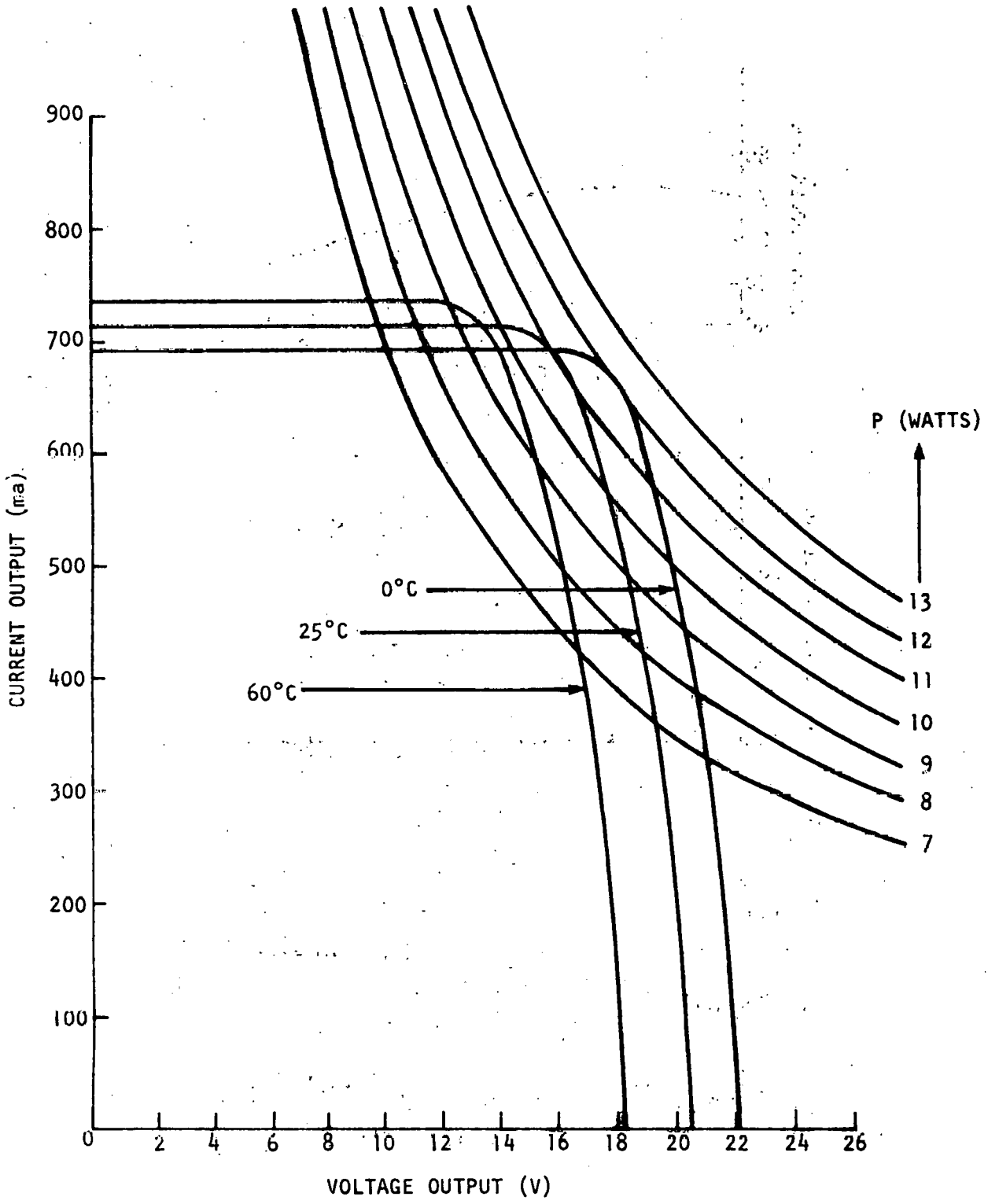

Figure IV-8. Effects of Temperature on Output Characteristics

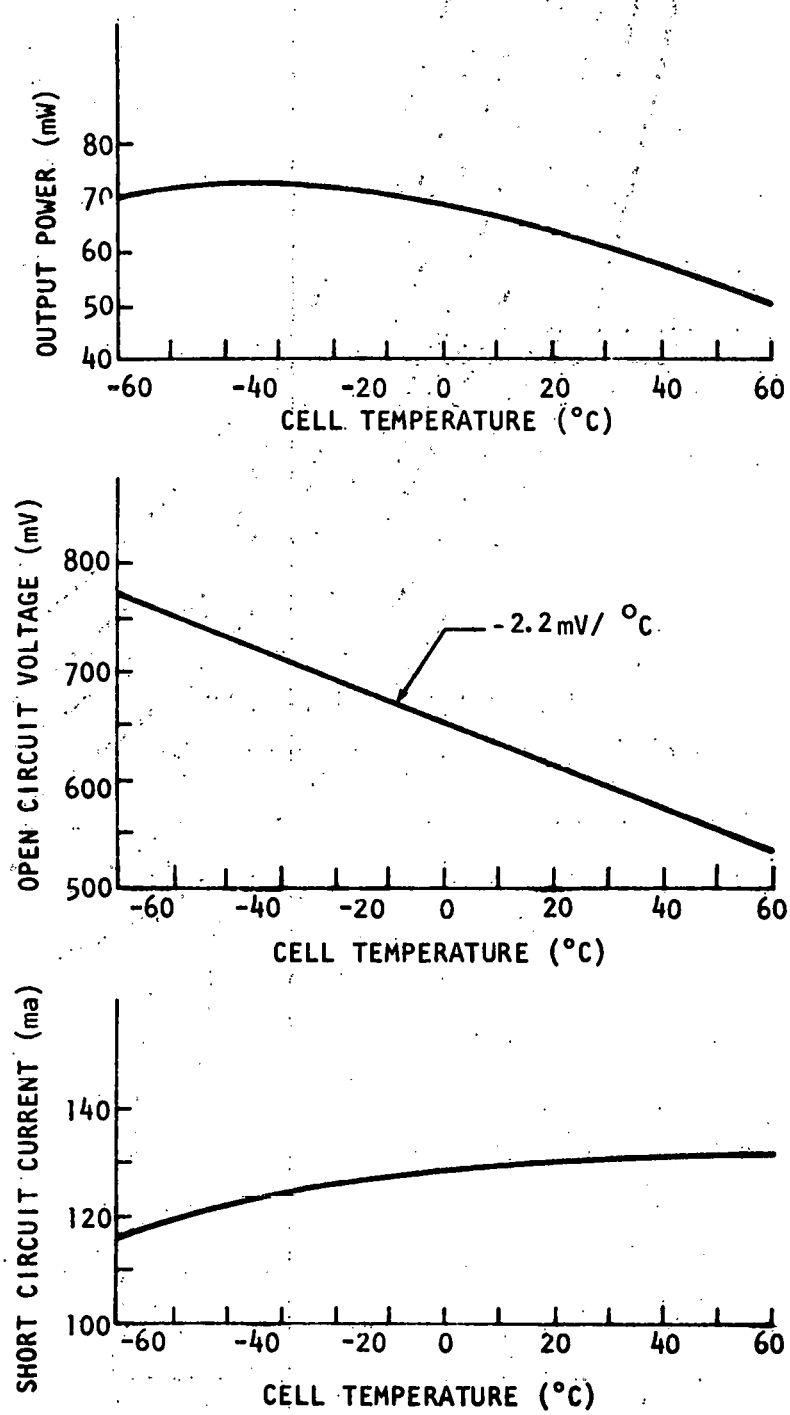

Figure IV-9. Effect of Temperature on Power, Open-Circuit Voltage, and Short-Circuit Current (2)

5. Insolation

Insolation is the intensity of solar radiation per unit area. There are two reference points for identifying and quantifying solar radiation, air mass zero (AM0) and air mass one (AM1). Beyond the earth's atmosphere the solar radiation has an intensity of 1.38 kW/m^2 and is referred to as AMD. At sea level, or AM1, the intensity is approximately 1.0 kW/m^2 (2).

The electrical output of a photovoltaic array at a given time depends on both the air mass and the incident angle between the sun's rays and the plane of the array. For a two-axis tracking array, the array plane is always oriented with its normal axis directed toward the sun. The elecrical output of two-axis tracking arrays is, thus, only affected by the air mass. Figure IV-10 illustrates the electrical output on a clear June day for a two-axis sun-tracking array. For a fixed array, the incident angle changes with the sun's apparent movement throughout the day. Figure IV-11 illustrates the electrical output (on clear day) of a fixed array, aligned so that, at noon, its normal axis points toward the sun.

6. Cost

The major impediment to large-scale commercialization of photovoltaic arrays is their high cost. The largest cost item in an array is the photocell. In concentrating systems, the reflectors account for a large portion of the array area and the cells, a smaller portion. Since manufacturing reflectors is cheaper than manufacturing photocells, much consideration is being given to using concentrators as a means of reducing costs. Even in concentrating systems, the photocell cost as a percentage of the system is high.

The main cost factors in photocell production are: (1) raw material availability, (2) raw material use in the photocell, and (3) the manufacturing process of the photocell itself.

If the raw material is scarce, its cost will be high, as different markets compete for the scarce resource. Commercial arrays use silicon or cadmium sulfide cells. Cadmium [205 x 10^6 kg U.S. reserves, 850 x 10^6 kg world reserves (3)] is less plentiful than silicon [essentially unlimited (3)] but it is not scarce. There are sufficient quantities of both materials for today's demands. If future expectations materialize, very large quantities of photocells will be needed; under such circumstances, cadmium would become scarce while silicon would still be in abundance. This abundance of silicon is one reason why much research is being done on polycrystalline and amorphous silicon photocells.

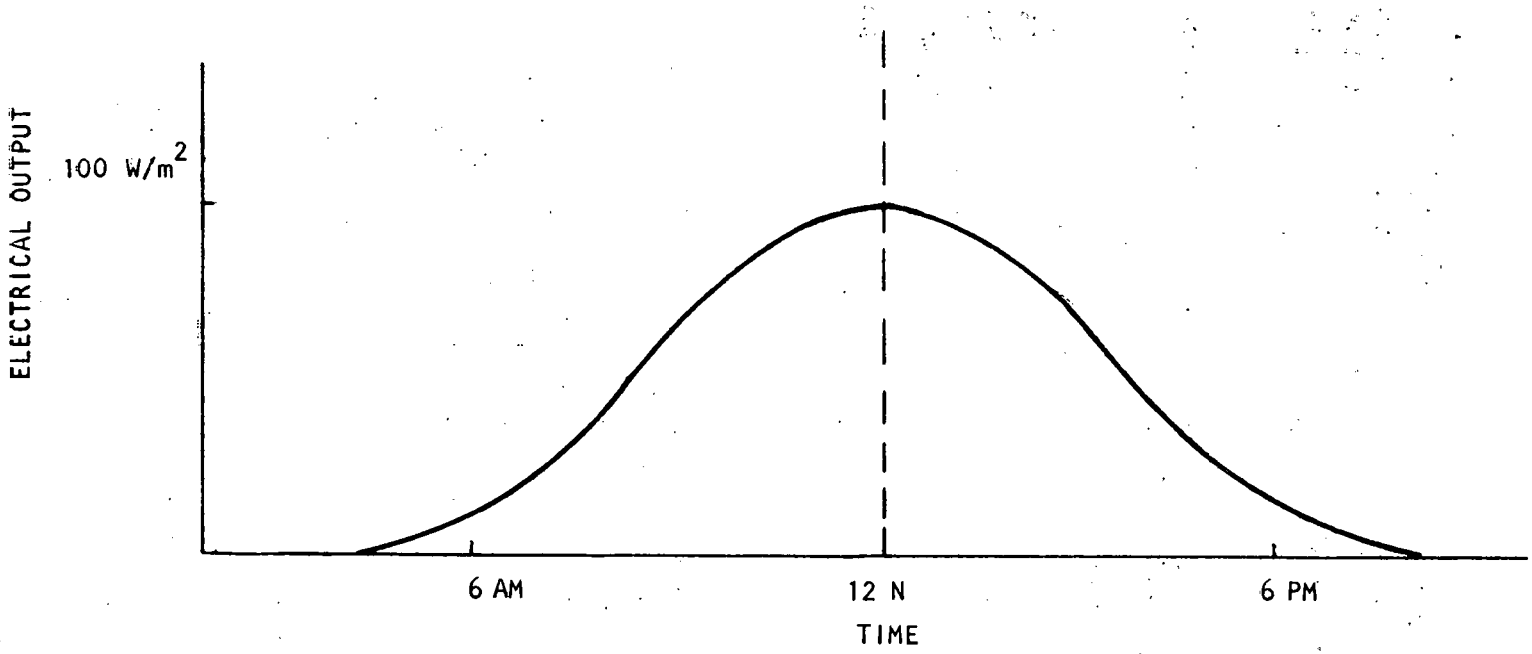

Figure IV-10. Fixed-Array Output Profile

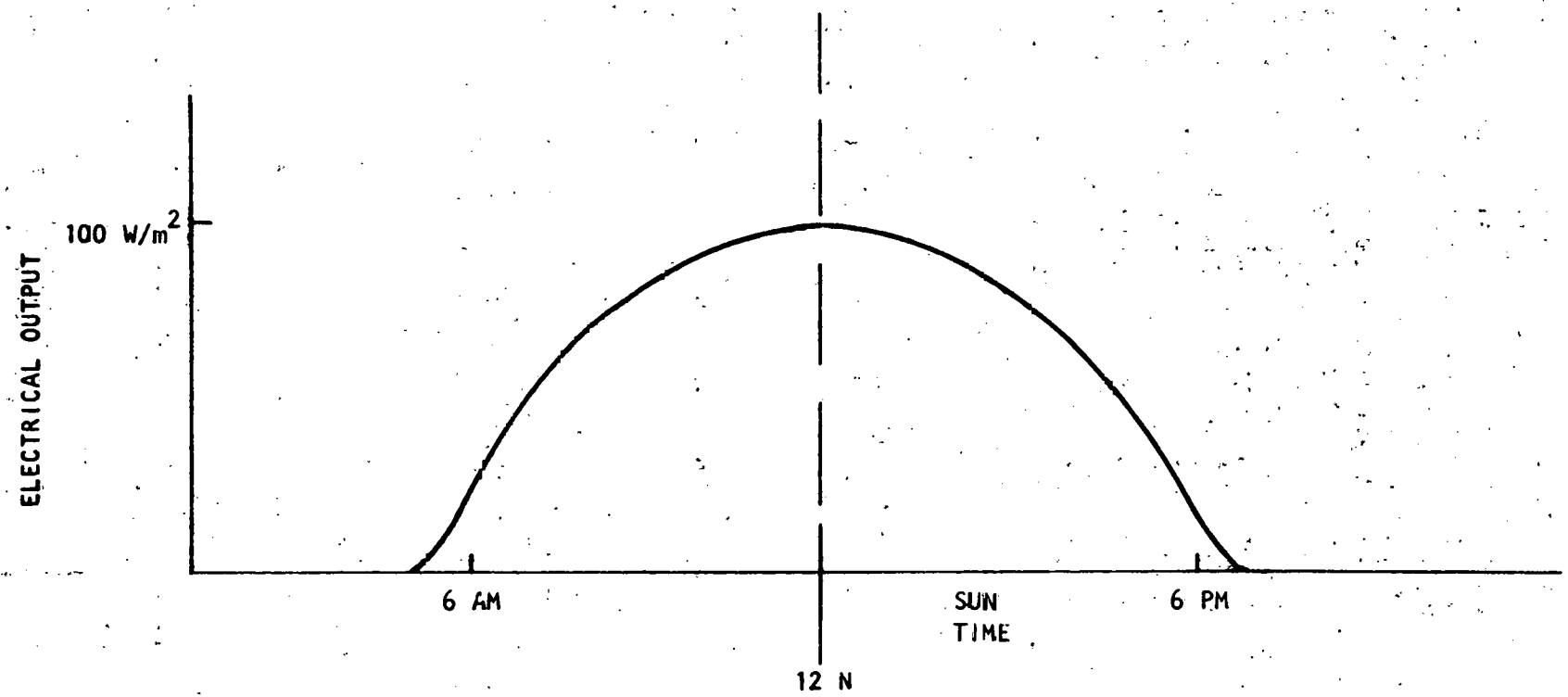

Figure IV-11. Two-Axis Sun-Tracking Array Output Profile

The cost of raw materials use in photocells is dependent upon the quantity of material used per unit of power and the preparation cost of that material. (Preparation cost will be discussed later.) This is apparent, for example, in the use of silicon cells. The monocrystalline cell is presently the most popular type of silicon cell. This use requires high-quality silicon. One way of growing this silicon is shown in Figure IV-12. The silicon cylinder is then cut into wafers of 50 to 300 μm thickness (2). Each wafer becomes the basis for an individual photocell. Another fabrication technique under experimentation employs "thin-film" cells. This technique has a thin film of silicon (3 μm thick) deposited onto a substrate (2). The thin-film cell efficiency is about half that of the monocrystalline cell efficiency, so two thin-film cells are needed to obtain the power output of one monocrystalline cell. Even under these conditions, there is a large difference in the quantity of silicon needed: 50 μm/6 μm = 8.3 times. For a given power output, thin-film cells would require 88 percent less silicon than current monocrystalline cells. It is not the quantity of material that is of prime importance, but rather the quality. Silicon as a raw material is plentiful and inexpensive. The cost problem is associated with the production of pure monocrystalline silicon. Because the use of thin films can eliminate the need for costly pure monocrystalline silicon, they are the focus of present research.

Both the processing of the material and the fabrication of the cell have the potential for cost reduction. In the cell fabrication process, the crystal is cut into wafers. Each water is then enclosed and a current collection grid is attached to it. These steps are not adaptable to low-cost mass production techniques. Thin films, on the other hand, can use spray deposition techniques which are particularly suited for continuous process production and are less costly. Additional cost reductions will come about as production quantities are increased and economies of scale come into play.

7. Maintenance and Repair

The following maintenance is required for solar arrays (8):

(a) Solar modules should be inspected for dirt, dust, bird droppings, insects, or other foreign material on the glass. Warm water and a soft cloth should be used for cleaning.

(b) Module mounting bolts should be inspected for tightness and tightened as required.

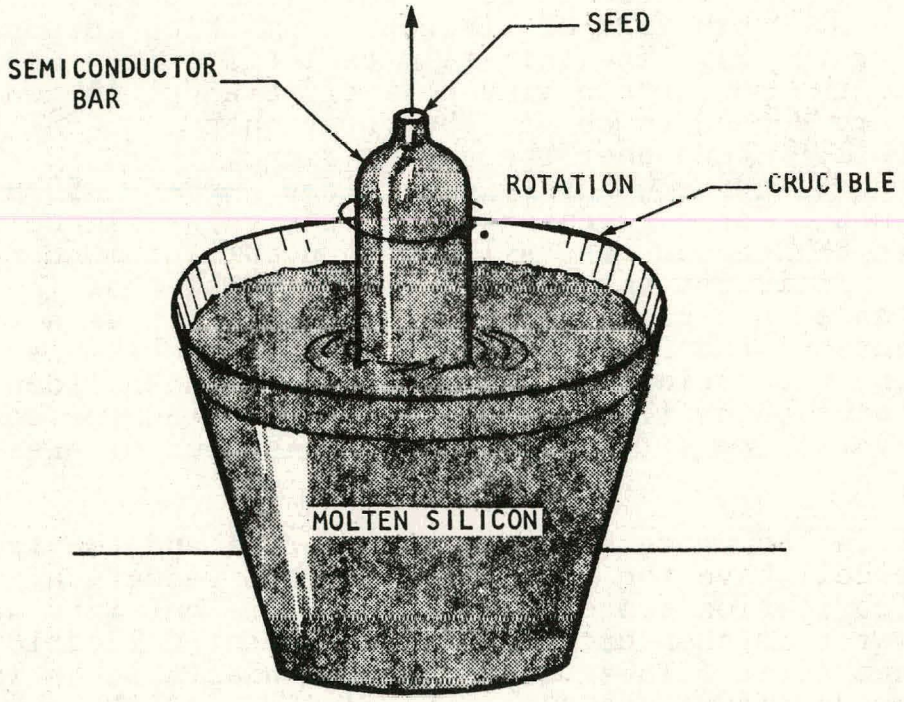

Figure IV-12. The Crystal-Growing Process in Schematic Form

(c) Module labels should be inspected for legibility and adherence. Labels should be cleaned, re-attached, or replaced as necessary.

(d) Rubber boots, silicone weatherization, and terminals of each module should be inspected for adequate weatherization. Terminals should be tightened and silicone weatherization repaired as required.

(e) Electrical wiring insulation should be inspected for cracking, peeling, or other defects and replaced as required.

(f) Installation sites should be inspected for any weeds, shrubs, trees, or other growth which could shade the array from sunlight. All such obstructions should be removed or cleared as required.

(g) Tracking mechanisms should be inspected for proper operation. Replacements should be made as required.

(h) Tracking mechanisms should be lubricated.

Table IV-1 shows the frequency of repair for a photovoltaic array.

TABLE IV-1. FREQUENCY OF REPAIR FOR A PHOTOVOLTAIC ARRAY

Item	Activity	Frequency
Solar Module Glass Cover	Inspect, clean as necessary	yearly
Solar Module Mounting Bolts	Inspect, tighten as necessary	yearly
Electrical Connections	Inspect, tighten as necessary	yearly
Solar Module Electrical Terminal Weatherization	Inspect, repair as necessary	yearly
Electrical Wiring Insulation	Inspect, replace as necessary	yearly
Obstructions that Can Cause Shade on the Array	Inspect, remove or clear as necessary	yearly
Tracking Mechanism	Inspect, lubricate, replace parts if necessary	twice yearly

Repairs to flatplate systems consist of replacing broken or faulty modules and making electrical connections. A module which has cracked cells is defined as a broken module. Cracked cells may be caused by vandalism, extremely heavy hail, or structural and thermal stress. Modules become faulty when their encapsulation breaks down. Repairs on concentrating and hybrid (combined photovoltaic and solar thermal) systems would involve those concerns which are common to fluid flow systems, electro-mechanical drives, and heat exchangers.

8. Life-Reliability-Degradation

These three variables are interdependent and involve two areas of concern: (1) physical capability and (2) electrical performance. Life is defined as the length of time the array may be expected to last while providing a given level of performance in a given environment. Reliability is defined as the array's expected level of performance over a period of time. Degradation is the expected amount of deterioration in performance over a given period of time.

Little reliable data is available on these subjects for cell materials other than silicon. Data on silicon exist because of its extensive use in the space program and because it is the most widely used terrestrial array. Endurance testing on photovoltaic modules shows that module failure is less than one percent annually (4). The majority of these failures are due to cracked cells. Reasons for cell cracking need more research but two causal factors have been identified: (1) projectiles impacting the array, and (2) temperature cycling. In addition, structural support for the cell in the module stresses the cell, and if it is not mechanically strong enough (a function of thickness) it will crack.

Electrical degradation in the above tests has shown that power loss due to the accumulation of dirt ranges from 1 to 28 percent, with a loss of less than 10 percent being the predominant value. Physical degradation appeared in the form of cracked cells, a delamination of the cell encapsulant, and cell discoloration.

The failure of any particular module generally does not put the system out of action. Depending on the degree of the failure, the range of its impaction system performance can be anywhere from moderate to severe.

Cell life is also sensitive to the environment. Cadmium-sulfide cells cannot tolerate moisture and must be well sealed. Silicon is not affected by moisture; however, the grid on the silicon cell corrodes in the presence of moisture,

so it too must be sealed. Sealing is accomplished by encapsulating the cells in silicone or glass. When the encapsulant is destroyed, moisture seeps in and, over time, destroys the cell. Silicone can discolor over long time periods and is more susceptible to dirt degradation than is glass. Silicone, however, is not as rigid as glass and can better withstand impacts from projectiles. Glass, on the other hand, washes better, yielding a higher electrical performance over its life, but shatters easily. Silicone is also susceptible to the attack of birds. Their beaks deform and sometimes penetrate the encapsulant. Both materials are used by manufacturers.

C. Photovoltaic Cells: Principle of Operation

Solar cells operate on the principle of photovoltaic effect: photons are absorbed to create equal numbers of positive and negative charges. The charges can be separated to generate a photovoltage and photocurrent, and power flows to the load.

Solid semiconductors are the most suitable materials for solar cells. The electrostatic inhomogeneity in semiconductors can be incorporated to separate the electrons and holes. Both homojunction and heterojunction structures can be used in semiconductors.

Figure IV-13 shows the basic principle of operation of photovoltaic cells. Semiconductors are made up of atoms. Large numbers of atoms are grouped together to make a crystal. The crystal consists of a p-type region, n-type region, and a junction. The junction consists of semiconductor material with p-type doping on one side and n-type doping on the other. The purpose of doping is to increase the quantity of free-charge carriers roaming around the crystal. The semiconductor becomes substantially more conductive after doping.

Energy conversion is triggered when a photon of sufficient energy penetrates the cell and dislodges an electron in the p-type region. In other photovoltaic devices, the process may occur in the n-type region or both. The electron moves into the n-type region and leaves behind a hole that moves toward the lower contract. The electron flows through the external circuit, producing electric current, and recombines with a hole near the p-type contact. The limitation on photovoltaic conversion efficiency is that some photons lack the energy to initiate this process, whereas other photons have more energy than the system can use. The excess energy is, however, wasted (7).

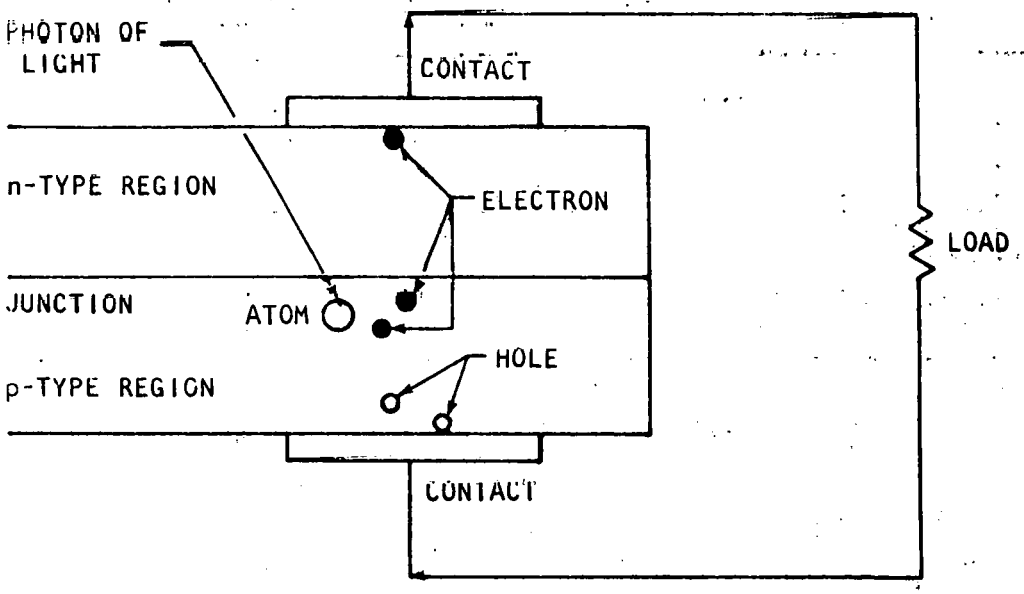

Figure IV-13. Principle of Operation of a Photovoltaic Cell (7)

D. Types of Cells

Research and development on photovoltaic materials has focused primarily on semiconductors since they exhibit the photoelectric effect. Each material used exhibits different properties and has its own idiosyncrasies. Each, for example, exhibits a different spectral response. Materials that have been used and researched extensively include (1) silicon, (2) cadmium sulfide, and (3) gallium arsenide. Other materials such as cuprous indium selinide, indium phosphorus, cadmium telluride, and cuprous oxide are being investigated for their potential in photovoltaic applications. Efficiencies for common cell materials are shown in Table IV-2.

TABLE IV-2. EFFICIENCY DATA (2)

Cell Type	Theoretical Cell (%)	Actual Cell (%)	Array* (%)
Silicon	23	10-15	4-10
Cadmium sulfide	11-14	5	3.68
Gallium arsenide	27	13	----

NOTE:
*Calculated from manufacturer's advertising literature.

Although any one of these materials can be used in the presence of light to produce electricity, very few of the materials are technologically or economically feasible at the present time. Of these, silicon is the most widely used photovoltaic cell material.

The most common photocell is the silicon monocrystalline cell. A typical cell is shown in Figure IV-14. Monocrystalline cells are made from a pure semiconductor material which is sliced into wafers. Doping agents of the N and P type are applied to create the junction (also called the barrier). Next, a grid is attached to both sides of the barrier. The grid will collect the current generated in the cell and direct it to the load. Since the grid is attached to the surface of the cell, part of the cell surface is covered by the grid and cannot receive light. This shaded portion of the cell cannot generate power. To minimize the grid shading factor, an antireflective coating is given to the cell. The coating is designed to minimize the amount of light reflected from the surface of the cell, thereby increasing the amount

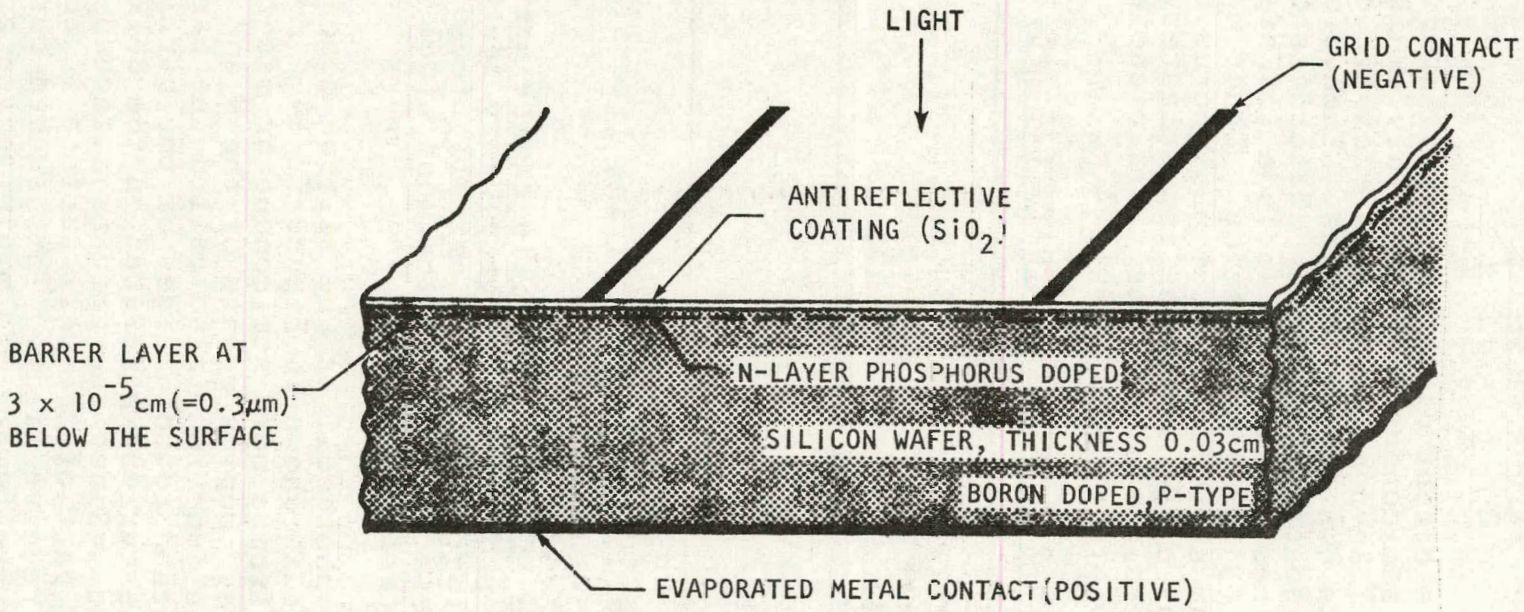

Figure IV-14. Cross-Section of a Conventional Silicon Solar Cell (2)

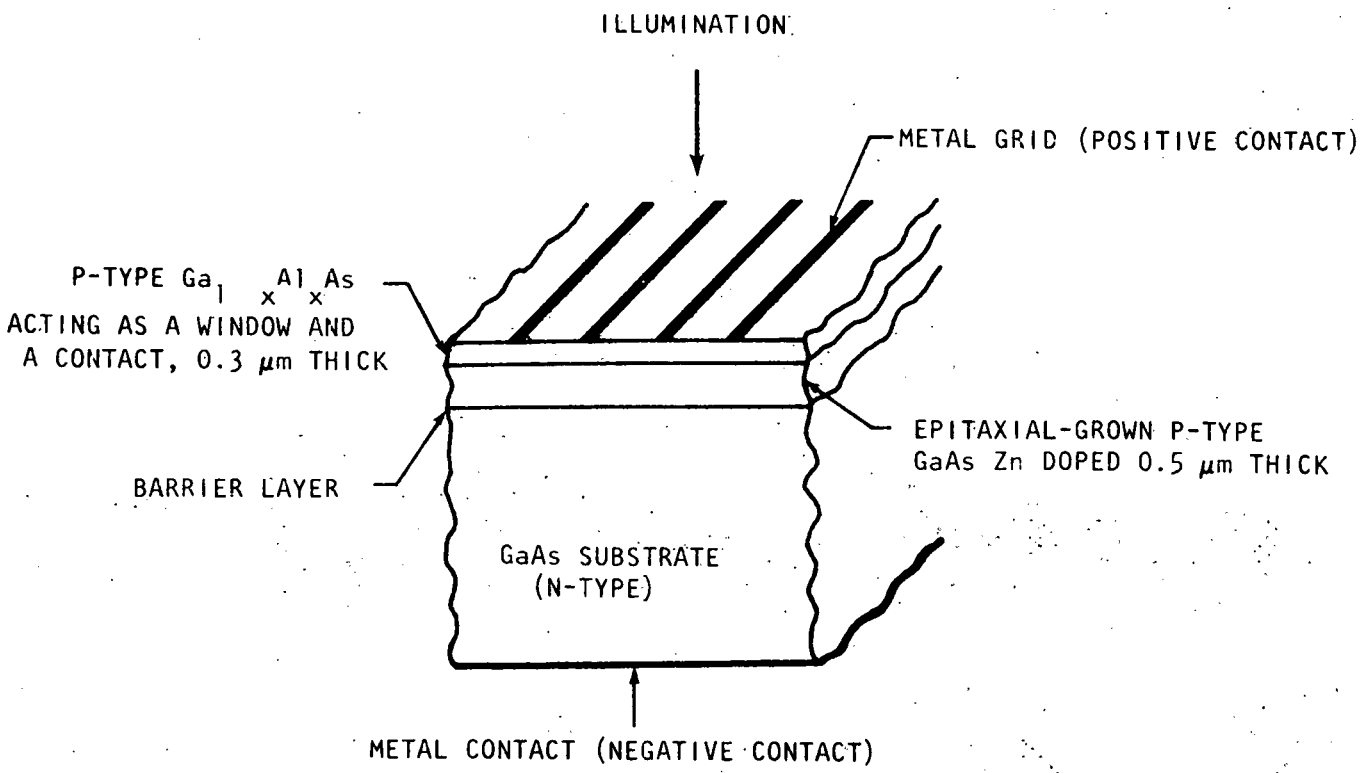

Figure IV-15. Cross-Section of a GaAs Solar Cell (2)

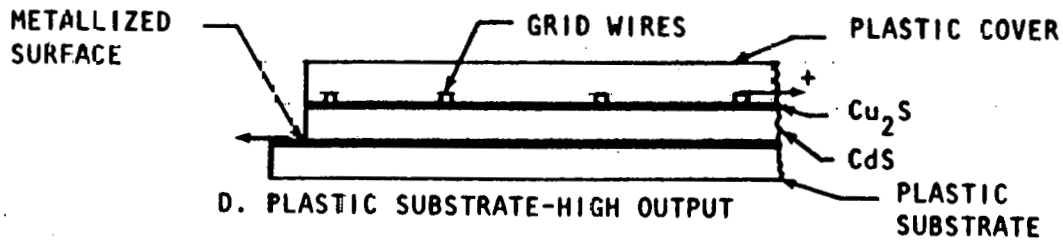

Figure IV-16. Frontwall CdS Film Solar Cells (5)

absorbed by the cell. This is important since the electricity generated is dependent upon the amount of light absorbed by the cell, not on the amount of light striking the cell. Finally, the cell is encapsulated to protect it from the environment.

The area receiving the most research and development today is thin-film cells. Figure IV-15 shows a gallium arsenide cell with a semiconductor substrate, while Figure IV-16 shows a cadmium-sulfide cell with a plastic substrate. The main purpose of a substrate is to provide mechanical support for the thin films which will be deposited on it. Thin films may be applied onto the substrate in the form of polycrystalline or amorphous matter. Figure IV-15 clearly shows how films are deposited in layers on top of a substrate. Thin-film cells are receiving the bulk of R&D attention because the cost of producing such cells is projected to be substantially less than that of monocrystalline cells.

E. Types of Arrays

There are two types of photovoltaic arrays: flat-plate (see Figure IV-2) and concentrating. Flat-plate collectors are generally mounted facing south at a fixed tilt angle. The tilt angle selected is close to the angle of the latitude of the site's global position, except in tropical latitudes. In tropical latitudes between 23°N and 23°S, the solar declination exceeds the latitude during part of the year. In these regions, the optimum design may have part of the array facing north and part facing south. Concentrating collectors make use of the photocell characteristics: power output increases as the light intensity on the cell surface increases. Concentrators therefore require less photocell area than flat-plate collectors for a given power output. Since photocells are more expensive than concentrators, this reduction in cell area makes concentrating systems an interesting area for R&D. Figure IV-17 shows a fixed-position configuration. All configurations gather the rays of sunlight and concentrate them on the cell surface. Either reflectors or lenses are used. The fresnel lens is a popular lens. Its principle of operation is shown in Figure IV-18. The lens may be used in rectangular or circular form. In circular form, the lens concentrates the sunlight onto a single cell. In rectangular form, the lens concentrates the light onto a row of cells. Although concentrators can reduce the cell area required, the concentrator system requires just as much collector aperture area as the flat-plate collector system.

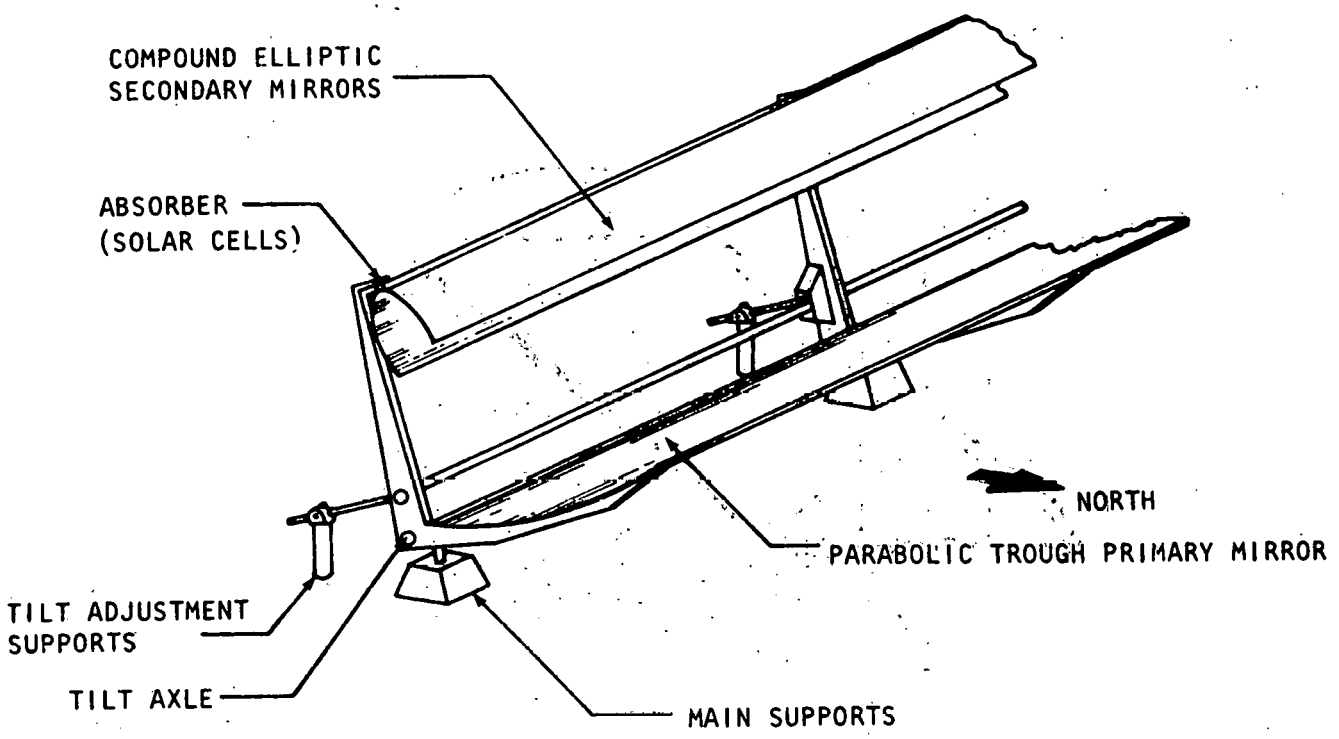

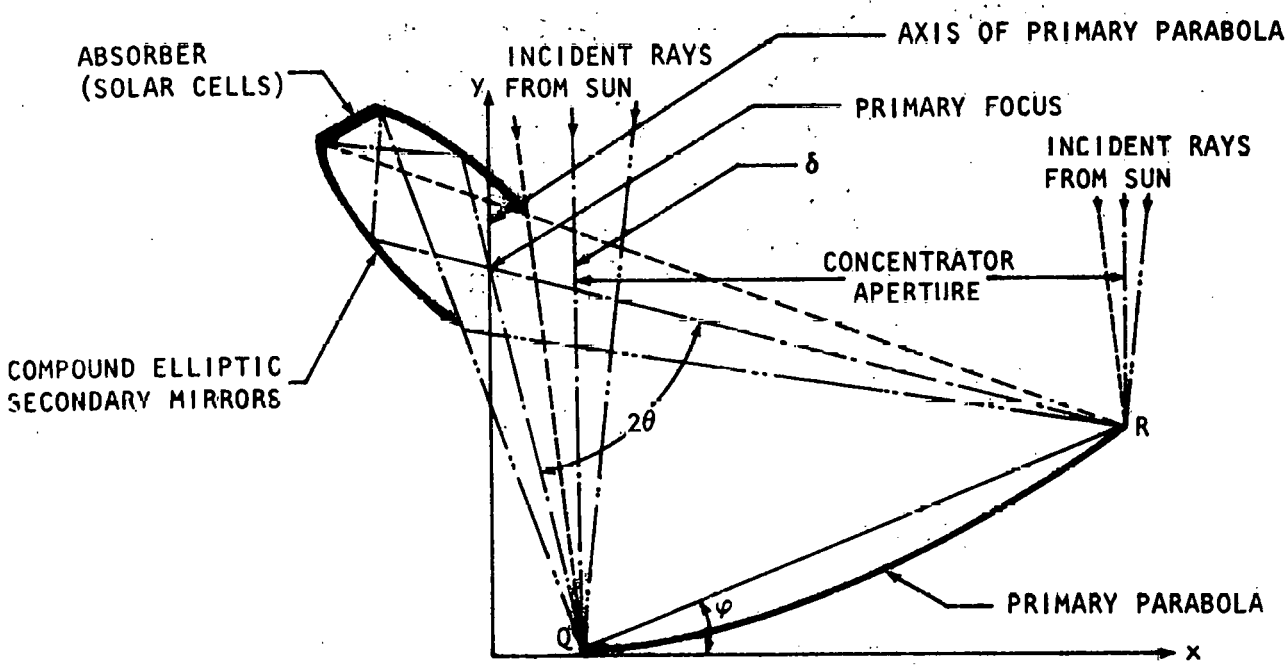

Figure IV-17. Off-Axis, Parabolic Trough, Compound-Elliptic Concentrator; Ray-Trace Diagram (2)

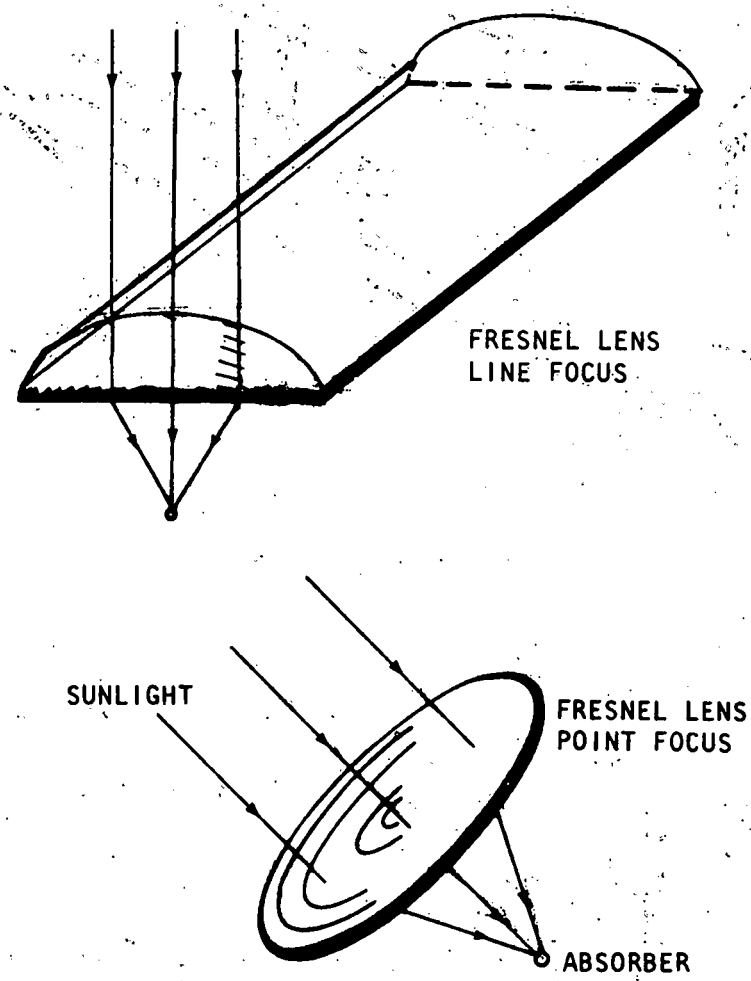

Figure IV-18. Fresnel Lenses (2)

A major difference between the two collection methods is the amount of sunlight each system can use. Concentrating systems use only direct sunlight and focus it onto the cells with the help of a tracking mechanism. Flat-plate collectors use both direct and diffuse sunlight. The concentrating system does not work when there is cloud cover, while the flat-plate system does although at a much reduced output level. On an average day in a temperate climate, 40 percent of the sun's energy that is received on the earth's surface is diffuse while 60 percent is direct (2). Even in an arid climate, at least 20 percent of the sun's energy is diffuse radiation (2).

Flat-plate or concentrating systems can be mounted in either a fixed position or be provided with a tracking system. Most flat-plate collectors are mounted in a fixed tilted position, while most concentrating systems employ a tracking method. In order for a concentrating system to operate at its optimum capacity, it must continuously track the sun. The greater the concentration ratio of the reflection or lens, the more important it is to track the sun with a high degree of accuracy. With high concentration units, a small error in aiming directly on the sun causes a substantial loss in system efficiency. This error becomes very small for concentrations of 10 or less. Precise tracking requires altitude variation as well as azimuth rotation. Such systems are very complex and costly; as a result, some manufacturers sacrifice a percentage of the incident energy and track only through the vertical angle. A typical two-axis tracking mechanism is shown in Figure IV-19. A graphic summary of concentrator types is provided in Figure IV-20.

Hybrid arrays make use of both the electric power and thermal energy in a common collector. As the sun strikes the collector, the temperature of the collector surfaces and solar cells increases. By the use of a circulating coolant, the thermal energy is made available for space heating or other use. This results in two immediate favorable effects: (1) as the cells warm up, their efficiency is reduced, so more power can be obtained by keeping them cool; (2) when the thermal energy can be used effectively, the system will operate much more efficiently than if the thermal energy is dissipated to the environment and thermal energy needs are supplied by other means. Accordingly, the array cost per unit of energy output will be reduced. (Other system costs, such as heat transfer equipment, must be considered before drawing conclusions on the system cost per unit of energy.) Figure IV-21 is a cross-section of a flat-plate hybrid system, while Figure IV-22 is a sketch of a concentrating hybrid collector.

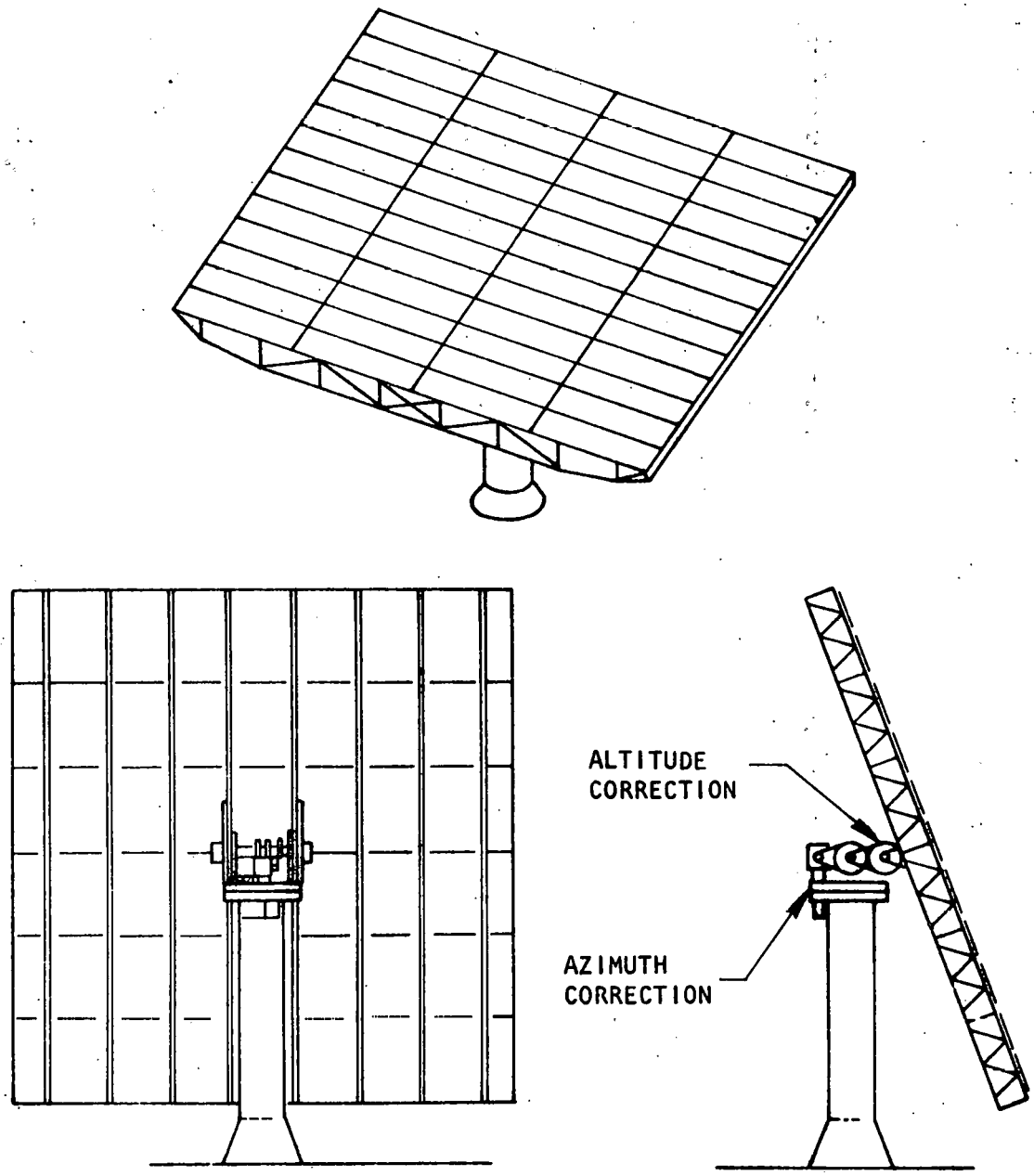

Figure IV-19. Two-Axis Tracking (6)

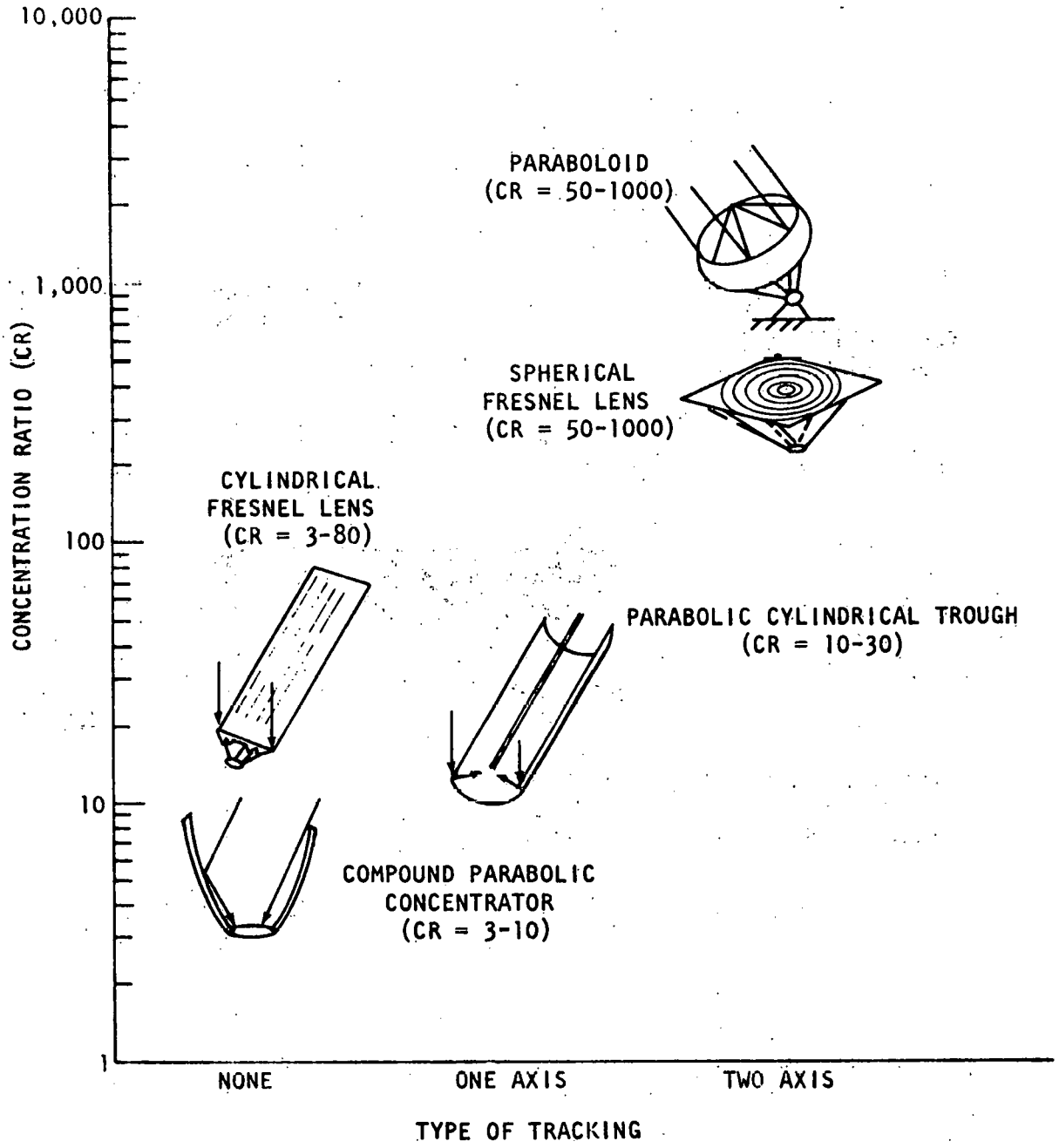

Figure IV-20. Concentrator Optics

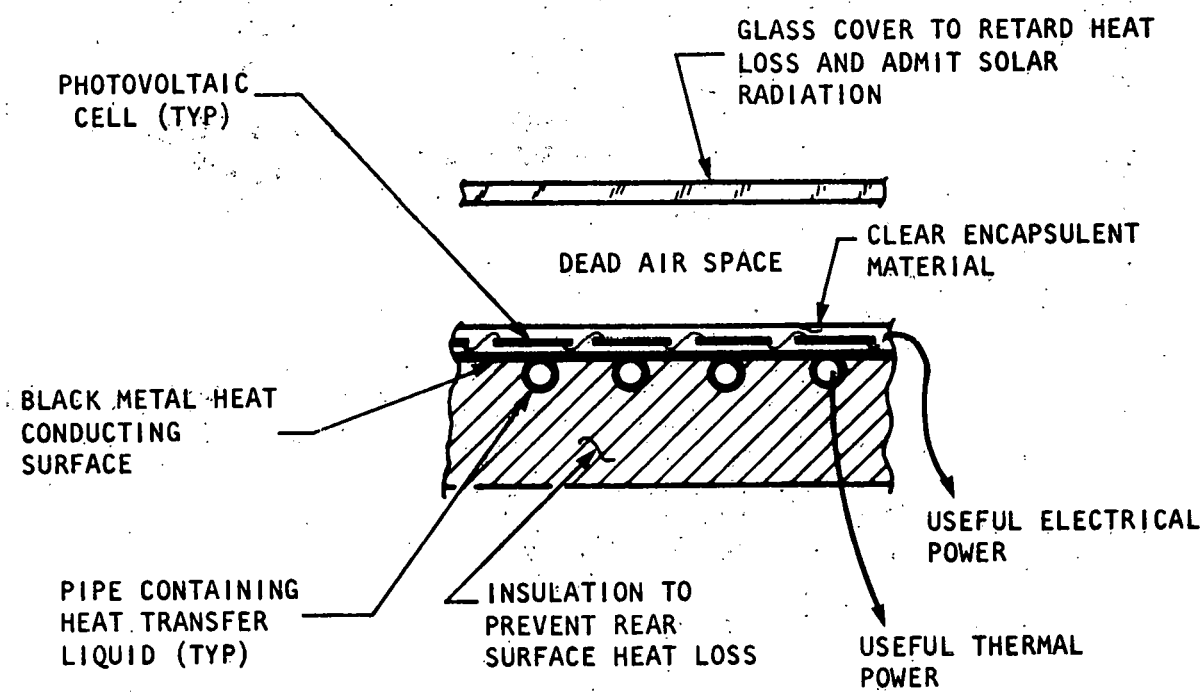

Figure IV-21. Hybrid Photovoltaic/Thermal Solar Energy Collector Section

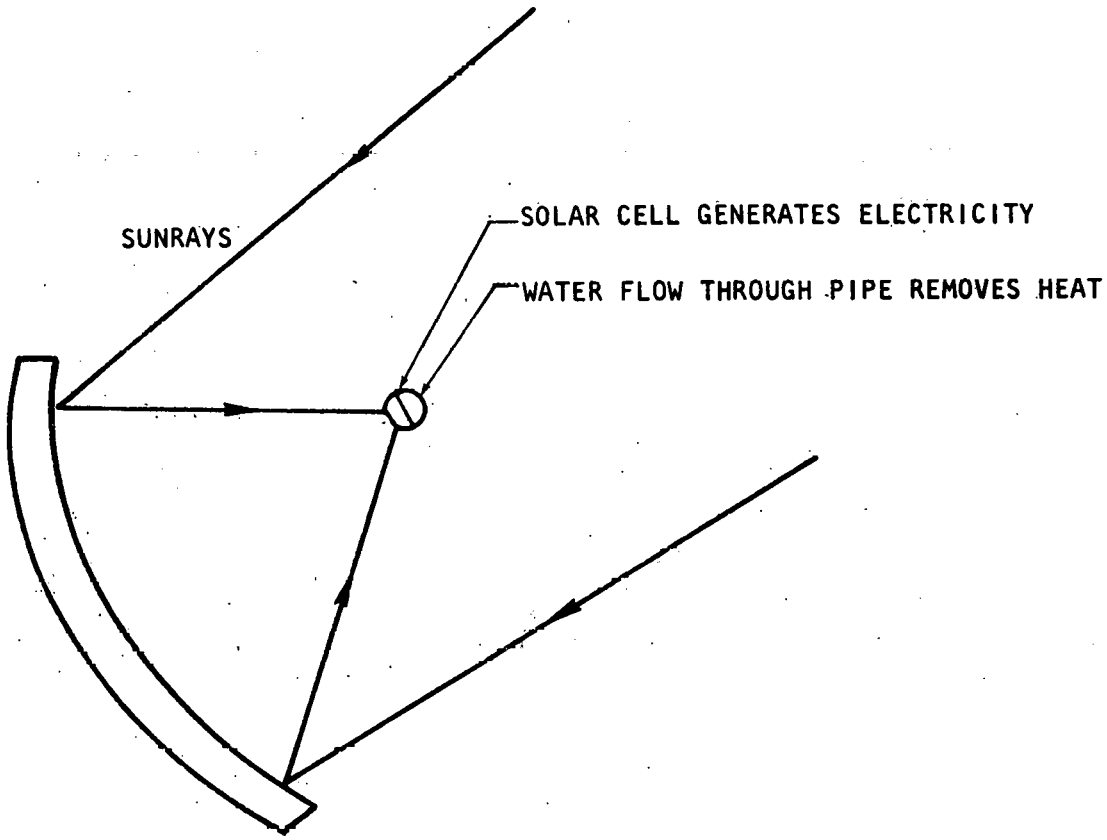

Figure IV-22. Concentrating Hybrid Collector (Parabolic Trough)

F. Array Manufacturers

1. Introduction

The photovoltaic market is a high-risk business. Access to this marketplace lies in three areas: (1) photovoltaic cell manufacture, (2) flat-plate photovoltaic array manufacture, and (3) concentrating collector manufacture. A closer look at each area is required to determine how the market is currently being approached.

Photovoltaic cell manufacture technology is well known by all semiconductor manufacturers, but since the market is not large, few firms are serving it. Market entry in the future would only require costs for gearing up for production and minor technology perfections, neither of which would involve large periods of time. Most semiconductor manufacturers are content with manufacturing only the cells and have no current interest in selling arrays or photovoltaic systems.

Most photovoltaic arrays are manufactured by companies which are either independent or backed by parent corporations in the energy field. Many of these firms manufacture their own solar cells, but several buy cells from semiconductor manufacturers. The sale of flat-plate collectors to the public is the only area being actively pursued within the terrestrial marketplace.

Concentrating photovoltaic collectors are in the early stages of development and are not actively marketed to the public. Firms involved in concentrator research will custom-design a system, but only one firm has a standard developed concentrating (hybrid) system for which it has published literature. Concentrators require more development before they can be commercialized. Several manufacturers performing research on collectors feel that the only viable market for concentrators is for very large systems.

The following is a list of those manufacturers known to be actively involved in the commercial sale of photovoltaic arrays:

Acurex Corporation
485 Clyde Avenue
Mt. View, California 94042
(415) 964-3200

Amperex Electronic Corporation
Providence Pike
Slatersville, Rhode Island 02876
(401) 762-3800, 762-9000

Applied Solar Energy Corporation
15251 E. Don Julian Road
City of Industry, California 91746
(213) 968-6581

Arco Solar, Inc.
20554 Plummer Street
Chatsworth, California 91311

Mobile Tyco Solar Energy Corporation
16 Hickory Drive
Waltham, Massachusetts 02154
(617) 890-0909

Motorola
P.O. Box 20924
Phoenix, Arizona 85036
(602) 244-5459

National Semiconductors Ltd.
331 Cornelia Street
Plattsburgh, New York 12901
(518) 561-3160

The Pioneer Electric & Research Corporation
743 Circle Avenue
Forest Park, Illinois 60130
(312) 771-8242

SES, Inc.
Tralee Industrial Park
Newark, Delaware 19711
(302) 731-0990

Sensor Technology, Inc.
21012 Lassen Street
Chatsworth, California 91311
(213) 882-4100

Solar Power Corporation
20 Cabot Road
Woburn, Massachusetts 01801
(617) 935-4600

Solarex Corporation
1335 Piccard Drive
Rockville, Maryland 20850
(301) 948-0202

Solargenics, Inc.
20319 Nordhoff Street
Chatsworth, California 91311
(213) 998-0806

Spectrolab
12500 Gladstone Avenue
Sylmar, California 91342
(213) 365-4611

Tideland Signal Corporation
P.O. Box 52430
Houston, Texas 77052
(713) 681-6101

2. Performance Variables

Each of the module manufacturing companies that provided data for this document has a line of photovoltaic modules. The products cannot be compared on a module basis because they are all different. Each company has a series of modules which can be interconnected in series or in parallel to obtain the desired current, voltage, or power level. In order to make comparisons, one must compare arrays sized to meet a particular load requirement.

The following subsections describe the range of products available in the photovoltaic industry. Table IV-3 shows the characteristics of arrays of different manufacturers.

a. Current. The available current output from a single module can range anywhere from 0.1 ampere to 7.0 amperes. The majority of the modules available provide less than 2.0 amperes each. The modules can be connected in parallel to obtain any value of current desired.

b. Voltage. The available voltage output from a single module can range anywhere from 3.0 to 30.0 volts at rated load. Any value in this range is readily available. Higher voltages can be obtained by connecting the modules in series.

c. Power. The power output for these modules ranges from 10 to 84 watts. Modules are available for every 2-watt increment in power up to 30 watts. After 30 watts there are only a few sizes available. Larger power requirements can be obtained by combining modules into an array.

TABLE IV-3. PHOTOVOLTAIC MODULE DATA

	MANUFACTURER										
	Amperex				Applied Solar Energy Corp.			Arco Solar			Mobil Tyco
Model	BPX-47A	BPX-47B-18	BPX-47B-20	BPX-47C	CPS-14	609-3039	60-3040	16-500	16-1000	16-2000	M28
Electrical Performance[1]:											
V_{oc} (V)	-	-	-	-	-	-	-	20.3	20.3	20.3	-
I_{sc} (A)	-	-	-	-	-	-	-	0.6	1.2	2.3	-
Pmax (W)	1.	16.5	18.3	33.0	1.4	23.4 23.4 23.4	84 84	8.2	16.6	33	41.3
V_{Pmax} (V)	11.5	8.2	9.1	16.4	14.0	18 9 6	30 15	16.1	16.1	16.1	8.6
I_{Pmax} (A)	0.7	2.01	2.01	2.01	0.1	1.3 2.6 3.9	2.8 5.6	0.51	1.03	2.05	4.8
η (%)	5.4	6.1	6.9	7.3	4.4	10.1	12.4	5.8	8.5	8.9	8.5
Dimensions[2]:											
(in)	18.4 x 16.9	23 x 18.4	23 x 18.4	41.5 x 16.9	7.3 x 6.75	30 x 12	47.75 x 22	35.9 x 11.9	25.9 x 11.9	47.9 x 11.9	-
(cm)	47 x 43	58 x 47	58 x 47	105 x 43	19 x 17	76 x 30	121 x 56	90 x 30	66 x 30	122 x 30	-
Surface Area[3]:											
(ft^2)	2.2	2.9	2.9	4.5	0.34	2.5	7.3	1.3	2.1	4.0	-
(m^2)	0.2	0.27	0.27	0.46	0.03	0.23	0.66	0.12	0.20	0.37	-
Weight: (lb)	5.29	8.8	8.8	24.3	2	9	-	3.3	5.4	10	20
(kg)	2.40	3.99	3.99	11.0	0.91	4.08	-	1.50	2.45	4.54	9.07

Notes: 1. *All modules are monocrystalline silicon except for SES which is cadmium sulfide.*

2. a. *Tolerance on data is ± 10%.*

b. *All data was measured at 100 mw/cm of light intensity.*

c. *All data was measured with a cell temperature of 25-29°C. Information is not available from manufacturers to calculate compensating differences for this 3°C temperature differential. However, the error due to this temperature difference is negligible (< 1%).*

3. *All dimensions are approximate.*

TABLE IV-3. (CONTINUED)

Model	MSP01E	MSP10D	MSP01B	MSP01A	MSF02A	MSP26A	2018 BXX17	2018 JXX19	2036 EXX19	2036 FXX11	3035 JXX18
	MANUFACTURER: Motorola						MANUFACTURER: Sensor Technology				
Electric Performance[2]:											
V_{oc} (V)	4.1-4.5	6.25-6.75	12.5-13.5	25-27	18.75-20	18.75-20	-	-	-	-	-
I_{sc} (A)	6.6-7.8	4.4-5.2	2.2-2.6	1.1-1.3	1.1-1.3	0.5-0.6	-	-	-	-	-
P_{max} (W)	21.7-26.5	21.7-26.5	21.7-26.5	21.7-26.5	16.3-20	7.3-9.1	3.6	4.32	4.32	2.16	8.4
$V/_{Pmax}$ (V)	3.52	5.28	10.55	21.1	15.84	15.84	7.2	7.2	14.4	14.4	14.0
$I/_{Pmax}$ (A)	5.88-7.19	3.92-4.8	1.96-2.4	.98-1.2	.98-1.2	.44-.55	0.5	0.6	0.3	0.15	0.6
η(%)	7.0	7.0	7.0	7.0	6.3	2.8	4.8	5.2	5.2	4.7	6.5
Dimensions[3]:											
(in)	23 x 23	23 x 23	23 x 23	23 x 23	22.8 x 19.3	22.8 x 19.3	6.5 x 17	6.5 x 19	6.5 x 19	6.5 x 11	11.28 x 18.5
(cm)	58 x 58	58 x 58	58 x 58	58 x 58	58 x 49	58 x 49	17 x 43	17 x 48	17 x 48	17 x 28	29 x 47
Surface Area[3]:											
(sq ft)	3.7	3.7	3.7	3.7	3.1	3.1	0.8	0.9	0.9	0.5	1.4
(m^2)	0.34	0.34	0.34	0.34	0.29	0.29	0.07	0.08	0.08	0.05	0.13
Weight: (lb)	12	12	12	12	9.2	9.2	-	-	-	-	-
(kg)	5.44	5.44	5.44	5.44	4.17	4.17	-	-	-	-	-

Notes: 1. *All modules are monocrystalline silicon except for SES which is cadmium sulfide.*

2. a. *Tolerance on data is ± 10%.*

   b. *All data was measured at 100 mw/cm of light intensity.*

   c. *All data was measured with a cell temperature of 25-28°C. Information is not available from manufacturers to calculate compensating differences for this 3°C temperature differential. However, the error due to this temperature difference is negligible (1%).*

3. *All dimensions are approximate.*

TABLE IV-3. (CONTINUED)

	MANUFACTURER									
	Solar Power Corp.				Spectrolab					Tideland Signal
Model	G-12-361	M12-401	M12-369	M12-361						MG-600
Electrical Performance[2]:										
V_{oc} (V)	-	-	21	21	-	-	-	-	-	9.35
I_{sc} (A)	-	-	1.63	2.05	-	-	-	-	-	0.62
P_{max} (W)	27.6	28.7	25	31	5.4	8.1	4 05	8.1	9.45	3.5
V_{Pmax} (V)	14.7	16.6	16.5	16.5	5.4	8.1	8 1	16.2	18.9	7
I_{Pmax} (A)	1.88	1.73	1.52	1.9	1	1	0.5	0.5	0.5	-
(%)	5.7	-	5.5	6.8	5.8	6.2	5.4	6.2	6.0	5.4
Dimensions[3]:										
(in)	44 x 17	-	45 x 15.3	36 x 15.3	4.88 x 28.9	4.88 x 42.1	4.88 x 22.4	4.88 x 42.1	4.88 x 48.7	10 x 10
(cm)	112 x 43	-	117-39	117-39	12 x 73	12 x 107	12 x 57	12 x 107	12 x 124	25 x 25
Surface Area[3]:										
(sq ft)	5.19	-	4.9	4.9	1.0	1.4	0.8	1.4	1.7	0.7
(m^2)	0.48	-	0.46	0.46	0.09	0.13	0.07	0.13	0.16	0.07
Weight: (lb)	20	-	18	18	3.6	5.2	2.8	5.2	6	20 lb
(kg)	9.07	-	8.16	8.16	1.63	2.34	1.27	2.34	2.72	9.07

Notes: 1. *All modules are monocrystalline silicon except for SES which is cadmium sulfide.*

2. a. *Tolerance on data is ± 10%.*

b. *All data was measured at 100 mw/cm of light intensity.*

c. *All data was measured with a cell temperature of 25-28°C. Information is not available from manufacturers to calculate compensating differences for this 3°C temperature differential. However, the error due to this temperature difference is negligible (1%).*

3. *All dimensions are approximate.*

TABLE IV-3. (CONTINUED)

	MANUFACTURER																	
	SES				Solarex													
Model	Basic	12-2	12-6	12-12	435	1480	480	4200	4200J	4300	220	230	1270	280	785	615	460	9200J
Electrical Performance[2]:																		
V_{oc} (v)	-	-	-	-	20	20	20	20	20	20	18	18	18	18	10	9	6.6	23
I_{sc} (A)	-	-	-	-	-	-	-		-	-	-	-	-	-	-	-	-	-
P_{max} (W)	1.52	3	6	12	6	10	12	20	22	36	2.5	5	9	11	10	2.5	6.5	25
$V/_{Pmax}$ (V)	8	16	16	16	14	14	14	14	14	14	12	12	12	12	7	6	4	16
$I/_{Pmax}$ (A)	0.19	0.19	0.38	0.76	0.4	0.65	0.8	1.3	1.5	2.1	0.18	0.4	0.65	0.8	1.3	0.4	1.3	1.5
(%)	3.68	3.68	3.68	3.68	8.1	7.7	8.1	7.7	7.0	8.1	6.7	6.7	7.5	7.9	7.2	6.7	7.0	7.5
Dimensions[3]:																		
(in)	8 x 8 Module	-	-	-	10 x 12	12.9 x 15.8	14.9 x 15.5	20 x 20	23 x 21	26 x 26.5	7 x 8.5	10 x 11	12.9 x 14	10.5 x 20	10.5 x 20	5.5 x 11	7.5 x 20	22.9 x 22.9
(cm)	20 x 20	-	-	-	25 x 31	33 x 40	38 x 39	51 x 51	58 x 53	66 x 67	18 x 22	25 x 28	33 x 36	27 x 51	27 x 51	14 x 28	19 x 51	58 x 58
Surface Area[3]:																		
(sq ft)	0.4	-	-	-	0.8	1.4	1.6	2.8	3.4	4.8	0.4	0.8	1.3	1.5	1.5	0.4	1.0	3.6
(m^2)	0.04	-	-	-	0.07	0.13	0.15	0.26	0.32	0.45	0.04	0.07	0.12	0.14	0.14	0.04	0.09	0.06
Weight: (lb)	-	6	12	24	-	-	-	-	-	-	-	-	-	-	-	-	-	-
(kg)	-	2.72	5.44	10.9	-	-	-	-	-	-	-	-	-	-	-	-	-	-

Notes: 1. *All modules are monocrystalline silicon except for SES which is cadmium sulfide.*

2. a. *Tolerance on data is ± 10%.*

b. *All data was measured at 100 mw/cm of light intensity.*

c. *All data was measured with a cell temperature of 25-28°C. Information is not available from manufacturers to calculate compensating differences for this 3°C temperature differential. However, the error due to this temperature difference is negligible (1%).*

3. *All dimensions are approximate.*

d. Module Efficiency. The efficiency of the individual modules ranges from 2.8 to 12.4 percent. A scatter diagram has been plotted of the module efficiency vs. power output and is shown in Figure IV-23. From the figure, it is apparent that there is very little correlation between module efficiency and power output. For power levels up to 8.0 watts, the efficiency of the various manufacturers' modules seems to be between 4.0 and 8.0 percent. For power outputs larger than 8.0 watts, the module efficiencies are slightly higher. A module efficiency of greater than 9.0 percent is a rarity, although continued progress is being made in this area.

e. Temperature. There appears to be a large variation in the effect of temperature on the arrays of the various manufacturers. Since the temperature affects both current and voltage, whose product equals power, any two variables determine the third variable when connected to a load. The temperature effect on voltage, as seen in manufacturers' literature, shows a voltage drop of 2.2 mV/°C per cell for silicon and 1.3 mV/°C per cell for cadmium sulfide. For silicon cells the power will drop by 0.3 percent/°C and for cadmium sulfide cells it will drop by 0.6 percent/°C.

Since the efficiency of an array is affected by temperature, it is important to know at what reference temperature the data were obtained. Manufacturers generally obtain their data at an array temperature of 25°C (77°F) or 28°C (82.4°F).

f. Insolation. Characteristic curves and their charge due to different insolation levels are available from all photovoltaic array manufacturers. In addition to these curves, manufacturers provide power output data and temperature variance curves. This information is taken at a reference insolation level. The reference used by most manufacturers is 100 mW/cm^2 which is equivalent to the approximate light intensity at high noon.

3. Physical Variables

Physical variables include size, maintenance, reliability, and life. As indicated in Table IV-3, the physical size of the various modules does not follow any recognizable pattern. The only observation that can be made is that as the power output increases, the area of the module must increase. Power outputs and physical sizes are plotted against one another in Figure IV-24. A straight-line correlation indicates an average value of 6.8 peak watts per square foot. Manufacturers' recommended maintenance of

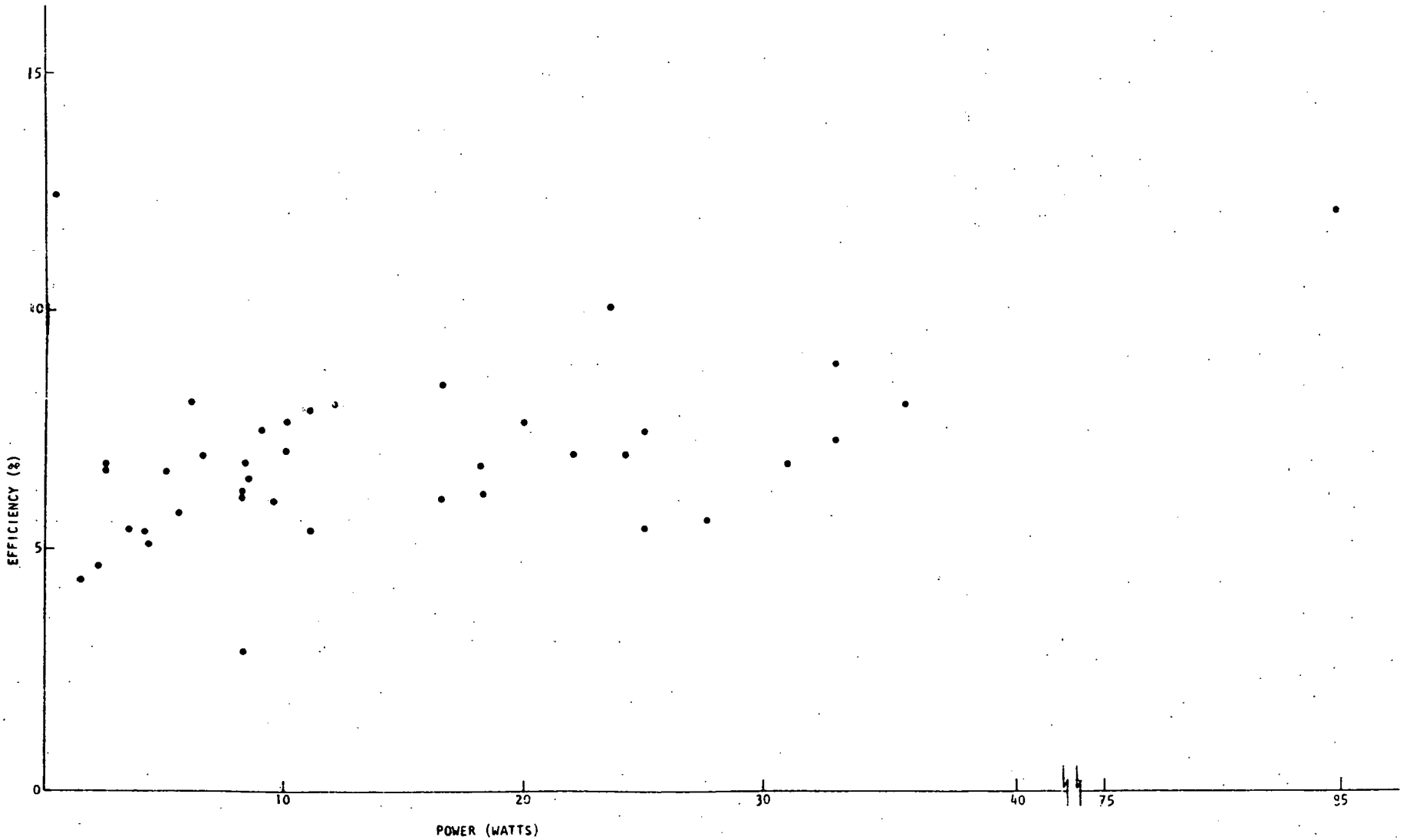

Figure IV-23. Scatter Diagram of Module Efficiency vs. Power Output

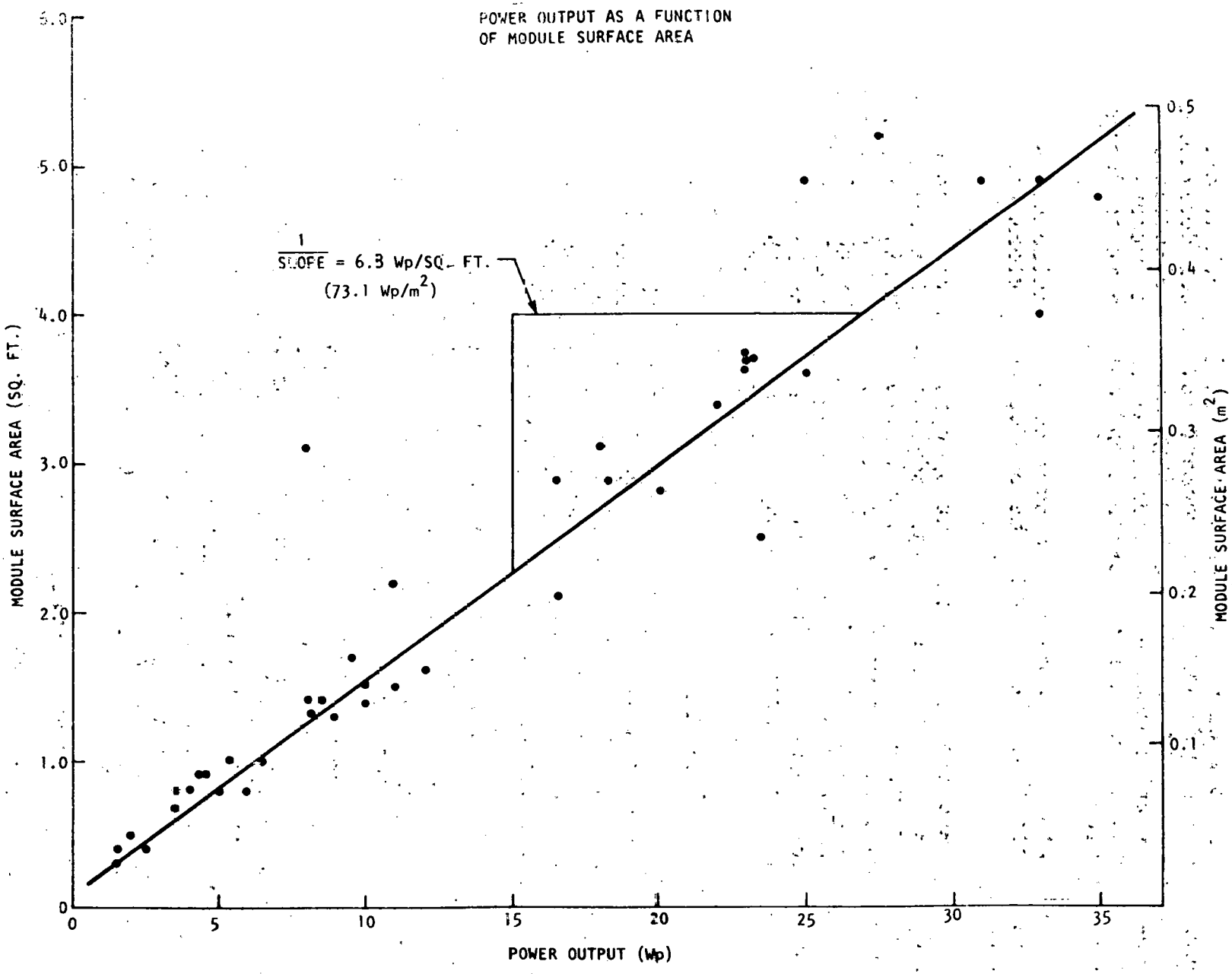

Figure IV-24. Flat-plate Module Surface Area Correlated to Power Output

modules consists of washing them at 6- or 12-month intervals, depending on how dirty the environment is. Other desirable maintenance includes checking the tightness of electrical connections and measuring the individual module outputs periodically to monitor performance and compare it to design specifications.

No data on reliability are available. Manufacturers merely state that they expect the product to perform as intended.

Life expectancy is dependent upon the materials used. Manufacturers of cadmium-sulfide modules guarantee their product for one year but project a life of over five years. Silicon modules have warranties of 1 to 5 years for materials and workmanship but a life expectancy of greater than 10 years. Although their literature states 10 years, most silicon manufacturers expect their product to last 20 or 25 years. No information is available to support either of these claims.

4. Costs and Delivery.

The cost of photovoltaic power should not be confused with the cost of a photovoltaic module. The module is a major cost contributor but other costs are also incurred, including the structure which will house the modules, electrical connections, and power conditioning equipment. Only module costs are considered in this section.

Since modules come in all sizes and a multitude of power outputs, a cost per module would be meaningless. A reasonable basis of comparison would be cost per peak watt. Even this base of comparison would not distinguish between the quality levels of any two given modules.

Most manufacturers operate on the block rate system. This system rewards mass purchases by reducing the cost per unit for large purchases. Figure IV-25 shows the cost per peak watt for photovoltaic modules and is based on data received from several manufacturers. Module costs for systems utilizing less than 500 watts are between $14 and $21 per peak watt. For purchases of more than 500 watts, the cost decreases to a range of $9.00 to $18.55 per peak watt. For systems larger than 50 kW, the price drops to between $8 and $10 per peak watt (1980$).

Delivery times for small quantities (less than 100 W) vary from 30 days to 120 days. Arrays in the kilowatt range would have longer waiting periods.

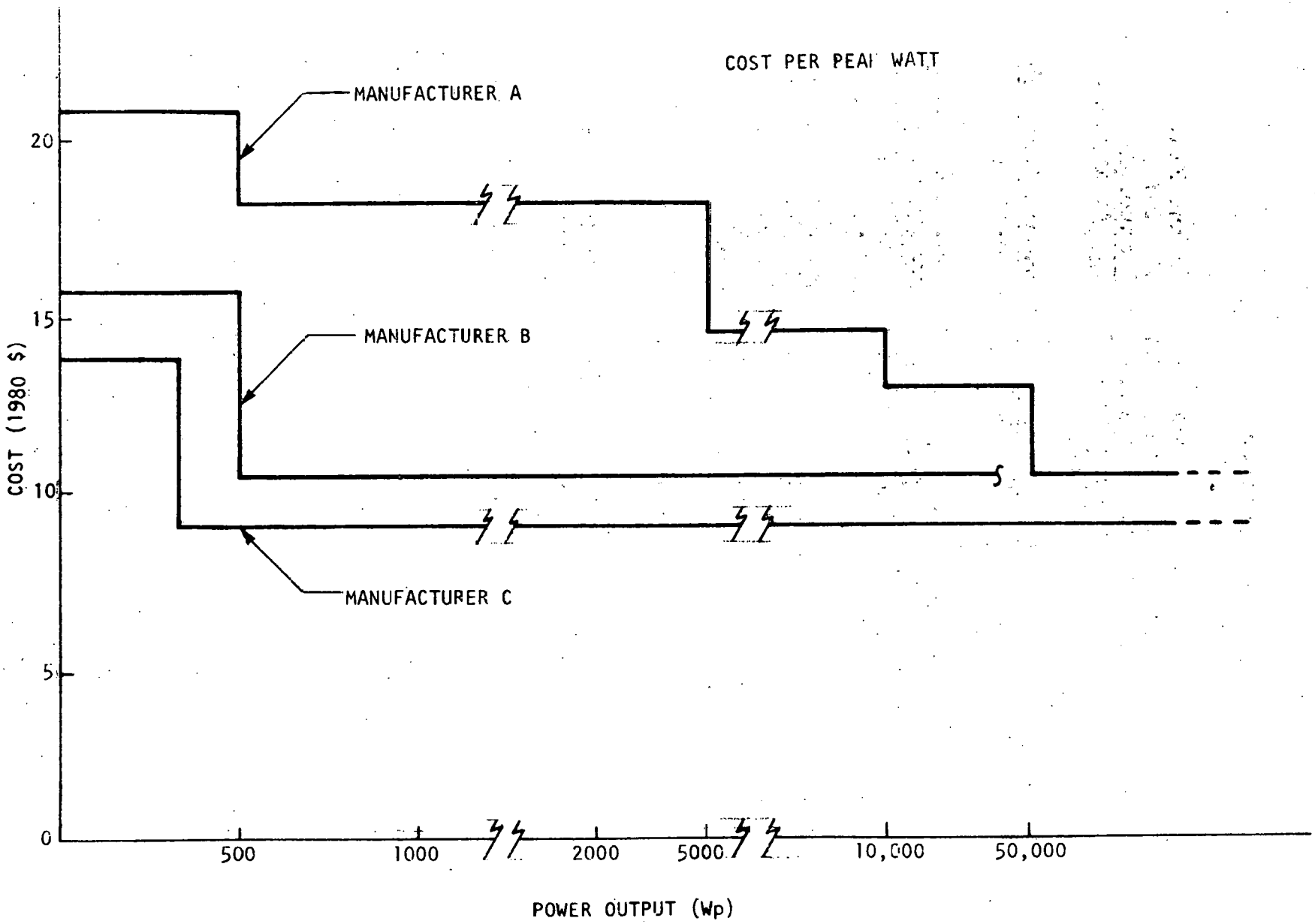

Figure IV-25. Photovoltaic Module Cost of Several Manufacturers

G. References

1. Ross, R.G., and B.D. Shafer. "Concentrator and Flat Panel Technology Alternatives for 50¢/Watt." In: Proceedings of the U.S. DOE Photovoltaic Technology Development and Applications Program Review, Arlington, Virginia, November 7 to 9, 1978.

2. Palz, Wolfgang. Solar Electricity, An Economic Approach to Solar Energy. Andover, England, Chapel River Press, 1978.

3. National Science Foundation. Assessment of the Technology Required to Develop Photovoltaic Power Systems for Large-Scale National Energy Applications, NSF-RA-N-74-072. Prepared by Jet Propulsion Laboratory, October 15, 1974.

4. Forman, S.E. Endurance and Soil Accumulation Testing of Photovoltaic Modules at Various MIT/LL Test Sites, EY-76-C-02-4094. Prepared for the U.S. Energy Research and Development Administration by Lincoln Laboratory, Lexington, Massachusetts, September 28, 1978.

5. Solar Cells. Ed. by Charles E. Backus. New York, IEEE Press, 1976.

6. Kern, E.C. Jr., and M.C. Russell. Hybrid Photovoltaic/Thermal Solar Energy Systems, COO-4577-1. Lincoln Laboratory, Lexington, Massachusetts, March 27, 1978.

7. Electric Power Research Institute. EPRI Journal, March, 1978.

8. The University of Alabama in Huntsville. A Survey of Photovoltaic Systems. Prepared for National Aeronautics and Space Administration, August 1979.

V. BIBLIOGRAPHY

Abacus Controls, Inc. Manufacturer's brochures, Somerville, New Jersey.

Abbondanti, A. and P. Wood. "A Criterion for Performance Comparison between High Power Inverter Circuits." IAS '75 Annual.

Acurex Corporation. Advertising literature.

Adams, G.B. and R.P. Hollandsworth. "Rechargeable Alkaline Zinc/Ferricyanide Redox Battery." In: Proceedings of DOE Battery and Electrochemical Contractors' Conference (U.S. DOE), December 10-12, 1979.

AiResearch Manufacturing Company of California. Manufacturer's published literature. Torrance, California.

American Institute of Aeronautics and Astronautics. 8th Intersociety Energy Conversion Engineering Conference Proceedings, August 13-17, 1973.

American Society of Mechanical Engineers. 9th Intersociety Energy Conversion Engineering Conference Proceedings, August 26-30, 1974.

Amperex Electronic Corporation (Philips). Advertising literature.

Anand, J.N. "Dow Sodium-Sulfur Battery for Energy Storage." Presented at the 14th Intersociety Energy Conversion Engineering Conference, American Chemical Society, 1979.

Anbar, M. Method and Apparatus for Electrochemical Generation of Power from Hydrogen, U.S. Patent 4,042,755. August 16, 1977.

Applied Solar Energy Corporation (Optical Coatings Laboratory, Inc.). Advertising literature.

ARCO Solar, Inc. Advertising literature.

Argonne National Laboratory. Cost and Design Study for Electric Vehicle Lead-Acid Battery. Prepared by ESB Incorporated, Philadelphia, 1977.

Argonne National Laboratory. Development of Lithium/Metal Sulfide Batteries at Argonne National Laboratory: Summary Report for 1977. March 1978.

Argonne National Laboratory. Development of Lithium/Metal Sulfide Batteries at Argonne National Laboratory: Summary Report for 1976. March 1977.

Argonne National Laboratory. Proceedings of the Symposium and Workshop on Advanced Battery Research and Design. March 22-24, 1976.

Argonne National Laboratory. Proceedings of the Workshop on Battery Storage for Solar-Photovoltaic Energy Systems. Denver, Colorado, January 11-13, 1978.

Argonne National Laboratory. Program Plan for Battery Systems for Photovoltaic Energy Storage. April 1978.

Battles, J. E., J. A. Smaga, and K. M. Myles. "Materials Requirements for High Performance Secondary Batteries." Metallurgical Transactions, Volume 9A. February 1978.

Bechtel Corporation. Battery Storage Performance Requirements for Terrestrial Solar Photovoltaic Power Systems. Prepared for Argonne National Laboratory under Contract No. 31-109-38-2962, Phase ID, July 1977.

Bechtel Corporation. Energy Storage and Power Conditioning Aspects of Photovoltaic Solar Power Systems. First Quarterly Report, Volume 1, COO/2748-75/T1. Prepared for ERDA, Division of Solar Energy, October 1975.

Bechtel Corporation. Final Report on Battery Storage Performance Requirements for Terrestrial Solar Photovoltaic Power Systems. August 1977.

Beck, James W. "Power Conversion Equipment for Storage Batteries." In: Near-Term Energy Storage Technologies, Workshop on Lead-Acid Batteries, Palo Alto, California, November 18-19, 1975. Prepared for Argonne National Laboratory by Electric Power Research Institute, March 1976.

Beck, J. W. et al. Purposes and Features of a Proposed National Battery Energy Storage Test (BEST) Facility. Electric Power Research Institute, April 1976.

Behrin, E. et al. Energy Storage Systems for Automobile Propulsion, Volume I Overview and Findings, W-7405-ENG-48. Lawrence Livermore Laboratory, December 15, 1977.

Behrin, E., et al. Energy Storage Systems for Automobile Propulsion, Volume 2, Detailed Report. Lawrence Livermore Laboratory, December 15, 1977.

Birk, J. R. Batteries for Energy Storage: Potential Applications and Alternative Technologies. Electric Power Research Institute, February 1976.

Birk, J. R. "Energy Storage, Batteries, and Solid Electrolytes: Prospects and Problems." In: Superionic Conductors, edited by G. O. Mahan and W. L. Roth. New York: Plenum Press, 1976, pp 1-14.

Birk, J. R. "The Lead-Acid Battery for Electric Utilities: A Review and Analysis." In: Proceedings of the ERDA/EPRI Lead-Acid Battery Workshop II, Electric Power Research Institute, December 9, 1976.

Birk, J. R., and N. P. Yao. Proceedings of Symposium on Load Leveling. Eloctrochemical Society, Inc., October 1977.

Birk, J. R., K. Klunder, and J. C. Smith. "Super Batteries: A Progress Report." IEEE Spectrum, March 1979, pp. 49-55.

Bradley, T. G. Bipolar Lithium/Iron Disulfide Cells. General Motors Research Laboratories, Society of Automotive Engineers, Inc., 1978.

Bridges, D.W., R.W. Minck, and D.G. Poquette. "Reproducibility and Performance of Large Prototype Na/S Cells." In: Proceedings of the 14th Intersociety Energy Conversion Engineering Conference, American Chemical Society, 1979.

Brodd, R. J., et al. Advanced Battery Material Resource Requirement Survey for Electric Vehicle Application. National Battery Advisory Committee to DOE (ad hoc), June 7, 1978.

Burris, L., et al. Chemical Engineering Division Research Highlights, 1977. Argonne National Laboratory, August 1978.

Cairns, E. J., and H. Shimotake. "High-Temperature Batteries." Science, Volume 164, Number 3886, (June 20, 1969).

Carlson, D.E. "Amorphous Silicon Solar Cells." RCA Engineer, Vol. 24, No. 5 (February/March 1979), pp. 24 to 28.

Carlson, D.E., and C.R. Wronski. "Solar Cells using Discharge-Produced Amorphous Silicon." Journal of Electronics Materials, Vol. 6, No. 2 (1977), pp. 95 to 106.

Catherino, H. et al. Cost Analysis of 50 kWh Zinc-Chlorine Batteries for Mobile Applications. Prepared for U.S. Department of Energy, by Energy Development Associates, January 1978.

Chalmers, B., et al. Continuous Silicon Solar Cells, GI-37067X. Prepared for National Science Foundation by Harvard University at Cambridge and Tyco Laboratories, Waltham, Massachusetts, January 1974.

Chatterji, D. Development of Sodium Sulfur Batteries for Utility Application. Electric Power Research Institute, December 1976.

Chatterji, D., et al. "Sodium-Sulfur Battery Development at General Electric." In: Proceedings of the Symposium on Load Leveling. Electrochemical Society, Inc., October 1977.

Chilenskas, A.A. Commercialization Planning for the Lithium/Metal Sulfide Battery. Prepared for Li 77 Symposium on Lithium Needs and Resources, October 1977.

Chilenskas, A.A. Questionnaire response.

Chin, O.T., et al. "An Electrochemically Regenerative Hydrogen-Chlorine Energy Storage System." J. Electrochem. Soc.: Electrochemical Science and Technology, Volume 126, No. 5 (May 1979), pp. 713-719.

Chreitzberg, A. M., et al. "Performance of Molten Salt Sodium/B-alumina/$SbCl_3$ Cells, 1978." Journal of Power Sources, Volume 3, No. 3 (November 1978), Elsevier Sequoia S. A., Lausanne, Switzerland.

Chreitzberg, A. M., J. B. Doe, and A. J. Salkind. "Batteries." In: Encyclopedia of Chemical Processing and Design, Volume 4. Marcel Dekker, Inc., 1977.

Ciprios, G., W. Erskine, Jr., and P. G. Grimes. Redox Bulk Energy Storage System Study, Volumes: 1 and 2. NASA-Lewis Research Center, January and February 1977.

Clark, R. P. Batteries for Specific Solar Applications. Sandia Laboratories, July 1979.

Cohn, E. M. "Redox, A New Energy Storage Scheme: Are We Asking the Right Questions?" Energy, Volume 4, No. 1 (Winter/1979).

D'Aiello, R.V. "RCA Progress in Flat-Plate Silicon Solar Panel Technology." RCA Engineer, Vol. 24, No. 5 (February/March 1979), pp. 16 to 23.

Deb, S., M.K. Mukherjee, and H. Saha. "Matching of Solar Cells and Performance of a Solar Battery." Solar Energy, Vol. 19, No. 2-E (1977), pp. 171 to 177.

Delavan Electronics, Inc. Advertising literature.

Delta Electronic Control Corporation. Manufacturer's published literature. Irvine, California.

Dennison, E. S. Metal-Hydrogen Secondary Battery System, U.S. Patent 4,098,962. Yardney Electric Corporation, July 4, 1978.

Dewey, C.G., et al. "Development of Experimental 20-KV, 36-MW Solid-State Converters for HVDC Systems." In: IEEE Transactions of Power Apparatus and Systems, Vol. PAS-87, No. 4, April 1968.

Dunlop, J. D., et al. Low Pressure Nickel Hydrogen Cell, U.S. Patent 3,959,018. Communications Satellite Corporation, May 25, 1976.

Dunlop, J. D., et al. Nickel Hydrogen Cell, U.S. Patent 3,867,199. Communications Satellite Corporation, February 18, 1975.

Dunlop, J. D., G. Van Ommering, and M. W. Earl. "Ni-H_2 Battery Flight Experiment." In: Power Source 6: Research and Development in Non-Mechanical Electrical Power Sources, Proceedings of the 10th International Symposium, Brighton, England, September 13-16, 1976, pp. 231-247.

Electric Power Research Institute. Development of High Efficiency Cost-Effective Zinc-Chlorine Batteries for Utility Peak-Shaving, 1976, EPRI EM-711. Energy Development Associates, March 1978.

Electric Power Research Institute. EPRI Journal, March, 1978.

Electric Power Research Institute. Near-Term Energy Storage Technologies: The Lead-Acid Battery. Prepared for Argonne National Laboratory, March 1976.

Elgar Corporation. Manufacturer's brochures. San Diego, California.

Eltimsahy, A.H., et al. "Experimental Investigations of a Solar Cell/Inverter System." In: Proceedings of the 1977 Annual Meeting, American Section of the International Solar Energy Society, Vol. 1, Section 14-25. Orlando, Florida, June 6-10, 1979.

Energy Development Associates. Flow Battery Project Review: The Zinc Chlorine Battery. July 17-18, 1979.

Exxon Research and Engineering Company. "Zinc-Bromine Battery System." Summary of Information presented at the Department of Energy - Division of Energy Storage Systems Flow Battery Project Review, Sheraton Potomac Inn, Rockville, Maryland, July 17-18, 1979.

Feduska, W., et al. Energy Storage for Photovoltaic Conversion, Volumes 1, 2, and 3. Prepared for U.S. Energy Research and Development Administration by Westinghouse R&D Center, September 1977.

Fink, J.L., et al. The Application of Static Inverters for Essential Loads. December 1963. Paper presented at IEEE Winter General Meeting, New York, January 27 - February 1, 1963.

Fischer, W. Questionnaire response. Brown, Boveri, Inc., Heidleberg, F.R.G.

Fischer, W., et al. "Recent Advances in Na/S Cell Development - A Review, 1978." Journal of Power Sources, Volume 3, No. 4 (December 1978), Elsevier Sequoia S.A., Lausanne, Switzerland.

Fischer, W., et al. "Sodium/Sulfur Batteries for Peak Power Generation." In: Proceedings of the 14th Intersociety Energy Conversion Engineering Conference, American Chemical Society, 1979.

Forman, S.E. Endurance and Soil Accumulation Testing of Photovoltaic Modules at Various MIT/LL Test Sites, EY-76-C-02-4094. Prepared for the U.S. Energy Research and Development Administration by Lincoln Laboratory, Lexington, Massachusetts, September 28, 1978.

Gahn, Randall F. Supply of Reactants for Redox Bulk Energy Storage Systems, DOE/NASA 1002-78/1. NASA-Lewis Research Center, September 1978.

George, J. H. B. Interim Cost Estimates for Advanced Battery Systems, Interim Report, July 1978. Electric Power Research Institute, July 1978.

Gibbons, J.F. Semiconductor Electronics. McGraw-Hill Book Company, New York, 1966.

Giner, J., and J. D. Dunlop. "The Sealed Nickel-Hydrogen Secondary Cell." J. Electrochem. Soc.: Electrochemical Science and Technology, Volume 122, No. 1 (January 1975), pp. 4-11.

Goodman, F.R., Jr. Los Angeles Department of Water and Power. "Power Conditioning Requirements for Application of Non-Conventional Energy Technologies in Electric Utility Systems." Presented at Workshop on Power Conditioning for Alternative Energy Technologies, Denver, Colorado, May 9-11, 1979.

Gould Incorporated. Develop Nickel-Zinc Battery Suitable for Electric Vehicle Propulsion. Rolling Meadows, Illinois: Prepared for Argonne National Laboratory, 1977.

Gould Incorporated. State-of-the-Art Lead-Acid Vehicle Batteries. Rolling Meadows, Illinois: Prepared for Argonne National Laboratory, August 26, 1977.

Graham, Robert W. Secondary Batteries, Recent Advances. Noyes Data Corporation, Park Ridge, New Jersey, 1978.

Hall, J.C., and J.T. McCormick. "Development of Intially Discharged Lithium-Silicon/Iron Sulfide Load-Leveling Cells." In: Proceedings of the Symposium on Load Leveling. The Electrochemical Society, Inc., 1977.

Hamilton, William. Prospects for Electric Cars, Final Report. General Research Corporation, March 15, 1978.

Hart, A. B., and A. H. Webb. "Batteries for Bulk Energy Storage on the U.K. Electricity Supply System." In: Power Source 6: Research and Development in Non-Mechanical Electrical Power Sources, Proceedings of the 10th International Symposium, Brighton, England, September 13-16, 1976, pp. 627-641.

Hedderson, George W. "Batteries." In: Standard Handbook for Electrical Engineers, Donald G. Fink, ed. McGraw-Hill, 1968.

Heinbockel, J.H., and A.S. Roberts. Analysis of GaAs and Si Solar Energy Hybrid Systems, NAS1-11707, Task No. 86. Prepared for National Aeronautics and Space Administration by Old Dominion University, Norfolk, Virginia, December 1975.

Heitner, K. and P. Skartvedt. Battery Technology - An Assessment of the State of the Art. TRW Inc. Energy Systems Group, March 27, 1978.

Iammartino, N. R. "New Batteries are Coming." Chemical Engineering, Volume 82, No. 2 (January 20, 1975).

International Rectifier. Advertising literature.

Jasinski, R. High Energy Batteries. Plenum Press, New York, 1967.

Johnson, A. C., et al. Economic Assessment of the Utilization of Lead-Acid Batteries in Electric Utility Systems, EY-76-C-02-4025. Prepared for U.S. Energy Research and Development Administration by Public Service Electric and Gas Company, Newark, New Jersey, April 1977.

Jones, I. W. "Recent Advances in the Development of Sodium-Sulphur Batteries for Load Leveling and Motive Power Applications." Electrochimica Acta, 1977, Volume 22, pp. 681-688.

Kelly, Henry. "Photovoltaic Power Systems: A Tour Through the Alternatives." Science, Vol. 199 (February 10, 1978), pp. 634 to 643.

Kern, E.C., Jr. Phase One Experiment Test Plan Solar Photovoltaic/Thermal Residential Experiment, EG-77-S-02-4577. Prepared for U.S. Department of Energy by Lincoln Laboratory, Lexington, Massachusetts, March 15, 1979.

Kern, E.C., Jr., and M.C. Russell. Hybrid Photovoltaic/Thermal Solar Energy Systems, COO-4577-1. Lincoln Laboratory, Lexington, Massachusetts, March 27, 1978.

Klein, M. and D. Dube. Design and Cost Survey of Nickel-Zinc Batteries for Electric Vehicle, ANL-K76-3541-1. Prepared for Argonne National Laboratory by Energy Research Corporation, October 1976.

Klein, M. Fabrication and Testing of Large Size Nickel-Zinc Cells. Prepared for NASA-Lewis Research Center by Energy Research Corporation, April 1977.

Klein, M., and M. George. "Nickel-Hydrogen Secondary Batteries." In: Proceedings of the 26th Power Sources Symposium, Atlantic City, New Jersey, April 29, 1974.

Klunder, K. W. "Battery Storage Program." In: Proceedings of the Interagency Coordination Meeting on Energy Storage, Washington, D.C., September 14 to 15, 1977. U.S. Department of Energy.

Kodali, S., et al. Safety and Environmental Aspects of Zinc-Chlorine Hydrate Batteries for Electric-Vehicle Applications. Prepared for U.S. Department of Energy by Energy Development Associates, March 1978.

Kordesch, K. V., and S. J. Cieszewski. "Nickel Oxide-Hydrogen Cells." In: Power Source 6: Research and Development in Non-Mechanical Power Sources, Proceedings of the 10th International Symposium, Brighton, England, September 13-16, 1976, pp. 249-258.

Kyle, M. L., et al. Lithium/Sulfur Batteries for Electric Vehicle Propulsion. Chemical Engineering Division, Argonne National Laboratory.

Landsman, E.E. "Static Inverters for PV Applications." Presented at: Workshop on Power Conditioning for Alternative Energy Technologies. Denver, Colorado, May 9-11, 1979.

Lazennec, Y. Improvements of Electrolyte and Seal Technology for Sodium-Sulfur and Sodium Antimony Trichloride Load-Leveling Batteries. Electric Power Research Institute, June 1977.

Lear, John W. "Nickel Hydrogen Cell Characterization and Simulated Low Earth Orbit Cycling." In: Proceedings of the 14th Annual Intersociety Energy Conversion Conference.

Levine, C. A. "Progress in the Development of the Hollow Fiber Sodium-Sulfur Secondary Cell." IECEC 1975 Record.

Levine, C. Old questionnaire, May 1977.

Levine, C. A. Sodium-Sulfur Battery System, Annual Report, May 19, 1975 - May 19, 1976. Dow Chemical Company, November 1, 1976.

Levine, C., and J. Anand. "The Sodium-Sulfur Battery with Glass Electrolyte." In: Proceedings of the Symposium on Load Leveling, Electrochemical Society, Inc., October 1977.

Lim, H. S., A. M. Lackner, and R. C. Knechtli. "Zinc-Bromine Secondary Battery." J. Electrochem. Soc.: Electrochemical Science and Technology, Vol. 124, No. 8 (August 1977), pp. 1154-1157.

Lindsley, E. F. "Exotic New Batteries - More Miles for Electric Cars." Popular Science, February 1979, pp. 78-83, 158.

Lund, T. J. and J. F. McCartney. "Battery and Fuel Cell Technology Survey." Automotive Engineering, Volume 86, No. 7 (July 1978).

Martino, F.J., et al. "Development of Li-Al/FeS Cells with LiCl-Rich Electrolyte." Prepared for Symposium on Battery Design and Optimization, Pittsburgh, Pennsylvania, October 1978.

Meyer, Hans. "Synchronous Inversion, Concept and Application." Windworks, c1976. In: Sharing the Sun, Solar Technology in the Seventies, Volume 7. A joint conference of the American Section of the International Solar Energy Society and the Solar Energy Society of Canada, Inc., August 15-20, 1979.

Miller, Lee E. "Air Force Nickel-Hydrogen Battery Space Experiment." In: Proceedings of the 14th Intersociety Energy Conversion Conference, American Chemical Society, August 1979.

Motorola, Inc. Advertising literature.

Mungeuast, John, and Del Kirk. Thyristor Voltage Safety Factor. Prepared for Electric Power Research Institute by Power Semiconductors, Inc., July 1978.

Napoli, L.S., et al. "High Level Concentration of Sunlight on Silicon Solar Cells." RCA Review, Vol. 38, No. 1 (March 1977), pp. 76 to 108.

National Aeronautics and Space Administration. Concentrating Solar Collector Subsystem (Preliminary Design Package and First Quarterly Report), NASB-32251. Prepared by Northrup, Inc., Hutchins, Texas, January 20, 1977.

National Aeronautics and Space Administration. Position Paper on the NASA Redox Flow Cell System. NASA-Lewis Research Center, September 1978.

National Science Foundation. Assessment of the Technology Required to Develop Photovoltaic Power Systems for Large-Scale National Energy Applications, NSF-RA-N-74-072. Prepared by Jet Propulsion Laboratory, October 15, 1974.

National Science Foundation. Characterization and Applications Analysis of Energy Storage Systems, AEC-75-20357. Prepared by the Aerospace Corporation, El Segundo, California, December 1977.

National Science Foundation. Proceedings of the Symposium on the Material Science Aspects of Thin Film Systems for Solar Energy Conversion, GI-43795. Organized by Optical Sciences Center, Tucson, Arizona, May 20-22, 1974.

National Semiconductors, Ltd. Advertising literature.

Nelson, P. A. and A. R. Landgrebe. "Battery Development Programs In Europe." Report on Foreign Travel, September 13 to October 5, 1977.

Nelson, P. A., et al. High-Performance Batteries for Stationary Energy Storage and Electric - Vehicle Propulsion, Progress Report for the Period October - December 1977. Argonne National Laboratory, March 1978.

Nelson, P. A., A. A. Chilenskas, and R. K. Steunenberg. "Lithium-Iron Sulfide Batteries for Electric Vehicles." The Fifth International Electric Vehicle Symposium, October 1978.

Nield, K. A Comparison of Battery Storage From Selected Studies of Photovoltaic Systems. Argonne National Laboratory, November 17, 1978.

Palz, Wolfgang. Solar Electricity, An Economic Approach to Solar Energy. Chapel River Press, Andover, England, 1978.

Personal comunication between Joseph King (United Technologies Corporation) and Amitava Podder (HAI), September 1979.

Personal communication between J.W. Main (AiResearch Manufacturing Company) and Amitava Podder (HAI), August 1979.

Personal communication between Donald Shireman (Westinghouse Electric Corporation) and Amitava Podder (HAI), July 1979.

Personal communication between Chuck Jobbinf (Delta Electronic Control Corporation) and Amitava Podder (HAI), July 1979.

Personal communication between S. Ohba (Soleq Corporation) and Amitava Podder (HAI), July 1979.

Personal communication between Charles Price (Elgar Corporation) and Amitava Podder (HAI), July 1979.

Personal communication between George A. O'Sullivan (Abacus Controls, Inc.) and Amitava Podder (HAI), July 1979.

Personal communication between David H. Matsen (Windworks, Inc.) and Amitava Podder (HAI), July 1979.

Personal communication (telephone) between Timothy Geisher (ARCO Solar Inc.) and Joseph Bondar (HAI), September 25, 1979.

Personal communication (telephone) between John Toro (Solarex Corporation) and Joseph Bondar (HAI), September 17, 1979.

Personal communication (telephone) between Robert O. Johnson (SES, Inc.) and Joseph Bondar (HAI), September 13, 1979.

Personal communication (telephone) between Eric Tornstrom (Mobil Tyco Solar Energy Corporation) and Joseph Bondar (HAI), September 13, 1979.

Personal communication (telephone) between Thomas Alexander, (Tideland Signal Corporation) and Joseph Bondar (HAI), September 12, 1979.

Personal communication (telephone) between John Sherwood (Solar Power Corporation) and Joseph Bondar (HAI), September 13, 1979.

Personal communication (telephone) between Lee E. Miller (Eagle-Pitcher Industries) and Amitava Podder (HAI), March 1980.

Phillips, G.A., et al. "Inverters for Commercial Fuel Cell Power Generation." In: IEEE Transactions of Power Apparatus and Systems, Volume PAS-95, No. 3, May/June 1976.

Photovoltaics and Materials. Ed. by K.W. Boer. Winnipeg: The American Section of the Solar Energy Society. 1976.

Pickett, D. F., et al. Electrochemistry of Some New Alkaline Battery Electrodes. Air Force Aero-Propulsion Laboratory, February 1976.

Pickrell, R. "10-kVA Inverter/Controller." In: Proceedings of the Semiannual Review Meeting-Silicon Technology Programs Branch, Williamsburg, Virginia, August 23, 1979.

Pickrell, Roy L., et al. An Inverter/Controller Subsystem Optimized for Photovoltaic Applications, DOE/NASA/1022-78/31. Technical paper presented at the Thirteenth Photovoltaic Specialists Conference sponsored by IEEE, Washington, D.C., June 5-8, 1978.

Pioneer Electric and Research Corporation. Advertising literature.

Pittman, P. F. Conceptual Design and Systems Analysis of Photovoltaic Power Systems, Volume I. Prepared for U.S. Energy Research and Development Administration by Westinghouse Electric Corporation, April 1977.

Pittman, P.F. Final Report Conceptual Design and Systems Analysis of Photovoltaic Power Systems, Volumes 1 through 5, E(11-1)-2744. Prepared for U.S. Energy Research and Development Administration by Westinghouse Electric Corporation, Pittsburgh, 1977.

Pittman, Paul F. "Implications of New Technology on Power Conditioner Design." Presented at Workshop on Power Conditioning for Alternative Energy Technologies, Denver, Colorado, May 9-11, 1979.

Pittman, Paul F. The Role of Batteries in Solar Photovoltaic Energy Systems. Presented at Sandia Labs, Albuquerque, New Mexico, July 27, 1979.

Posner, A. M. "Redox Fuel Cell." Fuel, Volume 34, No. 3 (July 1955), pp. 330-338.

Preto, Sandra. Questionnaire response. Argonne National Laboratory.

Preto, S.K., et al. "Calcium/Iron Sulfide Secondary Cells." Prepared for the meeting of the Electrochemical Society, Philadelphia, Pennsylvania, May 8-13, 1977.

Putt, R.A. "A Zinc Bromine Battery for Energy Storage." In: Proceedings of the 14th Intersociety Energy Conversion Engineering Conference, American Chemical Society, August 1979.

Putt, Ron. Zinc-Bromine Battery Program at Gould. Presented at DOE/STOR Flow Battery Project Review, Rockville, Maryland, July 17, 1979.

Read, Ed. Zinc-Bromine Battery System. Presented at DOE/STOR Flow Battery Project Review, Rockville, Maryland, July 17, 1979.

Remirez, Raul. "Battery Development Revs Up." Chemical Engineering, August 27, 1979.

Roberts, R. Status of the DOE Battery and Electrochemical Technology Program, MTR-8026. Mitre Corporation, September 1979.

Rosati, et al. AC/DC Power Converter for Batteries and Fuel Cells. Prepared for Electric Power Research Institute by United Technologies Corporation, August 1978.

Ross, R.G., and B.D. Shafer. "Concentrator and Flat Panel Technology Alternative for 50¢/Watt." In: Proceedings of the U.S. DOE Photovoltaic Technology Development and Applications Program Review, Arlington, Virginia, November 7-9, 1978.

Roy, A. S. and S. I. Kaplan. Analysis of Performance Capabilities of Redox-Flow Storage Batteries. Oak Ridge National Laboratory.

Schueler, D. G. and G. J. Jones. Energy Storage Considerations in Photovoltaic Central Station Utility Applications. Sandia Laboratory.

SES, Inc. Advertising literature.

Sensor Technology, Inc. Advertising literature.

Shirland, F.A. "The History, Design, Fabrication, and Performance of CdS Thin Film Solar Cells." Advanced Energy Conversion, Vol. 6, (1966), pp. 201 to 222.

Smith, D.R. "Power Conditioning for Photovoltaics." Presented at Workshop on Power Conditioning for Alternative Energy Technologies, Denver, Colorado, May 9-11, 1979.

Smith, J.L., W.R. Gates, and T. Lee. Historical Evidence of Importance to the Industrialization of Flat-Plate Silicon Photovoltaic Systems. Volumes I and II. Prepared for National Aeronautics and Space Administration by Jet Propulsion Laboratory, Pasadena, California, April 1978.

Solar Cells. Ed. by Charles E. Backus. New York, IEEE Press, 1976.

"Solar Power Conditioner." NASA's Jet Propulsion Laboratory, Pasadena, California. NASA Tech. Briefs, Spring 1979, p. 41.

Solar Power Corporation. Advertising literature.

Solarex Corporation. Advertising literature.

Soleq Corporation. Manufacturer's brochures. Chicago, Illinois.

Spectrolab. Advertising literature.

Springgate, W.F. "Integration of Solar Array and Power Conditioning Electronics." Presented at Intersociety Energy Conversion Engineering Conference, Boston, Massachusetts. August 3-5, 1971.

Srinivasan, S., R. Yea, and A. Beaufrere. "Hydrogen-Halogen Energy Storage Systems: Preliminary Feasibility and Economic Assessment." ERDA Contractors Coordination Meeting, January 1977.

Steunenberg, R. K. Lithium-Aluminum Metal Sulfide Batteries. Argonne National Laboratory, March 1977.

"Storage Batteries: The Case and the Candidates." EPRI Journal, October 1976, pp. 6-13.

Stover, John B. NASA-LeRC Photovoltaic Power System Tests on an 8-Kilowatt Single-Phase Line-Commutated Inverter. Prepared for U.S. Department of Energy by NASA-Lewis Research Center, February 1978.

Stump, et al. Design and Construction of a 50 kVA Power Conditioning Unit for Photovoltaic Power Streams. Prepared for Sandia Laboratories by Westinghouse Aerospace Electrical Division, under Contract No. 07-6940, April 1979.

Sudar, S. Old Questionnaire.

Sudar, S., et al. Development of Lithium-Metal Sulfide Batteries. Rockwell International, Atomics International Division, June 1978.

Sudar, S., et al. Development of Lithium-Metal Sulfide Batteries for Load Leveling. Atomics International, July 1977.

Sudworter, J.L., British Railways. Questionnaire response.

Svelzie, L.R. Delta Electronic Control Corporation, and D.J. Roseler, U.S. Department of Energy. Operational Characteristics of a 60kW Photovoltaic System Integrated With a Utility Grid.

Symons, P. C. and M. J. Hammond. Evaluation of a 1-kWh Zinc Chloride Battery System, Interim Report. September 1976.

Tajima, S., M. Nakamura, and T. Mori. "A Ni-Zn Rechargeable Cell of the Fixed Electrolyte Type." In: Power Source 6: Research and Development in Non-Mechanical Power Sources, Proceedings of the 10th International Symposium, Brighton, England, September 13-16, 1976, pp. 321-333.

Thaller, Lawrence H. Recent Advances in Redox Flow Cell Storage Systems, DOE/NASA 1002-79/4. Prepared for 14th Intersociety Energy Conversion Engineering Conference, Boston, 1979.

Thaller, Larry. Redox Energy Storage Systems. Presented at DOE/STOR Flow Battery Project Review, Rockville, Maryland, July 17, 1979.

Thaller, L. H. Redox Flow Cell Energy Storage Systems. Presented at AIAA Terrestrial Energy Systems Conference, June 4, 1979.

Tideland Signal Corporation. Advertising literature.

Towle, W. L., et al. Cost Estimate for the Commercial Manufacture of Lithium/Iron Sulfide Cells for Load-Leveling. Argonne National Laboratory, March 1976.

U.S. Department of Energy. An Assessment of Solar Photovoltaic Industry, Markets, and Technologies, EX-77-C-03-1978. Prepared by Booz, Allen and Hamilton, Inc., Bethesda, Maryland, September 30, 1978.

U.S. Department of Energy. Battery Technology: An Assessment of the State of the Art. Prepared by TRW, Inc., under Contract No. EX-76-C-10-3885, March 27, 1978.

U.S. Department of Energy. Electrochemical Storage System Multi-Year Program Plan. Draft Working Paper. Division of Energy Storage, June 15, 1979.

U.S. Department of Energy. Environmental Development Plan for Energy Storage Systems - FY 1979.

U.S. Department of Energy. National Photovoltaic Program Multi-Year Program Plan. Division of Solar Technology. June 6, 1979.

U.S. Department of Energy. Photovoltaic Tests and Applications Project Progress Report for April 1976 - June 1977. NASA-Lewis Research Center, November 1978.

U.S. Department of Energy. Proceedings of the Photovoltaics Program Semi-Annual Review, Advanced Materials R&D Branch, Golden, Colorado, October 4-6, 1977.

U.S. Department of Energy. Redox Flow Cell Development and Demonstration Project - Calendar Year 1976. Prepared by NASA-Lewis Research Center, December 1977.

U.S. Department of Energy. Second Annual Battery and Electrochemical Technology Conference - Agenda and Technical Presentations, June 5-7, 1978. Published May 1978.

U.S. Department of Energy. Technical and Economic Analysis Subprogram. Subprogram Overview FY 1979. Energy Storage Systems Division, February 1979.

U.S. Energy Research and Development Administration. The Best Facility - Workshop II, February 8 to 10, 1977. Electric Power Research Institute, April 1977.

U.S. Energy Research and Development Administration. Engineering Study of a 20 MW Lead-Acid Battery Energy Storage Demonstration Plant, ERDA-E (04-3)-1205. Prepared by Bechtel Corporation, San Francisco, October 1976.

U.S. Energy Research and Development Administration. Environmental Control Technology R&D Requirements for Energy Storage Systems, W-7405-Eng. 36. Prepared by Los Alamos Scientific Laboratory, Los Alamos, New Mexico, September 1977.

U.S. Energy Research and Development Administration. Environmental Development Plan (EDP) - Energy Storage Systems - FY 1978. September 1977.

U.S. Energy Research and Development Administration. First Annual ERDA Battery Contractors Coordination Meeting, January 27-28, 1977, Argonne National Laboratory.

U.S. Energy Research and Development Administration. Proceedings of the ERDA Semiannual Solar Photovoltaic Program Review Meeting, E(49-18)-2477. Prepared by University of Maine, Orono, Maine, August 3-6, 1976.

U.S. Energy Research and Development Administration. Proceedings of the Third International Electric Vehicle Symposium, Volume 1, February 19-21, 1974.

U.S. Energy Research and Development Administration. Study of the Auxiliaries for Lead-Acid Battery Systems for Peaking Power, ERDA - E (49-18)-2114. Prepared by Westinghouse Electric Corporation, Pittsburgh, December 1976.

U.S. Energy Research and Development Administration. Study of the Manufacturing Costs of Lead-Acid Batteries for Peaking Power, ERDA-E (49-18)-2114. Prepared by Westinghouse Electric Corporation, Pittsburgh, December 1976.

U.S. Environmental Protection Agency. Assessment of Industrial Hazardous Waste Practices: Storage and Primary Batteries Industries. Versar, Inc., 1975.

The University of Alabama in Huntsville. A Survey of Photovoltaic Systems. Prepared for National Aeronautics and Space Administration, August 1979.

Vissers, D. R., Z. Tomczuk, and R. K. Steunenberg. "A Preliminary Investigation of High Temperature Lithium/Iron Sulfide Secondary Cells." J. Electrochem Soc.: Electrochemical Science and Technology, May 1974, Volume 121, No. 5, pp. 665-667.

von Krusenstierna, O. "High-Energy Long-Life Zinc Battery for Electric Vehicles." In: Power Source 6: Research and Development in Non-Mechanical Electrical Power Sources, Proceedings of the 10th International Symposium, Brighton, England, September 13-16, 1976, pp. 303-319.

von Winbush, S. and A. F. Sammells. "A Zinc Chlorine Molten Salt Cell." J. Electrochem. Soc.: Electrochemical Science and Technology, Volume 123, No. 5 (May 1976).

Walsh, W. J. and H. Shimotake. Performance Characteristics of Lithium-Aluminum/Iron Sulfide Cells. Argonne National Laboratory, 1976.

Warshay, M. and L. O. Wright. "Cost and Size Estimates for a Redox Bulk Energy Storage Concept." J. Electrochem. Soc.: Electrochemical Science and Technology, Volume 124, No. 2 (February 1977).

Watson, T. Non-Hazardous Primary Lithium-Organic Electrolyte Battery. Prepared for U.S. Army ECOM by P. R. Mallory and Company, Inc., October 1974.

Weiner, S.A. Sodium/Sulfur Advanced Batteries. Ford Motor Company, May 1976.

Williams, B.F. "Do Photovoltaics Have a Future?" RCA Engineer, Vol. 24, No. 5 (February/March, 1979), pp. 12 to 15.

Windworks, Inc. Manufacturer's brochures. Mukwonago, Wisconsin.

Wittmann, A. Battery Design, Patent 4,000,350. Hughes Aircraft Company, December 28, 1976.

Wood, Peter. AC/DC Power Conditioning and Control Equipment for Advanced Conversion and Storage Technology. November 1976.

Wood, Peter. AC/DC Power Conditioning and Control Equipment for Advanced Conversion and Storage Technology. Prepared for Electric Power Research Institute, August 1975.

Wood, Peter. "Power Condition for Solar Photovoltaic/Battery Storage Systems." Presented at Workshop on Power Conditioning, Denver, Colorado, May 9-11, 1979.

Wood, Peter. "Power Conditioning Systems." In: Record of the Photovoltaics Power Conditioning Workshop, Albuquerque, New Mexico, October 13-14, 1976.

Wood, Peter, et al. "Power Conversion Equipment - A Key Component in New Power System Generation and Storage Concepts." In: Proceedings of American Power Conference 1976, Volume 38.

Wright, R.R. and H.R. Skutt. Electronics Circuits and Devices. New York: The Ronald Press Co., 1965.

Yao, N. P., and J. J. Barghusen. Proceedings of the Workshop on Battery Storage for Solar-Photovoltaic Energy Systems. Denver, Colorado, January 11 to 13, 1978. Sponsored by Argonne National Laboratory.

Zanio, K. and L. Fraas. Indium Phosphide/Cadmium Sulfide Thin-Film Terrestrial Solar Cells, Quarterly Report No. 4 EY-76-C-04-3717. Prepared for U.S. Energy Research and Development Administration by Hughes Research Laboratories, Malibu, California, October 1977.

Zeitner, E. J. and J. S. Dunning. High Performance Lithium/Iron Disulfide Cells. Society of Automotive Engineers, Inc., 1978.

Zivi, S.M., et al. "Battery Engineering Problems in Designing an Electrical Load Leveling Plant for Lithium/Iron Sulfide Cells." In: Proceedings of the 14th Intersociety Energy Conversion Engineering Conference, American Chemical Society, 1979.

VI. ABBREVIATIONS

air mass one (air mass at sea level)	AM1
air mass zero (air mass in space)	AM0
ampere	A
ampere-hour	Ah
centimeter	cm
current	i
degree centigrade	°C
degree Fahrenheit	°F
depth of discharge	DOD
distortion factor	df
efficiency	η
form factor	ff
gram	g
hertz	hz
kilogram	kg
kilovolt	kV
kilovolt-ampere	kVA
kilowatt	kW
kilowatt-hour	kWh
mean time between failures	MTBF
meter	m
microfarad	μF
micrometer (10^{-6} meter)	μm
miles per hour	mph

milliampere (10^{-3} ampere)	mA
millihenry	mH
millimeter	mm
millivolt (10^{-3} volt)	mV
milliwatt (10^{-3} watt)	mW
open circuit voltage	V_{oc}
output voltage	Vo
parts per million	ppm
phase	ø
pound	lb
power	P
"Q" point or operating point	Q
reactive volt amperes	VAR
root mean square	rms
short circuit current	I_{sc}
square centimeter	cm^2
square meter	m^2
temperature	T
total harmonic distortion	THD
volt	V
watt	W
watt-hour	Wh
Where N is an integer, designates the discharge rate, in amperes, equivalent to the battery rated capacity in ampere-hours, C, divided by N hours.	C/N

Chemical formulas use the standard symbols for the elements.

*U.S. GOVERNMENT PRINTING OFFICE: 1981-740-145/1288